

AKADEMIE DER WISSENSCHAFTEN DER DDR
Forschungsbereich Geo- und Kosmoswissenschaften
ZENTRALINSTITUT FÜR PHYSIK DER ERDE

Veröffentlichungen des Zentralinstituts für Physik der Erde

Nr. 81 Teil II

**5th International Symposium
„Geodesy and Physics of the Earth“**

G.D.R. Magdeburg, September 23rd to 29th, 1984

PROCEEDINGS

Part II

Editor: The Director of the Central Institute for Physics of the Earth

Als Manuskript gedruckt: Potsdam 1985

F 245/85

3623

C o n t e n t s
I n h a l t s v e r z e i c h n i s
Part II
Teil II

Fortsetzung "Planetary dynamics"

	Page Seite
P a p e r s	
HOLOTA, PETR: A new approach to iterations in solving geodetic boundary value problems for topography	4
IVANOV, I. B.: The irregularity in the Earth's annual rotation as a cause of systematic time variation	16
JENTZSCH, GERHARD: Ocean tidal loading along the "Blue Road Geotraverse" in Fennoscandia	18
JOCHMANN, H.: On the influence of coupling torques between the Earth's core and mantle on parameters and components of the rotation of the Earth	29
KELLER, WOLFGANG: Treatment of the geodetic boundary value problem by contact-transformation	32
KOLACZEK, B.; BRZEZINSKI, A.; KOSEK, W.; NASTULA, J.; SOLODUCHA, B.: On short periodical variations of polar motion and UT1 - UTC	35
MEINIG, M.: Influences of systematic differences between different star catalogues on the results of latitude and time determinations with the PZT 2	45
MELCHIOR, P.; DUCARME, B.; VAN RUYMBEKE, M.; POITEVIN, C.; DE BECKER, M.: Interactions between oceanic and gravity tides, as analysed from world-wide Earth tide observations and ocean models	55
MENTES, GY.: Capacitive pendulum with intelligent data collection	63
MENG JIACHUN: Research on the computational methods of gravity topographic effect	70
МЕЩЕРЯКОВ, Г. А.: ПОТЕНЦИАЛОГРАФИЧЕСКАЯ ЗАДАЧА И КОНЦЕПЦИЯ ГРАВИТИРУЮЩИХ ДИСКОВ	78
MORITZ, HELMUT: Variational principles for Earth rotation	88
POMA, A.; PROVERBIO, E.: Secular and long term variations in polar motion from classical and doppler observations	101
SJÖBERG, LARS E.: On the convergence problem of the satellite derived spherical harmonic expansion of the geopotential at the Earth's surface	108
SIMON, D.; KARMALEEVA, R. M.; LATYNINA, L. A.: On the comparison of the results of two different E-W-strainmeters operating at Tiefenort in the period 1978 - 1984	115
STEINERT, KLAUS-GÜNTER: Planets around Barnard's star?	126

	Page
	Seite
TRESL, JIRI: Geodynamic effects due to Earth's deformation	128
TSCHERNING, C. C.: On the long-wavelength correlation between gravity and topography	134
VONDRAK, J.: Polar motion between 1900.0 and 1984.0 as determined by different techniques	143
XIA JIONGYU: On the comparison and choice between the formulas of the Earth tidal correction in astronomical time and latitude observation	144
ЯЦКОВ, Я. С.: Н. Т. МИРОНОВ: ОБ УЧЕТЕ ВЛИЯНИЯ ГОРИЗОНТАЛЬНЫХ ПЕРЕМЕЩЕНИЙ ЛИТОСФЕРНЫХ ПЛИТ ПРИ ОБРАБОТКЕ НАБЛЮДЕНИЙ В ГЛОБАЛЬНОЙ СЕТИ ГЕОДИНАМИЧЕСКИХ СТАНЦИЙ (НА ПРИМЕРЕ ГЕОСС_РЕА) (On reducing the effect of horizontal displacements of the lithospheric plates from the observations carried out by global geodynamic network (on example the GEOSS-REA network)	150
ЮРКИНА, М. И.: О приливных поправках в геодезии	156
ZSCHAU, J.: Anelasticity in the Earth's mantle : Implications for the frequency dependence of love numbers	160

A New Approach to Iterations in Solving Geodetic
Boundary Value Problems for Real Topography

Petr Holota

RESEARCH INSTITUTE OF GEODESY,
TOPOGRAPHY AND CARTOGRAPHY

250 66 ZDIBY 98 / PRAGUE - EAST

CZECHOSLOVAKIA

1. Introduction

The solution of a geodetic (linear) boundary value problem generally means to find a harmonic function in the domain outside a telluroid which meets some conditions given on the surface of the telluroid. Following the definition, see (Krarup, 1973), (Hörmander, 1975, 1976), (Grafarend, 1978), (Brovar, Magnicky, Shimbirev, 1961, §34), the telluroid (or the surface of the Earth in the first approximation in Soviet literature) is about as irregular as the physical surface of the Earth's body. However, almost all formulas which are used for practical representation of the solution of the problem are valid for what is usually called a zero-order approximation of the solution based on a formal approximation of the real boundary surface (given by the telluroid) by a sphere. This kind of a spherical approximation is insomuch habitual in the respective computations as it is used even at the very cost of a high smoothing of the real topography.

There is a belief that there exists a convergent iterative (i.e. a constructive) process, in fact an analytical continuation in the interpretation by (Pellinen, 1974), (Marych, 1973) or (Moritz, 1980, §46), which modifies the

original boundary data in such a way that these, being used as boundary data on the sphere, define a harmonic function having the quality of an analytical continuation of the solution related to the original data and the boundary given by the rugged topography of the telluroid. However, it is not quite obvious whether the necessary perturbation of the zero-order solution which would represent an increment caused by the topography is small enough (and in which functional norm) to be determined by an iterative way as above. Anyway the iterative process must be highly unstable (which is also in agreement with the practical experience).

In this paper we will confine ourselves to the so-called simple Molodensky problem

$$(1.1) \quad \Delta T = \operatorname{div} \operatorname{grad} T = 0 \quad \text{in } \Omega,$$

$$(1.2) \quad r \frac{\partial T}{\partial r} + 2T = -r \Delta g \quad \text{on } \partial \Omega$$

where Δg is the gravity anomaly, $r = |x|$ and Ω is an unbounded domain with the boundary $\partial \Omega$ which is star-shaped at the origin of the system of coordinates x_1, x_2, x_3 . The simple Molodensky problem is the one considered in virtually all practical solutions of the geodetic boundary value problem. The term has been introduced by (Krarup, 1973) and is also explained in (Moritz, 1980, §§42,43).

It is well known that for the solution of the problem (1.1) - (1.2) the famous integral equation method has already been used by Molodensky. The basic integral equation for the unknown density is related to an irregular surface of the telluroid. However, for practical reasons it was reformulated and expressed as an integral equation of the second kind given on a spherical surface. This makes it possible to consider the integral operator involved as a perturbation of the one that corresponds to (1.1) - (1.2) in case of Ω being the exterior of a sphere. For the solution of the mentioned perturbation problem a technique has been developed inspired

by a method based on an asymptotic series expansion of the resolvent operator (with respect to a small parameter). The convergence problem related to a Neumann series solution has been investigated by (Moritz, 1973) and is an inspiring topic for further research.

From an abstract point of view the above perturbation problem can be taken for a consequence of a transition from the spherical coordinates r (radius vector), ν (polar distance), λ (geocentric longitude) to the new system of coordinates

$$(1.3) \quad \bar{r} = r - h(\nu, \lambda) \quad , \quad \bar{\nu} = \nu \quad , \quad \bar{\lambda} = \lambda$$

where the function h describes the telluroid's topography in relation to the reference ellipsoid. Following the concept of the so-called spherical approximation, the reference ellipsoid will be treated as a sphere of radius R (which is often defined as the radius of a sphere that has the same volume as the earth ellipsoid, i.e. $R = 6371$ km), for a more detailed explanation cf. (Heiskanen and Moritz, 1967) or (Moritz, 1980). In consequence (1.3) carries the surface of the telluroid into the sphere of radius R . However, it is necessary to express the Laplacian of T in terms of \bar{r} , $\bar{\nu}$, $\bar{\lambda}$.

In this paper a slightly more general transformation

$$(1.4) \quad \bar{r} = r - \omega(\bar{r})h(\nu, \lambda) \quad , \quad \bar{\nu} = \nu \quad , \quad \bar{\lambda} = \lambda$$

will be used instead of (1.3) where ω is a smooth and suitably chosen function such that $0 \leq \omega(\bar{r}) \leq 1 + \varepsilon$, $\varepsilon > 0$, for $R \leq \bar{r}$ and $\omega(R) = 1$. The simple Molodensky problem will again be solved by means of an iterative process. The proof of its convergence will be based on an a priori estimate of the solution of the problem, especially on an a priori estimate for its second derivatives.

For an actual representation of the solution there will be derived the so-called Green's function (more precisely

the Green-Stokes function in this case) making possible to write an explicit expression for the solution of the Poisson partial differential equation in case that it satisfies a boundary condition of the following type

$$(1.5) \quad \partial u / \partial |x| + 2u/R = f \quad \text{for} \quad |x| = R$$

which is well known in physical geodesy.

2. Laplacian

In spherical coordinates r , ν , λ the Laplacian of T has the following form

$$(2.1) \quad \Delta T = \partial^2 T / \partial r^2 + (2/r) \partial T / \partial r + (1/r^2) \partial^2 T / \partial \nu^2 + (\cos \nu / r^2 \sin \nu) \partial T / \partial \nu + (1/r \sin \nu)^2 \partial^2 T / \partial \lambda^2$$

Passing to the coordinates \bar{r} , $\bar{\nu}$, $\bar{\lambda}$, according to (1.4), we introduce, for any values of variables considered, the new function

$$(2.2) \quad u(\bar{r}, \bar{\nu}, \bar{\lambda}) = T(\bar{r} + \omega(\bar{r})h, \bar{\nu}, \bar{\lambda}) = T(r, \nu, \lambda)$$

To express the Laplacian of u in terms of \bar{r} , $\bar{\nu}$, $\bar{\lambda}$, which are not an orthogonal system, we have to calculate all the necessary derivatives:

$$(2.3) \quad \partial T / \partial r = \partial u / \partial \bar{r} \partial \bar{r} / \partial r$$

$$(2.4) \quad \partial^2 T / \partial r^2 = \partial^2 u / \partial \bar{r}^2 (\partial \bar{r} / \partial r)^2 + \partial u / \partial \bar{r} \partial^2 \bar{r} / \partial r^2$$

$$(2.5) \quad \partial T / \partial \nu = \partial u / \partial \bar{r} \partial \bar{r} / \partial \nu + \partial u / \partial \bar{\nu}$$

$$(2.6) \quad \partial^2 T / \partial \nu^2 = \partial^2 u / \partial \bar{r}^2 (\partial \bar{r} / \partial \nu)^2 + 2 \partial^2 u / \partial \bar{r} \partial \bar{\nu} \partial \bar{r} / \partial \nu + \partial u / \partial \bar{r} \partial^2 \bar{r} / \partial \nu^2 + \partial^2 u / \partial \bar{\nu}^2$$

$$(2.7) \quad \partial^2 T / \partial \lambda^2 = \partial^2 u / \partial \bar{r}^2 (\partial \bar{r} / \partial \lambda)^2 + 2 \partial^2 u / \partial \bar{r} \partial \bar{\lambda} \partial \bar{r} / \partial \lambda + \partial u / \partial \bar{r} \partial^2 \bar{r} / \partial \lambda^2 + \partial^2 u / \partial \bar{\lambda}^2 .$$

Thus

$$(2.8) \quad 0 = \Delta T = \Delta \bar{r} \partial u / \partial \bar{r} + |\text{grad } \bar{r}|^2 \partial^2 u / \partial \bar{r}^2 + (2/r^2) \partial \bar{r} / \partial \bar{\lambda} \partial^2 u / \partial \bar{r} \partial \bar{\lambda} + (2/r^2 \sin^2 \bar{\nu}) \partial \bar{r} / \partial \lambda \partial^2 u / \partial \bar{r} \partial \bar{\lambda} + r^{-2} (\partial^2 u / \partial \bar{\nu}^2 + (\cos \bar{\nu} / \sin \bar{\nu}) \partial u / \partial \bar{\nu}) + (1/\sin^2 \bar{\nu}) \partial^2 u / \partial \bar{\lambda}^2 .$$

After a small manipulation we obtain

$$(2.9) \quad \bar{\Delta} u = \Delta \bar{r} \bar{r} \bar{\lambda} u = ((2/\bar{r}) - (r/\bar{r})^2 \Delta \bar{r}) \partial u / \partial \bar{r} + (1 - (r/\bar{r})^2 |\text{grad } \bar{r}|^2) \partial^2 u / \partial \bar{r}^2 - (2/\bar{r}^2) (\partial \bar{r} / \partial \bar{\nu} \partial^2 u / \partial \bar{r} \partial \bar{\nu} + (1/\sin^2 \bar{\nu}) \partial \bar{r} / \partial \lambda \partial^2 u / \partial \bar{r} \partial \bar{\lambda})$$

and inserting from (1.4), we have

$$(2.10) \quad A = (2/\bar{r}) - (r/\bar{r})^2 \Delta \bar{r} = (2/\bar{r})(1 - (1 + h \partial \omega / \partial \bar{r})^{-1}) + (\omega/\bar{r}^2)(1 + h \partial \omega / \partial \bar{r})^{-1} (\Delta_1 h - 2h) - (1 + h \partial \omega / \partial \bar{r})^{-3} ((\bar{r} + \omega(\bar{r})h)/\bar{r})^2 + (\omega/\bar{r})^2 |\text{grad}_1 h|^2 h \partial^2 \omega / \partial \bar{r}^2 ,$$

$$(2.11) \quad B = 1 - (r/\bar{r})^2 |\text{grad } \bar{r}|^2 = 1 - ((\bar{r} + \omega(\bar{r})h)/\bar{r}(1 + h \partial \omega / \partial \bar{r}))^2 - (\omega/\bar{r}(1 + h \partial \omega / \partial \bar{r}))^2 |\text{grad}_1 h|^2 ,$$

$$(2.12) \quad C = - (2/\bar{r}) \partial \bar{r} / \partial \bar{\nu} = 2(\omega/\bar{r})(1 + h \partial \omega / \partial \bar{r})^{-1} \partial h / \partial \bar{\nu} ,$$

$$(2.13) \quad D = - (2/\bar{r} \sin \bar{\nu}) \partial \bar{r} / \partial \bar{\nu} = 2(\omega/\bar{r} \sin \bar{\nu})(1 + h \partial \omega / \partial \bar{r})^{-1} \partial h / \partial \lambda ,$$

provided that

$$(2.14) \quad h_{\max} \partial \omega / \partial \bar{r} > -1 .$$

Here

$$(2.15) \quad \Delta_1 h = \sin^{-1} \bar{\nu} \partial (\sin \bar{\nu} \partial h / \partial \bar{\nu}) + \sin^{-2} \bar{\nu} \partial^2 h / \partial \lambda^2$$

is the second and

$$(2.16) \quad |\text{grad}_1 h|^2 = (\partial h / \partial \bar{\nu})^2 + \sin^{-2} \bar{\nu} (\partial h / \partial \lambda)^2$$

the first Beltrami's differential operator related to the unit sphere. Thus

$$(2.17) \quad \bar{\Delta} u = A \partial u / \partial \bar{r} + B \partial^2 u / \partial \bar{r}^2 + C \partial^2 u / \bar{r} \partial \bar{r} \partial \bar{\nu} + D \partial^2 u / \bar{r} \sin \bar{\nu} \partial \bar{r} \partial \bar{\lambda} .$$

Omitting terms multiplied by

$$(2.18) \quad (h \partial \omega / \partial \bar{r})^2 \quad \text{or by} \quad h \partial^2 \omega / \partial \bar{r}^2 ,$$

we get

$$(2.10a) \quad A = (2/\bar{r}) h \partial \omega / \partial \bar{r} + (\omega/\bar{r}^2)(1 - h \partial \omega / \partial \bar{r})(\Delta_1 h - 2h) ,$$

$$(2.11a) \quad B = - (\omega/\bar{r}^2)(2\bar{r}h + \omega h^2) + 2((\bar{r} + \omega(\bar{r})h)/\bar{r})^2 h \partial \omega / \partial \bar{r} - (\omega/\bar{r})^2 (1 - 2h \partial \omega / \partial \bar{r}) |\text{grad}_1 h|^2 ,$$

$$(2.12a) \quad C = 2(\omega/\bar{r})(1 - h \partial \omega / \partial \bar{r}) \partial h / \partial \bar{\nu} ,$$

$$(2.13a) \quad D = 2(\omega/\bar{r} \sin \bar{\nu})(1 - h \partial \omega / \partial \bar{r}) \partial h / \partial \lambda .$$

Moreover, we will suppose in addition to the introductory section that

$$(2.19) \quad \omega(\bar{r}) = 0 \quad \text{for} \quad \bar{r} \geq R_e = \text{const.} > R .$$

Hence

$$(2.20) \quad A = B = C = D = 0 \quad \text{for} \quad \bar{r} \geq R_e .$$

Finally, extracting the dominant terms, we can put approximately

$$(2.10b) \quad A = (2/\bar{r}) h \partial\omega/\partial\bar{r} + (\omega/\bar{r}^2) \Delta_1 h ,$$

$$(2.11b) \quad B = -2\omega h/\bar{r} + 2h \partial\omega/\partial\bar{r} - (\omega/\bar{r})^2 |\text{grad}_1 h|^2 ,$$

$$(2.12b) \quad C = 2(\omega/\bar{r}) \partial h/\partial\psi ,$$

$$(2.13b) \quad D = 2(\omega/\bar{r} \sin\bar{\psi}) \partial h/\partial\lambda .$$

3. Boundary condition

Besides the Laplacian it still remains to express the condition (1.2) in terms of \bar{r} , $\bar{\psi}$, $\bar{\lambda}$. Inserting (1.4) and following the notation (2.2), we obtain

$$(3.1) \quad (R+h)(1+h\partial\omega/\partial\bar{r})^{-1} \partial u/\partial\bar{r} + 2u = - (R+h)\Delta g \quad \text{for} \quad \bar{r} = R$$

since

$$(3.2) \quad \omega(R) = 1$$

according to the definition. For practical reasons it would be desirable to have

$$(3.3) \quad (R+h)(1+h\partial\omega/\partial\bar{r})^{-1} = R .$$

It can be simply verified that this may be achieved for

$$(3.4) \quad \partial\omega(R)/\partial\bar{r} = 1/R .$$

In consequence the boundary condition (3.1) will be of the following form

$$(3.5) \quad R \partial u/\partial\bar{r} + 2u = - (R+h)\Delta g , \quad \bar{r} = R$$

or

$$(3.5a) \quad \partial u/\partial\bar{r} + 2u/R = - (1+h/R)\Delta g , \quad \bar{r} = R .$$

4. Green's - Stokes' function

Our aim is now to find an explicit expression for the solution of the following boundary value problem

$$(4.1) \quad \Delta u = g , \quad |x| > R ,$$

$$(4.2) \quad \partial u/\partial|x| + 2u/R = f , \quad |x| = R .$$

Following the general principles in constructing Green's function, we start with the fundamental solution

$$(4.3) \quad J = |x-y|^{-1}$$

of the Laplace differential equation. For $|y| < |x|$ we have

$$(4.4) \quad J = \sum_{n=0}^{\infty} (|y|^n/|x|^{n+1}) P_n(\cos\psi_{xy})$$

and

$$(4.5) \quad \partial J/\partial|y| = \sum_{n=0}^{\infty} n(|y|^{n-1}/|x|^{n+1}) P_n(\cos\psi_{xy})$$

where P_n is the usual Legendre polynomial of degree n and ψ_{xy} is the angle between the placement vector x and

y . In case of $|y| = R$ we obtain

$$(4.6) \quad F = \partial J / \partial |y| + 2J/R = \\ = R^{-2} \sum_{n=0}^{\infty} (2+n)(R/|x|)^{n+1} P_n(\cos \psi_{xy}) .$$

A function $H(y)$ which is harmonic for $|y| > R$ and for $|y| = R$ satisfies the condition

$$(4.7) \quad \partial H / \partial |y| + 2H/R = F$$

may simply be found as

$$(4.8) \quad H = \sum_{n=0}^{\infty} H_n, \quad H_n = (R/|y|)^{n+1} \bar{H}_n(y/|y|)$$

where, after the insertion into (4.7), we get the following equations for the individual surface spherical harmonics

$$(4.9) \quad \bar{H}_n = -R^{-1}(n+2)(n-1)^{-1}(R/|x|)^{n+1} P_n(\cos \psi_{xy}),$$

except for

$$(4.10) \quad \bar{H}_1 = (a_1 y_1 + a_2 y_2 + a_3 y_3) / |y|$$

with coefficients a_i which can be chosen arbitrarily.

Putting

$$(4.11) \quad H_s = R^{-1} \sum_{n=2}^{\infty} (n+2)(n-1)^{-1}(R^2/|x||y|)^{n+1} P_n(\cos \psi_{xy}),$$

we will now define a function

$$(4.12) \quad G(x,y) = J - H = |x - y|^{-1} - H_0 - H_1 + H_s$$

and we will call it Green's-Stokes' function since its restriction for $|y| = R$ (or, symmetrically, $|x| = R$) and $n \geq 2$ yields the famous (extended) Stokes function S , as it is known in physical geodesy. Thus

$$(4.13) \quad G(x,yR/|y|) = -|x|^{-1} - H_1 + S(x,y/|y|)$$

where

$$(4.14) \quad S(x,y/|y|) = R^{-1} \sum_{n=2}^{\infty} (2n+1)(n-1)^{-1}(R/|x|)^{n+1} P_n(\cos \psi_{xy}),$$

see (Shimbirev, 1975, eq. VIII.31) or (Moritz, 1980, eq. IV.155). Following the principle of symmetry, we can finally put

$$(4.15) \quad a_i = c_i x_i / R^2 |x|^3$$

to obtain

$$(4.16) \quad H_1 = \sum_{i=1}^3 c_i x_i y_i / (|x||y|)^3$$

where c_i , $i = 1, 2, 3$, are arbitrary constants.

The function $G(x,y)$ will enable us to express the solution of the problem (4.1) - (4.2). The natural point of departure is the formula

$$(4.17) \quad u(x) = - (1/4\pi) \int_{|y|>R} G(x,y) \Delta u(y) dy - \\ - (1/4\pi) \int_{|y|=R} (G(x,y) \partial u / \partial |y| - u(y) \partial G(x,y) / \partial |y|) d_y S$$

which is a slight modification of the well known Green's third identity for the exterior of the surface $|y| = R$. It is valid for functions u that, besides satisfying the general requirements for Green's identities, satisfy certain conditions at infinity, such as vanishing there. Since u should represent the solution of (4.1) - (4.2) and

$$(4.18) \quad \partial G / \partial |y| + 2G/R = 0 \quad \text{for } |y| = R$$

it follows, after inserting in (4.17), that

$$(4.19) \quad u(x) = - (1/4\pi) \int_{|y|=R} G(x,y) f(y) d_y S - \\ - (1/4\pi) \int_{|y|>R} G(x,y) g(y) dy$$

which is the desired explicit expression for the solution of (4.1) - (4.2), provided that for our g the volume integral converges, e.g. for g such that $g(y) = 0$ for $|y| \geq R_e$. However, considering that G involves the arbitrary term H_1 , it is clear that u is uniquely determined only in a quotient space with the zero vector given by a supplementary space spanned by the first degree harmonics $x_i |x|^{-3}$.

5. Calderon - Zygmund Inequality

As it will be clear from Section 7, we need an estimate "up to the second derivatives" for the second term on the right hand side of (4.19), i.e. an estimate for the solution u of

$$(5.1) \quad \Delta u = g, \quad |x| > R$$

in case of

$$(5.2) \quad \partial u / \partial |x| + 2u/R = 0 \quad \text{a.e. on } |x| = R$$

(a.e. means "almost everywhere" in the Lebesgue sense). For this purpose we will use the so-called L_2 - estimates for Poisson's equation which, in a certain sense, are an analogue of the Schauder theory in the Hölder spaces.

Let Ω be a domain in R^3 and g a function in the classical Banach space $L_2(\Omega)$ consisting of measurable functions on Ω that are square integrable. The norm in $L_2(\Omega)$ is defined by

$$(5.3) \quad \|u\|_2 = \left(\int_{\Omega} |u|^2 d\Omega \right)^{1/2}$$

In addition, we will use the Sobolev weight space $W_2^{(2)}(\Omega, R)$ equipped by the norm

$$(5.4) \quad \|u\|_{2,2}^2 = \sum_{|i| \leq 2} (R^{|i|} \|D^i u\|_2)^2 = \|u\|_2^2 + R^2 \| |\text{grad } u| \|_2^2 + R^4 \sum_{|i|=2} \|D^i u\|_2^2,$$

where

$$(5.5) \quad D^i u = \partial^{|i|} u / \partial r^j (\partial \lambda)^k (r \sin \lambda)^l$$

and $i = (j, k, l)$ is a multi-index with components j, k, l being non-negative integers. The number $|i| = j + k + l$ is called the length of the multi-index i . For the general definition of Sobolev weight spaces see (Kufner, John, Fučík, 1977, espec. sec. 8.10).

Recall now that the Newtonian potential of g is the function w defined by the convolution

$$(5.6) \quad w(x) = - (4\pi)^{-1} \int_{\Omega} |x - y|^{-1} g(y) dy$$

The desired L_2 - estimates are usually established through a consideration of the Newtonian potential w . Of the fundamental importance for the L_2 - theory is the Calderon-Zygmund inequality. It has deep roots in the general theory of elliptic equations and its proof, which is rather hard, goes beyond the scope of this paper. For that reason, following (Gilbarg and Trudinger, 1983, Theorem 9.9), we will confine ourselves, without proof, to

Theorem 5.1 (Calderon-Zygmund inequality). Let $g \in L_2(\Omega)$ and let w be the Newtonian potential of g . Then $w \in W_2^{(2)}(\Omega, R)$, $\Delta w = g$ a.e. and

$$(5.7) \quad \|D^i w\|_2 \leq C \|g\|_2 \quad \text{for } |i| = 2$$

where $C = \text{const}$. Moreover, Ω can be a bounded as well as an unbounded domain in R^3 , consistently with the note made in (Gilbarg and Trudinger, 1983, p. 235). Note, however, that here, for practical reasons, we have interpreted the Calderon-Zygmund inequality in a weight space and in spheri-

cal coordinates in contrast to Theorem 9.9 in (Gilbarg and Trudinger, 1983).

Considering now the Green-Stokes function (4.12), the L_2 - estimate for the second derivatives of the solution of (5.1) - (5.2) follows immediately from Theorem 5.1 and the explicit formula (4.19). Thus

$$(5.8) \quad \|D^2 u\|_2 \leq \text{const.} \|g\|_2$$

Our aim is now to find a quantitative estimate for the Sobolev norm of u .

6. Sobolev norm estimate

Starting with this section we will suppose that

$$(6.1) \quad g(y) = 0 \quad \text{for} \quad |y| \geq R_e = \text{const.} > R$$

According to (5.4) we have to estimate the terms

$$(6.2) \quad A_0 = \int_{\Omega} \left(\int_{\Omega} G(x,y) g(y) dy \right)^2 dx,$$

$$(6.3) \quad A_1 = (4\pi R)^2 \int_{\Omega} |\text{grad } u|^2 dx,$$

$$(6.4) \quad A_2 = (4\pi R^2)^2 \sum_{|i|=2} \|D^i u\|_2^2$$

with G being the Green-Stokes function (4.12) and

$$(6.5) \quad \Omega = \{x; R < |x| < R_e\}$$

to get the necessary estimate

$$(6.6) \quad \|u\|_{2,2}^2 = (4\pi)^{-2} (A_0 + A_1 + A_2)$$

for the solution of (5.1) - (5.2) in Ω .

Using Cauchy's inequality and the obvious inequality

$$(6.7) \quad (a + b + c)^2 \leq (1 + \varepsilon_1 + \varepsilon_2)a^2 + (1 + 1/\varepsilon_1 + \varepsilon_3)b^2 + (1 + 1/\varepsilon_2 + 1/\varepsilon_3)c^2,$$

with $\varepsilon_1, \varepsilon_2, \varepsilon_3$ being positive, we have

$$(6.8) \quad A_0 \leq k \|g\|_2^2$$

where

$$(6.9) \quad k = (1 + \varepsilon_1 + \varepsilon_2)A_{00} + (1 + 1/\varepsilon_1 + \varepsilon_3)A_{01} + (1 + 1/\varepsilon_2 + 1/\varepsilon_3)A_{02}$$

and

$$(6.10) \quad A_{00} = \iint_{\Omega} (J - H_0)^2 dy dx,$$

$$(6.11) \quad A_{01} = \iint_{\Omega} H_1^2 dy dx,$$

$$(6.12) \quad A_{02} = \iint_{\Omega} H_2^2 dy dx$$

since $G = J - H_0 - H_1 + H_2$.

To estimate A_{00} we, first, recall that for $|y| < |x|$

$$(6.13) \quad J = |x|^{-1} + \sum_{n=1}^{\infty} (|y|^n / |x|^{n+1}) P_n(\cos \psi_{xy})$$

and for $|x| < |y|$

$$(6.14) \quad J = |y|^{-1} + \sum_{n=1}^{\infty} (|x|^n / |y|^{n+1}) P_n(\cos \psi_{xy}).$$

Consequently

$$(6.15) \quad A_{00} = 2(A_{001} + A_{002})$$

where

$$\begin{aligned}
 (6.16) \quad A_{001} &= \int_{\Omega} \int_{R < |y| < |x|} (|x|^{-1} - H_0)^2 dy dx = \\
 &= \int_{\Omega} \int_{|x| < |y| < R_e} (|y|^{-1} - H_0)^2 dy dx = \\
 &= (11/12)(4\pi)^2 R^4 (1 - (28/11)(R_e/R) + \\
 &+ (24/11)(R_e/R)^2 - (8/11)(R_e/R)^3 + (1/11)(R_e/R)^4)
 \end{aligned}$$

and

$$\begin{aligned}
 (6.17) \quad A_{002} &= \sum_{n=1}^{\infty} Q_n (J_n^2 + \\
 &+ 4 \sum_{m=1}^n ((n-m)!/(n+m)!)^2 (G_{nm}^2 + S_{nm}^2))
 \end{aligned}$$

with

$$\begin{aligned}
 (6.18) \quad Q_n &= \int_R^{R_e} \int_R^{|x|} (|y|^n / |x|^{n+1})^2 |y|^2 d|y| |x|^2 d|x| = \\
 &= \int_R^{R_e} \int_{|x|}^{R_e} (|x|^n / |y|^{n+1})^2 |y|^2 d|y| |x|^2 d|x| = \\
 &= (1/4)(2n-1)^{-1} R^4 ((2n-1)(2n+3)^{-1} (R_e/R)^4 + \\
 &+ 4(2n+3)^{-1} (R/R_e)^{2n-1} - 1) ,
 \end{aligned}$$

$$(6.19) \quad J_n = \int_{\omega} P_n^2(\cos \nu) d\omega ,$$

$$(6.20) \quad G_{nm} = \int_{\omega} (P_{nm}(\cos \nu) \cos m\lambda)^2 d\omega ,$$

$$(6.21) \quad S_{nm} = \int_{\omega} (P_{nm}(\cos \nu) \sin m\lambda)^2 d\omega$$

and $d\omega$ denoting the surface element of the unit sphere.

Here we have used the famous decomposition formula

$$\begin{aligned}
 (6.22) \quad P_n(\cos \psi_{xy}) &= P_n(\cos \nu_x) P_n(\cos \nu_y) + \\
 &+ 2 \sum_{m=1}^n ((n-m)!/(n+m)!) (\cos m\lambda_x \cos m\lambda_y + \\
 &+ \sin m\lambda_x \sin m\lambda_y) P_{nm}(\cos \nu_x) P_{nm}(\cos \nu_y) ,
 \end{aligned}$$

cf. (Hobson, 1952, p. 140) where $P_{nm}(\cos \nu)$ is called the associated Legendre function of degree n and order m . Naturally $P_{n0} = P_n$. Since

$$(6.23) \quad J_n = 4\pi / (2n+1) ,$$

$$(6.24) \quad C_{nm} = S_{nm} = 2\pi (n+m)! / ((2n+1)(n-m)!) ,$$

see (Smirnov, 1958, sec. 131), we obtain

$$(6.25) \quad A_{002} = 3(4\pi)^2 \sum_{n=1}^{\infty} (2n+1)^{-2} Q_n .$$

Approaching now the estimate for A_{01} , we get, in view of (4.16),

$$\begin{aligned}
 (6.26) \quad A_{01} &= \sum_{i=1}^3 c_i^2 \left(\int_{\Omega} x_i^2 |x|^{-6} dx \right)^2 = \\
 &= (4\pi/3)^2 (R^{-1} - R_e^{-1})^2 |c|^2
 \end{aligned}$$

where

$$(6.27) \quad |c|^2 = c_1^2 + c_2^2 + c_3^2 .$$

For A_{02} (4.11) similarly yields

$$\begin{aligned}
 (6.28) \quad A_{02} &= R^{-2} \sum_{n=2}^{\infty} (n+2)^2 (n-1)^{-2} R_n^2 (J_n^2 + \\
 &+ 4 \sum_{m=1}^n ((n-m)!/(n+m)!)^2 (G_{nm}^2 + S_{nm}^2))
 \end{aligned}$$

with

$$(6.29) \quad R_{\Omega} = \int_R^{R_e} (R/r)^{2n+2} r^2 dr = \\ = R^3(2n-1)^{-1}(1 - (R/R_e)^{2n-1}) .$$

Thus

$$(6.30) \quad A_{02} = 3(4\pi)^2 R^4 \sum_{n=2}^{\infty} N^2(n)(1 - (R/R_e)^{2n-1})^2$$

where

$$(6.31) \quad N(n) = (n+2)/(n-1)(2n-1)(2n+1) .$$

Quantitatively, $N^2(2) < 0.0712$, $N^2(3) < 0.0052$, $N^2(4) < 0.0011$, etc.

Combining now (6.9) - (6.12), (6.15), (6.18), (6.25), (6.26) and (6.30), we obtain

$$(6.32) \quad A_0 \leq (4\pi R^2)^2 C_0 \|g\|_2^2$$

with

$$(6.33) \quad C_0 = (1 + \varepsilon_1 + \varepsilon_2)((11/6)(1 - (28/11)q + \\ + (24/11)q^2 - (8/11)q^3 + (1/11)q^4) + \\ + (3/2) \sum_{n=1}^{\infty} (2n-1)^{-1}(2n+1)^{-2}((2n-1)(2n+3)^{-1}q^4 + \\ + 4(2n+3)^{-1}(1/q)^{2n-1} - 1)) + \\ + (1 + 1/\varepsilon_1 + \varepsilon_3)(1 - (1/q))^2(c/3R)^2 + \\ + (1 + 1/\varepsilon_2 + 1/\varepsilon_3) 3 \sum_{n=2}^{\infty} N^2(n)(1 - (1/q)^{2n-1})^2$$

and

$$(6.34) \quad q = R_e/R .$$

In the next step we have to estimate A_1 given by (6.3). Using Green's identity, we get

$$(6.35) \quad \int_{\Omega} |\text{grad } u|^2 dx \leq \int_{|\mathbf{x}| > R} |\text{grad } u|^2 dx = \\ = - \int_{|\mathbf{x}|=R} (\partial u / \partial |\mathbf{x}|) u dS - \int_{|\mathbf{x}| > R} u \Delta u dx .$$

However, u is a solution of (5.1) - (5.2) which yields

$$(6.36) \quad \int_{\Omega} |\text{grad } u|^2 dx \leq (2/R) \int_{|\mathbf{x}|=R} u^2 dS - \int_{\Omega} u g dx \leq \\ \leq (2/R) \int_{|\mathbf{x}|=R} u^2 dS + (\eta/2) \int_{\Omega} u^2 dx + \\ + (1/2\eta) \int_{\Omega} g^2 dx$$

where we have used the well known inequality

$$(6.37) \quad ab \leq \eta a^2/2 + b^2/2\eta, \quad \eta > 0 .$$

Since

$$(6.38) \quad \int_{\Omega} u^2 dx \leq C_0 R^4 \|g\|_2^2 ,$$

according to (6.2) and (6.32), it remains to make an estimate of only the first term on the right hand side of (6.36). For this purpose we, first, put

$$(6.39) \quad z(\mathbf{x}) = z(|\mathbf{x}|) = 1 - (|\mathbf{x}| - R)/(R_e - R) ,$$

$R \leq |\mathbf{x}| \leq R_e$. Then

$$(6.40) \quad \int_{|\mathbf{x}|=R} u^2 dS = -R^2 \int_{\Omega} |\mathbf{x}|^{-2} (\partial z / \partial |\mathbf{x}|) u^2 dx - \\ - R^2 \int_{\Omega} |\mathbf{x}|^{-2} z(\mathbf{x}) (\partial u^2 / \partial |\mathbf{x}|) dx \leq$$

$$\begin{aligned} &\leq (R_e - R)^{-1} \int_{\Omega} u^2 \, dx + 2 \int_{\Omega} |u(\mathbf{x}) \partial u / \partial |\mathbf{x}| | \, dx \leq \\ &\leq (R_e - R)^{-1} \int_{\Omega} u^2 \, dx + \eta_1 \int_{\Omega} u^2 \, dx + \\ &+ (1/\eta_1) \int_{\Omega} |\text{grad } u|^2 \, dx \end{aligned}$$

where we have used again the inequality (6.37) with $\eta_1 > 0$ instead of η . The last result inserted in (6.36) yields

$$\begin{aligned} (6.41) \quad &(1 - 2/\eta_1 R) \int_{\Omega} |\text{grad } u|^2 \, dx \leq \\ &\leq (2R^{-1}(R_e - R)^{-1} + 2\eta_1 R^{-1} + \eta/2) \int_{\Omega} u^2 \, dx + \\ &+ (1/2\eta) \int_{\Omega} g^2 \, dx \end{aligned}$$

for

$$(6.42) \quad \eta_1 > 2/R.$$

Returning now to A_1 and combining (6.3), (6.38) and (6.41), we finally get

$$(6.43) \quad A_1 \leq (4\pi R^2)^2 C_1 \|g\|_2^2$$

with

$$(6.44) \quad C_1 = (C_0(2R(R_e - R)^{-1} + 2\eta_1 R + R^2 \eta/2) + R^{-2}/2\eta)/(1 - 2/\eta_1 R)$$

and C_0 given by (6.33).

It remains to estimate the term A_2 given by (6.4). However, we will confine ourselves to the qualitative estimate (5.8) which involves the use of the Calderon-Zygmund inequality. Accordingly,

$$(6.45) \quad A_2 \leq (4\pi R^2)^2 C_2 \|g\|_2^2$$

with C_2 which generally depends on R , R_e and $|c|$, i.e.

$$(6.46) \quad C_2 = C_2(R, R_e, |c|).$$

Conclusively, the desired estimate (6.6) results now from (6.32), (6.43) and (6.45). Hence

$$(6.47) \quad \|u\|_{2,2} \leq R^2 M^{1/2} \|g\|_2$$

where

$$(6.48) \quad M = M(R, R_e, |c|, \varepsilon_1, \eta, \eta_1) = C_0 + C_1 + C_2.$$

7. Iterative process

Resuming now the original purpose of this paper, we have to find a solution u of equation (2.17) under the boundary condition (3.5a). For this purpose we use the Green-Stokes representation formula (4.19) which, putting

$$(7.1) \quad f = -(1 + h/R) \Delta g$$

and

$$(7.2) \quad g = A \partial u / \partial r + B \partial^2 u / \partial r^2 + C \partial^2 u / r \partial r \partial \vartheta + D \partial^2 u / r \sin \vartheta \partial r \partial \lambda$$

with

$$(7.3) \quad A = B = C = D = 0 \quad \text{for } r \geq R_e,$$

in view of (2.20), changes into an integro-differential equation for u . Our aim is to solve it iteratively. (For simplicity reasons we are omitting here the bar-sign above

the coordinates r, ϑ, λ .)

Using again the inequality (6.37), with $\eta = 1$, we get

$$\begin{aligned}
 (7.4) \quad \|g\|_2^2 &\leq 4(\|A \partial u / \partial r\|_2^2 + \|B \partial^2 u / \partial r^2\|_2^2 + \\
 &+ \|C \partial^2 u / r \partial r \partial \vartheta\|_2^2 + \|D \partial^2 u / r \sin \vartheta \partial r \partial \lambda\|_2^2) \leq \\
 &\leq 4R^{-4}(\sup_{\Omega} |RA|)^2 (R \|\partial u / \partial r\|_2)^2 + \\
 &+ \sup_{\Omega} B^2 (R^2 \|\partial^2 u / \partial r^2\|_2)^2 + \\
 &+ \sup_{\Omega} C^2 (R^2 \|\partial^2 u / r \partial r \partial \vartheta\|_2)^2 + \\
 &+ \sup_{\Omega} D^2 (R^2 \|\partial^2 u / r \sin \vartheta \partial r \partial \lambda\|_2)^2 .
 \end{aligned}$$

Thus

$$(7.5) \quad \|g\|_2 \leq 2 R^{-2} L \|u\|_{2,2}$$

where

$$(7.6) \quad L = \max(\sup_{\Omega} R|A|, \sup_{\Omega} |B|, \sup_{\Omega} |C|, \sup_{\Omega} |D|) .$$

Treating now the right hand side of (4.19) with f, g given by (7.1), (7.2) as an operator defined on $W_2^{(2)}(\Omega, R)$ and denoted here by K , we can immediately deduce, under a supposition that f is a sufficiently smooth function, that K maps the Sobolev space $W_2^{(2)}(\Omega, R)$ into itself. Indeed, the second term of the right hand side of (4.19) belongs to $W_2^{(2)}(\Omega, R)$ simply due to the estimate (6.47) and (7.5). As regards the first term this is a harmonic function in the domain $|x| > R$. We will denote it by V_f for short. Due to the Green-Stokes representation formula (4.19) any function u which is harmonic for $|x| > R$ and such that its restriction to $\Omega = \{x; R \leq |x| \leq R_e\}$ belongs to $W_2^{(2)}(\Omega, R)$ may be uniquely represented (apart from the first degree

harmonic components) in terms of boundary values of the expression

$$(7.7) \quad U(x) = \partial u / \partial |x| + 2u / |x| ,$$

which for $|x| = R$ is an element of the so-called Sobolev-Slobodeckij space $W_2^{(1/2)}(|x|=R)$ with fractional derivatives. The last statement is a consequence of the fact that for functions from $W_2^{(k)}(\Omega)$, k is a positive integer, there exists a precise characterization of traces on the boundary $\partial\Omega$ of Ω in terms of functions from $W_2^{(k)}(\Omega)$ with k non-integr. E.g.:

$$(7.8) \quad U \in W_2^{(1)}(\Omega) \Leftrightarrow \text{Tr}(U) \in W_2^{(1/2)}(\partial\Omega) ,$$

see (Nečas, 1967) or (Kufner, John, Fučík, 1977). Here $\text{Tr}(U)$ means the trace of U on $\partial\Omega$. Conversely, for f (and thus also Δf) belonging to $W_2^{(1/2)}(|x|=R)$ the restriction to Ω of the harmonic function V_f is necessarily an element of $W_2^{(2)}(\Omega)$. Accordingly,

$$(7.9) \quad u \in W_2^{(2)}(\Omega, R) \Rightarrow Ku \in W_2^{(2)}(\Omega, R)$$

which is the property of K we wanted to prove. (Note that we have applied the above statements related to the characterization of traces of function from $W_2^{(2)}(\Omega)$ to the weight Sobolev space $W_2^{(2)}(\Omega, R)$, bearing in mind that $W_2^{(2)}(\Omega, R)$ and $W_2^{(2)}(\Omega) = W_2^{(2)}(\Omega, 1)$ are equipped with the equivalent norms.)

In addition, combining (6.47) and (7.5), we can simply deduce that

$$(7.10) \quad \|Ku - Kv\|_{2,2} \leq M^{1/2} L \|u - v\|_{2,2}$$

for $u, v \in W_2^{(2)}(\Omega, R)$. Thus K will have the quality of a contraction mapping from $W_2^{(2)}(\Omega, R)$ into itself if

$$(7.11) \quad M^{1/2} L < 1 .$$

Under the last condition there exists a unique solution $u \in W_2^{(2)}(\Omega, R)$ of the integro-differential equation $u = Ku$ and thus also of the problem (2.17), (3.5a) since we can apply the famous Banach fixed point theorem in the linear space $W_2^{(2)}(\Omega, R)$ which is complete, see (Lyusternik and Sobolev, 1965, p. 43). Moreover, u may be obtained by means of iterations

$$(7.12) \quad u = \lim_n u_n, \quad u_n = Ku_{n-1}$$

where $u_0 \in W_2^{(2)}(\Omega, R)$ is a starting approximation.

8. Conclusion

The preceding results contain a number of parameters. The preliminary estimates indicate that the condition (7.11) is satisfied for realistic topography and the parameter R_e great enough to have $R_e - R > h_{\max} - h_{\min}$. This is an essential prerequisite for a reasonable iterative process. Moreover, it is necessary to suppose that the constants c_i in the first degree harmonic function H_1 are sufficiently small since they are involved in the estimate for M . A natural consequence of this requirement is a need of a good starting approximation. However, the first term on the right hand side of (4.19) can be taken in quality of this approximation. It is formally identical with the famous Stokes integral. Thus the Stokes approximative solution of the simple Molodensky problem is imbedded in the sequence of approximations of our iterative process as originally desired.

References

- Brovar, V.V., Magnicky, V.A., Shimbirev, B.P. (1961): The Theory of the Figure of the Earth. Geodezizdat Publishers, Moscow, 1961 (in Russian).
- Gilbarg, D. and Trudinger, N.S. (1983): Elliptic Partial Differential Equations of Second Order. Springer-Verlag, Berlin-Heidelberg-New York-Tokyo, 1983.
- Grafarend, E. (1978): The Definition of the Telluroid. Bull. Géod. 52(1978), pp. 25-37.
- Heiskanen, W.A. and Moritz, H. (1967): Physical Geodesy. W.H. Freeman and Company, San Francisco and London, 1967.
- Hobson, E.W. (1952): The Theory of Spherical and Ellipsoidal Harmonics. Foreign Literature Publishers, Moscow, 1952 (in Russian).
- Hörmander, L (1975): The Boundary Problems of Physical Geodesy. The Royal Inst. of Technology, Division of Geodesy, Stockholm, 1975; also in: Archive for Rational Mechanics and Analysis 62(1976), pp. 1-52.
- Lyusternik, L.A. and Sobolev, V.I. (1965): Foundations of Functional Analysis. Nauka Publishers, Moscow, 1965.
- Krarup, T. (1973): Letters on Molodensky's Problem I. Unpublished manuscript communicated to the members of IAG spec. study group 4.31.
- Kufner, A., John, O., Fučík, S. (1977): Function Spaces. Academia, Prague, 1977.
- Marych, M.I. (1973): On the Solution of Molodensky's Problem by Means of Taylor's Series. Geodesy, Cartography and Aerophotography, vol. 17, Lvov, 1973, pp. 26-33 (in Russian).
- Moritz, H. (1973): On the Convergence of Molodensky's Series. Anno XXXII - Boll. di Geod. e Sci. Affini - N. 3, 1973, pp. 125-144.
- Moritz, H. (1980): Advanced Physical Geodesy. H. Wichmann Verlag Karlsruhe and Abacus Press Tunbridge Wells Kent, 1980; also in Russian by Nedra Publishers, Moscow, 1983.
- Nečas, J. (1967): Les méthodes directes en théorie des équations elliptiques. Academia, Prague, 1967.
- Shimbirev, B.P. (1975): The Theory of the Figure of the Earth. Nedra Publishers, Moscow, 1975 (in Russian).
- Smirnov, V.I. (1958): Lectures in Higher Mathematics, Vol. III. Fizmatgiz Publishers, Moscow, 1958 (in Russian).
- Pellinen, L.P. (1974): On the Identity of Various Solutions of the Molodensky's Problem. Izv. vuzov, Geod. i aerofotosyomka, 3(1974), pp. 65-71 (in Russian).

THE IRREGULARITY IN THE EARTH'S ANNUAL ROTATION AS
A CAUSE OF SYSTEMATIC TIME VARIATION

I. B. Ivanov

The Higher Institute of Mining and Geology,
Sofia, Bulgaria

Seasonal variations in the Earth's rotational velocity ω were established in 1937 by N. Stoyko [1]. Since then, all the authors who have discussed their causes have pointed out that they are mainly causes of a meteorological character. There is a general consensus, however, that the effect of the meteorological factors, in the broadest sense of the term, although considered very important, can explain only about half of the observed values of these seasonal variations, and at that with quite a few reservations. Usually no explanation is given about the other 50% or, if given, it is based on a variety of causes, some of which run counter to the meteorological factors [2].

Here we submit an explanation precisely of the unexplained 50% of the values of these variations in the Earth's angular velocity. It is based on a transport of masses through the equatorial plane established by us [3].

The angular moment of a rotational body is given by the expression

$$(1) \quad M = C \omega$$

where C is the body's inert moment vs the axis of this rotation. If the body is isolated, i.e. not subject to external effects, this moment is constant.

As is known, if a rotational body has an equatorial plane, i.e. a plane perpendicular to its rotation, in relation to which plane the body is symmetric, when this symmetry is violated, then its inert moment C increases. In our epoch, according to [4], theoretically about July 2nd, i.e. summer in the northern hemisphere, the Earth is closest in shape to the rotational ellipsoid with which it approximates, and about January 2nd its shape deviates most from this ellipsoid. As Kozai [5] established from observation, these two dates deviate in reality from the theoretical ones by about 20 days by retarding, as is natural to expect because of the Earth's rheological properties. It follows then that the Earth's inert moment C , when considered as a rotational body, is smallest about July 20th and biggest about January 20th.

In all the investigations of the Earth's angular velocity, its angular moment M is assumed to be constant. From (1) we have

$$(2) \quad M = C \omega = \text{const}$$

and consequently, when taking into consideration the above about seasonal variations in the Earth's inert moment C , it follows

from (2) that its angular velocity ω should be biggest about July 20th and smallest about January 20th.

Thus, theoretically, proceeding from the result obtained in [4] one reaches the conclusion which Stoyko established with the observings. At that, this conclusion is obtained only from changes caused by factors which refer to the body of the Earth.

Bearing in mind the above about the discussions following Stoyko's finding about the causes of seasonal variations in the Earth's rotational velocity which, as all authors stressed, are meteorological in character, i.e. external to the Earth's body, it naturally follows that the unexplained 50% in the change in value of the seasonal variations in the Earth's angular velocity ω are due to causes within the Earth. In the light of this deduction, the doubt may be expressed that meteorological phenomena are responsible for 50% of the magnitude of these variations.

Comments. 1) On the basis of 7-year observations of the Earth's rotational velocity, Belocerkovsky [6] added trimestrial variations in the Earth's angular velocity ω to the annual and semestrial known until then, nothing that they "apparently are due to meteorological phenomena". Moreover, an exact coincidence of the phases can not be expected, because "meteorological phenomena recur but not at the same time". If the diagrams adduced in Belocerkovsky's article are examined, it can be seen that the extrema in the change of the Earth's rotational velocity ω in one year are about four typical points around the Earth's orbit: perihelion, aphelion, vernal and autumnal equinox. The results obtained refer to 17 stations on Soviet soil.

Let us analyze the third formula about T_{LZ} from [3]:

$$(3) \quad \begin{aligned} T_{LX} &= -g M_{\odot} \left[\frac{1}{\rho_L^2} \cos(\delta_L - \delta_E) - \frac{1}{\tau_E^2} \right] \sin \alpha, \\ T_{LY} &= -g M_{\odot} \left[\frac{1}{\rho_L^2} \cos(\delta_L - \delta_E) - \frac{1}{\tau_E^2} \right] \cos \alpha \cos \varepsilon - \\ &\quad - \frac{g M_{\odot}}{\rho_L^2} \sin(\delta_L - \delta_E) \sin \varepsilon, \\ T_{LZ} &= -g M_{\odot} \left[\frac{1}{\rho_L^2} \cos(\delta_L - \delta_E) - \frac{1}{\tau_E^2} \right] \cos \alpha \sin \varepsilon - \\ &\quad - \frac{g M_{\odot}}{\rho_L^2} \sin(\delta_L - \delta_E) \cos \varepsilon. \end{aligned}$$

$(\alpha = (2\pi + \frac{\pi}{13000})t)$, t is recorded in parts of the year (days) for a presentation of the algebraic projections of the Sun's tide-forming force \vec{T} on the Earth in one geocentric equatorial coordinate system (see Fig.). This projection is responsible for the seasonal transport of masses in the direction of the Earth's rotational axis, i.e. perpendicular to the Earth's equatorial plane, and it changes its sign in the perihelion and the aphelion, being annulled in the points of the vernal and autumnal equinox.

OCEAN TIDAL LOADING ALONG THE
"BLUE ROAD GEOTRAVERSE" IN FENNOSCANDIA

by

Gerhard Jentzsch *

The 29-year observations on the Earth's rotational velocity of the U.S. Naval observatory station, elaborated by Mihailov [7], confirmed the existence of trimestrial variations for the Washington station as well. It should be added, though, that the trimestrial variations for this station are much smaller than the corresponding ones in Belocerkovsky's diagrams.

2) For the station in Washington the maximum of ω is in May and the minimum in October. This is obviously connected with meteorological factors but the movement of the North American plate probably interferes as well. Supplementary investigations are called for.

Description of the magnitudes participating in the formulas(3) and figure: G - gravitational constant, M_s - solar mass, $Z_E = |SE|$ - distance between points S and E, $\delta_L = |SL|$ - distance between points S and L, δ_L, δ_E - declinations of points L and E, ξ - angle of precession $\approx 23^\circ 27'$, α - angle connected linearly with the true anomaly ν . The last one is supposed, for the sake of convenience, to change uniformly in the course of a year, i.e. $\nu = 2\pi t$, where t is recorded in days (parts of a year).

Acknowledgements are due to Dr.G.M.R.Winkler, Director of Time Service Division, U.S. Naval Observatory in Washington, for kindly supplying the 23-year observation data.

R E F E R E N C E S

- 1 . STOYKO,N. Sur la périodicité dans l'irrégularité de la rotation de la terre.-C o m p t. Rend.Sciences Acad.Sci., 205,79 (1937).
- 2 . MUNC,W.H., Mac Donald G.J.F. The Rotation of the Earth.- Cambridge University Press, 1975.
- 3 . IVANOV,I.B. On Seasonal Variations in Kimura's Correction Z(t).-C o m p t.Rend.Acad.Bulg.Sci.,t.33, No 6, 1980.
- 4 . IVANOV,I.B. Periodic Variations in Coefficients I_n ($n = 2$) of Geopotential Development.-I b i d e m, t.32, No 6,1979.
- 5 . KOZAI,Y. Seasonal Variations of Geopotential Inherred from Satellite Observation.-S A O Special Report No 312, Cambridge, Massachusetts, April 2, 1970.
- 6 . БЕЛОЦЕРКОВСКИЙ,А.Ю. Короткопериодическая неравномерность вращения Земли, сб. Вращение Земли,изд.АНУССР,Киев,1963.
- 7 . МИХАЙЛОВ,П.И. Извещдана на неравномерността в ротацията на Земята от разлики TU_2-TU_1 за периода 1956-1979 година. Дипломна работа,Висш институт по архитектура и строителство, Геодезически факултет,1982 год.

Summary

Some results from gravity tidal measurements along the Fennoscandian "Blue Road Geotraverse" are presented here. The residual vectors for constituents O1 and M2 are compared to ocean tidal loading, calculated for modified Schwiderski maps. The coherence of the results for O1 shows the sufficient intercalibration of the different gravimeters. The results for M2 indicate, that an improvement of the models for the spatial distribution of the marine tide of the Norwegian shelf has to be applied to fit the observed residuals near the coast. Data acquisition of the gravimeters, calibration, and data analysis are shortly discussed.

Zusammenfassung

Einige Ergebnisse der gravimetrischen Gezeitenmessungen entlang der Geotraverse "Blaue Straße" in Fennoskandien werden vorgestellt und die Residualvektoren für die Partialtiden O1 und M2 mit den berechneten Auflastwirkungen für ein modifiziertes Meereszeitenmodell von Schwiderski verglichen. Die Übereinstimmung der Ergebnisse der O1-Residuen zeigt die Güte der Eichung der beteiligten Gravimeter. Die Ergebnisse für M2 lassen erkennen, daß eine Verbesserung des Meereszeitenmodells für den Bereich des norwegischen Schelfs nötig ist, um eine Übereinstimmung der berechneten mit der beobachteten Auflastwirkung zu erzielen. Weiterhin werden die Datenerfassung, die Kalibrierung und die Analyse kurz diskutiert.

1. Introduction

Between spring 1980 and autumn 1983 tidal gravity measurements were carried out at seven sites in Norway, Sweden, and Finland along the "Blue Road Geotraverse", which starts near the polar circle at the Norwegian coast and leads nearly south - east through

* Institut für Geophysikalische Wissenschaften der Freien Universität Berlin, Rheinbabenallee 49, 1000 Berlin 33

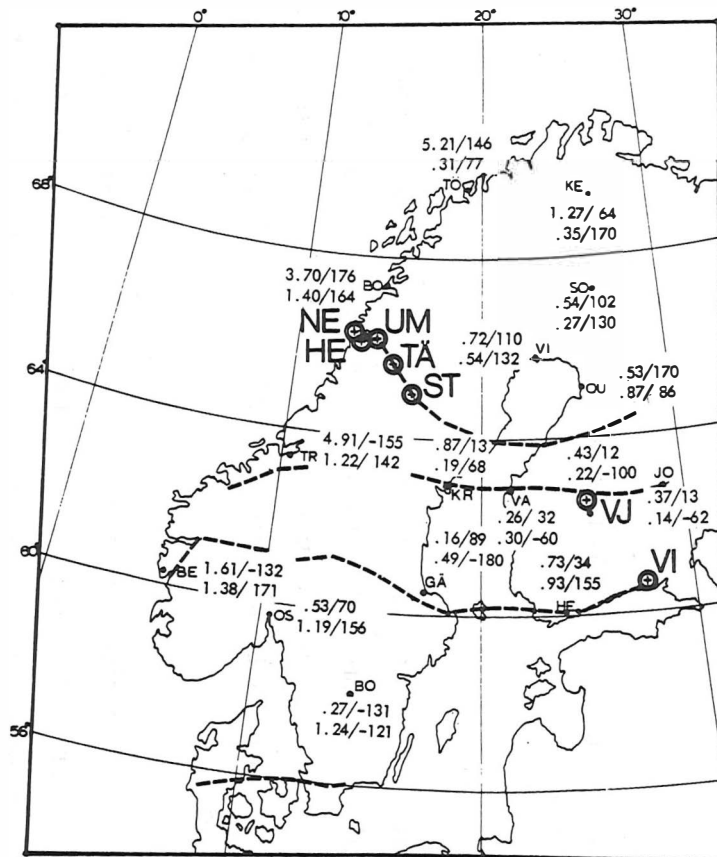


Fig. 1: Tidal residuals already obtained in Fennoscandia in micro-gals and degrees for M2 (upper) and O1 (lower), from Ducarme and Kääriäinen (1980); the dashed lines show the "land-uplift-lines" for repeated precise gravity surveys; the circles denote the tidal gravity stations along the Blue Road: NE - Nesna, HE - Hennesberget, UM - Umbukta, TÄ - Tärnaby, ST - Storuman, VJ - Vaajakoski, VI - Virojoki.

Sweden and Finland (see fig. 1). The recording periods varied between ten months and about two years (see tab. 1). The five instruments used were calibrated by parallel recordings at the Berlin Tidal Observatory.

The aim of these measurements can be summarized as follows (Jentzsch, 1983a):

- 1) Determination of realistic tidal parameters along this line for the correction of precise gravity surveys in addition to the measurements which have already been carried out (Ducarme and Kääriäinen, 1980);
- 2) Study of the interaction of ocean tidal loading and the structure of the lithosphere in that area;
- 3) Development of an ocean tidal model of the shelf esp. for the constituent M2 in order to augment the respective global model of Schwiderski (1979).

Tab. 1: Stations, instruments, and recording periods

Station	Instrument	Period
NESNA	GS - 15/206	April 1980 - March 1981
HEMNESBERGET	GS - 15/206	August 1982 - October 1983
UMBUKTA	LCR - ET 18	April 1980 - August 1981
TÄRNABY	LCR - ET 18	August 1981 - April 1983
STORUMAN	GS - 11 / BN 06	August 1981 - October 1983
VAAJAKOSKI	GS - 15/210	April 1981 - July 1982
VIROJOKI	GS - 11 / BN 20	August 1982 - October 1983

2. Experimental problems and realization of the measurements

In this project five tidal gravimeters were used, provided by different institutes (see tab. 1). These gravimeters were inter-compared by recording at the Berlin Tidal Observatory (int. nr. 0750) before and after the measurements on the profile. The LCR-ET meter served as a reference.

Only the ET 18 was already provided with analog and digital recording equipment; therefore the four Askaniacs could be equipped with equal data acquisition systems. In order to apply the measuring station to the field conditions along the profile new power supply units were developed including a power failure protection, and a buffer circuit to attach and to recharge a storage battery. 61

The components of the station are given in fig. 2: Directly to the gravimeter output a preamplifier is attached for pre-filtering and adjustment of impedance to recording equipment. The digital recording system is based on a Datel cassette recorder. After a suitable alias-filtering and amplification the signal is sampled with a rate of 30 sec, converted into 12 bit samples, and stored on the tape cassette. A monitor output provided with an hourly time mark is connected to a chart recorder.

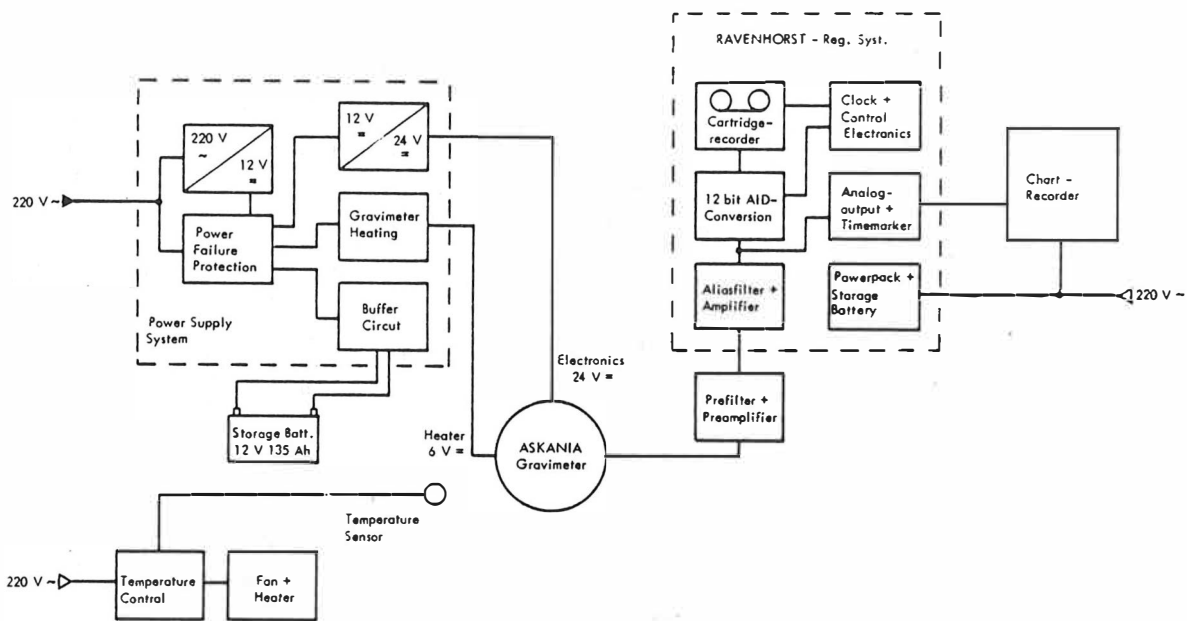


Fig. 2: Station components of the tidal gravimeter station (from Asch, 1983)

Further, the measuring stations consisted of an insulated and temperature stabilized gravimeter room (constant near 30°C). Whenever possible this room was built up in a cellar space which was also temperature controlled to provide a fairly stable temperature gradient, too.

The LCR - ET 18 was also provided with a buffer battery, but according to the necessary adaption to the European system the applied conversion of voltages caused energy loss due to waste heat which could not be buffered over a longer period. The feedback signal of the ET 18 was decoded by an angular decoder and converted into a 14 bit data word. The resolution of the digital records is

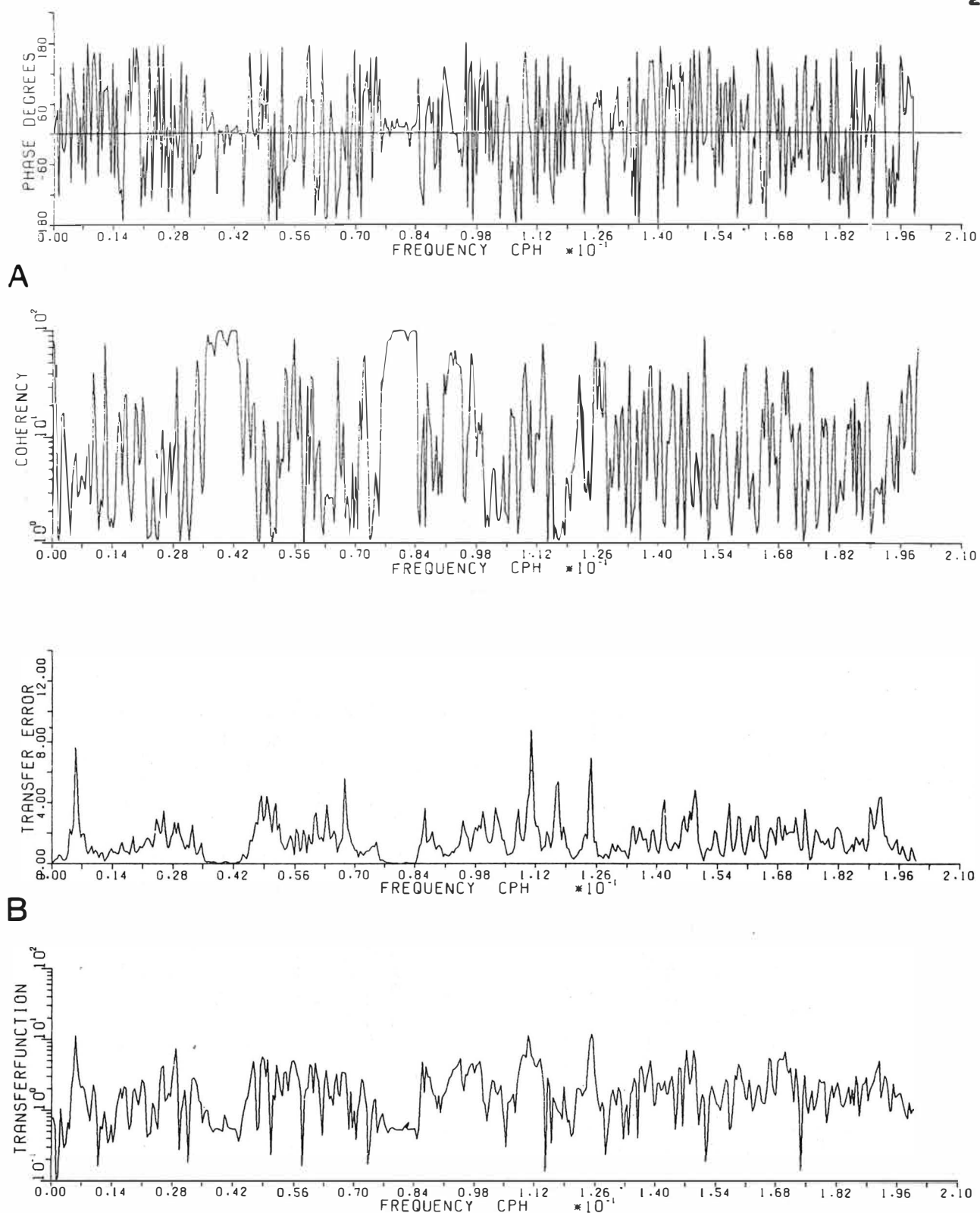


Fig. 3: Coherence (in percent), and phase difference (A), transfer function, and transfer error (B) between the gravimeters ET 18 and GS - 15/206 at the Berlin Tidal Observatory (from Jahr, 1984)

about 0.1 μ gal; in the case of the ET 18 a dynamic range of 84 dB is achieved, and 72 dB in the case of the Askanias. For more details see Asch (1983).

Although special efforts concerning stable recording conditions were applied, esp. with regard to stable temperatures and power failure, several gaps were introduced into the records. These gaps were caused not only by failures of electronic circuits, but also by mechanical problems of the chart recorders. Later, when reading the cassettes, errors occurred due to the insufficient data security of the incremental recording. The stations were maintained by local people, who were very helpful, but only trained to do some proper manipulations. Regarding the stations being far away, and nearly unreachable during winter within acceptable time, we got better data than expected. Only two stations out of seven (Storuman and Virojoki) caused difficulties; but here maintenance problems also met instrumental problems. Therefore the analysis of these records is not yet finished.

3. Calibration

Since the ET 18 as the most sensitive instrument was calibrated very carefully before, it was used as a reference. With this instrument the tidal parameters of our Berlin Tidal Observatory were determined. There, all Askanias have recorded for at least half a year. In the case of the GS - 15/206 a parallel record with the ET 18 could be realized, and thus not only tidal amplitudes and phases could be compared, but also transfer function and coherence could be calculated. Fig. 3 gives the coherence and the phase differences as well as the transfer function and transfer error. In fig. 4 sections of the continuous transfer function are compared to the ratios of the individual tidal amplitudes. The errors are small; esp. for the main tidal waves they are better than 0.5%, reaching nearly the 0.1% level. This provides calibration errors in the order of 0.1 μ gal and less for the amplitude, and less than 0.2° for the phase.

Due to the different drift properties of the two gravimeters (the ET 18 nearly without any linear drift), outside the tidal bands the

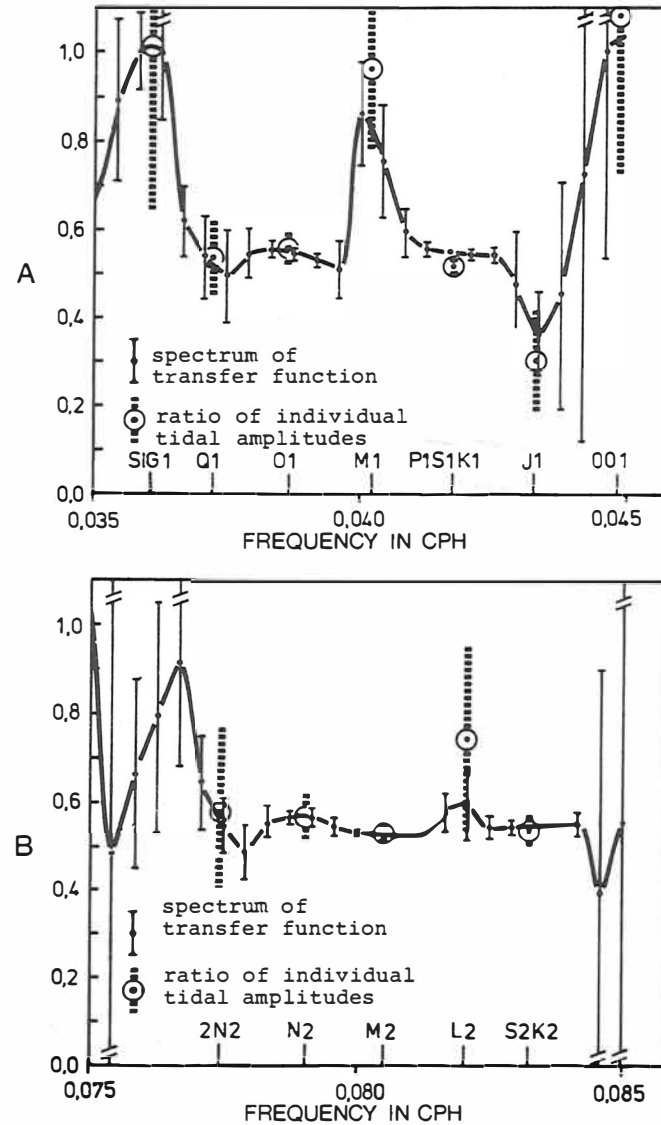


Fig. 4: Diurnal (A) and semidiurnal (B) sections of the continuous transfer function compared to the ratios of the individual tidal amplitudes; error bars are given for both (from Jahr, 1984)

coherence of the spectra is small, and even the minor tidal constituents show significant deviations from the smooth transfer function expected within the tidal bands.

4. Results of the measurements and tidal residuals

Many efforts had to be applied in data preparation, filtering, and analysis. Both the continuously and the digitally recorded data were processed. Special attention was paid to the elimination of disturbances, the separation of the drift, and the interpolation of small gaps. Algorithms had to be developed and adapted to the properties of the individual time series. The drift was removed using physical models as well as spline - functions in order to increase the signal-to-noise ratio, and to minimize filter problems. The analysis was performed using a modified least squares method. The errors calculated are referred to the Fourier spectrum of the residuals. More details are given by Plag and Jahr (1983).

The results for the constituents O1 and M2 are summarized in tab. 2. With A_0 as observed amplitude, and the gravimetric factor δ_0 the expected body tidal amplitude A_b is assuming $\delta = 1.160$:

$$(1) \quad A_b = \delta / \delta_0 A_0$$

The phase denotes the difference

$$(2) \quad \alpha = \alpha_0 - \alpha_b$$

usually used. Thus, referring to the Greenwich meridian, a negative phase means Greenwich phase lag, and a positive phase a lead. The signal-to-noise ratio s/n refers to the noise level of the Fourier spectrum of the residual noise; the mean noise levels for the diurnal and the semidiurnal tidal bands are used as errors.

The residual tidal vector \vec{L}_0 with amplitude A_1 and phase λ denotes the observed loading signal, and is given by

$$(3) \quad \vec{L}_0 = \vec{O} - \vec{B}$$

where \vec{O} is the observed tidal vector from A_0 , α , and \vec{B} the vector of the expected body tide from A_b and zero phase shift.

The record of Tärnaby is of very high quality due to stable station conditions and a very keen maintenance. The preliminary results for the two stations Nesna and Umbukta, as given by Asch et al. (1983) can be improved now. Differences are due to higher state of data processing and longer time series available.

Tab. 2: Results for the constituents O1 and M2 (see text)

Station	A_0 [μ gal]	δ	α [$^\circ$]	s/n	A_b [μ gal]	A_1 [μ gal]	λ [$^\circ$]
O1							
NESNA	26.253 $\pm .133$	1.143 $\pm .005$	1.11 $\pm .16$	362	26.636	.640 $\pm .133$	127.37 ± 11.91
HEMNES- BERGET	26.265 $\pm .167$	1.145 $\pm .007$.65 $\pm .36$	157	26.621	.464 $\pm .167$	140.36 ± 20.62
UMBUKTA	26.543 $\pm .128$	1.151 $\pm .006$	1.35 $\pm .28$	207	26.683	.643 $\pm .128$	103.29 ± 11.45
TÄRNABY	26.920 $\pm .032$	1.154 $\pm .001$.68 $\pm .07$	846	27.053	.345 $\pm .032$	112.86 ± 5.25
VAAJA- KOSKI	29.577 $\pm .227$	1.154 $\pm .009$.54 $\pm .43$	132	26.728	.154 $\pm .227$	10.50 ± 84.56
M2							
NESNA	11.289 $\pm .056$.922 $\pm .005$	-2.05 $\pm .20$	368	14.203	2.960 $\pm .056$	-171.04 ± 1.08
HEMNES- BERGET	8.592 $\pm .076$.703 $\pm .006$	-4.68 $\pm .50$	113	14.182	5.662 $\pm .076$	-172.89 $\pm .77$
UMBUKTA	12.321 $\pm .079$	1.002 $\pm .006$	1.53 $\pm .37$	156	14.263	1.974 $\pm .079$	170.40 ± 2.29
TÄRNABY	13.358 $\pm .009$	1.050 $\pm .001$	1.08 $\pm .04$	1535	14.763	1.430 $\pm .009$	169.88 $\pm .35$
VAAJA- KOSKI	19.107 $\pm .105$	1.172 $\pm .007$	1.05 $\pm .32$	181	18.918	.397 $\pm .105$	62.02 ± 15.17

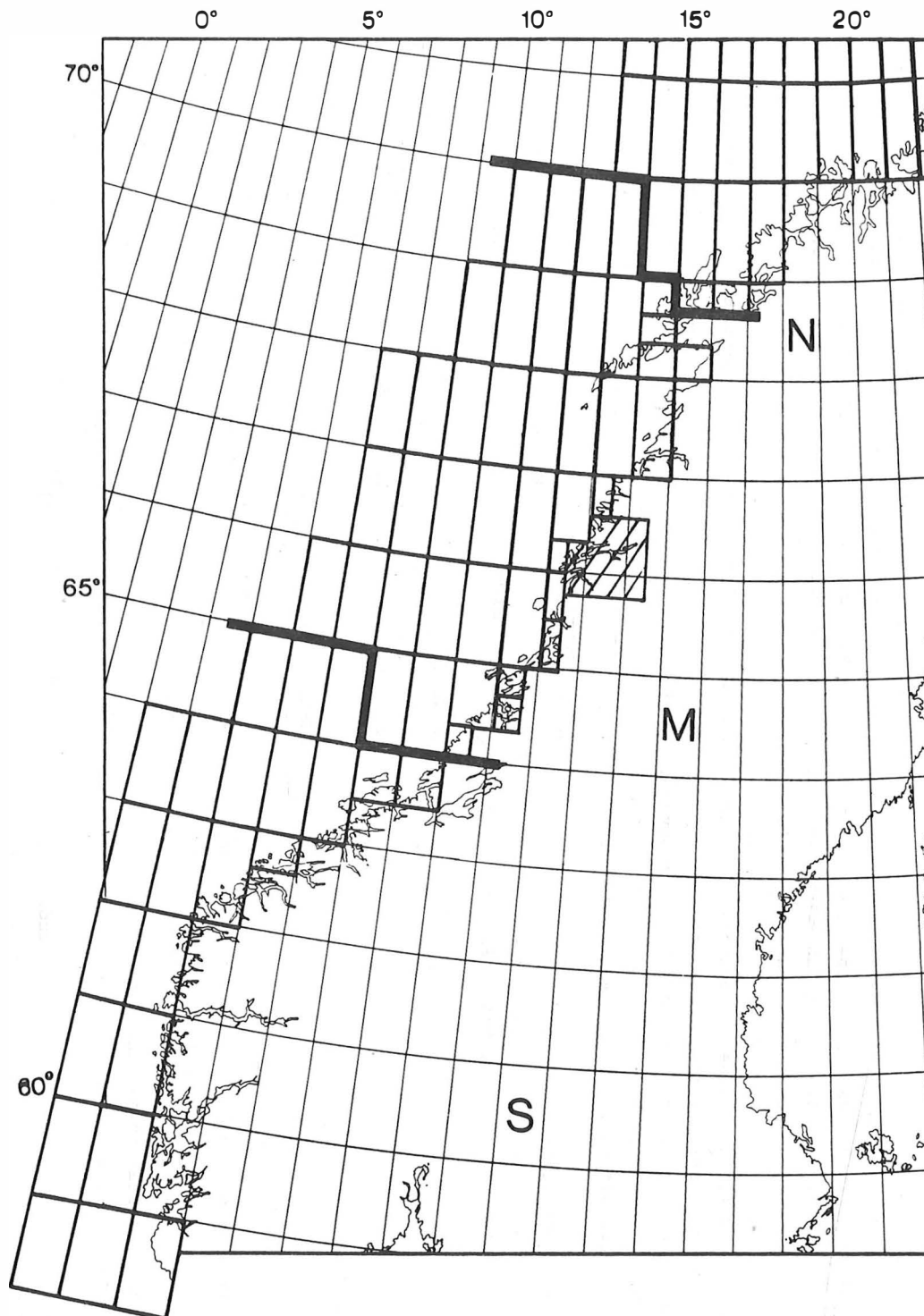


Fig. 5: The ocean cells of the shelf model separated into three parts: south, middle, and north; the Rana fjord area (hatched) is added using empirical data.

Although the stations in Norway are not far apart, their M2 residuals differ much. This is due to different station elevations, which causes varying Newtonian attraction of the marine load of the adjacent seas (see also sec. 5).

5. Ocean tidal loading and observed tidal residuals

The response of the earth to tidal loading was calculated according to Farrell (1972). The Green's function for an appropriate earth model was convolved with a model of the ocean tide distribution. The results for the "Blue Road" presented here were obtained by applying this method in a similar way as described by Baker (1980) for Britain: The theoretical gravity load, \vec{L} , at a point on the surface of the earth is given by

$$(4) \quad \vec{L}(\vec{r}) = \rho \iint_{\text{oceans}} G(|\vec{r} - \vec{r}'|) \vec{H}(\vec{r}') dA$$

where \vec{r} is the positioning vector, $\vec{H}(\vec{r}')$ is the complex amplitude of the ocean tide over a surface dA , usually approximated by a spherical disk, and ρ is the density of the sea water. $G(|\vec{r} - \vec{r}'|)$ is the Green's function describing the elastic and Newtonian attraction effects of a point mass on the surface of the earth.

Different earth models were used: the "Blue Road Crust" (BLC) as derived by Lund (1979) with a Moho depth of about 45 kilometers, a model with a rather thin crust of about 20 kilometers (C20), and a model with a Moho depth of more than 50 kilometers (C50). It turned out, that the response of the model C20 fitted best to the observations. Therefore in the following all results are referred to this model.

The algorithm used to calculate the loading vector allows to integrate over different ocean patches separately in order to determine their individual signals. Thus, the Norwegian shelf was separated into three main parts: south, middle, and north (see fig. 5). The Rana fjord area was modelled using a local distribution derived from empirical data (Plag, 1982a/b). Compared to earlier results obtained for Fennoscandia on the basis of the M2 - map of Hendershott (Jentzsch, 1983b) instead of Schwiderski's

here, it can be stated, that now more realistic values are available. Near the coast the calculated loading of both maps is similar, but the differences of the results increase with increasing distance from the coast. This seems to be due to the fact, that the Schwiderski table fits better to open ocean amplitudes. E.g. for the Indian Ocean Schwiderski gives a maximum amplitude of 47 centimeters, whereas Hendershott (1973) calculates 138 centimeters. This produces a load amplitude of nearly 1 microgal for Fennoscandia, but only 0.1 microgal in the case of Schwiderski's. Generally, comparing the results for both maps for M2 for Fennoscandia, distant oceans of Schwiderski's map provide about 10 percent of the amplitude of Hendershott's.

Figs. 6 and 7 contain the results for constituents O1 and M2 (compare to tab. 2). Wave O1 provides a test for the calibration of the different gravimeters: Since the observed amplitudes of O1 are varying between 25.9 and 29.6 microgals, the amplitude ratios to the observed M2 are varying between ~1.6 and ~3.1. Therefore, regarding the smaller amplitude of M2, the coincidence of the O1 amplitudes, parameters and loading residuals is satisfying. Thus the differences between observed and calculated M2 residuals are significant: Close to the sea the observations never fit the responses calculated with the original Schwiderski map (see fig. 7, vectors "ORIG" and "OBS"). Near the coast the different elevations of the stations are responsible for the differences of the signal: For Hemnesberget, situated in the fjord area, at sea level we calculate a load vector $A_1 = 2.62 \mu\text{gal}$, $\lambda = 173.7^\circ$; for an elevation of 40 meters these values change to $A_1 = 4.10 \mu\text{gal}$, $\lambda = 179.3^\circ$, and for the station elevation of 84 meters we get $A_1 = 6.01 \mu\text{gal}$, $\lambda = -177.6^\circ$.

Further, the calculations show, that close to the ocean the load vector is controlled by the adjacent seas. Thus, the middle section of the Norwegian shelf covers more than 60 percent of the total load. Therefore, this part was subject to change in order to test the fit of the calculated to the observed load. The phase was modified by plus and minus 20 degrees, respectively. Since the coherence is significantly improved by a shelf model incorporating a -20 degrees phase shift, this was repeated with -15 degrees. In

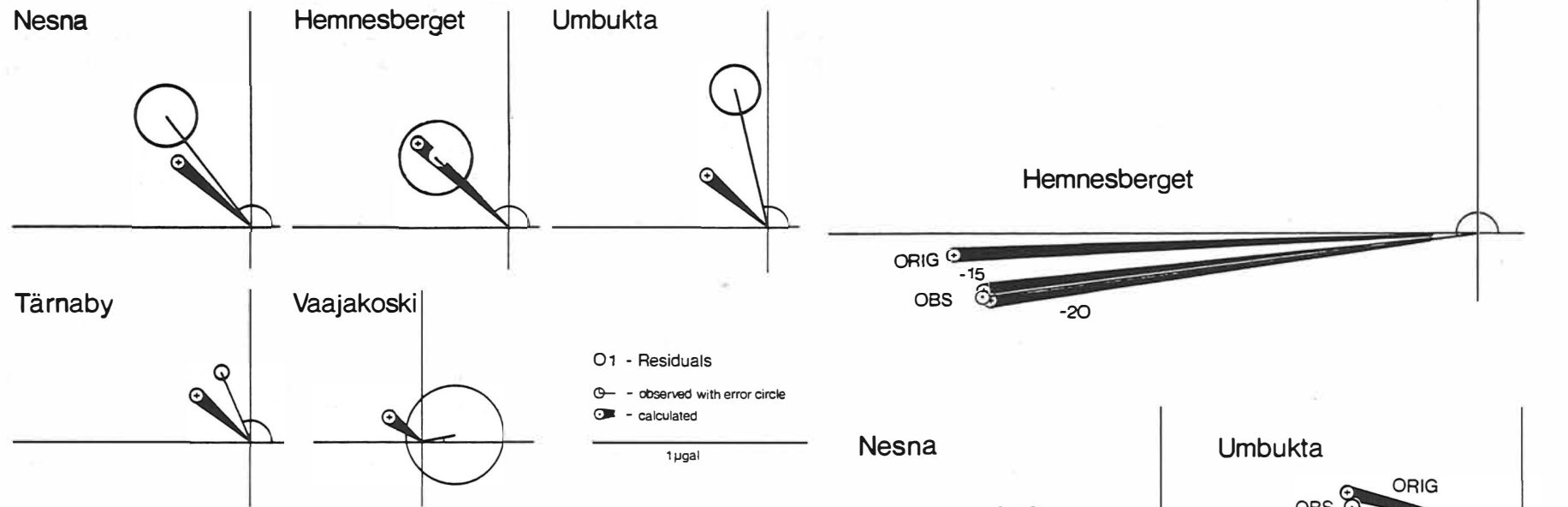


Fig. 6: Observed tidal residuals for constituent O1 compared to calculated load vectors; note different scale to fig. 7.

fig. 7 the results for "-15" and "-20" degrees are also given (see tab. 3). Compared to the numerical tidal model of the Norwegian shelf provided by Mathisen and Johansen (1982, see also Blankenburgh et.al., 1983), a significant difference arises: The phases given are smaller by about 10 degrees with respect to Schwiderski's phases in that area.

This result leads to an investigation of the residual load \vec{R} ,

$$(5) \quad \vec{R} = \vec{L}_o - \vec{L}$$

which was already carried out by Baker (1980) for the marine load around Britain, in order to improve local models for the spatial

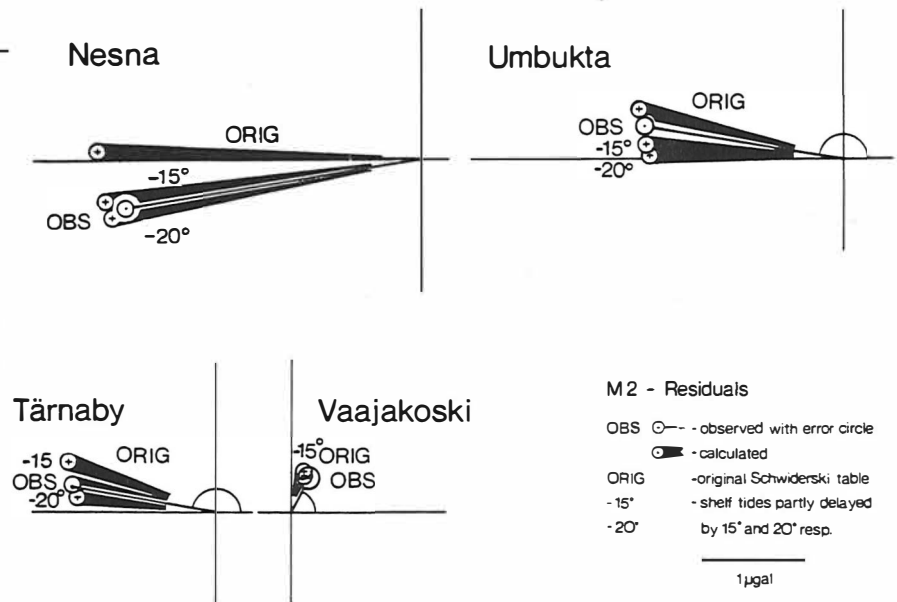


Fig. 7: Tidal residuals of constituent M2: Observed vectors compared to calculated load vectors for original and modified Schwiderski shelf tides.

Tab. 3: Theoretical load of O1 and M2 for Schwiderski's maps modified at the coast ("ORIG", see fig. 5); "-15" and "-20" denote phase shift applied to middle section of the Norwegian shelf (height corrections applied, compare to tab. 2)

Station	O1 ORIG		ORIG		M2 -15		-20	
	[μgal]	[°]	[μgal]	[°]	[μgal]	[°]	[μgal]	[°]
NESNA	.45	138.7	3.29	168.1	3.16	-172.9	3.10	-170.2
HEMNES- BERGET	.58	138.6	6.01	-177.6	5.67	-173.8	5.64	-172.4
UMBUKTA	.36	138.8	2.04	166.3	1.92	175.8	1.88	178.9
TÄRNABY	.33	139.6	1.53	160.8	1.44	170.5	1.39	173.4
VAAJA- KOSKI	.19	143.4	.43	71.4	.39	70.3	not calc.	

distribution of the marine tide. The results obtained for the "Blue Road" seem to be promising and encourage such a study using available shelf models of that area.

6. Conclusions

(1) Regarding the interaction of ocean loading and the structure of the lithosphere the responses to different crustal structures are too small to develop a detailed crust/mantle model for that area. Nevertheless, all calculations had to be referred to a crust of about 20 kilometers depth to fit the observations. A crust of greater depth (mountain root or even remnants of a downgoing slab of the crust) would provide a significant amplification of the M2 tidal residual by about 10% at sea level. The Wahr model as a reference instead of $\delta = 1.160$ provides smaller residuals, which would require a thinner crust.

Generally, this question could be answered better by tidal tilt observations. But in that area the respective interpretations would depend much more on the modelization of the ocean tidal input. Up to now it seems to be impossible to provide a model of the marine tide of the fjords which would fulfill these requirements.

(2) M2 and O1 ocean tidal charts were tested, using tidal gravimeters in that area. According to the significant phase shift

indicated, a further investigation of the response to local models of the distribution of the marine tide seems to be promising.

(3) More realistic tidal corrections for precise gravity surveys are provided by these measurements along the "Blue Road". Generally, for that purpose a standard earth is sufficient for loading corrections. But close to the fjords only tidal measurements can provide results incorporating the tidal admittance with regard to the distribution of the water masses, and the elevation of the station. Close to the sea or even to an inlet the loading signal can be amplified by factor two or three or even more, only by attraction. This is an individual property of each station. Therefore overall calculations lead to wrong values in that area. To avoid systematic errors due to loading the total tidal correction should be determined with an accuracy of one microgal or better.

7. Acknowledgements

The preparation and the performance of the measurements as well as the data analysis required the cooperation of many institutes and scientists. The support of the Finnish Geodetic Institute (FGI), the Swedish Land Survey, and the Norwegian Geographical Survey was the key to starting and to carrying out the measurements. Gravimeters were provided by the FGI (A. Kiviniemi) and different German institutes of the Universities of Bonn (M. Bonatz), Clausthal (O. Rosenbach), Kiel (J. Zschau), and the Observatory Schiltach (W. Zürn). The instruments were carefully maintained by local people with the help of our Fennoscandian colleagues. All this is gratefully acknowledged.

From our side G. Asch was mainly responsible for the experimental part of the work; Th. Jahr, H.-P. Plag, and W. Thiel did the data analysis of the time series. Together we established the measuring sites, installed the instruments, and discussed the results. I take this opportunity to thank them for their intense cooperation.

We are thankful to the German Research Society (Deutsche Forschungsgemeinschaft) for the financial support.

8. References

- Asch, G., 1983: Digital data acquisition and preprocessing of tidal data.- BIM, 89, 5742-5758.
- Asch, G., T. Jahr, G. Jentzsch, H.-P. Plag, and H. Scholz, 1983: A gravity tidal profile along the "Blue Road Geotraverse".- Proc. Ninth Int. Symp. Earth Tides, 585-592, Schweitzerbart'sche Verlagsbuchhandlung, Stuttgart.

- Baker, T. F., 1980: Tidal gravity in Britain: tidal loading and the spatial distribution of the marine tide.- Geophys. J. R. astr. Soc., 62, 249-267.
- Blankenburgh, J. C., B. A. Fossum, and J. P. Mathisen, 1983: Project proposal: Sea level prediction and co-tidal charts.- IKU, Trondheim.
- Ducarme, B., and J. Kääriäinen, 1980: The Finnish tidal gravity registrations in Fennoscandia.- Publ. of the Finish Geodetic Institute, No. 90.
- Farrell, W. E., 1972: Deformation of the earth by surface loads.- Rev. Geophys. Space Physics, 10(3), 761-797.
- Hendershott, M. C., 1973: Ocean tides.- Trans. Am. Geophys. Un., 54, 76-86.
- Jahr, T., 1984: Kalibrierung und Vergleich von Erdzeitengravimetern als Vorbereitung zur Auswertung der Gezeitenregistrierungen entlang des Profils "Blaue Straße" in Skandinavien.- Diploma Thesis, Institut für Geophysikalische Wissenschaften der Freien Universität Berlin (unpublished).
- Jentzsch, G., 1983a: A gravity tidal profile along the "Blue Road Geotraverse" - aims of research and present state of the project.- BIM, 89, 5737-5741.
- Jentzsch, G., 1983b: Ocean loading in Fennoscandia.- Proc. Ninth Int. Symp. Earth Tides, 723-30, Schweitzerbart'sche Verlagsbuchhandlung, Stuttgart.
- Lund, C.-E., 1979: Crustal structure along the Blue Road in northern Scandinavia.- Geol. Förr. Stockh. Förrh. (GFF), 101(3), 191-204.
- Mathisen, J. P., and Ö. Johansen, 1982: A numerical tidal and storm surge model for the North Sea.- Marine Geodesy, 6(3&4), 267-291.
- Plag, H.-P., 1982a: Analysen von Pegelstandsregistrierungen entlang der norwegischen Küste - Entwicklung und Anwendung eines Programmsystems sowie Ergänzungsmessungen im Bereich des Rana Fjordes.- Diploma Thesis, Institut für Geophysikalische Wissenschaften der Freien Universität Berlin (unpublished).
- Plag, H.-P., 1982b: Analysis of tidal data from the Norwegian coast.- IKU report P-203/1/82, Trondheim.
- Plag, H.-P., and T. Jahr, 1983: On processing of earth tidal data.- BIM, 89, 5759-5786.
- Schwiderski, E. W., 1979: Global ocean tides, part II: The semidiurnal principal lunar tide (M2), tlas of tidal charts and maps.- NSWC, Dahlgren.

On the influence of coupling torques between the Earth's core and mantle on parameters and components of the rotation of the Earth

by

H. Jochmann

Akademie der Wissenschaften der DDR
Zentralinstitut für Physik der Erde
DDR-1500 Potsdam, Telegrafenberg A 17

Summary

The physical reliability of correlations between magnetic field quantities and components and parameters of the Earth's rotation was investigated. It was found that only the correlations between variations of the magnetic field intensities and of the length of day are physically significant, while the correlations between the magnetic field and parameters of the CHANDLER-wobble are dubious.

Zusammenfassung

Die physikalische Realität von Korrelationen zwischen magnetischen Feldgrößen und Komponenten und Parametern der Erdrotation wurde untersucht. Es wurde festgestellt, daß nur Korrelationen zwischen den Variationen des magnetischen Feldes und der Tageslänge signifikant sind, während die Korrelationen zwischen dem magnetischen Feld und den Parametern der CHANDLER-Welle angezweifelt werden müssen.

Since MUNK and REVELLE (1952) proved that the decade fluctuations of the Earth's rotation are not excited by geophysical surface-phenomena, it is usual to look at the core for the excitation of that phenomenon.

The only indications of variations in the core or at the core-mantle boundary are variations of the magnetic field and indeed, as we see by Fig. 1, exist fairly good correlations between the magnetic field intensity and the components and parameters of the Earth's rotation.

The first curve shows the variation of the total intensity of the magnetic field at Niemegk, after a linear trend is being removed. Further in the figure the variations of the length of day and of the amplitude and period of the CHANDLER-wobble are exhibited.

It could be objected that we have compared global phenomena with a local variation of the magnetic field, but it should be mentioned that there exist similar trends of the magnetic field variations at all magnetic observatories, only the amplitudes are different as it should be. Relations between magnetic field variations and variations of the Earth's rotation are produced by coupling torques between the core and the mantle.

As generally assumed and sufficiently proved the geomagnetic field is maintained by a dynamo process taking place in the liquid core. Temporal variations of this process cause similar variations of the magnetic field and coupling parameters. The magnetic fields and currents of this process react with the conducting part of the lower mantle and produce LORENTZ-forces which are the reason for torques

$$L = \int_V (\vec{r} \times (\vec{j} \times B)) dV \quad (1)$$

exciting variations of the rotation of the Earth.

Before considering the evaluation of this integral from magnetic field quantities we shall evaluate the amount of the torque necessary to excite the observed variations of the length of day. From the Eulerian equations emerges the relation between the relativ length of day (u_3) and the exciting component of the torque

$$L_3 = C \omega_0 \frac{du_3}{dt} \quad (2)$$

where C is the axial moment of inertia and ω_0 the velocity of rotation. For decade fluctuations a mean value

$$|L_3| \approx 10^{17} \text{ Nm} \quad \text{and a maximum value} \quad |L_3| \approx 10^{18} \text{ Nm}$$

were obtained.

To evaluate these values from the geomagnetic field, we must know the field quantities and its variations at the core mantle boundary. These values can be obtained by solving the induction equation

$$\text{curl} \left(\frac{1}{\mu_0} \text{curl} B \right) = -\dot{B}$$

provided that a conductivity law for the mantle and a relative velocity between core and mantle are known. According to STIX and ROBERTS (1983) we applied a conductivity law of form

$$\sigma(r) = \sigma_a (r/a)^{-\alpha}$$

($\sigma_a = 3 \cdot 10^3 \Omega^{-1} \text{ m}^{-1}$ and $\alpha = 30$) and a relative angular velocity between core and mantle of -10^{-10} 1/s corresponding to the westward drift of the magnetic field. Using a spherical harmonic model of the surface magnetic field and its secular variations we obtained by iterative solution of the induction equation and applying equation (1) following components of the electromagnetic torque

$$\left. \begin{array}{l} L_1 = 0.4 \\ L_2 = 0.1 \\ L_3 = -14.0 \end{array} \right\} \cdot 10^{17} \text{ Nm}$$

Although these values are first results, we can assume that the correlation between variations of the magnetic field and the length of day are physically significant.

Let us now have a look at the variation of the CHANDLER-period. Applying an input-output-analysis using the annual wobble of polar motion, I found that the variations of the CHANDLER-period are much smaller than the variations shown by the curve of Fig. 1.

To investigate this discrepancy we introduce a notation of the torque given by ROCHESTER (1976)

$$L = - (k + k' \bar{i}_3 \times) (\bar{\chi} - \lambda_3 \bar{i}_3) - k'' \lambda_3 \bar{i}_3 \quad (3)$$

where k , k' and k'' are coupling constants. \bar{i}_3 is the vector of unity nearly in the direction of the rotation axis and $\bar{\chi}$ is the relative rotation between core and mantle.

Assuming isotrope conductivity and magnetic permeability we obtain

$$L_M = -k_M (i - \bar{i}_3 \times) \bar{\chi} \quad (4)$$

where $k_M \approx 10^{27}$ Nm s.

The influence of L_M on the CHANDLER-period can be obtained by analyzing an Earth model consisting of fluid core and solid mantle. We shall apply an Earth model derived by POINCARÉ's variational principle which was demonstrated by MORITZ (1982). The version of MORITZ consists of a fluid core and an elastic mantle. This model was modified allowing for viscosity of the mantle.

To estimate the influence of the electromagnetic torque we must investigate the eigenvalue solution of polar motion equations. In first order approximation these equations are independent of the equation governing rotational variations. Following equations are valid for the considered Earth model:

$$\begin{aligned} \dot{u} - i (\sigma_0 + i\alpha) u + \frac{A_c + D_{12} \omega_0}{A + D_{11} \omega_0} (\dot{v} + i \omega_0 v) &= \frac{-L_E}{A + D_{11} \omega_0} \\ \dot{u} + \frac{A_c + D_{22} \omega_0}{A_c + D_{12} \omega_0} \dot{v} + i \frac{C_c \omega_0}{A_c + D_{12} \omega_0} v &= \frac{L_E}{A_c + D_{12} \omega_0} \end{aligned} \quad (5)$$

where

$$L_E = -k_M (1 + i) v \quad (6)$$

are the equatorial components of the electromagnetic torque in complex notation.

u are the polar motion components in complex notation,
 v describes the polar motion of the core relative to the mantle,

A , A_c and C_c are moments of inertia of the whole Earth and the core respectively,

D_{12}, D_{11}, D_{12} are coefficients depending on the elastic deformation of the mantle and the influence of these deformations on the fluid core.

σ_0 is the CHANDLER-period of an elastic Earth model and

α a damping factor depending on the viscosity of the mantle.

The eigenvalue solution of (5) yields following frequencies of the free wobbles:

$$\begin{aligned} \sigma_1 &= \frac{A}{A_M} \left(1 + \frac{2 k_M}{A_M \omega_0} (1 - i) \right) (\sigma_0 + i\alpha) \\ \sigma_2 &= -\omega_0 \left(1 + \frac{A}{A_M} \left(\varepsilon - \frac{D_{22}}{A_C} \omega_0 \right) - \frac{k_M}{A_M \omega_0} (1 - i) \left(1 + \frac{A}{A_C} \right) \right) \end{aligned} \quad (6)$$

σ_1 is the frequency of the CHANDLER-wobble and σ_2 the frequency of the diurnal free wobble. It is seen that damping and period of both wobbles are influenced by coupling torques, but we must notice that in both frequencies k_M is divided by the moment of inertia of the mantle A_M . Since $k_M/A_M \approx 10^{-10}$ period and damping of both wobbles are not significantly influenced by electro-magnetic core mantle coupling.

Similar dubious is the correlation between the magnetic field intensity and the amplitude of the CHANDLER-wobble. As mentioned before the equatorial components of the coupling torque are much smaller than the axial component, but really the equatorial components should be larger to excite a wobble comparable with the observed quantities.

RUNCORN (1982) suggested to explain the excitation of CHANDLER-wobble by acting electromagnetic torques which could be described by DIRAC-functions. He assumed that the equatorial components are of the same order of magnitude as the axial component. This is in contradiction to our first results.

Regarding to the present state of investigation we can only expect that the correlation between the variations of the length day and of the magnetic field intensity correspond to physical relations.

References

- MORITZ (1982): Theories of nutation and polar motion III. Rep. of the Dept. of Geodetic Science and Surveying. Rep. No 342 Ohio State University Columbus (Ohio)
- MUNK, W.; REVELLE, R. (1952): On the geophysical interpretation of irregularities in the rotation of the Earth. Monthly Not. of the Royal Astron. Soc. Geoph. Suppl. No 6. pp. 331 - 343
- ROCHESTER, M. G. (1976): The secular decrease of obliquity due to dissipative core-mantle coupling. Geophys. J. R. astr. Soc. 43 pp. 109 - 116
- RUNCORN, S. K. (1982): The role of the core in irregular fluctuations of the Earth's rotation and the excitation of the CHANDLER-wobble. Phil. trans. R. Soc. London A 306 pp. 261 - 272
- STIX, M.; ROBERTS, P. H. (1983): Time dependent electromagnetic core-mantle coupling. Paper pres. to Symp. 12 of IUGG Meeting, Hamburg August 1982

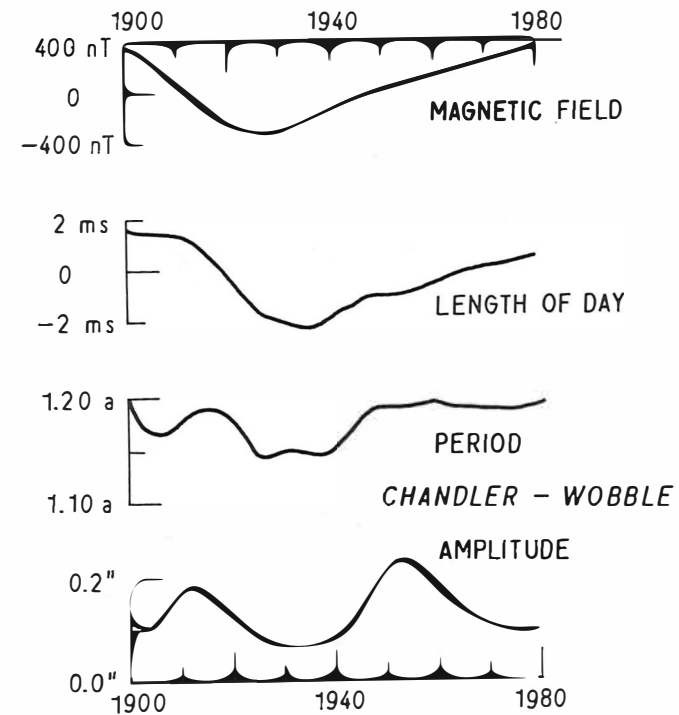


Fig. 1

Treatment of the Geodetic Boundary Value Problem by Contact-Transformation

Wolfgang Keller

Technical University Dresden

1. Introduction

One possibility to study free boundary value problems for elliptical differential equations is to use the searched function V for the definition of a contact-transformation. This contact-transformation transforms the free boundary value problem for V into a boundary value problem with fixed boundary for a coordinated function ψ .

This approach was intensively studied by Kinderlehrer, Nirenberg [1] and Kinderlehrer, Nirenberg, Spruck [2]. The application of this principle in geodesy goes back to Sanso' [3]. He applies the most simple case of a contact-transformation, Legendre's transformation.

A new function ψ , the adjoint potential, new co-ordinates $\xi_i, i=1,2,3$ and new impulses $\pi_i = \partial\psi/\partial\xi_i, i=1,2,3$ are coordinated to the old function V , the gravitational potential of the earth, to the old Cartesian co-ordinates $x_i, i=1,2,3$ and to the old impulses $p_i = \partial V/\partial x_i, i=1,2,3$ in the following manner :

$$\psi = x_i \xi_i - V$$

$$\xi_i = p_i, \quad i=1,2,3$$

$$\pi_i = x_i, \quad i=1,2,3$$

Under the hypothesis, that Marussi's condition

$$\det \left(\frac{\partial^2 V}{\partial x_i \partial x_j} (x) \right) \neq 0, \quad x \in \text{ext } \sigma \quad (4)$$

is fulfilled in the exterior of the earth and the impulses $p_i, i=1,2,3$ are known on the surface σ of the earth, the adjoint potential ψ solves the following boundary value problem

$$\text{Tr } \Phi^2 - [\text{Tr } \Phi]^2 = 0, \quad \xi \in \text{int } \Sigma \quad (5)$$

$$\Phi := \left(\frac{\partial^2 \psi}{\partial \xi_i \partial \xi_j} (\xi) \right) \quad (6)$$

$$\left(\xi_i \frac{\partial \psi}{\partial \xi_i} - \psi \right) \Big|_{\Sigma} = V \quad (6')$$

$$\Sigma = \{ \xi \in R^3 \mid \exists x \in \sigma : \xi_i = p_i(x), i=1,2,3 \} \quad (7)$$

Hence the linear free boundary value problem for V was transformed into an equivalent boundary value problem with a fixed boundary for ψ .

In the trivial case of a spherical earth with homogeneous mass distribution, the solution of (5), (6), (6'), (7) is known:

$$\psi_0(\xi) = \mu^{1/2} |\xi|^{1/2} \quad (8)$$

Evidently, ψ_0 is not differentiable in the origin $\xi = 0$ and we can expect, that a singularity appears also in the general case. As the cause of that singularity we have to consider the fact, that Legendre's transformation maps the point at infinity onto the origin $\xi = 0$.

- (1) Because there isn't any sense to speak about differentiability of V in the point at infinity, we can't expect differentiability of ψ in the origin.
- (2)

- (3) Therefore the aim of this notice is, to find a new contact-transformation, which also transforms the free boundary value problem into a new one with a fixed boundary, but with the point at infinity as a fixed point. In this way the mentioned singularity is avoided.

2. Contact-transformation

A new function ψ , new co-ordinates ξ_i , $i=1,2,3$ and new impulses $\pi_i = \partial\psi/\partial\xi_i$, $i=1,2,3$ are to be coordinated now to the searched function V , to the Cartesian co-ordinates x_i , $i=1,2,3$ and to the impulses $p_i = \partial V/\partial x_i$, $i=1,2,3$ in the following way:

$$\psi = x_i \xi_i - V \quad (9)$$

$$\xi_i = -\mu^{1/2} \frac{p_i}{|p|^{3/2}}, \quad i=1,2,3 \quad (10)$$

$$\pi_i = \alpha_{ik} x_k, \quad i=1,2,3 \quad (11)$$

$$\alpha_{ik}(\xi) = -\frac{\mu}{|\xi|^3} (\delta_{ik} - 3 \frac{\xi_i \xi_k}{|\xi|^2}), \quad i,k=1,2,3 \quad (12)$$

Lemma 1: It holds:

$$d\psi - d\xi_i \cdot \pi_i = (-1) (dV - dx_i \cdot p_i) \quad (13)$$

i. e., the transformation (9) - (12) is indeed a contact-transformation.

If Marussi's condition (4) is fulfilled additionally, the point-transformation (10) is even one-to-one. In this case, we can interpret (10) intuitively:

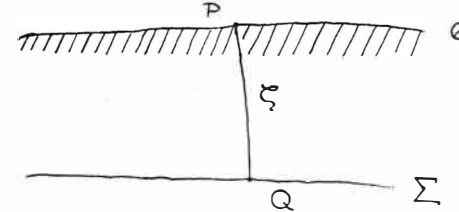
If we use the rotationally symmetric potential

$$V_0 = \mu/|x|$$

as reference potential, we recognise:

$$\frac{\partial V_0}{\partial x_i}(\xi) = -\frac{\mu \xi_i}{|\xi|^3} = -\frac{\mu (-\mu^{1/2} p_i)}{|p|^{3/2} (\mu^{1/2} p^{-1/2})^3} = p_i = \frac{\partial V}{\partial x_i}(x), \quad i=1,2,3$$

This means, that the point-transformation (10) maps every point P of the surface σ of the earth onto belonging point Q of the gravimetric telluroid Σ .



If we suppose again, that the impulses p_i , $i=1,2,3$ are known on the surface of the earth, the gravimetric telluroid is a known surface. The function ψ induces by (11) the mapping of the known telluroid onto the unknown surface of the earth.

In the same way like in the case of Legendre's transformation, we get ψ as the solution of the following boundary value problem:

$$\text{Tr } \Phi^2 - [\text{Tr } \Phi]^2 = 0, \quad \xi \in \text{ext } \Sigma \quad (14)$$

$$\Phi = (\gamma_{im} \gamma_{kn} \frac{\partial^2 \psi}{\partial \xi_m \partial \xi_n} - \beta_{imk} \frac{\partial \psi}{\partial \xi_m}) \quad (15)$$

$$\gamma_{ik}(\xi) = -\frac{|\xi|^3}{\mu} (\delta_{ik} - 3 \frac{\xi_i \xi_k}{|\xi|^2}), \quad i,k=1,2,3 \quad (16)$$

$$\beta_{imk}(\xi) = -\frac{3}{2} \frac{|\xi|^4}{\mu^2} (\delta_{mi} \xi_k + \delta_{mk} \xi_i + \delta_{ik} \xi_m - 2 \frac{\xi_i \xi_m \xi_k}{|\xi|^3}) \quad (17)$$

$$(-\frac{1}{2} \xi_i \frac{\partial \psi}{\partial \xi_i} - \psi) \Big|_{\Sigma} = V \quad (18)$$

The problem has an analogue structure like the problem, which arises from Legendre's transformation.

Of course it is an exterior problem but this is only a pure technical difficulty. We can overcome this difficulty by applying the Kelvin transformation.

3. Linearization

Usually, the problem is to be linearized. The function

$$\psi_0(\xi) = - 2\mu/|\xi| \tag{19}$$

is assumed to be the adjoint reference potential. This reference potential solves the boundary value problem (14) - (18) in the trivial case of a spherical earth with a homogeneous mass distribution. In the opposite to (8) it does not appear any singularity in (19).

If we denote the adjoint disturbing potential by $u = \psi - \psi_0$, we arrive to :

Theorem 1: The linearization of (14) - (18) is given by

$$- \Delta u(\xi) = 0 \quad , \quad \xi \in \text{ext } \Sigma \tag{20}$$

$$\left(- \frac{1}{2} \xi_1 \frac{\partial u}{\partial \xi_1} - u\right) \Big|_{\Sigma} = (\nabla - \mu/|\xi|) \Big|_{\Sigma} =: \varphi \tag{21}$$

The linearized problem is an oblique boundary value problem for Laplace's equation. Theorem 2 describes the solvability of this problem.

Theorem 2: Let be the domain $\text{ext } \Sigma$ belonging to the regularity class $C^{2,1}$ and let it differ from the exterior of a sphere only "a little". Then it exists three and only three real constants α_i , $i=1,2,3$ and one and only one function u , such that

$$- \Delta u(\xi) = 0 \quad , \quad \xi \in \text{ext } \Sigma$$

$$\left(- \frac{1}{2} \xi_1 \frac{\partial u}{\partial \xi_1} - u\right) \Big|_{\Sigma} = \varphi + \alpha_i S_i(\xi) \Big|_{\Sigma}$$

$$u(\xi) = O(1/|\xi|^3) \text{ for } |\xi| \rightarrow \infty$$

hold.

(S_i are the three linearly independent spherical harmonics of degree one.)

With the help of the implicit - function theorem we obtain a local existency- and uniqueness result from theorem 2.

Theorem 3: Let be fulfilled the same hypothesis as in theorem 2. Furthermore let be

$$\Sigma \sup_{|\alpha| \leq 1} |D^\alpha \varphi(x)|$$

sufficient small.

Then exists three and only three real constants α_i , $i=1,2,3$ and a function ψ , such that

$$\text{Tr } \Phi^2 - [\text{Tr } \Phi]^2 = 0 \quad , \quad \xi \in \text{ext } \Sigma$$

$$\left(- \frac{1}{2} \xi_1 \frac{\partial \psi}{\partial \xi_1} - \psi\right) \Big|_{\Sigma} = \varphi + \alpha_i S_i \Big|_{\Sigma}$$

$$\psi = O(1/|\xi|^3) \text{ for } |\xi| \rightarrow \infty$$

hold.

Except of this solution any other solution does not exist in a neighbourhood of ψ_0 .

References :

- [1] Kinderlehrer, D., Nirenberg, L.: Regularity in Free Boundary Problems. Ann. Scuola Norm. Sup. Pisa Ser. IV, 4(1977) , pp 373 - 391
- [2] Kinderlehrer, D., Nirenberg, L, Spruck, J.: Regularity in Elliptic Free Boundary Problems, I, Journal d'Analyse Math. , 34(1978) , pp 86 - 119
- [3] Sanso', F.: The Local Solvability of Molodensky's Problem in Gravity Space. Manuscr. Geod. , 3(1978) , pp 157 - 227

ON SHORT PERIODICAL VARIATIONS OF POLAR MOTION
AND UT1 - UTC

B.Kożaczek, A.Brzeziński, W. Kosek
J.Nastula, B. Słoducha
SPACE RESEARCH CENTRE, PAS
Warsaw, POLAND

ABSTRACT. The MERIT data of pole coordinates, UT1-UTC and l.o.d. from the period between October 1983-July 1984 have been used for analysing spectra of their variations in the short periodical part from 10 - 90 days by the Maximum Entropy Spectral Analysis-MESA. A few short periodical variations detected by MESA in all series of data determined by different techniques seem to be real short periodical variations of polar motion and UT1-UTC. Their amplitudes, which are of the order of a few miliardseconds only, are weakly determined, and they can be changeable.

1. INTRODUCTION

Simultaneous observations made by different techniques during the MERIT Campaign have given the most accurate and the most dense data for the Earth rotation study. The MERIT observational data from the period of ten months, October 1983 - July 1984, have been used for analysing spectra of the polar motion and UT1-UTC in the short periodical part, from 10 to 90 days, by the Maximum Entropy Spectral Analysis - MESA.

2. SPECTRAL ANALYSIS OF THE MERIT DATA OF POLE
COORDINATES AND UT1-UTC

First, all time series of pole coordinates determined by BIH-Astrometry, IPMS-Astrometry, DMA-DOPPLER, CSR-LASER, NGS-VLBI as well as UT1-UTC determined by BIH and l.o.d. determined by CSR have been smoothed using a Gaussian filter with 3 different Gaussian windows, whose width at half maximum amplitude-FWHM was 5, 30 and 50 days, respectively. The series of smoothed data have been computed with different steps of 1, 2 and 5 days.

In order to diminish the influence of long periodical variations on short periodical part of spectra, differences of each series of pole coordinates, UT1-UTC and l.o.d. smoothed using a Gaussian filter with two different FWHM of 5 and 30 days as well as 5 and 50 days have been computed and used for further spectral analysis. Transfer function of such filters is shown in Figure 1.

Diagrams of power spectral densities of differences computed with FWHM of 5 and 30 days of chosen series of pole coordinates, UT1-UTC and l.o.d. are shown in Figures 2a-2c, respectively.

The short periodical part of spectra of pole coordinates determined by BIH-Astrometry and DMA (44) -Doppler are the most noisy. LPMS-Astrometry data are very strongly smoothed in this part of the spectrum. The spectra of variations of x coordinate determined by DMA-67 and CSR are the most similar. It can be seen in the diagrams of logarithms of power spectral densities presented in Figure 3. Most of detected by MESA periods of short periodical terms appear in three or four series of pole coordinates determined by different techniques.

It is noteworthy to stress that the order of magnitude of short periodical variation amplitudes is two times smaller than in the case of Chandler or annual periodical variations. Amplitudes of short periodical variations detected by MESA in the range of periods of 10-90 days are of the order of a few milliarcseconds, mostly 2-5 mas and are comparable with the 1 mas order of their errors.

Performed test, in which time series consisting of a sum of several periodical terms with amplitudes of 2-5 mas and the noise with $\sigma = 5$ mas have been analysed by MESA, revealed that MESA detects well such periodical terms (Table 1) .

The list of periods and amplitudes of short periodical variations detected by MESA in the analysed time series of pole coordinates, UT1-UTC and l.o.d. is given in Table 2. Amplitudes and phases have been determined by the least squares method, on the basis of data of resolution of 1 day.

The accuracy of amplitude determinations increases with the increase of resolution of smoothed data. In the case of smoothing resolution of 5 days, comparable with the resolution of original data, accuracies of amplitude determinations are of the order of 1 mas. Phases are very weakly determined. Errors of phases are usually of the order of tens

of degree.

Amplitudes of periodical terms with periods longer than 60 days are considerably diminished by the used filter with FWHM of 5 and 30 days, Figure 1. So, MESA of differences of smoothed series of pole coordinates with FWHM of 5 and 50 days was performed, too. The results are given in Table 3. Amplitudes of the periodical terms with periods longer than 30 days are greater than before, but their errors are higher.

Periods of the most energetic periodical variations and their amplitudes or power spectral densities are different in different series of pole coordinates, but these differences are within the range of their errors.

Some most energetic short periodical variations were detected by MESA in each analysed series, although maxima of power spectral density have different shapes of high sharp peaks or of wider and lower peaks divided into two parts. These periodical variations detected nearly in all series have approximately the following periods: 75 or longer, 55-60, 45, 35, 27, 24, 18, 14, 12 days. Taking into account the errors of the analysed data and of determined parameters of short periodical variations, we decided to add power spectral densities of several series of x and of y coordinates, separately, in order to increase the effects of real short periodical variations of polar motion. These variations of polar motion ought to have the same periods in all series of the data determined by different techniques. Combined spectra of pole coordinates of the most accurate techniques are presented in Figure 4. In combined spectra there are the short periodical variations with the greatest amplitudes detected in the single series of pole coordinates, and their amplitudes are greater. However, in the combined spectra the maxima of power spectral densities for longer periods like: 24, 27, 35, 45, 50-60, 75 days are more increased than in the case of a shorter part of these spectra. It means that these periodical terms are detected by all techniques, and can be real periodical terms of polar motion.

The data of UT1-UTC determined by BIH-Astrometry and of l.o.d. determined by CSR-LASER have been analysed in the same way as the data of pole coordinates. Spectra of UT1-UTC and l.o.d., obtained by MESA, are presented in Figure 2c. In both series of the data short periodical variations, with the following periods, have been detected: 60-70, 35, 27, 19, 15, 13, 12 days. Additionally, there are high peaks for periods of 14 and 21 days in the case of BIH data and for periods of 45 days in the case of CSR data.

Amplitudes of these short periodical variations computed by the least squares method are given in Table 2.

Short periodical variations with periods longer than 50 days are not so well determined on the basis of the present MERIT data, due to the short period of observations. Thus, we have analysed the longer series of pole coordinates determined by BIH-Astrometry, CSR-LASER and DMA-Doppler in the last few years between 1978 - 1984 (B.Koźaczek et al., 1984). These data of pole coordinates have been used for computation of an instantaneous velocity vector of a pole - v_i for each 15 days.

$$v_i = \sqrt{(x_i - x_{i-1})^2 + (y_i - y_{i-1})^2}.$$

In order to remove long periodical variations, differences of instantaneous velocities and mean velocity values for 60 days have been computed. The spectra of these differences of pole velocities obtained by MESA for different techniques as well as for combined spectra of all techniques are presented in Figure 5.

Short periodical variations with the greatest amplitudes have approximately the following periods : 75 , 60 , 40-35 , 30 , 26 days, which are similar to the periods detected in pole coordinates.

In conclusion we can say that the present accuracy of pole position data and UT1-UTC allow to detect some short periodical variations of polar motion and UT1-UTC, and estimate the order of their amplitudes. This part of spectrum of polar motion and UT1-UTC needs further careful investigations.

REFERENCES

- EIH, 1983-1984 , MERIT Monthly Circular No 1-10 , Paris, France.
 Koźaczek B., King R.W., Erzeziński A., Kosek W., 1984. Intern. Symposium "On Space Techniques for Geodynamics , Sopron, Hungary, July 1984.

Table 2. Amplitudes of differences of pole positions determined by one technique and smoothed with FWHM of 5 days and 30 days and with the step of 1 day

Per. /days/	Ampl. /mas/	Per. /days/	Ampl. /mas/	Per. /days/	Ampl. /mas/	Per. /days/	Ampl. /mas/
VLBI-X		VLBI-Y		CSR-X		CSR-Y	
97	4+0.4			77	4+0.4	77	6+0.7
74	5 0.4			50	2 0.4	54	5 0.7
62	5 0.4			41	2.0.4	28	2 0.7
36	3 0.4			32	2 0.4	22	2 0.6
26	2 0.4			24	3 0.4	14	1 0.6
18	2 0.4			18	2 0.4		
16	2 0.2			14	2 0.4		
				12	2 0.4		
DMA67-X		DMA67-Y		DMA44-X		DMA44-Y	
97	3+0.4	73	2+0.6	99	3+0.4	76	5+0.7
62	5 0.4	53	4 0.5	65	3 0.4	54	3 0.7
44	3 0.4	38	4 0.5	48	3 0.4	43	2 0.7
32	2 0.4	28	4 0.5	33	4 0.4	34	2 0.7
24	2 0.4	23	3 0.5	16	2 0.4	25	1 0.7
19	2 0.4	15	4 0.5	14	1 0.4	19	1 0.7
14	2 0.4	12	2 0.5	11	1 0.4	15	1 0.7
BIH-X		BIH-Y		UT1-UTC/BIH /ms/		L.O.D/CSR /ms/	
72	4+0.8	76	5+0.8	59	6+2.2	44	8+1.2
45	6 0.8	52	5 0.8	28	5 2.2	36	4 1.2
32	5 0.8	33	8 0.8	21	5 2.2	25	6 1.2
29	5 0.8	24	3 0.8	15	5 2.2	19	8 1.2
25	7 0.8	16	3 0.8	14	9 2.2	16	4 1.2
22	5 0.8	15	6 0.8	11	3 2.2	12	6 1.2
14	4 0.8	13	4 0.8				

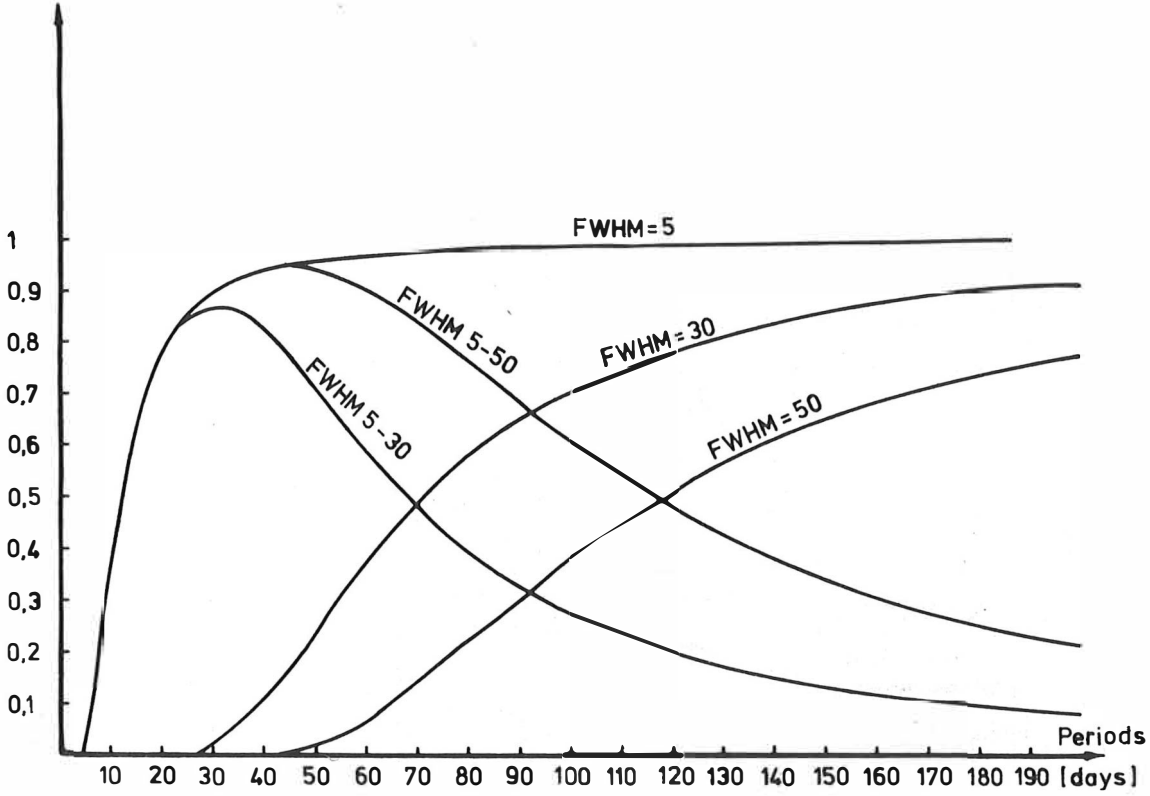


Fig 1. Transfer function of the Gaussian filters

Table 1. Results of spectral analysis of a modeled series of periodical variations with the noise of $\sigma = 5$ mas

Modeled series		Detected terms from 55 data		Detected terms from 271 data	
Period /days/	Amplitudes /mas/	Period /days/	Amplitudes /mas/	Period /days/	Amplitudes /mas/
70	5	70	6 ± 0.7	70	5 ± 0.2
55	4	58	3	58	3
45	3	44	2	44	2
27	3	33	2	33	2
21	2	27	2	27	2
		23	1	23	1
		19	3	19	2
		17	2	17	2
15	2	15	3	15	2

Table 3. Amplitudes of differences of pole positions determined by one technique and smoothed with FWHM of 5 days and 50 days, and with the step of 5 days

Period /days/	Ampl. /mas/	VLBI-Y	Period /days/	Ampl. /mas/	CSR-X	Period /days/	Ampl. /mas/	CSR-Y
80	6+2		82	8+2		80	11+4	
62	5-2		57	4-2		58	5-4	
36	4-2		41	3-3		-	-	
			32	3-2		28	5-4	
DMA67-X		DMA67-Y			DMA44-X			DMA44-Y
60	9+2	76	8+3		-	80	11+4	
44	5-2	56	3-3		66	4+2	59	3-4
32	3-2	38	7-3		48	5-2	-	-
		28	6-3		32	5-2	28	5-4
BIH-X		BIH-Y						
73	9+3	76	10+4					
55	8-3	56	4-4					
31	6-3	42	5-4					
26	8-3	32	9-4					
22	6-3	-	-					

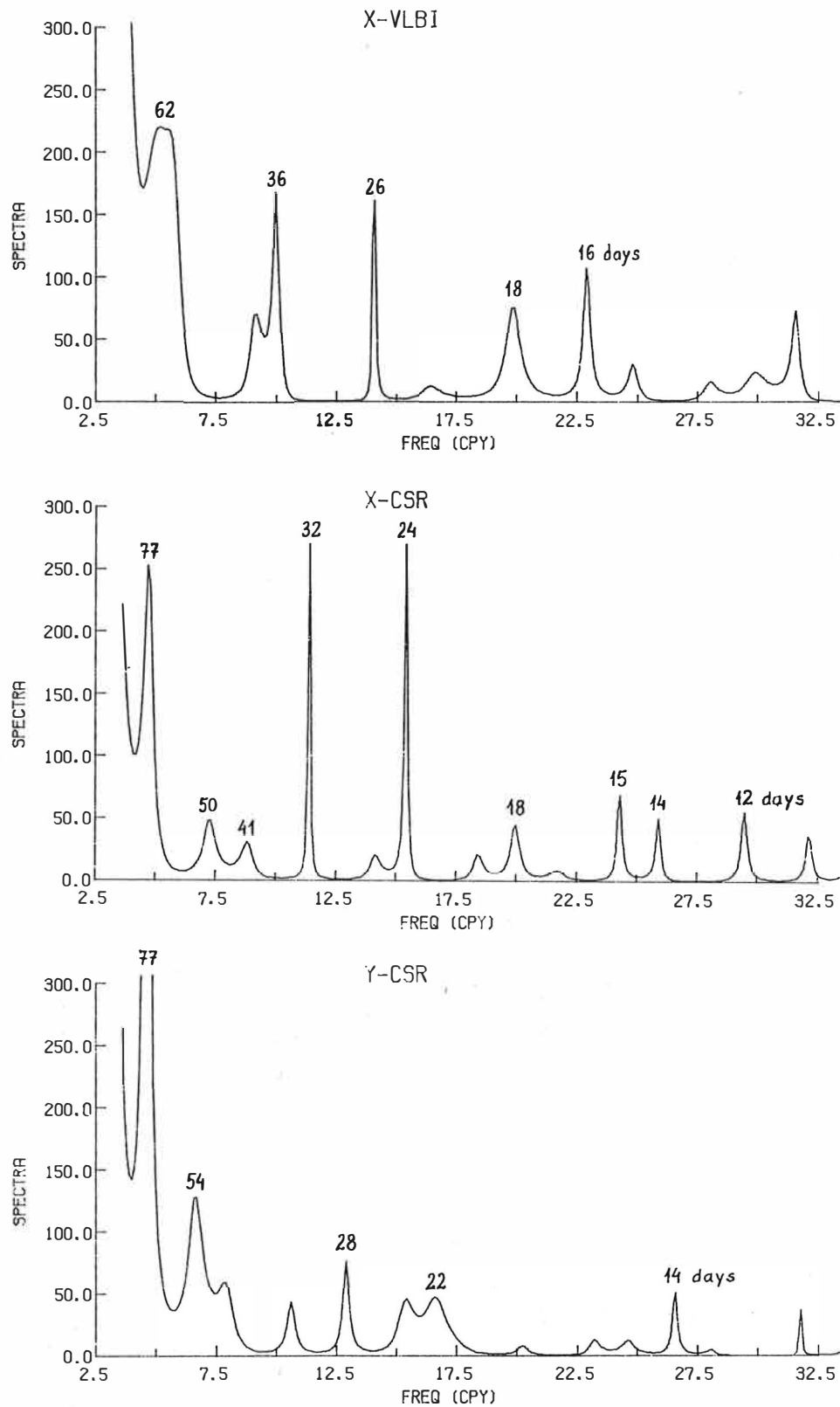


Fig 2a. Power spectral density of pole coordinates variations in units of $1''^2 \times \text{day} \times 10^{-5}$

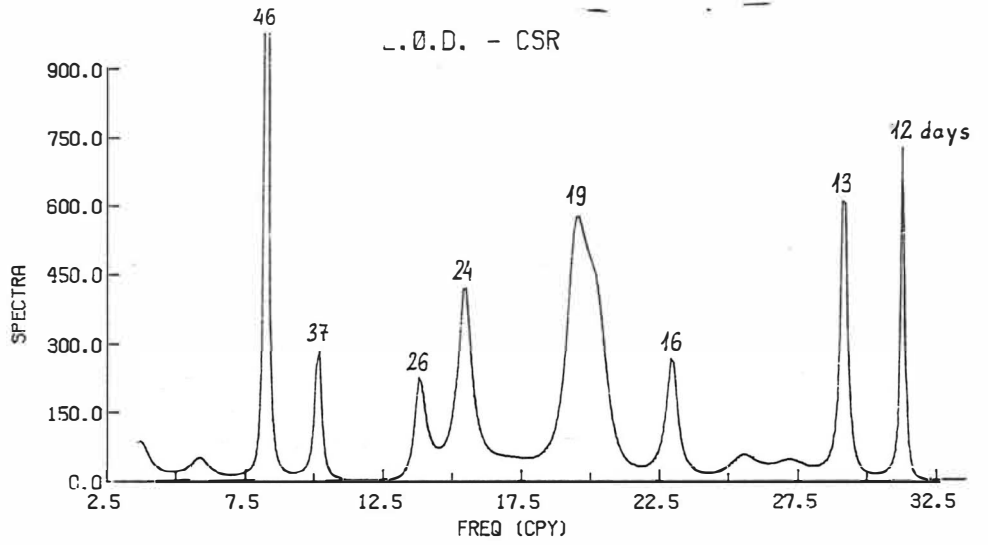
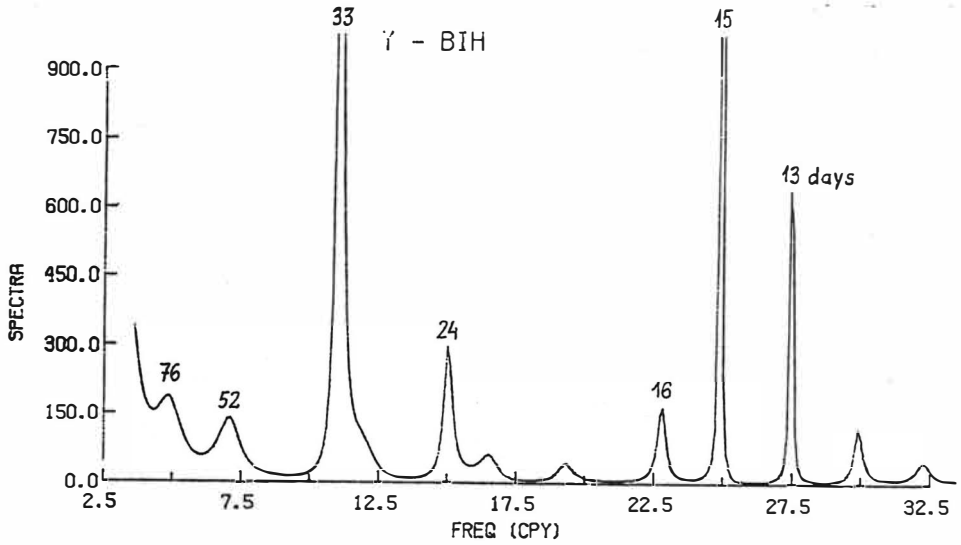
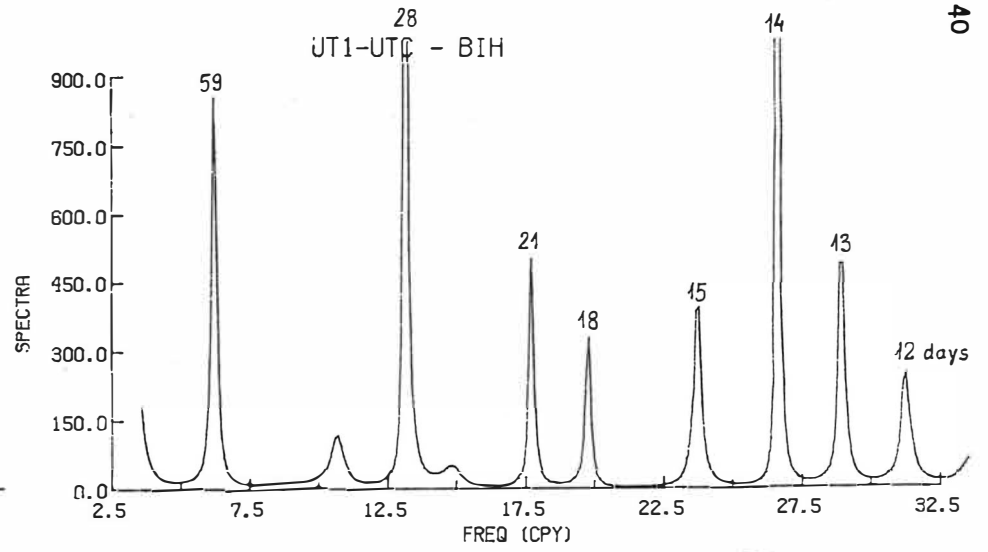
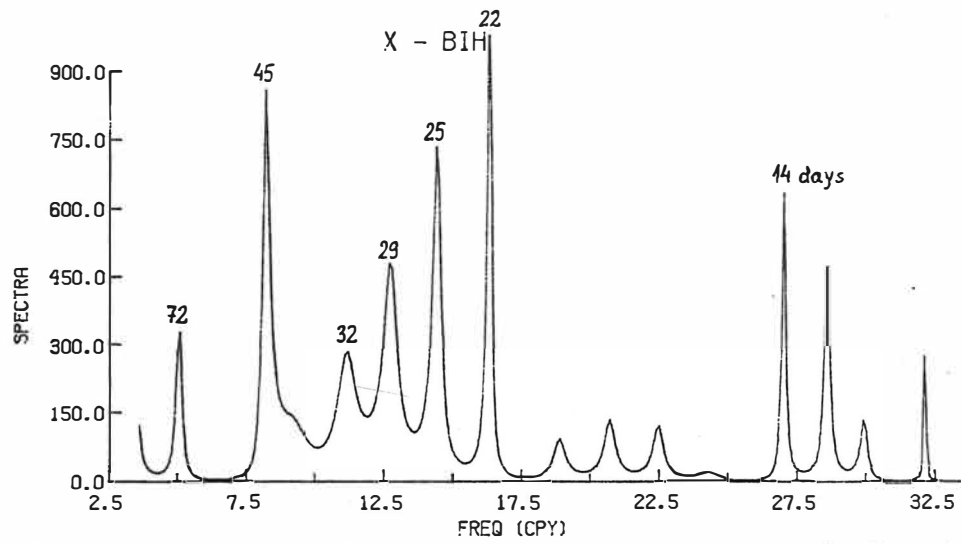
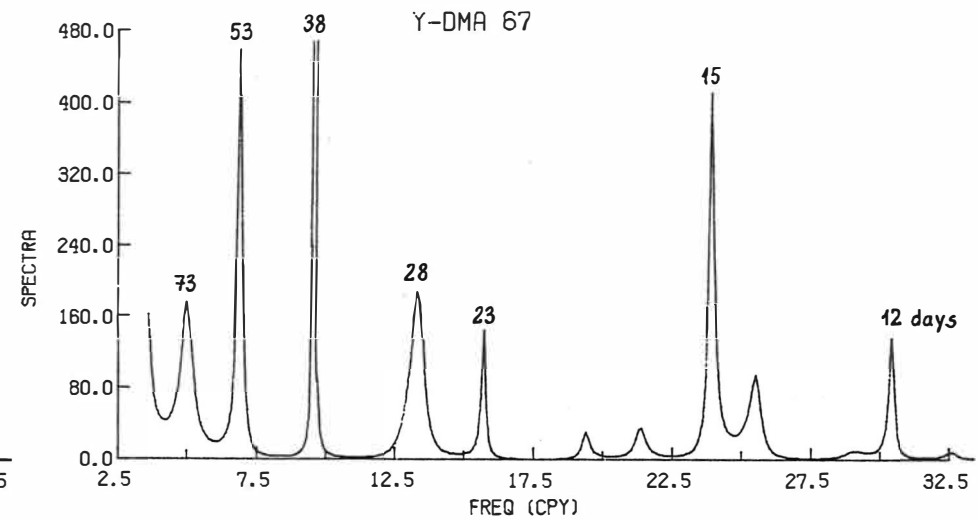
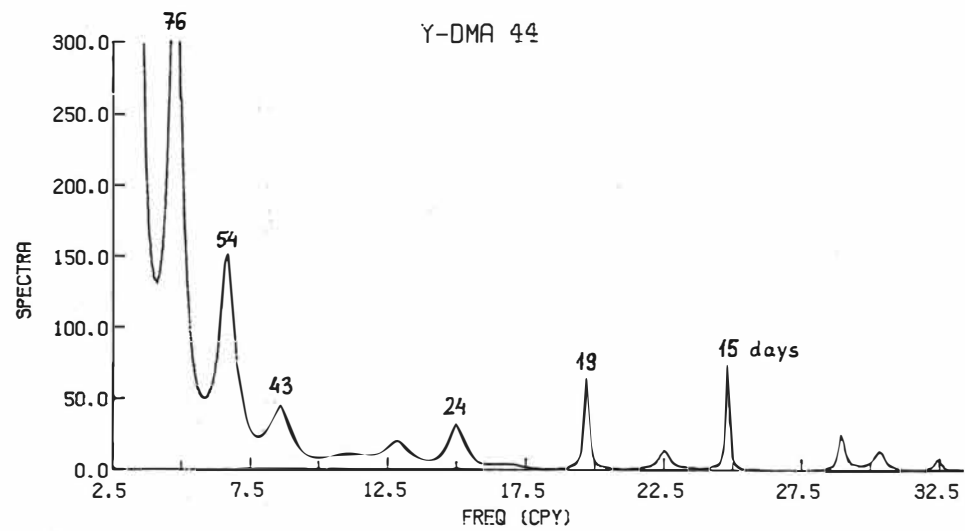
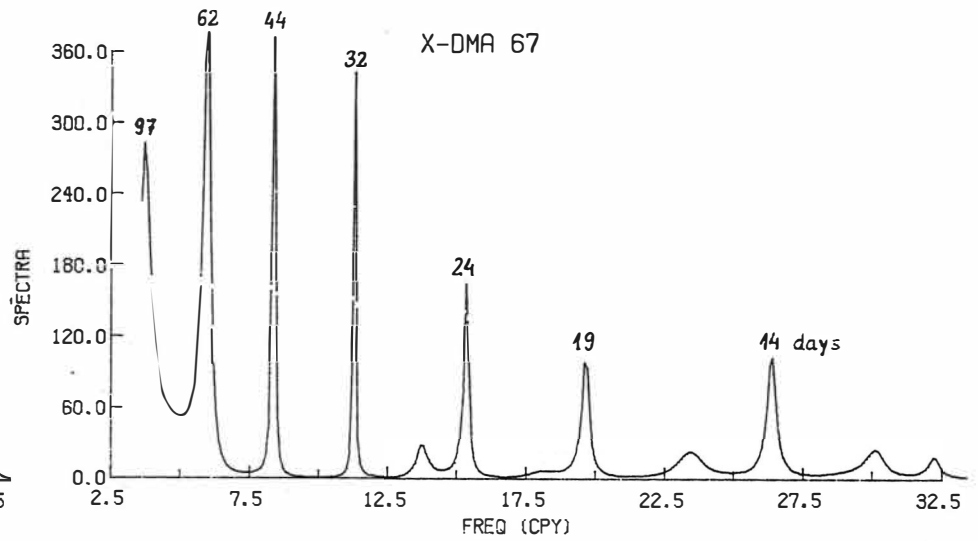
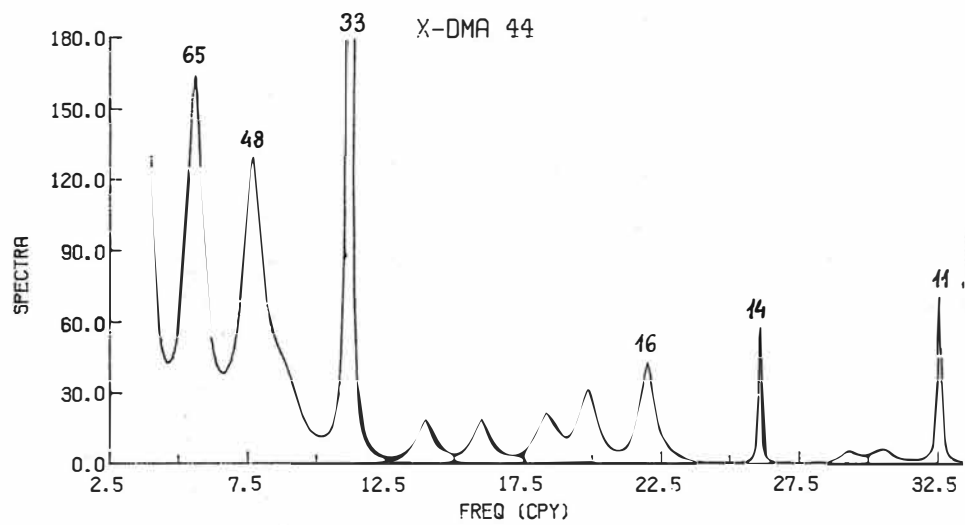


Fig 2c. Power spectral density of pole coordinates variations

UT1 - UTC and l.o.d. in units of $1''^2 \times \text{day} \times 10^{-3}$



**Fig 2b. Power spectral density of pole coordinates variations
in units of $1''^2 \times \text{day} \times 10^{-5}$**

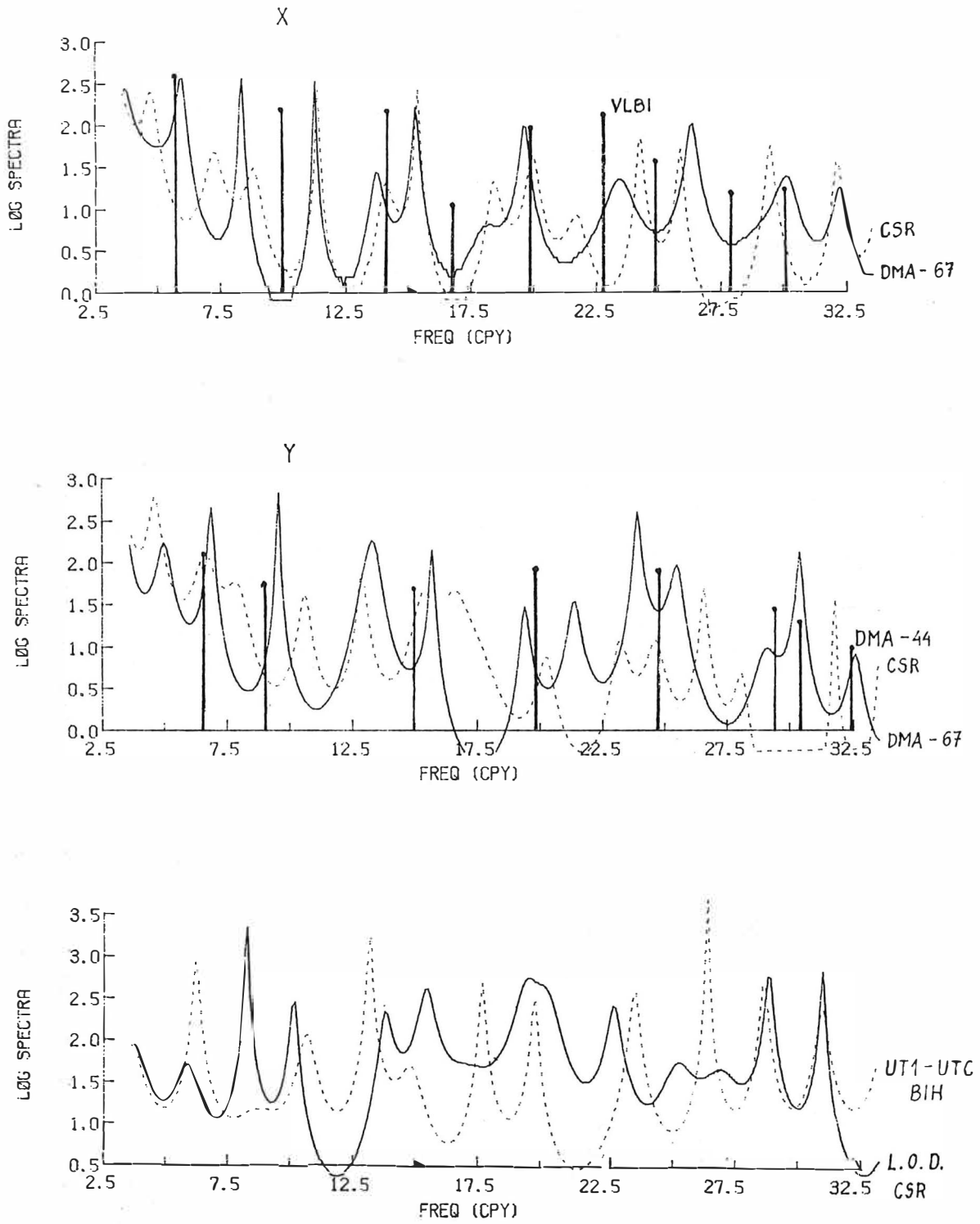


Fig 3. Logarithm of power spectral density of variations of pole coordinates. UT1 - UTC and l.o.d.

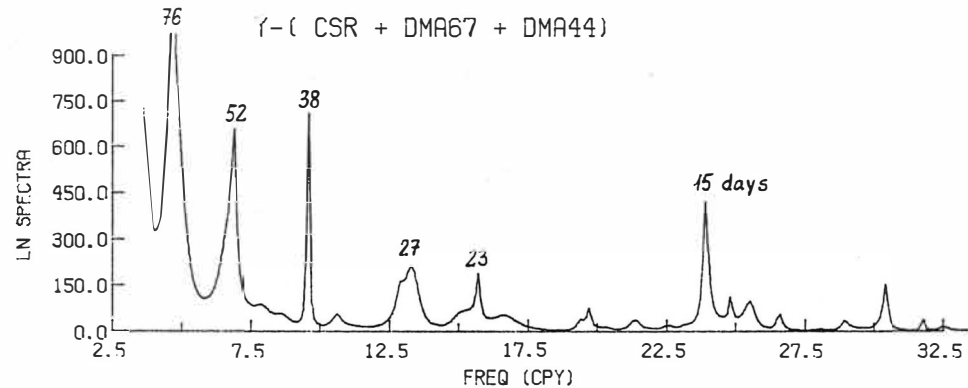
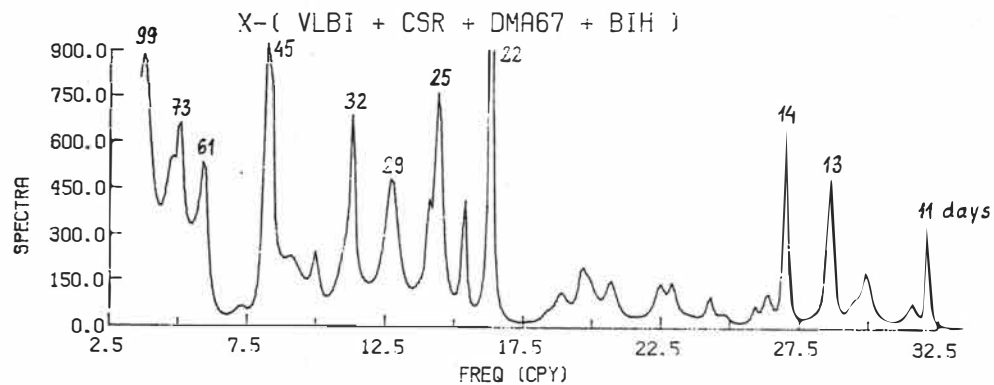
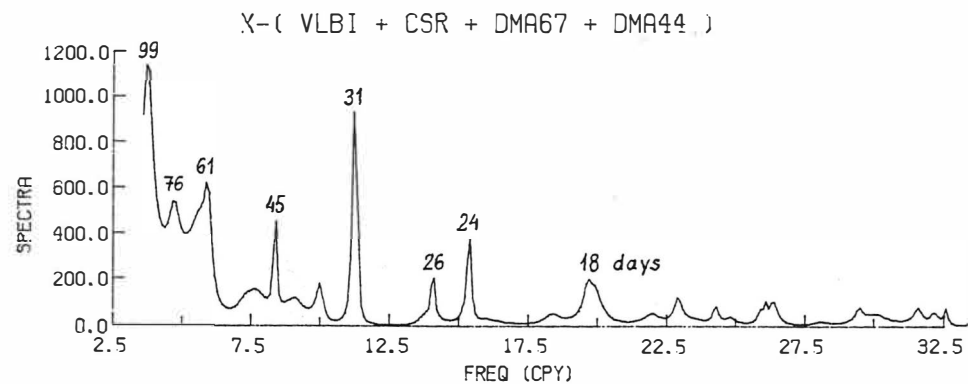
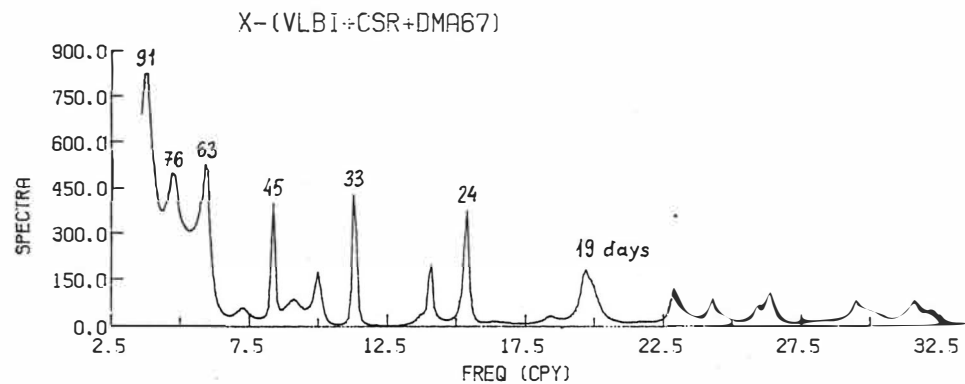


Fig 4. Power spectral density of combined spectra of pole coordinates variations in units of $1'' \times \text{day} \times 10^{-5}$

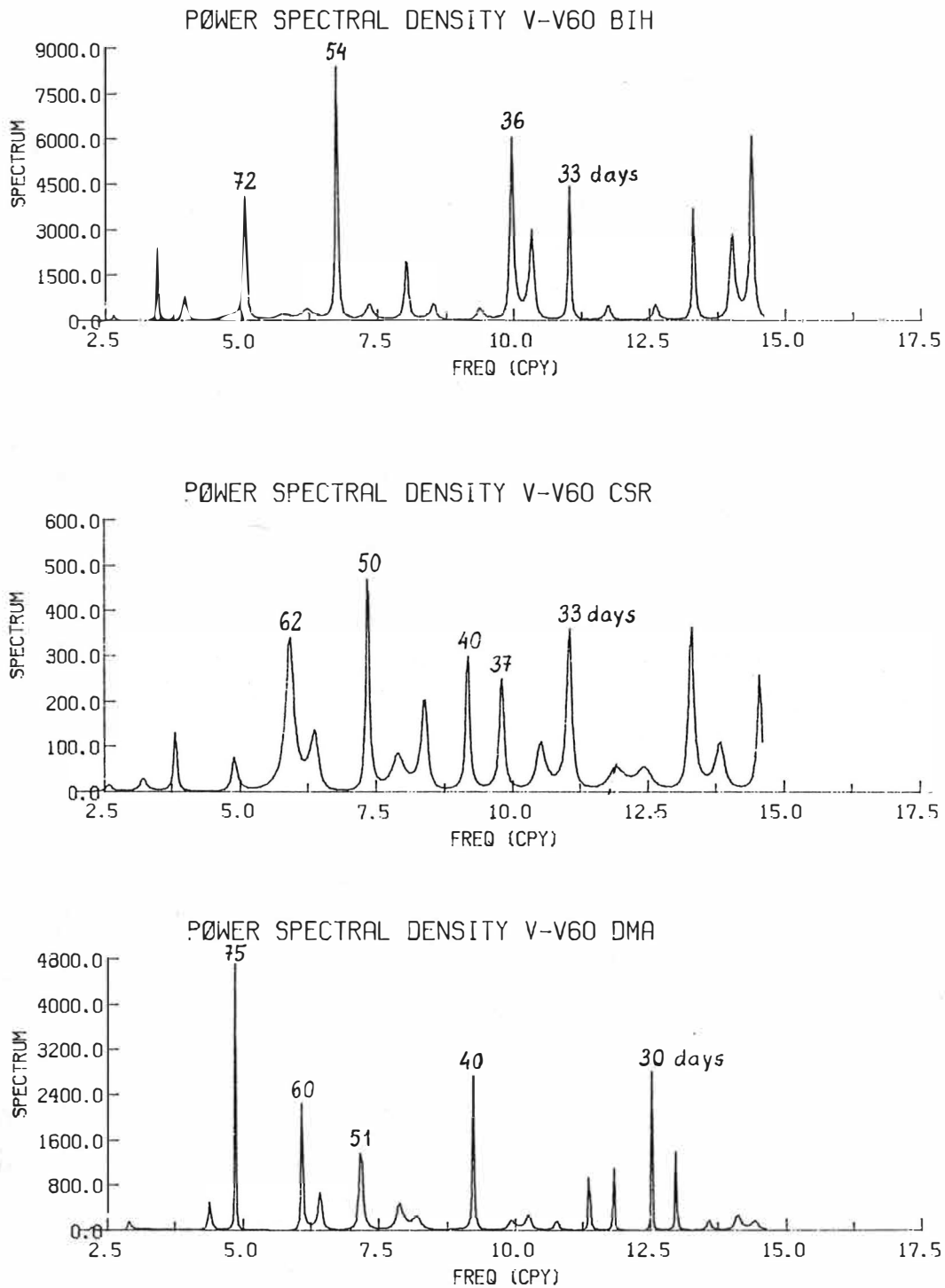


Fig 5. Power spectral density of pole motion velocity differences $\nabla - V60$ in units of $1''^2 \times \text{day} \times 10^{-3}$

Influences of systematic differences between different star catalogues on the results of latitude and time determinations with the PZT 2

by
M. Meinig¹⁾

Summary

Systematic errors in the star catalogues, used for the reduction of PZT observations, affect directly the results of latitude and time determinations and therefore also the Earth rotation parameters which are being derived from these results. In the geodetic-astronomical observatory of the Central Institute for Physics of the Earth the catalogue PZT 80 is presently being used. This catalogue contains star places, which were improved by own PZT results. The systematic differences between this catalogue and the catalogue of northern PZT stars NPZT 74 are approximated by analytical expressions in dependence on the right ascension. The influence of these differences on the latitude and time determinations is presented for the observation series with the PZT 2 in the years 1981 - 83. The obtained results are compared with values calculated from data of the Bureau International de l'Heure.

Zusammenfassung

Systematische Fehler in den Sternkatalogen, die bei der Reduktion der PZT-Beobachtungen verwendet werden, wirken sich direkt auf die Ergebnisse der Breiten- und Zeitbestimmungen aus und beeinflussen somit die aus diesen Ergebnissen abgeleiteten Erdrotationsparameter. Im geodätisch-astronomischen Observatorium des Zentralinstituts für Physik der Erde wird gegenwärtig der Katalog PZT 80 verwendet, der Sternörter enthält, die auf Grund eigener PZT-Ergebnisse verbessert wurden. Die systematischen Differenzen zwischen diesem Katalog und dem Katalog der nördlichen PZT-Sterne NPZT 74 werden durch analytische Ausdrücke in Abhängigkeit von der Rektaszension approximiert. Der Einfluß dieser Unterschiede auf die Ergebnisse der Breiten- und Zeitbestimmungen wird anhand der Beobachtungsreihen mit dem PZT 2 für die Jahre 1981 - 83 dargestellt. Die erhaltenen Ergebnisse werden Vergleichswerten gegenübergestellt, die aus BIH-Daten berechnet wurden.

When making observations with photographic zenith telescopes (PZT) special star catalogues must be used for the reduction, since fundamental stars can hardly be observed. In general, there exist individual star catalogues at the PZT stations. For standardization of these catalogues and for adaptation to the system of the fundamental catalogue FK4 an observation programme was carried out upon the recommendation of the International Astronomical Union in the seventies according to which the stars of the PZT stations on the northern hemisphere were observed together with FK4 stars with meridian circles. 10 meridian circles were involved in this programme. As a result of this international cooperation the catalogue of the northern PZT stars NPZT 74 was issued /1/.

The systematic differences between catalogue PZT 80 /2/ which is presently being used at Potsdam for the reduction of the PZT observations and catalogue NPZT 74 are

¹⁾ Academy of Sciences of the G.D.R., Central Institute for Physics of the Earth, DDR-1500 Potsdam, Telegrafenberg

approximated by analytical expressions in dependence on the right ascension and are graphically presented in Fig. 1 and 2. The resulting maximum amounts of the systematic differences are 0.09" for the declination and 0.013^s for the right ascension.

For the latitude and time determinations with the PZT 2 of the geodetic-astronomical observatory of the Central Institute for Physics of the Earth corresponding corrections were calculated by groups for consideration of the systematic catalogue differences. The corrected data were graphically presented together with the uncorrected results after smoothing of the data series for the years 1981 - 83 (Fig. 3 and 4). For comparison the curves of the latitude changes and (UT1-UTC)-values calculated from data of the Bureau International de l'Heure (BIH) were also plotted.

In Fig. 5 to 8 the differences between the individual curves are graphically presented in a scaled-up manner. The differences between the curves obtained on the one hand from the results with the Yasuda-catalogue (NPZT 74) and on the other hand with our own catalogue PZT 80 show an annually recurrent periodic behaviour (Fig. 5 and 6). The deviations vary between -0.05" and +0.09" for the latitude and between -0.012^s and +0.008^s for the time. For comparison, the differences of the results obtained in the old system and in the new system of astronomical constants introduced from 1. 1. 1984 for the period from the beginning of the MERIT main campaign till the end of 1983 were also graphically presented. Although the differences mentioned last are smaller than the differences between the two star catalogues considered, their influences are of such a magnitude that they must be considered for the calculation of new star coordinate corrections from our own observation results.

Further graphical presentations include the difference curves of the results obtained with the Yasuda catalogue and our own catalogue, respectively, regarding the BIH system (Fig. 7 and 8). These difference curves can be considered as local z-term for the latitude and as local τ -term for the time, respectively. The variations of the z-term are within the limits of -0.10" and +0.09" for our own catalogue and within the limits of -0.04" and +0.14" for the Yasuda catalogue. The τ -term varies between -0.036^s and -0.005^s for our own catalogue and between -0.033^s and -0.003^s for the Yasuda catalogue. A constant portion could be split off from the τ -term and eliminated by a correction of the conventional longitude used for the reduction.

The graphical presentations show that the curve behaviour largely depends on the catalogue used. Therefore, it cannot be excluded that residual systematic star coordinate errors still have an influence on the local z-term and τ -term, respectively. Although it would be formally possible to derive improvements for the star coordinates from the deviations compared with the BIH system on condition that the remaining local terms of the latitude and time determinations are minimized, this procedure does not seem justified, because then errors resulting from other causes (refraction, temperature influences, instrumental errors) might falsely be transferred to the star coordinates.

The differences between various systems for the years 1981 - 83 were represented in the analytical form

$$\Delta = X_0 + X_1 \sin 2 \pi t + X_2 \cos 2 \pi t + X_3 \sin 4 \pi t + X_4 \cos 4 \pi t$$

(t = time in Besselian years). The coefficients X_0 to X_4 were determined by the method of

least squares and are given in Tab. 1. The quantity $A = \sum_{i=1}^4 x_i^2$ also given in Tab. 1 is a criterion for the mutual approximation of the compared systems. It becomes evident that the results obtained with the catalogues PZT 80 and NPZT 74 respectively are in better agreement with the BIH system than the both catalogues between each other.

A decision upon which of the two catalogue systems (Potsdam PZT 80 or NPZT 74) is better suited for the reduction of the observation data of the PZT 2 cannot be taken on the basis of the present investigations.

Tab. 1: Differences between various systems for the years 1981 - 83

<u>Latitude</u>	x_0	x_1	x_2	x_3	x_4	$A = \sum_{i=1}^4 x_i^2$
PZT 80 - BIH	0.003"	0.002"	0.047"	0.010"	-0.011"	$0.2434 \cdot 10^{-2}$
NPZT 74 - BIH	0.039	-0.055	0.022	-0.003	0.001	$0.3519 \cdot 10^{-2}$
NPZT 74 - PZT 80	0.036	-0.057	-0.025	-0.013	0.012	$0.4187 \cdot 10^{-2}$
<u>Time</u>						
PZT 80 - BIH	-0.0213 ^s	-0.0018 ^s	-0.0043 ^s	-0.0039 ^s	-0.0001 ^s	$0.3695 \cdot 10^{-4}$
NPZT 74 - BIH	-0.0211	-0.0057	0.0032	-0.0027	-0.0027	$0.5731 \cdot 10^{-4}$
NPZT 74 - PZT 80	0.0002	-0.0039	0.0075	0.0012	-0.0026	$0.7976 \cdot 10^{-4}$

Literature

- /1/ Yasuda, H.; Hurukawa, K.; Hera, H.: Northern PZT Star Catalog (NPZT 74).
Ann. Tokyo Astron. Obs., Second Ser., Vol. XVIII. No. 4 (1982), 367.
- /2/ Meinig, M.: Verbesserung der Sternörter des Potsdamer PZT-Katalogs.
Astron. Nachr. 305 (1984) 4, 195 - 202.

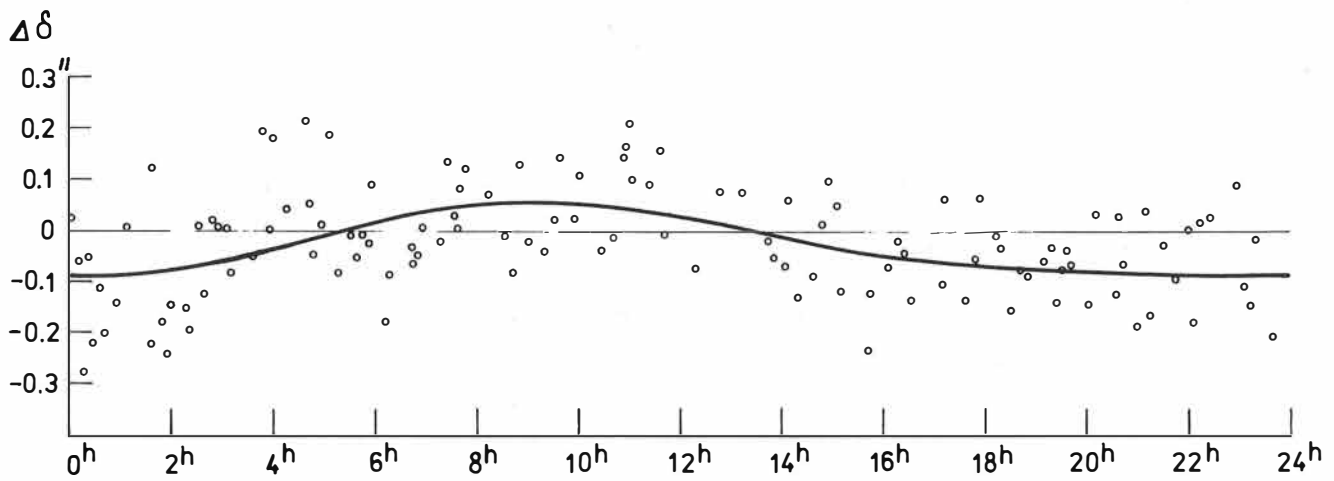


Fig.1 Systematic differences $\Delta\delta$ between the catalogs PZT 80 and NPZT 74
 $\Delta\delta = -0.027'' + 0.042'' \sin \alpha - 0.057'' \cos \alpha - 0.015'' \sin 2 \alpha - 0.002'' \cos 2 \alpha$

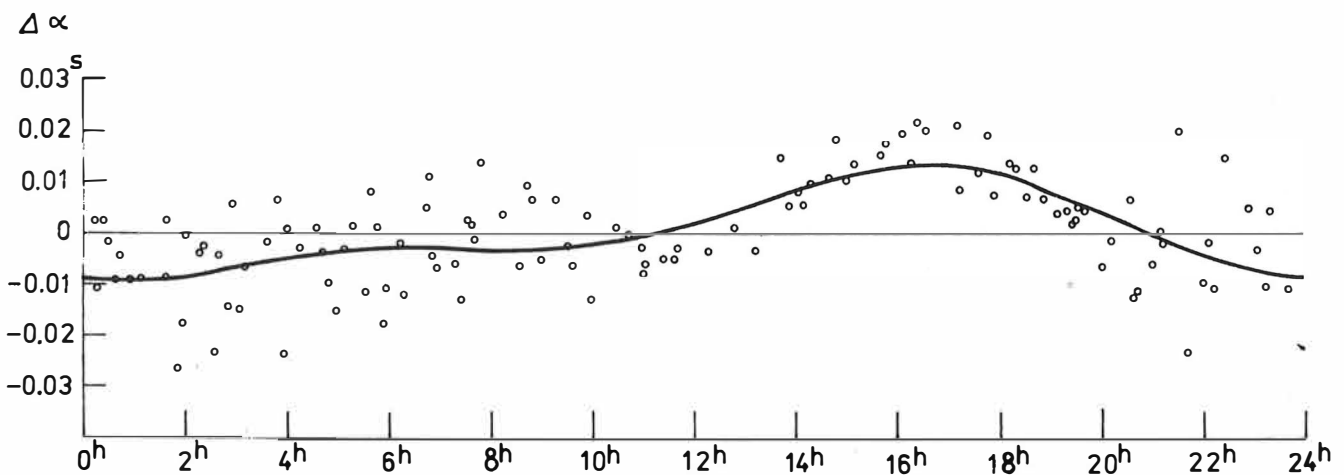


Fig.2 Systematic differences $\Delta\alpha$ between the catalogs PZT 80 and NPZT 74
 $\Delta\alpha = 0.0004^s - 0.0072^s \sin \alpha - 0.0053^s \cos \alpha + 0.0021^s \sin 2 \alpha - 0.0036^s \cos 2 \alpha$

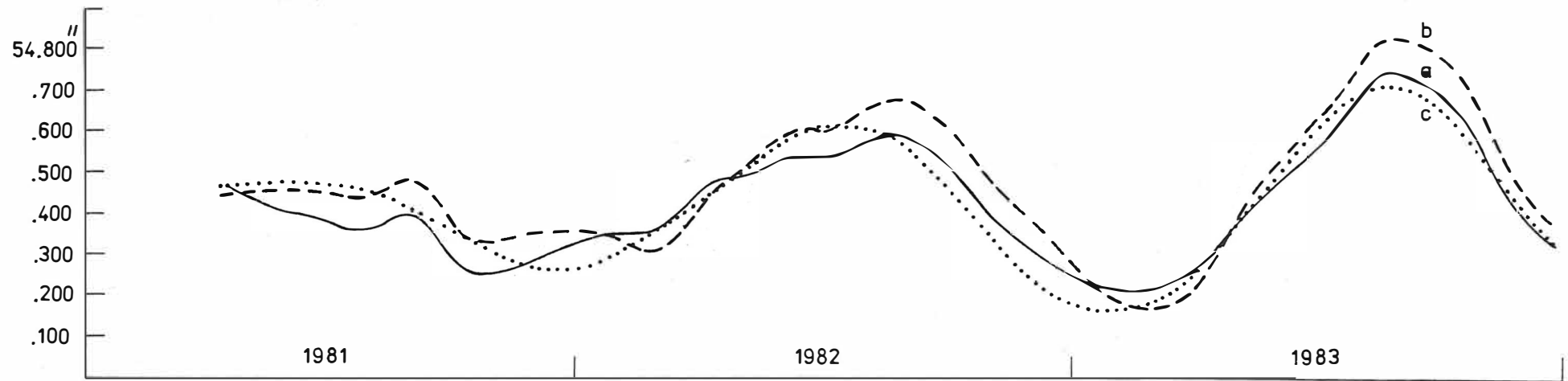


Fig.3 Latitude variations of the Station Potsdam in the years 1981 - 1983

- a) PZT 2 observations refered to catalog PZT 80
- b) PZT 2 observations refered to catalog NPZT 74
- c) according to BIH

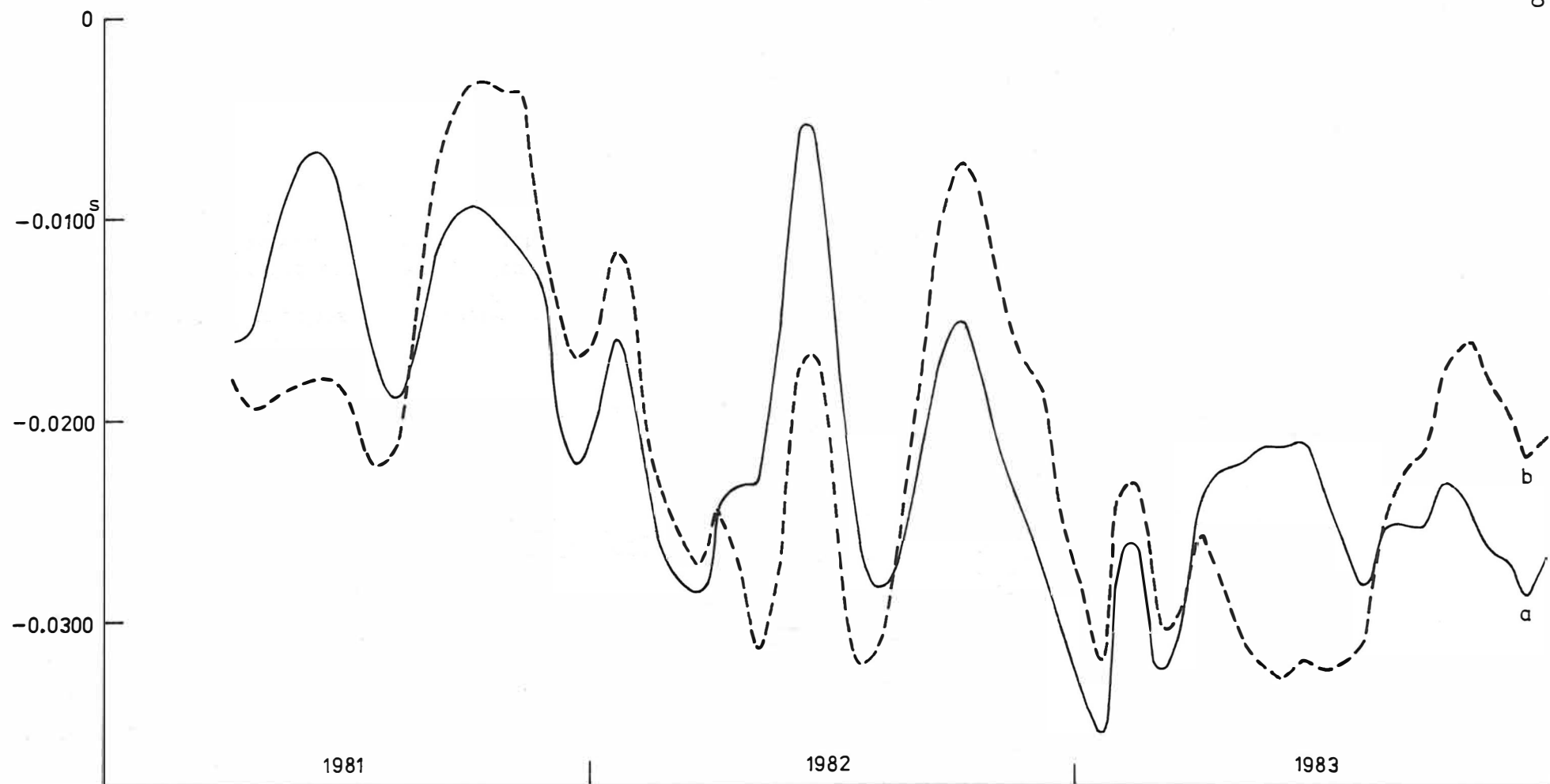


Fig.8 Difference of the time determinations in the systems of the catalogs PZT 80 (a) and NPZT 74 (b) respectively in reference to the BIH system

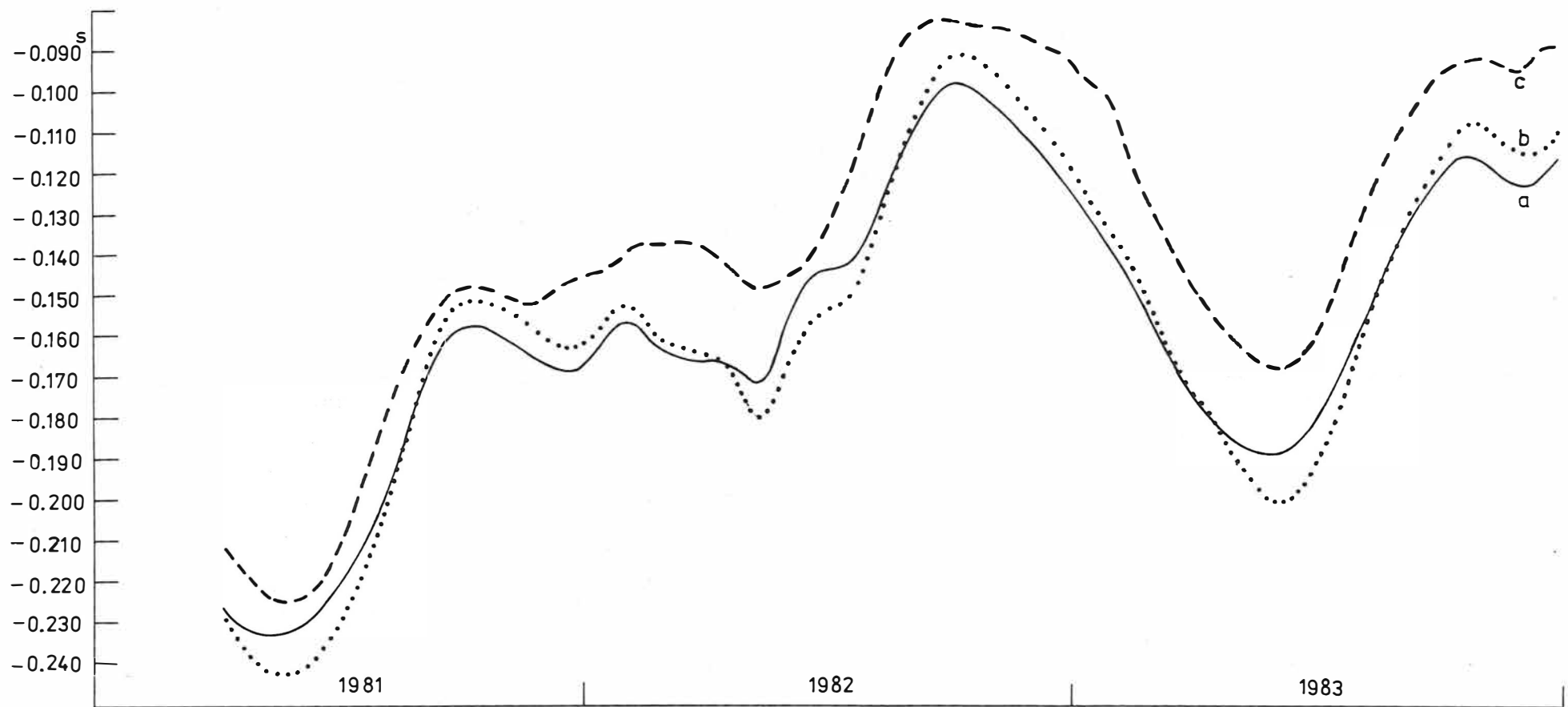


Fig. 4 $(UT1 - UTC) + (MJD - 44605) \cdot 0.0023^S + K$ in the years 1981-1983

$K = 0$ for 1.1.1981 - 30.6.1981
 $K = -1^S$ 1.7.1981 - 30.6.1982
 $K = -2^S$ 1.7.1982 - 30.6.1983
 $K = -3^S$ 1.7.1983 - 30.12.1983

a) PZT2 observations referred to catalog PZT 80
 b) PZT2 observations referred to catalog NPZT 74
 c) according to BIH

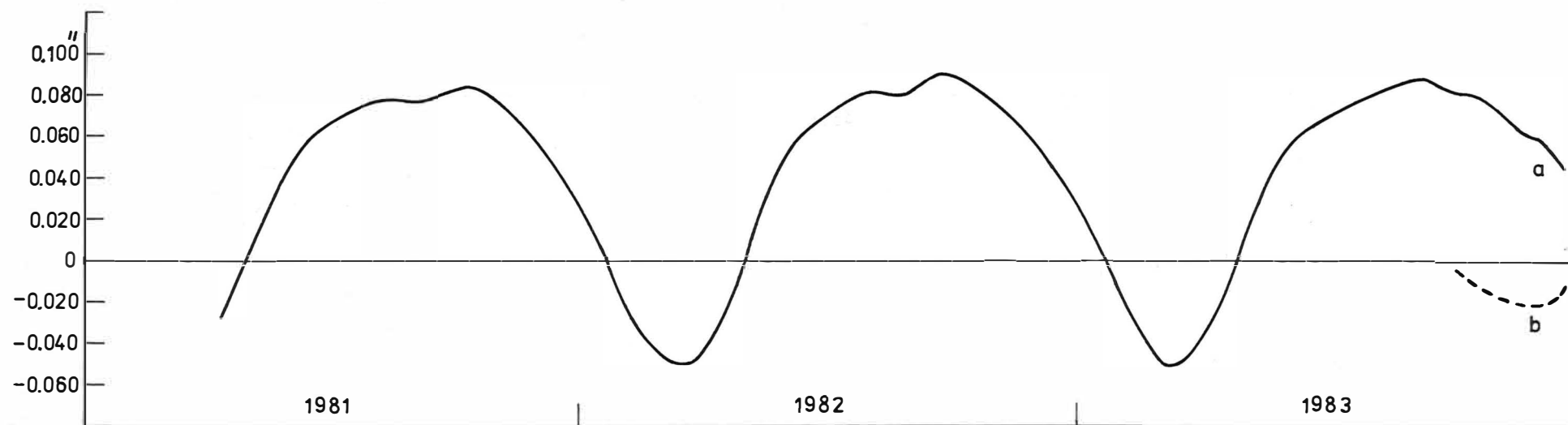


Fig. 5 Differences of the latitude determinations

- a) between the systems of the catalogs PZT 80 and NPZT 74
- b) between the old and the new systems of astronomical constants

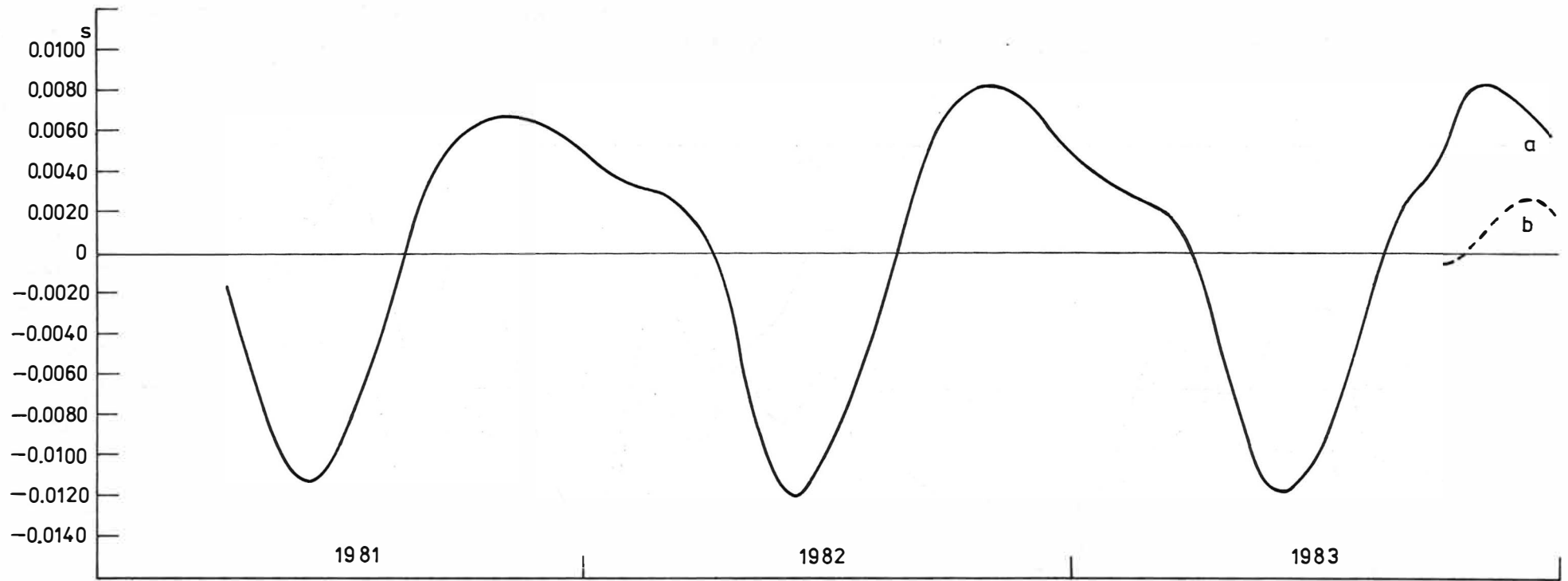


Fig. 6 Differences of the time determinations

- a) between the systems of the catalogs PZT 80 and NPZT 74
- b) between the old and the new systems of astronomical constants

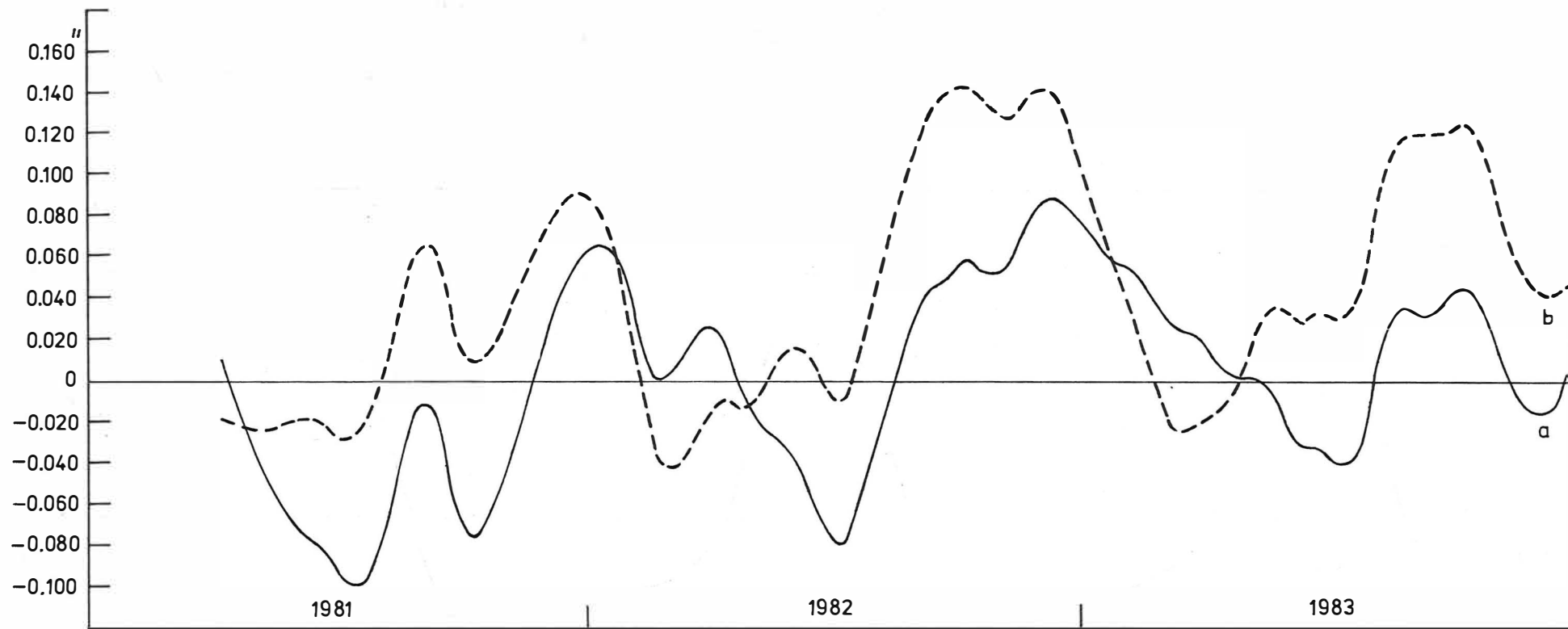


Fig.7 Differences of the latitude determinations in the systems of the catalogs PZT 80 (a) and NPZT 74 (b) respectively in reference to the BIH system

INTERACTIONS BETWEEN OCEANIC AND GRAVITY TIDES, AS ANALYSED FROM
WORLD-WIDE EARTH TIDE OBSERVATIONS AND OCEAN MODELS.

P. Melchior, B. Ducarme, M. Van Ruymbeke, C. Poitevin, M. De Becker

Observatoire Royal de Belgique
Avenue Circulaire 3, 1180 Bruxelles, Belgium.

ABSTRACT

The problem of interactions between earth tides and oceanic tides is rather complex as it involves effects of newtonian attraction, loading and associated change of earth potential, tangential pressure and friction on the moving ocean floor which are not always easy to evaluate, principally for coastal or island stations.

This paper takes advantage of two facts :

- (1) By the end of 1983 the International Center of Earth Tides has collected and evaluated a considerable amount of data from 223 stations including those of the Trans World Profiles developed by the same group of authors (102 stations). This ensures, for the first time, a World wide distribution including the tropical areas and the southern hemisphere.
- (2) In 1978-80, new oceanic cotidal maps of high quality, established by E.W. Schwiderski, became available.

We have calculated, for the eight principal tidal waves, the correlations between the observed gravity variations and those resulting from a calculation based upon the Schwiderski maps. This correlation is highly significant.

At the level of accuracy of the best transportable gravimeters the agreement is perfect except at a few places where effects of lateral heterogeneities in the mantle can perhaps be suspected.

These cotidal maps can therefore be safely used as working standards for other geodetic and geophysical applications.

INTRODUCTION

There are presently in geodynamics a number of problems where a very precise correction (or prediction) for tidal effects is needed :

gravimetry, altimetry, VLBI, laser ranging to the Moon and satellites, etc. As an example, in terms of the vertical component of gravity, "precise" means $1 \mu\text{gal}$ ($= 10^{-8} \text{ ms}^{-2}$), and, probably soon, better than $1 \mu\text{gal}$ (Melchior, 1983). A working standard to be used as a model for such precise tidal computations is not easy to select because of the complication of ocean-continent tidal interactions which consist in a number of intricated effects. These are :

- the direct attraction of the periodically moving masses of water upon the ground based instruments
- the flexure of the ground under the load of these masses
- the change of the earth's potential due to this load deformation of the earth
- a modification of oceanic tide height due to the body tide of the ocean's bottom.

These interactions can be predicted using Farrell's procedure (1972) based upon Green's functions, provided that a good model of the various oceanic tidal components is available. Their evaluation depends upon the chosen rheological model of the earth's interior.

Thus, precision Earth Tide measurements carry much information about the tides of the Ocean, about heterogeneities in the lithosphere and mantle as well as about liquid core dynamics. All these informations are to be extracted now.

At first sight we believed that a model composed of homogeneous isotropic spherical layers is much more likely to be valid for the body tide, having significant displacements through most of the earth's volume, than for the load tide whose displacements are appreciable only in the lithosphere and upper mantle. Differences in lithospheric structure, as beneath ocean basins and continents, would therefore affect the load more than the body tide.

Near the load the surface deformation is very sensitive to the properties of sediments. At larger distances from the load one has to take into account structures down to generally a depth two or three times the horizontal distance between the load and the point of observation. Lack of knowledge of these lithospheric features is the reason why the loading effects are presently not accurately predictable. Eventually these features must be determined in order to produce correct tidal predictions for precision measurements.

However, the most recent results, derived from world wide tidal gravity measurements, lead Melchior and De Becker (1983) to conclude that some anomalies observed in specific tectonic areas could be due to very deep lateral heterogeneities.

TRANS WORLD TIDAL GRAVITY PROFILES

There was a considerable handicap to the use of such a method of

investigation which was due to the complete lack of reliable observations in some 80 % of the surface of the Earth and particularly in all the Southern hemisphere.

To fulfil these gaps in data the Royal Observatory of Belgium (Bruxelles) and the International Centre for Earth Tides have jointly organized measurements in Asia, Africa and the South Pacific. Starting in 1973, a first tidal gravity profile extending over 17400 km from Istanbul to Papeete (Tahiti) involves 36 stations. A second profile from Cape to Cairo involves 20 stations in East Africa. A program in East Asia involves 10 stations in China, 5 in Japan and 1 in Korea.

Transportable recording instruments (Geodynamics and LaCoste Romberg gravimeters) were used, precise enough to reach a precision of few tenths of microgals on the amplitude of the tidal waves after 4 to 6 months of continuous recordings which was, at each place the duration of observations indeed but rather more extended measurements have been made at Brussels, Canberra, Alice Springs and Wuhan. Before starting the experiment all the instruments were first very carefully compared at the Brussels station to determine their instrumental constants (Ducarme, 1975). A check was made at Canberra and at Wuhan by comparing again five or four of the instruments.

When this programme started - in 1973 - no one of the existing oceanic tide models fitted the earth tide observations. Therefore the initial objectives of these measurements were :

- (1) To determine to what extent measurements in continental stations like Urumqui, Lanzhou or Alice Springs are free from oceanic tidal influence and can thus be considered as "load amphidromic points".
- (2) To compare coastal station results with those from continental stations and to see if the tidal parameters (amplitude factor δ and phase difference α) exhibit any regional behaviour and what is the extent of such regions.
- (3) To check if any one of the existing cotidal charts permit adequate correction of the observed data so that one will obtain identical tidal parameters at all the places, that moreover fit the Love numbers obtained by the integration of the fundamental equations of the spherical elasticity when using the best models of the earth's interior.
- (4) In the event that is proved to be impossible, to see if any improvement or correction of the cotidal charts may be done or if another geodynamical process or geophysical parameter has to be invoked to explain the observed anomalies.

Since 1979, Schwiderski (1979, 1980a,b) has constructed new cotidal maps for the nine main tidal waves Q_1 , O_1 , P_1 , K_1 , N_2 , M_2 , S_2 , K_2 , M_f by integration of the classical Laplace equations completed with terms allowing for bottom friction, turbulent dissipation and tidal vertical movements of the ocean bottom. This integration is based upon a $1^\circ \times 1^\circ$ grid which means that most of the coastal areas are included.

It consequently became one of our major aims to compare the on-shore gravimetric tide measurements with the effect calculated with the Schwiderski maps (as well as with other available maps). We can consider indeed that a cotidal map which allows generation of computed attractions and loads in agreement with the Earth tide gravity measurements over a sufficiently broad area can be used with confidence as a working standard for height, tilt and strain tidal corrections or to apply the necessary corrections to high-precision measurements performed by new techniques like altimetry, very long-baseline interferometry (VLBI), Moon and satellite laser ranging and absolute gravity. Such measurements are extremely important for earthquake prediction by allowing to control crustal uplifts, fault motions and stress-strain accumulation.

To correctly control the minute changes involved, tidal corrections must be applied with a precision of $1 \mu\text{gal}$ or better, which corresponds to about 3 millimeters in height. This is not an easy task.

On the other hand valuable information about global oceanic and solid Earth tides has been derived from satellite perturbation data over the last years by many authors (Melchior, 1983, ch. 15). Because they all have exactly the same frequencies, it is impossible to separate in this way the individual contributions of the oceans, of the Earth tide and of the interactions between ocean and crust (even if a dependence of the satellite orbit inclination is apparent). Therefore, a net of ground measurements is essential to serve as a ground base and should complement the satellite measurements.

INTERPRETATION OF THE RESULTS BY A VECTOR DIAGRAM

In our previous papers we introduced the following definition of the "residual vector" \vec{B}_i (B_i , β_i) :

$$B_i \cos (\omega_i t + \beta_i) = \{ \delta_i A_i \cos (\omega_i t + \alpha_i) - \delta_i^{\text{th}} A_i \cos \omega_i t \} f(\phi) \quad (1)$$

where i refers to the tidal component considered (Q_1 , O_1 , P_1 , K_1 , N_2 , M_2 , S_2 , K_2). A_i is the "theoretical" tidal amplitude calculated for a rigid Earth model with the Cartwright-Tayler-Edden tidal potential, ω_i being the tidal frequency, α_i the observed phase lag. $f(\phi)$ is the dependence on the latitude ϕ for the various tidal families, and δ_i^{th} and δ_i are respectively the theoretical and the observed amplitude factors. The δ_i^{th} allow the deformation of an elastic Earth model to be taken into account. Hydrodynamic effects of the flattened liquid core are sufficiently well established that this Earth model should include them : they reach up to 2 % of the amplitude of the most important diurnal wave (K_1).

In terms of Love numbers :

$$\delta = 1 + h - \frac{3}{2} k \quad (2)$$

Equation (1) can be written

$$\vec{B} = \vec{A} - \vec{R} \quad (3)$$

as shown on the figure 1, $\vec{A} (\delta_1 A_1, \alpha_1)$ being the observed tidal vector and $\vec{R} (\delta_1^{\text{th}} A_1, 0)$ the calculated tidal vector for an oceanless elastic earth model with liquid core. The mean square error on the experimental determination of \vec{A} is represented by the error circle of radius ϵ .

We also define the corresponding "load vector" $\vec{L} (L_1, \lambda_1)$ which contains the periodic attraction as well as loading effects of oceanic tides. This is calculated by the Farrell procedure (1972) based upon Green's functions, on the basis of the Schwiderski cotidal maps.

Our computation program, written by M. Moens (Melchior et al. 1980), is based upon the following principles.

- (1) The Newtonian attraction is directly calculated taking the altitude of the stations into account.
- (2) The load deformation of the ground is calculated by polynomial interpolation in the Farrell tables without considering the altitude, this effect being considered as negligible.
- (3) Mass conservation of oceanic waters has been ensured by two alternative procedures : (a) a uniform correction which consists in the introduction of a sheet of water of constant thickness with a constant phase; (b) a correction proportional to the tidal amplitude, which is thus larger in the coastal areas. Both procedures give the same result at the 0.1 μgal level. Procedure (b) was employed rather than (a).

There are about 45000 polygons $1^\circ \times 1^\circ$ in each Schwiderski cotidal map but, for near-shore stations, the nearby oceanic $1^\circ \times 1^\circ$ zones have been redivided into smaller and smaller squares up to $0.125^\circ \times 0.125^\circ$ in size. When the centre of a small square is less than 10 km from a station the corresponding effect has not been taken into account. This is essential because if the observing station is very near to the centre of such a square, the evaluation loses any physical meaning.

To compare the vectors \vec{B} and \vec{L} , we calculate the correlation of $B \cos \beta$ with $L \cos \lambda$ and the correlation of $B \sin \beta$ with $L \sin \lambda$ as well. This is done for the eight main waves and, in each case, for three Earth models which differ in the latitude dependence of the δ parameter.

This latitude dependence results from the flattening of the Earth as well as from Coriolis and centrifugal force. It was theoretically demonstrated by Love (1911) and Wahr (1981) and experimentally established by Melchior (1981), Melchior and De Becker (1983).

Ocean-continent tidal interactions have total amplitudes reaching 2-3 μgal in continental Europe but 5-10 μgal in Spain or the United Kingdom. Around the Indian Ocean (East Africa and South East Asia) they also reach 30 μgal , while up to 40 μgal interactions have been observed in the South Pacific Islands (Melchior et al., 1981).

A very important feature is that, as clearly shown by Fig. 1, the correlation between $B \sin \beta$ and $L \sin \lambda$ is not affected by the choice of the Earth model, $B \sin \beta$ being independent of it on the condition that the viscous phase lag of the Earth is negligible, which has been demonstrated by Zschau (1978). This can provide a check for the instrumental calibrations and/or for the oceanic cotidal maps.

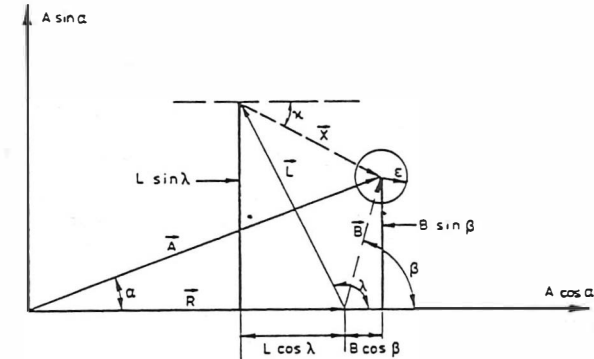


Fig. 1. Comparison of observed and calculated ocean-continent tidal interactions. For the semi-diurnal M_2 wave, the correct scale of this figure should be : $R \approx A \approx 40$ (Europe)-90 (Equator) μgal ; $\alpha \approx 0 - \pm 5^\circ$; $L \approx B \approx 2$ (Europe)-10 (South Pacific) μgal ; $X \approx 0.5-5$ μgal ; $\epsilon \approx 0.5$ (Europe)-1 (Equatorial zone) μgal ($\vec{B} = \vec{A} - \vec{R}$, $\vec{B} - \vec{L} = \vec{X}$).

The essential result was that the recent Schwiderski maps (1979, 1980a,b) fulfil these requirements to a large extent, so that it seems appropriate to use these cotidal maps as working standards to correct Earth tide parameters (amplitude factors and phases) for the influence of oceanic tides. The use of the same maps for all stations preserves the homogeneity of the network.

A final residue vector $\vec{X} (X, \chi) = \vec{B} - \vec{L}$ is then calculated :

$$X_1 \cos (\omega_1 t + \chi_1) = B_1 \cos (\omega_1 t + \beta_1) - L_1 \cos (\omega_1 t + \lambda_1). \quad (4)$$

This vector shown in fig. 1, contains the unexplained part of the observed residual vector \vec{B} . When $|\vec{X}| > \epsilon$ it is suspected to contain the following systematic effects :

Instrumental systematic errors :

- Calibration (frequency-dependent)
- Thermal influences
- Barometric effects
- Power supply, ground connection, dead band of the recorder
- Drift.

Geophysical effects :

Lateral heterogeneity of lithosphere and upper mantle
Local distortions of the oceanic cotidal maps
Load barometric effect.

Computation errors :

Map digitization, computer processing
Errors in coordinates, imperfections of analysis method.

An important result of our analysis was that the sine component $X \sin \chi$ appears quite always smaller than 0.5 μgal while the cosine component $X \cos \chi$ may reach at some specific places up to 5 μgal . This is reflected in the correlation coefficients given in the Table 1. One may logically suspect therefore an effect of deep lateral heterogeneities of the lithosphere and upper mantle (Melchior and De Becker, 1983).

TABLE 1
Correlation coefficients between observed residue \vec{B} and oceanic loading \vec{L}

Wave	N	Cosine component	Sine component
Q ₁	32	0.776	0.702
O ₁	175	0.516	0.778
P ₁	55	0.567	0.720
K ₁	177	0.459	0.643
N ₂	171	0.698	0.776
M ₂	180	0.848	0.929
S ₂	179	0.717	0.634
K ₂	53	0.723	0.770

Note that S₂ wave contains a non negligible contribution from atmospheric tides.

N : number of ground based tidal gravity stations.

CONSIDERATIONS ABOUT SOME TYPICAL AREAS

A detailed analysis of the different areas where measurements have been made is given in (Melchior et al. 1981). We will here restrict ourselves to a few typical examples.

Europe

There is a very high density of tidal stations in Europe, occupied with many different instruments from different institutions.

The observed residues \vec{B} exhibit an outstanding fitting with the loading effects \vec{L} well under the noise estimation ϵ (0.3 μgal). Six stations present however a $X \cos \chi$ residue of 1 to 2 μgal . These stations are located in the two different areas of extreme lithosphere's thickness existing on both sides of the Alps (Melchior and De Becker, 1983; Melchior et al. 1983b).

Indian Ocean

The considerable discrepancies between the Indian Ocean cotidal maps proposed by the different authors were attributed by some of them to the fact that this area is very near to a resonance with tidal frequencies, so that slight changes or errors in the dimensions (which depend of course upon the grid dimensions) displace the eigen-frequencies and cause great differences in the results.

Schwiderski refuted this point of view. In his model the M₂ tide is only 40 cm in the centre of the Indian Ocean while it reaches 138 cm in the Hendershott model.

Our measurements around the Indian Ocean fit in general quite well the Schwiderski cotidal map. In particular our station at Antananarivo which, with its geographical position in the centre of Madagascar, 150 km from the sea, is surely a strategic place for checking the cotidal maps of this ocean.

Far East (China, Japan, Korea)

This area is also interesting because of the complicate pattern of the tides inside the gulf of Chihli and the Korea Bay.

With some 10 stations all around we have been able to show that the M₂ world Schwiderski map leaves a final unexplained residue of about 1 μgal but with a rather systematic negative phase. This is larger than the noise. By introducing corrections from local cotidal maps of this gulf, this residue reduces to 0.5 μgal while the phase got a large dispersion showing that it more or less represents noise.

THE DIURNAL TESSERAL WAVES IN SOUTHEAST ASIA AND INDONESIA

We expected that this zone would be the most crucial test for three essential reasons.

- The South China Sea is a resonant diurnal system : the amplitudes of the K₁ and O₁ tidal waves reach more or less 0.5 m in the area.
- Because of obvious geographical reasons all our stations are more or less coastal.
- The diurnal direct Earth tide is extremely small as all our stations are very close to the equator.

This explains why our O₁, K₁ and occasionally P₁ load vectors amount to 1-3.5 μgal over all this area.

A first typical feature to be observed is that the phase difference in the K₁ and O₁ load signals fits everywhere with the corresponding difference in the neighbouring harbours, with only one exception in Manila, as shown in Table 2. This shows evidently that the experimentally obtained load vector is mainly sensitive to the near-sea tides.

An remarkable check is also offered by the wave P₁ which, in general, is difficult to extract from earth tide data, its period being

TABLE 2

South East Asia and Indonesia

$K_1 - Q_1$ residual phase difference in degrees : (a) observed with gravimeters;
(b) in the nearest sea.

		(a)	(b)
Southeast Asia			
2460	Colombo (Sri Lanka)	18	29
2501	Bangkok (Thailand)	-56	-43
2551	Penang (Malaysia)	-32	-58
2550	Kuala Lumpur (Malaysia)	-46	-58
2601	Hong Kong	-15	-50
4010	Baguio (Philippines)	-20	-40
4011	Manila (Philippines)	-3	-41
2555	Kota Kinabalu (Malaysia)	-33	-50
2701	Saigon (Vietnam)	-43	-20
Indonesia			
4105	Banjar Baru (Indonesia)	-36	-40
4100	Bandung (Indonesia)	-34	-23
4110	Ujung Pandang (Indonesia)	-13	-22
4111	Manado (Indonesia)	-15	
4150	Jaya Pura (Indonesia)	-14	-21
4160	Port Moresby (Papua)	-36	
4210	Darwin (Australia)	-47	-23

equal to 23h 53m 57s makes its frequency very close to the K_1 and S_1 frequencies so that only very good instruments, carefully protected against barometric as well as thermal disturbances, have been able to isolate it (Melchior, 1978).

However, this tidal component, which is the third in amplitude in the tesseral family, is of major interest for investigations of the liquid core hydrodynamical oscillations. It is with great satisfaction that we can point out here that the load effects computed from the Schwiderski P_1 cotidal map are in close agreement with the observed P_1 loads in all the thirteen stations where we could separate it from K_1 and S_1 and where, of course, this P_1 signal was not too weak (see Table 3).

SMALLER COMPONENTS Q_1 AND K_2

In a paper presented at the IAG Commission on Earth Tides, Melchior, Ducarme and Chueca (1983a) show that a fair agreement is also found for these waves between observed and calculated ocean-continent interactions. Q_1 wave has a maximum amplitude of 6 microgals at 45° latitude. K_2 wave

TABLE 3
 P_1 wave. Observed and calculated loading and attraction effects.
Observed residues with respect to Molodensky Model I.
(All stations where $B \geq 0.3 \mu\text{gal}$ are considered).

Station	Observed residue		Schwiderski map		Vectorial difference	
	B(μgal)	β (°)	L(μgal)	λ (°)	X(μgal)	χ (°)
9904 Kerguelen (TAF)	0.40	-82	0.37	-106	0.16	-14
2600 Guangzhou (China)	0.33	-94	0.40	-92	0.07	97
2612 Shanghai (China)	0.38	-28	0.43	-32	0.06	123
2823 Kyoto (Japan)	0.60	-26	0.64	-7	0.21	-118
2847 Mizusawa (Japan)	1.13	4	0.76	5	0.37	4
3019 Djibouti (Afar)	0.62	139	0.65	147	0.10	36
3020 Mogadiscio (Somalia)	0.57	104	0.78	137	0.43	2
4105 Banjar Baru (Indonesia)	1.57	-125	0.90	-115	0.70	-137
4115 Kupang (Indonesia)	0.85	-116	0.92	-118	0.11	42
4160 Port Moresby (Papua)	0.87	-16	0.91	-19	0.06	113
4209 Alice Springs (Australia)	0.28	-106	0.18	-133	0.18	-27
4205 Armidale (Australia)	0.46	7	0.26	38	0.27	-24
6004 Uwekahuna (Hawaii)	1.17	83	1.03	102	0.39	23

has a maximum amplitude of 9.5 microgals at the equator. The residues reach a maximum of 0.5 μgal for Q_1 , 1 μgal for K_2 . Despite these very low amplitudes their phases are in fair agreement which shows that the noise in our measurements seems to be less than 0.3 μgal .

LOADING AMPHIDROMIC POINTS

For many years it has been of interest to find points where the oceanic effects are minimized, even possibly zero. The question is whether such points exist. If they could be discovered it would be worthwhile to install there the best gravimeter to investigate the hydrodynamic effects of the Earth's liquid core. It is also interesting to look at such points for absolute gravity measurements. However the geographical position of such a point will be different for each tidal component.

At a certain distance from a sea the direct attraction of its water masses and their loading effect are equal and opposite, cancelling in such a way that the effect of the ocean is virtually zero. This is true only for the nearest sea and as the more distant oceans have a significant effect it is not easy to predict where the effects of all the oceans together will cancel. This not necessarily happens just in the centre of each continent.

We have calculated such maps for each continent (Melchior, Ducarme 1983). The M_2 map for Africa is given on the figure 2. It shows indeed

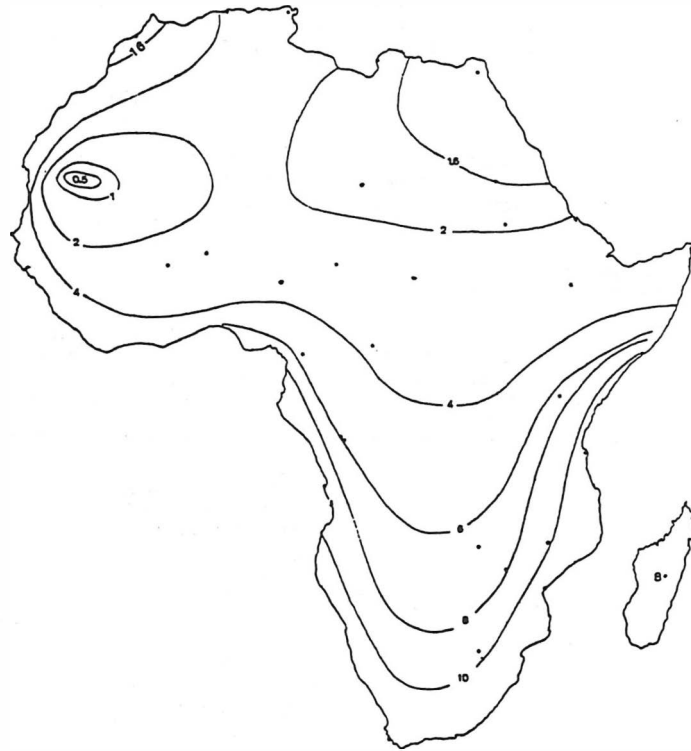


Fig. 2. Tidal loading and attraction effects in Africa. Tidal wave M_2 amplitudes, given in μgal , are peak to peak.

that the minimum of attraction and loading is not located in the middle of the continent at all but in the Republic of Mauretania.

It is clear from our Trans-World Tidal Gravity Profile that one such point must exist in Australia for the M_2 wave, between Alice Springs and Broken Hill, which is indeed confirmed by the Parke map (1979) (at $\phi = -28^\circ 30'$, $\lambda = 137^\circ 30'$) but not by the Schwiderski or any other map. The M_2 Parke map indicates, moreover, that such points exist also in Argentina, near Tucuman ($\phi = -28^\circ$, $\lambda = 297^\circ$) and in Texas, west of Dallas ($\phi = +33^\circ$, $\lambda = 260^\circ$) while the M_2 Schwiderski map gives amphidromic points at $\phi = 33.5^\circ \text{ N}$, $\lambda = 106.5^\circ \text{ W}$ in New Mexico and north-west of Lanzhou ($\phi = +37^\circ$, $\lambda = 103^\circ 30'$) in China.

With the O_1 Schwiderski map we have not found any amphidromic point in Australia even if the load is everywhere very small there. We also found that over a broad area in China (between 25° and 35° N , 84° and 92° E) the O_1 load is nearly uniformly small as it does not exceed $0.1 \mu\text{gal}$. The situation is similar in Africa (northern Nigeria, Tamanrasset, Bangui).

CONCLUSIONS

At the level of some parts in 10^{-10} of g , we obtain a general agreement between two completely independent methods of investigation i.e. the mathematical construction of oceanic cotidal maps on one side and the on shore tidal gravity variations observations on the other side.

It is time now to consider new refinements of both types of approach. In the modelisation of interactions, we should introduce viscosity and lateral heterogeneities in the mantle and, as pointed out by Schwiderski some contributions which have been discarded until now: horizontal pressure of the sea on the shelf slopes, self loading of earth tides and Coriolis force.

The world coverage of tidal gravity measurements has been considerably improved since 1973 by the Trans World Tidal Gravity Profiles (figure 3) but is still far from being sufficient. By the end of 1983 there are only very few measurements available on the American continent. Our team starts measurements in Brazil just by the end of this year. The great number of data already compiled required the organization of an Earth Tides Data Bank (Ducarme, 1983). This Data Bank is extremely flexible, allowing now the statistical investigation of different oceanic and earth tides models.

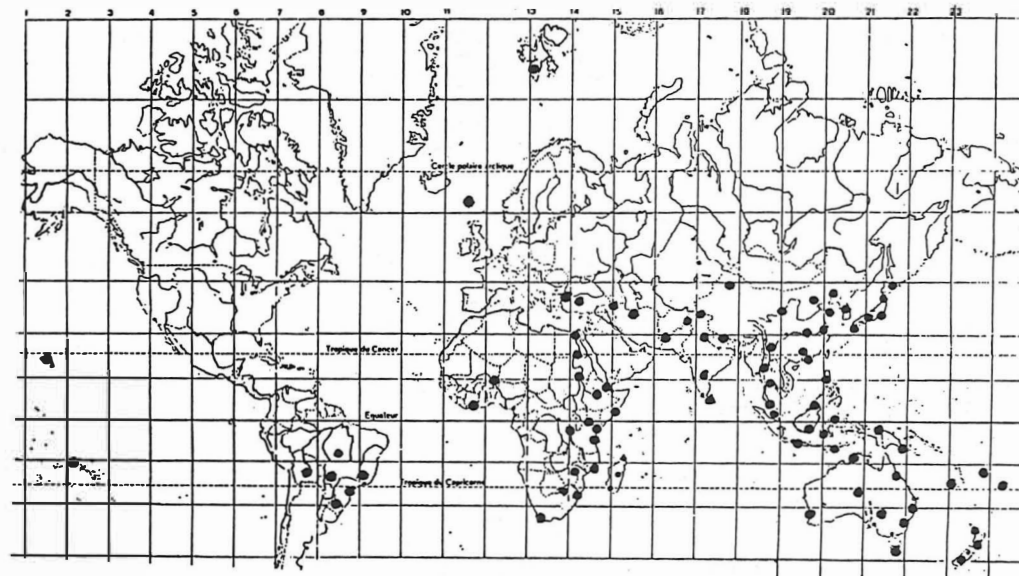


Figure 3. Trans World Tidal Gravity Profiles 1973-1984
 performed by the Royal Observatory of Belgium and the International Center for Earth Tides, Brussels
 (because of their high density in Europe, stations are not indicated in this area).

REFERENCES

- Ducarme, B. : 1975, A fundamental station for trans-world tidal gravity profiles.
Phys. Earth Planet. Inter., 11 : 119-127.
- Ducarme, B. : 1983, A Data Bank for Earth Tides.
IUGG General Assembly, Hamburg - Symposium 6 : Data Management.
Bull. Inf. Marées Terrestres 91 : 5963-5980.
- Ducarme, B. and Melchior, P. : 1978, A Trans-world tidal gravity profile.
Phys. Earth Planet. Inter., 16 : 257-276.
- Farrell, W.E. : 1972, Deformation of the Earth by surface loads.
Rev. Geophys. Space Phys., 10 : 761-797.
- Love, A.E.H. : 1926, Some problems of Geodynamics.
Dover Publications, Inc. New York.
- Melchior, P. : 1981, An effect of the earth ellipticity and inertial forces is visible from M_2 and O_1 tidal gravity measurements in the Trans World Profiles.
9th Intern. Symposium on Earth Tides, New York. Comm. Obs. R. Belg., A 63, S. Geoph. 141 : 1-9.
- Melchior, P. : 1983, The Tides of the Planet Earth.
Pergamon Press, 2nd edition, 641 pages.
- Melchior, P., Moens, M. and Ducarme, B. : 1980, Computations of tidal gravity loading and attraction effects.
Bull. Obs. Marées Terrestres, Obs. R. Belg. 4, fasc. 5 : 1-94.
- Melchior, P., Moens, M., Ducarme, B. and Van Ruymbeke, M. : 1981, Tidal loading along a profile Europe - East Africa - South Asia - Australia and the Pacific Ocean.
Phys. Earth Planet. Inter., 25 : 71-106.
- Melchior, P. and De Becker, M. : 1983, A discussion of world-wide measurements of tidal gravity with respect to oceanic interactions, lithosphere heterogeneities, Earth's flattening and inertial forces.
Phys. Earth Planet. Inter., 31 : 27-53.
- Melchior, P., Ducarme, B. and Chueca, R.M. : 1983a, The small tidal waves Q_1 and K_2 as an evidence of the accuracy of the trans world tidal gravity measurements.
IUGG General Assembly, Hamburg - IAG Commission on Earth Tides.
Bull. Infor. Marées Terrestres 91 : 5981-5986.
- Melchior, P., De Becker, M., Ducarme, B., Poitevin, Ch. and Van Ruymbeke, M. : 1983b, Effect of lateral heterogeneities in the lithosphere on tidal measurements.
IUGG General Assembly, Hamburg - IAG Commission on Earth Tides.
Bull. Infor. Marées Terrestres 91 : 5987-5991.
- Parke, M., E. and Hendershott, M., C. : 1979, M_2 , S_2 , K_1 models of the Global Ocean Tide on an Elastic Earth.
Marine Geodesy, 3 : 379-408.
- Schwiderski, E.W. : 1979, Global Ocean Tides. Part II. The Semidiurnal Principal Lunar Tide (M_2), Atlas of Tidal Charts and Maps.
Naval Surface Weapons Center, Dahlgren Laboratory TR 79-414, Dahlgren, VA.
- Schwiderski, E.W. : 1980a, On charting global ocean tides.
Rev. Geophys. Space Phys., 18 : 243-268.
- Schwiderski, E.W. : 1980b, Ocean tides. Part I. Global ocean tidal equations. Part II. A hydrodynamical interpolation model.
Mar. Geodesy, 3 : 161-255.
- Wahr, J. : 1981, Body tides on a elliptical, rotating, elastic and oceanless earth.
Geophys. J. R. Astron. Soc. 64 : 677-704.
- Zschau, J. : 1978, Tidal Friction in the Solid Earth : Loading Tides Versus Body Tides.
Tidal Friction and the Earth's Rotation, Springer-Verlag Berlin : 62-94.

CAPACITIVE PENDULUM WITH INTELLIGENT DATA
COLLECTION

Gy. Mentés

Geodetical and Geophysical Research Institute
of Hungarian Academy of Sciences /GGRI/ Sopron,
Hungary

Abstract

In order to find new application fields for horizontal pendulums in geodynamic measuring techniques their improvement is very important. Conventional recording systems are not very convenient for geodynamic phenomena, therefore a new capacitive horizontal pendulum with electric output and an intelligent digital data recorder has been constructed. For the reproduction of the original signal this latter also uses logical decisions besides mathematical filtering of the data. That is the reason why analog recording can be abandoned and it is not necessary to store all sampled data. The recorder can be programmed for various kinds of tasks.

Zusammenfassung

Um neue Anwendungsmöglichkeiten für Horizontalpendel in der geodynamischen Messtechnik zu finden ist die Verbesserung von Horizontalpendeln sehr wichtig. Die herkömmlichen Registrierungssysteme sind für Registrierung der verschiedenen geodynamischen Phänomene nicht völlig geeignet, deshalb wurde ein neues kapazitives Horizontalpendel mit elektrischem Ausgang und einem intelligen-

ten digitalen Datenregistrierungssystem konstruiert. Um das originale Signal wiederherzustellen benutzt das letztere gewisse logische Entscheidungen neben den mathematischen Filtermethoden für Filterung der Daten. Aus diesem Grund kann die analoge Registrierung weggelassen werden und es ist nicht nötig alle gemessene Werte zu speichern. Das digitale Registrierungsgerät kann für verschiedene Messaufgaben programmiert werden.

1. Introduction

Recently more and more data are needed for the study of geodynamic phenomena. To acquire this mass of data with the required accuracy new measuring instruments and automatic digital data acquisition systems are to be developed. The conventional horizontal pendulums with photorecorder used for Earth tide recording do not comply with requirements of modern measuring and computation technique. This is the reason why we have developed a horizontal pendulum with capacitive transducer which supplies an electric signal and therefore it can be easily integrated with digital data acquisition and processing systems. The traditional analogous pendulum records are read out manually or by means of a curve digitizer /indirect digitizing/ at hourly time marks. In this case the quality of the digitization is completely depending on the evaluating person making a manual prefiltering of the tidal curve which always contains some microseismic oscillations, spikes, steps and gaps.

By sampling the output signal of the capacitive pendulum by means of a simple digitizer at hourly time marks the error of the digitizing can be very high because of the above-mentioned properties of the tidal signal. In this case an analog record is also needed to verify the digital data. Another solution is the

increasing of the sampling rate what increases the number of data to be stored /Jentzsch, 1981; Plag and Jahr, 1983/.

To solve this problem we have developed an intelligent digital data acquisition system which works with a high sampling rate and is capable to prefilter tidal data by means of mathematical filtering algorithms and logical decisions. Therefore it gives out correct and reliable tidal data at hourly time marks and need no large storage capacity for tidal recording.

2. The construction and functioning of the capacitive pendulum

Our horizontal pendulum is a metal pendulum and has a Zöllner suspension. Figure 1 shows the top- and profile-view of the pendulum. Its base /1/ is a right-angled triangular plate which is rigid enough to hold the whole pendulum with high stability. The base plate is standing on a fixed foot /L/ which is placed in the right angled corner and on two levelling screws /L₁; L₂/ in the acute-angled corners. On the base plate there is a bracket /8/ with clamps /6, 7/ for suspension wires. The two wires clamped at points A and B hold the pendulum beam /9/, in horizontal position. The wires are made of tungsten and have a diameter of 20 µm.

The sensitivity of the pendulum is depending on the deviation of rotation axis AB of the pendulum beam from the vertical. The deviation can be decreased or increased by means of the levelling screw L₁ denoted "sensitivity screw". The smaller this angle is the more sensitive the pendulum is. At zero angle the sensitivity is infinitely high and the pendulum is in an instable state. If the vertical changes perpendicularly to the vertical plane of the pendulum beam the latter will move to a new vertical plane containing the rotation

axis AB i.e. the pendulum beam rotates around the axis AB in the horizontal plane. The same effect can be caused by tilting the pendulum around the axis containing the top of the fixed foot /L/ and one of the sensitivity screw /L₁/ by means of the "drift screw" /L₂/.

In this latter case the position of the rotation axis AB is changed against the vertical. A capacitive transducer is applied to measure electrically the rotation angle of the pendulum beam. The capacitive transducer is a differential plane condenser, the functioning of which is based on the change of the surface of opposite-standing plates. The moving plate /11/ is fixed and electrically connected to the pendulum beam because the output of the capacitive transducer is led out via the suspension wires. That is the reason that a glass plate is under the bracket to insulate it from the base plate.

The standing plates /12/ of the differential condenser are insulated from each other and from the console /13/ by a glass plate, too. The differential condenser connected together with two fixed capacitances of equal value forms a capacitive bridge circuit. The console holding the standing plates is adjustable to balance the bridge at the middle position of the pendulum beam.

Figure 2 shows the electric construction of the capacitive pendulum. The bridge is supplied by a sinewave oscillator of high amplitude stability. The amplitude of the supply voltage is 20 V and the frequency is 15 kHz. The output voltage of the bridge is detected by the high input impedance preamplifier /15/ placed near to the transducer under the console. The input of the preamplifier is connected to the wire

clamp /7/ and its output voltage is transferred on a low impedance via the connector /16/ to the separate electronical unit which contains all other electric parts with the exception of the preamplifier. The preamplifier is followed by a selective amplifier and phase-sensitive rectifier which enables the sign-correct measurement of the deviation of the pendulum beam from its zero position. The phase-sensitive rectifier is followed by a third-order Butterworth low-pass filter for filtering the self-swinging of the pendulum. The output signal of the low-pass filter is amplified by a DC amplifier, the output of which is the filtered output. In most cases we need an unfiltered output which is the output of a DC amplifier amplifying directly the output signal of the phase-sensitive rectifier. If the capacitive pendulum is inserted into a measuring system it is very important to know its transfer function which is depending on the eigenperiod of the pendulum. Figure 3 shows the transfer function of the pendulum relative to the unfiltered output at different eigenperiods.

3. The intelligent digital data acquisition system

Figure 4 shows the block diagram of the data acquisition system. It is controlled by a microprocessor MC 6802 from MOTOROLA. The controller program is stored in the EPROM memory. The RAM memory is used for calculations and temporary storage of data as a buffer memory. When the buffer memory is full, the sampled or preprocessed data can be transferred in blocks into the exchangeable non-volatile semiconductor memory which can be exchanged as a cassette, or into the cassette unit, or the data can be directly transferred via a telephone line to a large computer.

The exchangeable semiconductor memory is more reliable under conditions of an Earth tide observatory than the cassette unit which contains moving mechanical parts. The storage capacity of the exchangeable semiconductor memory is sufficient for about 15 days to store the prefiltered hourly value of tidal data measured by a pair of horizontal pendulums including the storage of environmental parameters too. The digital recorder system has 16 analog input channels, an analog multiplexer, and a 12-bits analog to digital converter. The sampling and converting of the analog channels is controlled by the master processor.

The exact time is given by the real-time clock which can be synchronized by means of a DCF-77 receiver. The speed of the system can be increased applying a slave processor which can be a high speed arithmetic or a FFT processor depending on the desired filtering algorithm. The data acquisition system has a keyboard and a display too, for manual control and for input and display parameters needed for data sampling and filtering.

On the one hand the intelligent digital data acquisition system can be used as a simple digitizer. In this case it samples and digitizes the analog input signals with the given sampling rates and stores them in blocks on cassette tape. This is advantageous if both the preprocessing and the processing are to be made on a large computer /e.g. recording of the free oscillation of the Earth/. On the other hand the intelligent digital data acquisition system can do the preprocessing.

That means in the case of Earth tide recording that the system works with a high sampling rate /1-30 s/, filters the self-swingings of the pendulum excited by earthquakes or microseismic activity, then removes the steps, using linear prediction and logical decision and

after a second filtering it stores only the hourly values of the Earth tide /Fig. 5/.

The first and the second filtering method can be a simple or a Fox-Schuller averaging for tidal records. The microprocessor can execute these algorithms with high speed.

Steps are removed as follows: the microprocessor calculates after each sampling a new smoothed and step-corrected value $s/n/$, then from previous values calculates a predicted value $s/n/p$, for $s/n/$.

Whenever $|s/n/ - s/n/p| > S$, a step is assumed and $s/n/$ is substituted for $s/n/p$ and the step correction value is corrected according to the new step. The value $s/n+1/$ will be step-corrected with this new correction value. If there is no step, $s/n/$ is stored. Because some parts of the above described system are still under construction, the filter method was tested with different sampling rates and limits S on a computer. The simulated input signal is shown in Fig. 6. The eigenperiod of the self-swinging superposed on the "simplified" tidal signal /a sinus wave of one day period/ was 50 s, the spikes and steps had half of the amplitude of the signal. The accuracy of the method depends on the quality of the linear prediction, the sampling rate and the limit S . Table 1 shows the errors of the method at different sampling rates and limits. It can be seen that both parameters have an optimum. When the limit is too low the error will be very high because the program always substitutes $s/n/$ for $s/n/p$. If the limit is too high, the program will not sense the small steps in the input signal.

Table 1.

Limit S	Sampling period [s]	Average error of the filtering in percentage of amplitude with RMS error
0.1	5	0.29 ± 0.32
0.1	10	0.72 ± 0.75
0.1	20	1.94 ± 2.14
0.05	5	0.48 ± 0.51
0.05	10	0.08 ± 0.08
0.05	20	0.33 ± 0.40
0.02	5	0.19 ± 0.07
0.02	10	0.07 ± 0.08
0.02	20	0.57 ± 0.63
0.01	5	0.37 ± 0.11
0.01	10	0.25 ± 0.10
0.01	20	0.60 ± 0.42

4. Conclusion

The microprocessor techniques makes it possible to build an intelligent digital data acquisition system which can preprocess or process tidal data automatically decreasing manual work. The above described system can be very easily reprogrammed for recording other geophysical phenomena, only the parameters /linear prediction coefficients, limit, etc/ must be chosen properly. This makes it possible together with the capacitive solution for the pendulum to record free oscillations of the Earth parallel with continuous Earth tide recording what is out of capability of conventional pendulums and recording system.

References

- Jentzsch, G., 1981: Automatic Treatment and Preprocessing of tidal data recorded at 1 min intervals, BIM, 85, 5415-5428.
- Plag, H.-P. and Jahr, T., 1983: On processing of Earth Tidal Data, BIM, 89, 5759-5786.

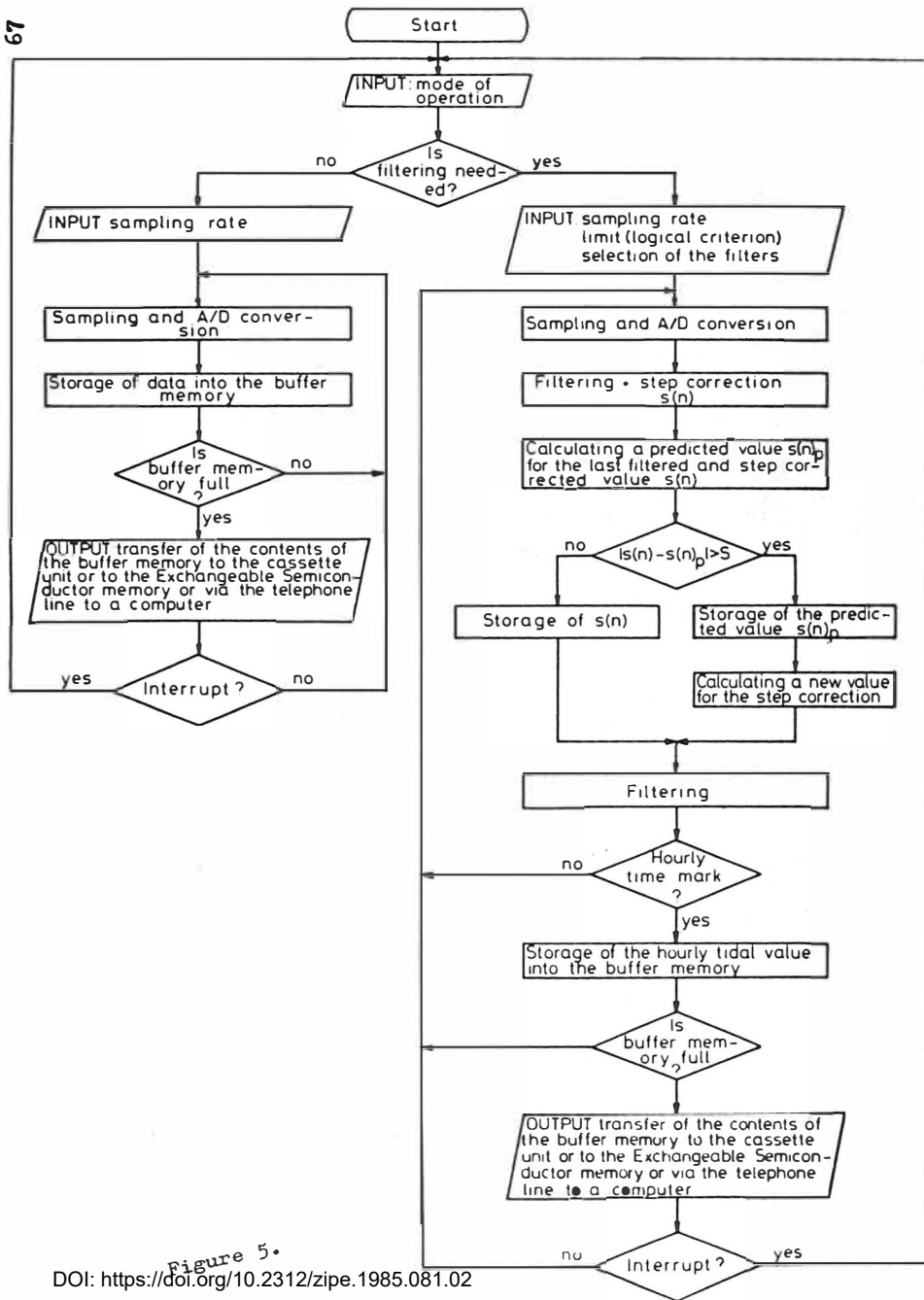


Figure 5.

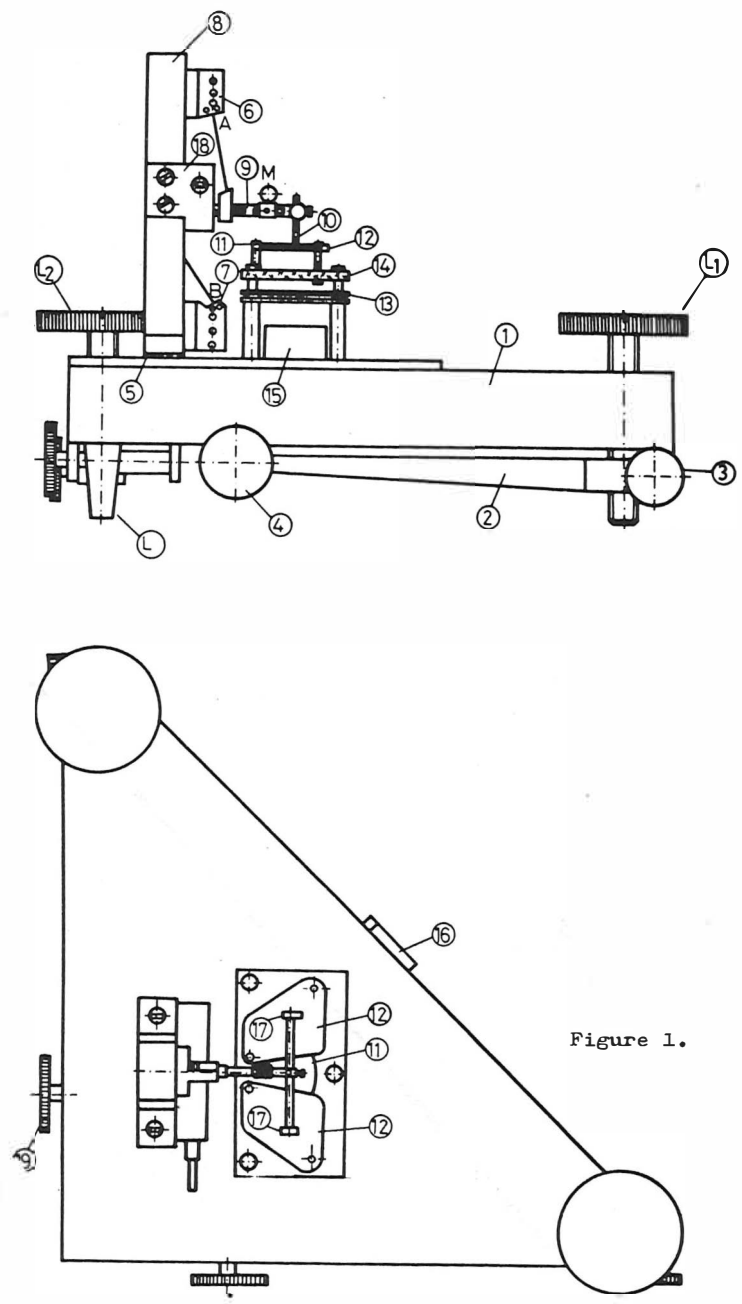


Figure 1.

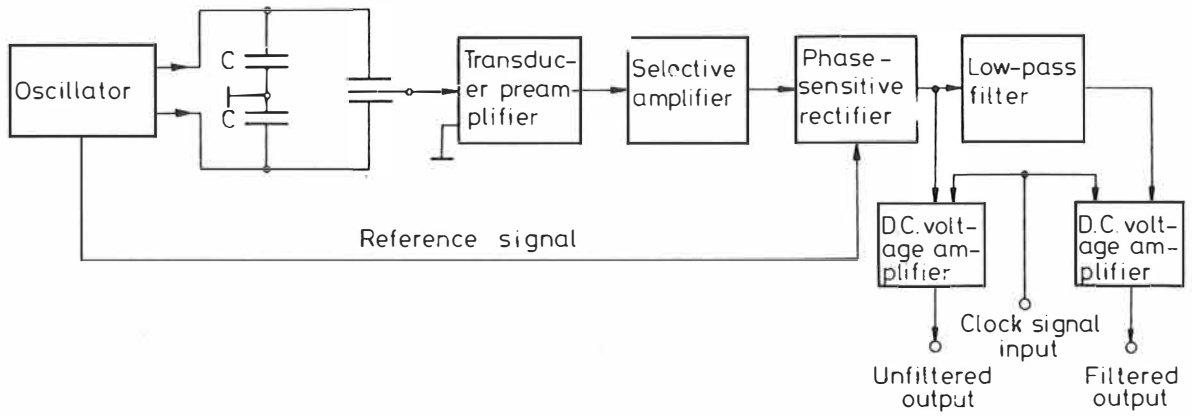


Figure 2.

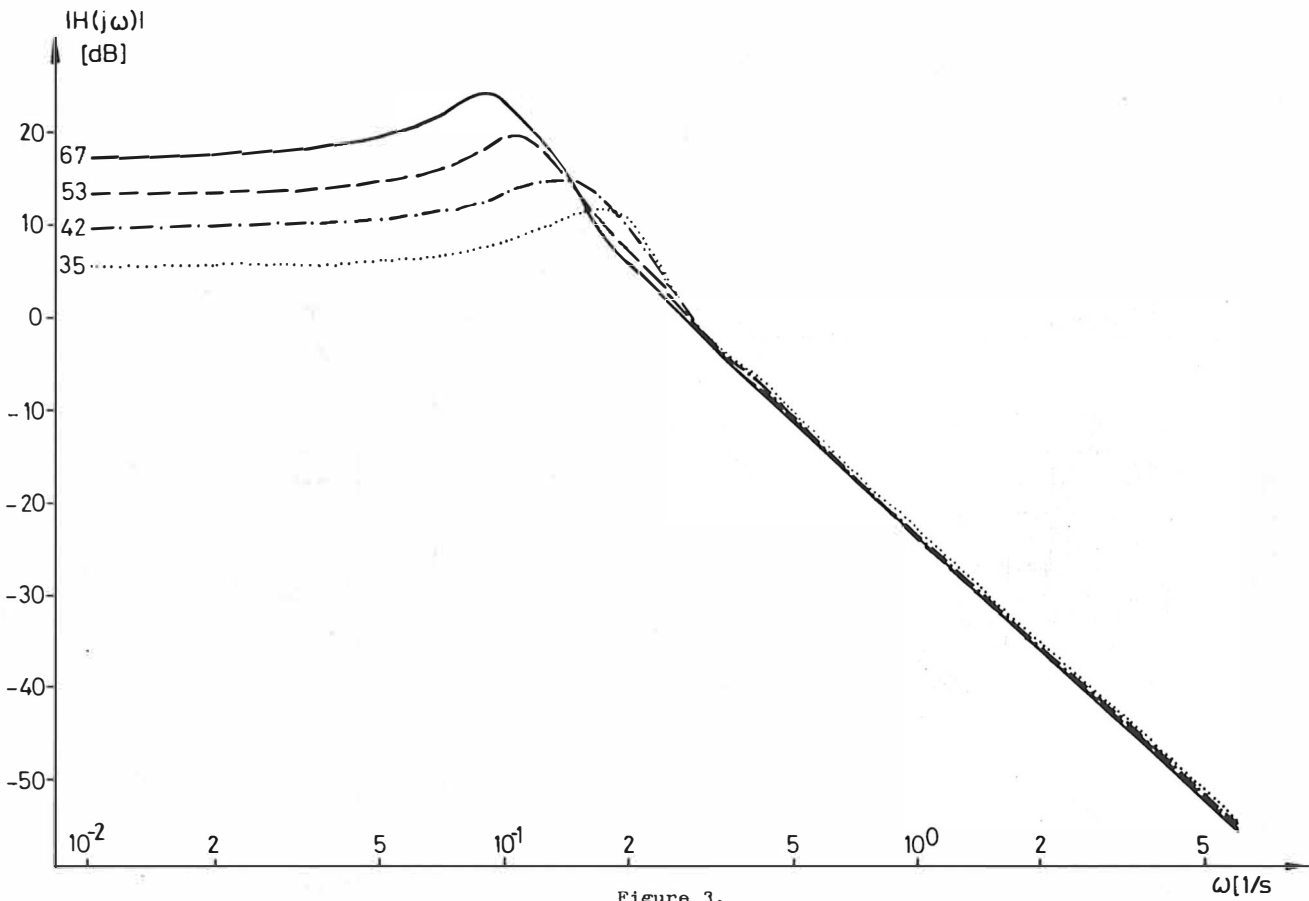
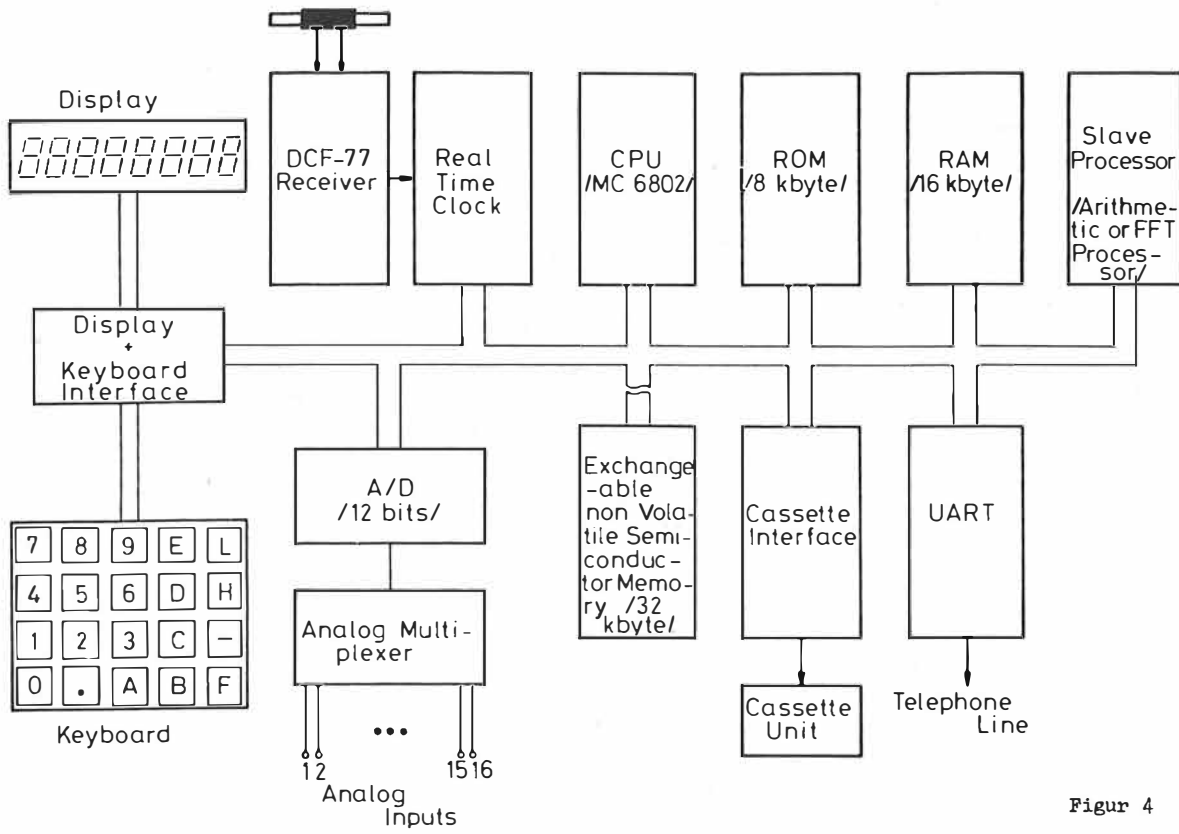


Figure 3.



Figur 4

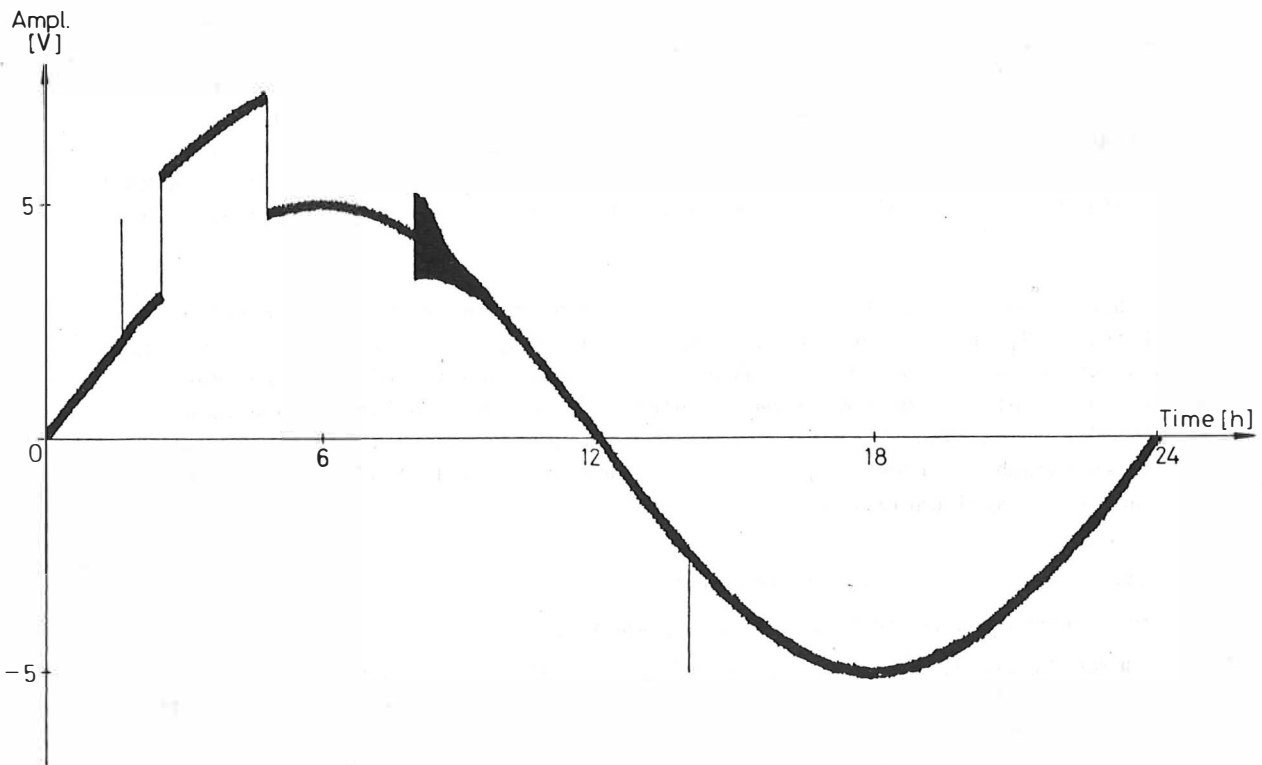


Figure 6.

Meng Jiachun

(Institute of Geodesy and Geophysics, Academia Sinica)

Abstract

This paper deals with all kinds of methods for computing the gravity topographic effect. These methods include: topographic correction solution C, MOLODENSKY's series solution G_1 , PELLINEN's formula G' , analytic continuation solution g_n (including that carried out stepwise and separated-rings) and BJERHAMMAR's solution. The paper proves the interrelation between the formulas of topographic correction, derives the relation between the analytic continuation solution and BJERHAMMAR's solution and deduces some of their natures. In these methods, each has a common operator L. Generally speaking, there exists in them certain connections with each other, but they can not be replaced mutually. The linear solution (or it may be called gradient solution) of analytic continuation solution is respectively the approximate value of MOLODENSKY's series solution G_1 and BJERHAMMAR's solution. When solving with these methods, the basic question encountered is the same. The paper also puts forward that, to use reduction of separated rings may decrease difficulties brought about in iterative computation.

I. Introduction

In the computation of geodetic gravimetry, the effect of topography on gravity can not be neglected. Generally gravity topographic effect is classified into two parts, i. e. effect on normal gravity and that on gravity anomaly. In the topographic correction of gravity anomaly, there are topographic correction solution C, MOLODENSKY's series solution G_1 , PELLINEN's formula G' , analytic continuation solution g_n (including that carried out stepwise and separated-rings) and BJERHAMMAR's solution, etc. The analytic continuation solution demands to compute the vertical gradient of gravity anomaly. Whether we operate on the basis of linear reduction or not, we can divide it according to linear reduction or nonlinear reduction up to 2nd order⁽¹⁾ (or n-th order⁽²⁾). Owing to different data one used, three kinds of representation of gravity vertical gradient may be classified in accordance with gravity anomaly, height anomaly and vertical deflections^(3a). But nonlinear reduction is resolved according to gravity anomaly. When classifying them by using reduction surface, the surface gravity anomaly may be extended analytically to the point-level, geoid or a certain sphere surface within the earth.

In these methods, their starting points, forms of formulas and their results are all different. G_1 is given out in accordance with MOLODENSKY's problem, the analytic continuation solution draws support from TAYLOR series and is solved in the way of analytic continuation, and BJERHAMMAR's solution is derived in line with poisson equation. But we still pay close attention to the questions about the interrelation of these topographic correction formulas, the advantages and disadvantages of each method and their applicabilities.

II. Discussion about formulas correlation

In the topographic correction of gravity anomaly, all of the topographic correction C, MOLODENSKY's series solution G_1 , PELLINEN's formula G' and analytic continuation solution g_n ($n = 1, 2, \dots$) have a common operator. It will be seen here after that, all formulas of topographic correction have something to do with gravity vertical gradient L_1 (Δg). HENCE, this operator is expressed by L. It may be explained as

vertical derivative. For example, the topographic correction solution is expressed to be

$$(1) \quad C = \frac{1}{2} G \delta R^2 \iint_{\sigma} \frac{(h - h_p)^2}{l_o^3} d\sigma$$

$$(2) \quad l_o = 2R \sin \frac{\psi}{2}$$

G is gravitational constant, δ , density of topographic masses, R , radius of the earth, ψ , spherical distance between the computing point P and moving point (surface element) Q , and h_p and h are relief heights of p and Q respectively. By using the operator, it may be simplified as

$$(3) \quad C = \pi G \delta L (h - h_p)^2$$

Similarly, there are

$$(4) \quad G_1 = L (h - h_p) \Delta g \quad (5) \quad G' = L (h - h_p) (\Delta g - \Delta g_p)$$

$$(6) \quad L_1 = L, (\Delta g) = L (\Delta g - \Delta g_p)$$

As to the free-air anomaly in the mountain areas, owing to the proportion which BOUGUER layer holds is much larger than the proportion which the absolute value of BOUGUER anomaly makes up, therefore it may be approximately assumed

$$(7) \quad \Delta g - \Delta g_p \approx 2\pi G \delta (h - h_p)$$

HENCE, under the condition that the free-air anomaly Δg has linear correlation with the height h , PELLINEN's formula G' may be written as

$$(8) \quad G' = 2C$$

Therefore we may conclude: (1) When there is short of gravity data, according to the hypothesis $\Delta g = ah + b$, G' may be obtained by computing C with data of topographic height. (2) Avoiding the hypothesis of the crustal density δ , topographic correction solution C may be replaced by computing G' directly.

As for G_1 , HEISKANEN and MORITZ have expressed it to be the sum of the following two terms (3b, 4):

$$(9) \quad G_1 = G_{11} + G_{12} = -\frac{h_p R^2}{2\pi} \iint_{\sigma} \frac{\Delta g - \Delta g_p}{l_o^3} d\sigma + \frac{R^2}{2\pi} \iint_{\sigma} \frac{h \Delta g - h_p \Delta g_p}{l_o^3} d\sigma$$

By using the operator L , it is written as

$$(10) \quad G_1 = -h_p L (\Delta g - \Delta g_p) + L (h \Delta g - h_p \Delta g_p) \quad (11) \quad G_{11} = -h_p L (\Delta g)$$

Here, G_{11} is the linear solution g_1 of the analytic continuation of gravity anomaly, which corresponds to the free-air correction carried out by reducing the gravity anomaly from earth surface to the sea level. To do reduction like this has to use earth surface height of the computing point, but the physical meaning of G_{12} is not clear.

Taking notice of formula (7), it may be written approximately as

$$(12) \quad G_p = L (h-h_p) (\Delta g - \Delta g_p) + L (h-h_p) \Delta g_p \\ \approx G' + \frac{\Delta g_p}{2\pi G\delta} L, (\Delta g)$$

However, by using formula (7), YOICHIRO FUJII⁽⁶⁾ has derived

$$(13) \quad G_p = G_{11}^* + G_{12}^* \approx 2\pi G\delta L (h-h_p)^2 + L (h-h_p) \Delta g_p \\ \approx 2C + \frac{\Delta g_p}{2\pi G\delta} L, (\Delta g)$$

In FUJII's paper, G_{11}^* and G_{12}^* were originally written as G_{11} , G_{12} respectively. Here, in order to avoid mixing up with the forementioned signs adopted by HEISKANEN and MORITZ, the author adds an asterisk to each sign to differentiate them from the original signs. In view of the approximation of BOUGUER layer, G_{11}^* is twice as much as the topographic correction solution C. The meaning of FUJII's formula (13) reverts with that to make clear the physical meaning of G_{11}^* and G_{12}^* .

After comparing formulae (10), (12) and (13), we may conclude: (1) In all of the formulae given by HEISKANEN and MORITZ, the author and FUJII, G_1 has a bearing on the 1st-order vertical gradient L_1 of gravity anomaly. And the interrelation between G_1 and the formulae of L_1 , G' and C has been also given out. In quantity, G_1 is equal to the linear combination of gravity vertical gradient L_1 with $L (h \Delta g - h_p \Delta g_p)$ or with PELLINEN's solution G' , or with topographic correction solution C) respectively.

(2) By using the same grid, YUKIO HAGIWARA⁽⁴⁾ has computed G_1 , G_{11} and G_{12} respectively for the gravity stations on the 35°30' latitude circle in Tanzawa mountain areas of Japan. The results calculated show that, in the formula (10) of HEISKANEN and MORITZ, though the amplitudes of G_{11} and G_{12} are not equal, and yet the waveform are nearly alike. While according to FUJII's formula (13) and using the same grid, the result obtained after computing Tanzawa mountain areas shows that, G_{11}^* is much smaller than G_{12}^* . Herefrom we may conclude like this: G_1 is a quantity which is approximately proportional to $L_1 (\Delta g)$.

With the aid of TAYLOR series of the vertical gradient of the gravity anomaly $L (\Delta g)$, the analytic continuation solution can solve the gravity topographic effect. It may be a linear solution (which is also called gradient solution) by taking into account of 1st-order vertical gradient L_1 , and may be also a non-linear reduction by giving consideration to n-th-order vertical gradient L_n . Generally speaking, to attend to the second order L_2 is enough. This way, when earth surface gravity anomaly Δg is extended analytically to the geoid with TAYLOR series up to 2nd order, it may be written as

$$(14) \quad \Delta g^* = \Delta g - hL_1 (\Delta g) + hL_1 (hL_1 (\Delta g)) - h^2 L_2 (\Delta g)$$

where

$$L_1 (\Delta g) = \frac{\partial \Delta g}{\partial h} \quad L_2 (\Delta g) = \frac{\partial^2 \Delta g}{\partial h^2}$$

If earth surface gravity anomaly Δg is extended analytically to the point level, then

$$(15) \quad \Delta g' = \Delta g - 3L_1 (\Delta g) + 3L_1 [3L_1 (\Delta g)] - 3^2 L_2 (\Delta g)$$

As it does not have the difficulty to compute deflection of the vertical when using MOLODENSKY's series solution, so it is considered as the most wide-ranging and ingenious method for solving MOLODENSKY's problem. If Δg is extended analytically to the point level and then to the geoid (or a certain sphere surface within the earth), we may have stepwise and separated-rings analytic continuation⁽⁵⁾.

$$(16) \quad \Delta g^* = \Delta g' - h_p L_1 (\Delta g) + h_p L_1 [3L_1 (\Delta g)] + h_p^2 L_2 (\Delta g)$$

Where, $\Delta g'$ is gravity anomaly on the point level, h and h_p are elevations of arbitrary point and computing point respectively, Z is their elevation difference. Apparently, when leaving out the 2nd order vertical gradient term, we get the gradient solution of gravity anomaly continuation^{2, 3)}

$$(17) \quad \Delta g_* = \Delta g' - h_p L_1 (\Delta g) \quad (18) \quad \Delta g' = \Delta g - \partial L_1 (\Delta g)$$

Under the condition of $h_p = 0$, i. e. when the point level and geoid are coincident, we have $\Delta g_* = \Delta g'$. This makes the method of continuation to the point level become a special case of formula (16).

According to the description of this section and the next one, we can see that, all the computing methods of computing gravity topographic effect on hand have a common operator. Generally speaking, there exists certain relation between each of these methods, but they are not replaced mutually. As to their differences in numerical solution, they may be different depending on the kinds of regional topography.

III. Analytic continuation solution and BJERHAMMAR's solution

In analytic continuation solution, one of the most important questions is the computation of the vertical gradient of the gravity anomaly $L_1 (\Delta g)$. Under the condition to use enough accuracy to carry out plane approximation about sphere and in the case of projection of earth's surface to a plane with an azimuthal equidistant projection, the integration of the earth's surface will be transformed into one on the tangent plane at the computing point. Now if let the computing point p be the origin and set up plane polar coordinates and rectangular coordinates systems, then, the integrated coefficients of $L_1 (\Delta g)$ may be written as⁽⁵⁾

$$(19) \quad K_{ij} = \frac{1}{\pi} \left(\frac{1}{r_i} - \frac{1}{r_{i+1}} \right) = \frac{\Delta r}{\pi r_i (r_i + \Delta r)}$$

n is the numbers of subblock in the i th circular zone, r_i is the inner radius of this zone and Δr is the width.

$$(20) \quad K_{ij} = \sum_{i,j=1,2} (-1)^{i+j+1} \frac{\sqrt{x_i^2 + y_j^2}}{2\pi x_i y_j}$$

x_i, y_j are the plane rectangular coordinates of the corner point of the i th and j th subnetwork. Thus we have

$$(21) \quad L_1 (\Delta g) = \sum K_{ij} (\Delta g - \Delta g_p)$$

In order to avoid man-made hypothesis to be introduced during the course of computing the disturbing potential, BJERHAMMAR presented out to extend downwards the earth surface gravity anomaly to the equivalent sphere within the earth, and let

$$(22) \quad \Delta g_p^* = \Delta g_p - \frac{t^2(1-t^2)}{4\pi\sigma} \iint_{\sigma} \frac{\Delta g^* - \Delta g_p^*}{D^3} d\sigma$$

Where

$$(23) \quad t = \frac{R}{r_p} \quad r_p = R + h_p$$

$$(24) \quad D = \frac{l}{r_p} = \sqrt{1 + t^2 - 2t \cos \psi}$$

$$l = (R^2 + r_p^2 - 2Rr_p \cos \psi)^{1/2}$$

(25)

or it may be also written as

$$(26) \quad \Delta g_p^* = \Delta g_p - \frac{R^2(r_p^2 - R^2)}{4\pi r_p} \iint_{\sigma} \frac{\Delta g^* - \Delta g_p^*}{l^3} d\sigma$$

R is the radius of equivalent sphere, h_p is the distance from earth surface point to the equivalent sphere.

As to the two arbitrary points on the earth surface, within a certain limit they may be written as ⁽²⁾

$$(27) \quad \ell^2 = \ell_0^2 + (h - h_p)^2$$

Besides, we have

$$(28) \quad \frac{R^2 - R_p^2}{2R_p} = \frac{h_p(2R+h_p)}{2(R+h_p)} = h_p \left(1 - \frac{h_p}{2R} + \frac{h_p^2}{2R^2} - \dots \right)$$

On the tangent plane of equivalent sphere where the computing point lies, if the polar coordinates system is chosen and the rest is similar to what the author did in paper ⁽⁵⁾ then from the second term at the right side of formula (26) we may write:

$$(29) \quad K_{ij}^B = \frac{1}{\pi} \left(1 - \frac{h_p}{2R} + \frac{h_p^2}{2R^2} \right) \frac{1}{2\pi} \iint_S \frac{r dr dA}{[r^2 + (h - h_p)^2]^{3/2}}$$

$$= \frac{1}{\pi} \left(1 - \frac{h_p}{2R} + \frac{h_p^2}{2R^2} \right) \int_{r_i}^{r_{i+1}} \frac{r dr}{[r^2 + (h - h_p)^2]^{3/2}}$$

$$= \left(1 - \frac{h_p}{2R} + \frac{h_p^2}{2R^2} \right) \frac{1}{\pi} \left\{ [r_i^2 + (h - h_p)^2]^{-1/2} - [r_{i+1}^2 + (h - h_p)^2]^{-1/2} \right\}$$

apparently, when $\Gamma \rightarrow \infty$, the integration constant C=0. So we obtain:

$$(30) \quad \Delta g_p^* = \Delta g_p - h_p \sum K_{ij}^B (\Delta g_i^* - \Delta g_p^*)$$

Now, we shall make inferences as follows:

(1) In the downward continuation of gravity anomaly, BJERHAMMAR's solution may be expressed as the sum of the gradient solution extended analytically to the same spherical surface with the effects related to gravity vertical gradient of every surface element and its topographic elevation difference.

Because of that, when expanding the right-hand side of formula (29) according to the binomial theorem, we have

$$(31) \quad K_{ij}^B = \left(1 - \frac{h_p}{2R} + \frac{h_p^2}{2R^2} \right) \frac{1}{\pi} \left\{ \frac{1}{r_i} - \frac{1}{r_{i+1}} + \frac{1}{r_i} \sum_{m=1}^{\infty} \binom{n'}{m} \left(\frac{h - h_p}{r_i} \right)^{2m} - \frac{1}{r_{i+1}} \sum_{m=1}^{\infty} \binom{n'}{m} \left(\frac{h - h_p}{r_{i+1}} \right)^{2m} \right\}$$

$$= \left(1 - \frac{h_p}{2R} + \frac{h_p^2}{2R^2} \right) K_{ij} (1 + B)$$

$$B = \sum_{m=1}^{\infty} \binom{n'}{m} (h - h_p)^{2m} \left(\frac{1}{r_i^{2m}} + \frac{1}{r_i^{2m-1} r_{i+1}} + \frac{1}{r_i^{2m-2} r_{i+1}^2} + \dots + \frac{1}{r_i r_{i+1}^{2m-1}} + \frac{1}{r_{i+1}^{2m}} \right)$$

$$= -\frac{1}{2} (h - h_p)^2 \left(\frac{1}{r_i^2} + \frac{1}{r_i r_{i+1}} + \frac{1}{r_{i+1}^2} \right) + \dots$$

where
(32)

n' is an arbitrary real number, where $n' = -\frac{1}{2}$, $\left| \left(\frac{h - h_p}{r} \right)^2 \right| < 1$. HENCE, formula (30) may be written as:

$$(33) \quad \Delta g_p^* = \Delta g_p - h_p \left(1 - \frac{h_p}{2R} + \frac{h_p^2}{2R^2} \right) \left\{ L_i (\Delta g_i^*) + \sum L_{ij} B \right\}$$

$$(34) \quad L_i (\Delta g_i^*) = \sum K_{ij} (\Delta g_i^* - \Delta g_p^*) \quad L_{ij} = K_{ij} (\Delta g_i^* - \Delta g_p^*)$$

While $g_1^* = -h_p L_1 (\Delta g^*)$ is gradient solution, and the initial value of Δg^* is Δg . Now the proof is at an end.

(2) If analytic continuation solution and BJERHAMMAR's solution of gravity

anomaly are not extended simultaneously to the same spherical surface, BJERHAMMAR's solution may be expressed approximately as stepwise analytic continuation solution extended to the same spherical surface.

All of us know that, when the distance h_p from earth surface point to the equivalent sphere is equal to 300m, $h_p/R = 4.7088 \times 10^{-5}$; even under the condition of $h_p = 10000m$, $h_p/R = 1.5696 \times 10^{-3}$ is still smaller than the spherical approximate error ($\frac{1}{R} = 3.352836 \times 10^{-3}$). Generally speaking, L_1 (Δg) is about a magnitude of 10^{-2} . Therefore, h_p/R in formula (33) and the above each term may be generally omitted.

Let h_p be the distance from earth surface point to equivalent sphere with the earth, h'_p is the distance from point level (or the geoid) to the equivalent sphere, and z is the distance from earth surface point to point level (or the geoid), and if h_p in (33) is replaced by $h'_p + z$, then the preceding two terms in (33) will become (18) and (17). And the inference (3) shows that, so long as the value $h-h_p$ in the central zone is far smaller than 250m, ΣL_{ij}^B will be probably smaller.

(3) In plain, plateau, hilly terrain and parts of low mountain areas, BJERHAMMAR's solution may be equivalent to the analytic continuation solution.

In absolutely ideal plain and plateau areas, i.e. under the condition of $h-h_p = 0$, formula (33) may be written as:

$$(35) \quad \Delta g_p^* = \Delta g_p - \rho_p \left(1 - \frac{h_p}{2R} + \frac{h_p^2}{2R^2} \right) L_1(\Delta g^*)$$

In areas where the topographic undulation is smaller, e. g. in plain, plateau, hilly terrain and parts of low mountain areas (the elevation difference is about 250m), their value $\left(\frac{h-h_p}{R} \right)^2$ may be still smaller than the spherical approximate error. Because of that, at the place $r = 4.625km$ away from the computing point, and when $h-h_p=100m$, the magnitude of $\left(\frac{h-h_p}{R} \right)^2$ is 10^{-4} ; when $h-h_p=250m$, $\left(\frac{h-h_p}{R} \right)^2 = 2.9218 \times 10^{-3}$. According to the definition, we have

$$\frac{1}{r_\lambda^2} > \frac{1}{r_\lambda r_{\lambda+1}} > \frac{1}{r_{\lambda+1}^2}$$

HENCE, so long as the value $h-h_p$ in the central zone is smaller than 250m, L_{ij}^B in formula (33) may be possibly smaller. This way, BJERHAMMAR's solution will be equivalent to the analytic continuation solution. Contrarily, in low mountain areas $\left(\frac{h-h_p}{R} \right)^2$ will be close to or greater than the spherical approximate error. Therefore, the effect of topographic height on gravity topographic effect should not be neglected.

(4) In the case to demand accuracy alike, no matter how far the radii of templet circular zones of analytic continuation solution and BJERHAMMAR's solution we compute, they may be the same.

We know that, K_{ij}^B shown in formula (29) is the integrated (templet) coefficient of BJERHAMMAR's solution. It is the function of elevation h_p of computing point, the circular zone radii r_i, r_{i+1} of templet and the topographic elevation difference $h-h_p$. When $h-h_p = 0$, K_{ij}^B obtained at the right-hand side of formula (29) is the integrated (templet) coefficient of analytic continuation solution. As for any circular zone, the coefficient K_{ij}^B will decrease with the increase of value $h-h_p$. But as to different values $h-h_p$, the difference value of K_{ij}^B on a certain circular zone may still remain certain magnitude. For example, on the circular zone apart from 30' of the computing point, the difference value of K_{ij}^B

of this circular zone may be taken as a magnitude of $10^{-7} - 10^{-5}$ for the different values of $h-h_p$; on the circular zone apart from l^0 , the difference between their coefficients may have a magnitude of $10^{-8} - 10^{-6}$. In the case of that the requirements of data unit and accuracy are definite, if we use different values of $h-h_p$ for certain circular zone, then, the radius of this circular zone computed how far may be identical. HENCE, the templet of BJERHAMMAR's solution may be the same as with analytic continuation solution.

IV. The Advantages and Disadvantages of Every Method

In computation, all solutions such as the topographic correction solution C, MOLODENSKY's series solution G_1 , PELLINEN's formula G' , analytic continuation solution g_n ($n = 1, 2, \dots$) and BJERHAMMAR's solution g_B have a common operator L. Judging from this, the problems such as the precise solution of integrated (templet) coefficient K_{ij} , computation of central zone, the division of templets and how far do we compute the circular zone radius of templet, etc. are all similar. HENCE the difficulties encountered when operate them are also the same.

In the preparation of data, some methods only require data of topographic height h , for example, C; some requires gravity anomaly Δg besides topographic height, e. g. G_1, G' ; some only requires data of topographic height at the place of computing point besides Δg , e.g. g_n, g_B .

In these methods, they require separately the data of $h-h_p$ or $\Delta g - \Delta g_p$, or they use both of them. In numerical values, $h-h_p$ is generally greater than $\Delta g - \Delta g_p$, or it is even greater by a magnitude than it. Therefore, under the condition when the operators are alike, the convergence (rate) of L_1, g_B is fast; G_1, G' take second place; and owing to $(h-h_p)^2$ is greater, the convergence rate of C is the slowest. According to the same reason, the circular zone radius of G_1, G' may be computed farther than that computed for L_1, g_B .

As to iterative computations, BJERHAMMAR's solution may be iterated to the n -th order, e.g. in WUHAN area iteration requires 2-3 times, in WUDU area, it requires 6-7 times at most. In theory, analytic continuation solution may be iterated to the n -th order. In application, to iterate 2 times is enough ([2], p.420). But the methods of C, G_1, G' do not require iterative computations. From this point of view, it is their advantage. The distinguishing features of geodetic gravimetry computation are: the computing templet will be displaced with the change of computing point, the scale of templet and how far will be the circular zone radius computed are not altered with the change of computing point. Thus, if the circular zone radius remains unchanged, to do one time of iterative computation will require the data of 2ψ . So the problem of iterative computation of BJERHAMMAR's solution is more prominent than that of analytic continuation solution.

In BJERHAMMAR's solution, the value $\Delta g^* - \Delta g_p^*$ will be gradually decreased after doing every iterative computation, and at the first several times its reduced range is greater. HENCE, when computing the idea of separated-ring reduction presented by the author in literature (5) may be used. This idea is: according to the given accuracy required, for different values of $\Delta g - \Delta g_p$ the reduction may be carried out by choosing different block distance (or circular zone radius). Here, we may

consider the reducing range of $\Delta g^* - \Delta g_p^*$ reduces one by one and in unequal interval the circular zone radius, and it may reduce it in equal interval.

By using it in BJERHAMMAR's solution in WUDU area, the result shows that, the value $\Delta g^* - \Delta g_p^*$ after the first iteration is reduced smaller by 70 - 90 % or more than the initial value; iterative computation is chiefly the first 2-3 times; to adopt the principle of separated-ring reduction is reasonable and it may quicken the rate of iteration.

V. Conclusion

To sum up all mentioned above, we may have conclusions as follows:

(1) All the computing methods of gravity topographic effect now available have a common operator L , and certain relation between these methods may be found out. HENCE, the value of gravity topographic effect obtained by using a certain method may be transformed into a value got by another method. But, generally speaking, these methods can not be replaced mutually.

(2) The linear solution (i. e. gradient solution) of analytic continuation solution is the approximate value of MOLODENSKY's series solution G_1 and BJERHAMMAR's solution respectively. C and G' are also the partial value of G_1 .

(3) In the downward continuation of earth surface gravity anomaly, BJERHAMMAR's solution may be expressed as the sum of the gradient solution extended analytically to the same spherical surface with the effect related to topographic height. If they are not extended to the same spherical surface, BJERHAMMAR's solution may be expressed approximately as the stepwise continuation solution extended to the same spherical surface. In plain, plateau, hilly terrain and parts of low mountain areas, BJERHAMMAR's solution may be equivalent to the analytic continuation solution.

(4) Some basic problems we meet when we use all methods in computation are the same. Let us examine from iterative computations, G_1 , G' are different from analytic continuation solution and BJERHAMMAR's solution, and it is not necessary to operate iterative computation; in the respect of number of times of iteration, the number of times of analytic continuation solution may be less than that of BJERHAMMAR's solution; in the respect of forced conformity, the latter is better than the former; in iterative computation, to adopt separated-ring reduction presented by the author is reasonable. It can not detract accuracy, and may cut down many related data, furthermore, the rate of iterative computation is fast.

References

- (1) NOE, H., Numerical investigations on the problem of MOLODENSKY, Mitteilungen der Geodätischen Institute der Technischen Universität Graz, Folge 36, Graz, 1980.
- (2) MORITZ, H., Advanced Physical Geodesy, Herbert Wichmann Verlag / Abacus Press, 1980, pp. 377-388, p. 420.
- (3) HEISKANEN, W. A. and MORITZ, H., Physical Geodesy Reprint Institute of Physical Geodesy, Technical University Graz, Austria, 1979, a) pp. 115-117, b) pp. 307-310.
- (4) YUKIO HAGIWARA, Practical Computations of G_1-G_1 Ovar Tanzawa Mountains. Journal of the Geodetic Society of Japan, Vol. 18 (1972), No. 4, pp. 161-171.
- (5) 孟嘉春, 重力异常的解析延拓及其计算,
测量与地球物理集刊, 第6号 (1984年).
- (6) YOICHIRO FUJII, Significance and limitation of the gradient method in the geodetic boundary value problem, Journal of the Geodetic Society of Japan, Vo. 16 (1970), No. 3, pp. 111-126.

РЕЗЮМЕ. Рассмотрено два подхода к потенциалографической задаче-ПЗ, под которой понимается уже давно решаемая задача удобного аналитического представления внешнего потенциала притяжения планеты. Первый - дескриптивный; соответствующие ему известные способы представления потенциала доставляют решение прямой ПЗ. Второй подход - конструктивный; он приводит к обратным ПЗ, являющимся новым видом обратных задач теории потенциала.

Обсуждена постановка обратной ПЗ, в которой известный потенциал планеты представлен суммой потенциалов простого и двойного слоев, расположенных на заданной поверхности внутри планеты; искомыми являются плотность и момент этих слоев. Частный случай такой задачи, когда слои предполагаются в экваториальной плоскости, приводит к концепции гравитирующих дисков - КГД.

Согласно КГД потенциал планеты представлен суммой потенциалов трех плоских круговых одноцентренных дисков: фокального - ФД, безмассового материального - БМД и дипольного - ДД. ФД (с четными зональными гармониками) отвечает планете в предположении гидростатически равновесного ее состояния; БМД (с гармониками, четными относительно плоскости экватора) и ДД (с нечетными - в том же смысле - гармониками) отражают негидростатичность планеты: соответственно ее симметричную и несимметричную часть относительно экваториальной плоскости.

Обсуждены альтернативы в установлении нормального поля Земли. Указаны механические предпосылки КГД.

Abstract. Here are considered two approaches as to the potentialographical problem PP, under which we understand for a long time a solving problem of convenient analytical representation of external potential planet gravitation. The first one is descriptive to which corresponds known methods of solution of direct PP. The second is a constructive one; it brings to inverse PP, which is a new kind of inverse problems of potential theory.

Here is discussed inverse PP in which a known potential of the planet represented as sums of potentials of the simple and double layers, situated on the given surface in the interior of the planet density and moments of these layers are to be sought. A particular case of this problem, when layers are supposed to be in equatorial plane, brings to the conception of gravitating disks - CGD.

According to CGD potential of planet is represented as the sum of three potentials of the plane circular one-centered disks: focal disks - FD, material, massless MMD and dipole disk - DD. FD /with even zonal harmonics/ corresponds to a planet supposing hydrostatics of its balanced state; MMD /with harmonics even as to equator plane / and DD /with odd harmonics in the same sense / represent a planet non-hydrostatically: namely its symmetrical and non-symmetrical parts as to equator plane.

Here are also discussed alternatives in setting normal Earth gravitation and given mechanical prerequisites of CGD.

Мещеряков Г.А.

(СССР, Львовский политехнический институт)

ПОТЕНЦИАЛОГРАФИЧЕСКАЯ ЗАДАЧА И КОНЦЕПЦИЯ ГРАВИТИРУЮЩИХ ДИСКОВ

§I. Ниже будем рассматривать задачу удобного аналитического представления внешнего потенциала притяжения планеты, совершенно не связывая ее ни с определением формы последней, ни с ее внутренним строением. Эту задачу мы называем потенциалографической^{*)}. Она не нова. Впервые ее решил еще Лаплас, разложив потенциал притяжения планеты в ряд шаровых функций, который и поныне является основным аппаратом как при теоретических исследованиях, так и при решении разнообразных практических задач. Однако предлагались и другие формы описания потенциала. И даже в последнее время усиленно изыскиваются новые нетрадиционные способы его представления, именно такие, которые не теряя в точности, позволяли бы эффективную и экономичную реализацию на ЭВМ.

История рассматриваемого вопроса и его актуальность вынуждают подойти к нему с некоторых общих позиций. Но сначала отметим кратко многообразие возможных подходов к нему. Даже классический лапласов ряд шаровых функций допускает различные интерпретации [1,2,3] и разные формы записи его [4,5]. А кроме него даны были еще описания потенциала по гармоникам сжатого эллипсоида вращения, рядами по функциям Ламе, потенциалом простого слоя, суммой потенциалов точечных масс, при помощи мультиквадрикковых и других видов функций, с использованием так называемых неподвижных центров (мнимых или комплексных), комбинированием различных способов его

*) Лекция "Обратные задачи теории геопотенциала", прочитанная автором на международной зимней школе "Теоретические и экспериментальные вопросы планетарной геодинамики" (29.IX-9.X.1983, Киев).

аппроксимации в отдельных областях пространства и др., - и все это, скажем, - суть разные методы решения потенциалографической задачи. Обзор и библиография их имеются в [6,7].

Как видно, некоторые из перечисленных методов отвечают дескриптивному подходу: как наилучшим образом (в каком-то определенном смысле, например, с позиций теории квадратических приближений) описать потенциал (V или T) аналитически - при помощи специальных функций или разложений в ряды. Такому подходу следуют представления потенциалов рядами по шаровым функциям, по гармоникам сжатого эллипсоида, по функциям Ламе, методом конечных элементов и некоторые другие. Если исходить из принципа теории наилучших квадратических приближений, то для получения удовлетворяющего ему решения задачи необходимо знать форму планеты [1], и - в соответствии с этим - из только-что указанных представлений V первые дают строгое решение для планет сферической формы, вторые и третьи - для планет эллипсоидальной формы (соответственно в виде эллипсоидов вращений и трехосных эллипсоидов). Использование конечных элементов предусматривает наиболее полное описание потенциала реальной планеты. Все эти подходы осуществляют математическую аппроксимацию V ; будем считать, что они доставляют решение прямой потенциалографической задачи.

Но к описанию потенциала реальной планеты возможен и другой подход - конструктивный, которому соответствуют обратные потенциалографические задачи: надо отыскать поверхность S и на ней расположить два слоя - простой и двойной (или один из них), сумма потенциалов которых выражала бы потенциал планеты и допускала бы более простые вычисления его, нежели традиционным образом по ряду шаровых функций.

Возможность постановки таких обратных задач вытекает из сле-

дующих соображений. Пусть поверхность σ тела известна, будем полагать, что она принадлежит к классу поверхностей Ляпунова (к ним относятся, например, ограниченные замкнутые поверхности класса C^2). И пусть на σ известны значения потенциала V и его нормальной производной $\frac{\partial V}{\partial n}$. Тогда, как известно, внешний потенциал V тела τ может быть представлен суммой потенциалов простого и двойного слоев, расположенных на σ :

$$V(P) = -\frac{1}{4\pi} \int_{\sigma} \frac{1}{l_{PQ}} \left(\frac{\partial V}{\partial n} \right)_Q d\sigma_Q + \frac{1}{4\pi} \int_{\sigma} V_Q \frac{\partial}{\partial n_Q} \left(\frac{1}{l_{PQ}} \right) d\sigma_Q, \quad (Q \in \sigma, P \notin \sigma) \quad (1)$$

Указанный факт возможности представления объемного потенциала суммой потенциалов двух слоев

$$V = V' + V'' \quad (2)$$

или даже одного из них, имеет основополагающее значение в математической физике при исследовании и решении краевых задач теории потенциала. Здесь же обсуждается иной вопрос - вопрос о разнообразии форм описания внешнего объемного потенциала V . Значит, имея образец его выражения в виде (1) и учитывая непрерывность потенциалов слоев (простого и двойного) во внешнем по отношению к ним пространстве, можно предположить, что изучаемый потенциал представим суммой

$$V = k' V' + k'' V'', \quad (3)$$

в которой коэффициенты k' и k'' - постоянные или даже переменные, а потенциалы V' и V'' (именно, - потенциал простого слоя

$$V'(P) = \int_S \frac{\mu_Q dS_Q}{l_{PQ}}, \quad (Q \in S, P \notin S) \quad (4)$$

и потенциал двойного слоя

$$V''(P) = \int_S \nu_Q \frac{\partial}{\partial n_Q} \left(\frac{1}{l_{PQ}} \right) dS_Q, \quad (Q \in S, P \notin S) \quad (5)$$

- соответственно с плотностью μ и моментом ν) отнесены к

некоторой ограниченной гладкой двухсторонней поверхности S , 8 расположенной внутри σ и не имеющей с ней общих точек. Предположим также, что сумма (3) выражает на σ и в области между σ и S аналитическое продолжение внешнего потенциала (V или T) во внутрь тела τ , если, конечно, оно существует.

Ясно, что, если для заданного тела τ мы сможем каким-то образом разделить его потенциал на две части, которые хотим затем трактовать потенциалами слоев (соответственно простого и двойного), лежащих на выбранной априори поверхности S , объемлемой поверхностью σ тела τ , то будем иметь здесь две типичные обратные задачи теории потенциала с присущими им свойствами некорректности. При этом описывающие их выражения (4) и (5) - относительно плотностей μ и ν этих слоев - являются интегральными уравнениями I рода с непрерывными ядрами; причем условия разрешимости этих уравнений должны дать как подтверждение правильности выбора поверхности S , так и правомочность принятого разделения V на части V' и V'' .

Обратные задачи теории потенциала, в которых заданный внешний потенциал (V или T) тела τ неизвестной формы, должен быть представлен суммой (3), мы называем обратными потенциалографическими задачами. Коэффициенты k' и k'' при этом могут считаться заданными. Если один из них равен 0, а второй единице, то потенциал представляется только одним слоем - простым или двойным. Поверхность S , несущая в таких задачах слой (или слой) может считаться либо известной, либо даже подлежащей определению. Эти задачи объединяют в себе ряд задач, известных из практики геодезии. Например, при $k''=0$ и $k'=1$ имеем представление внешнего потенциала планеты потенциалом простого слоя: за S здесь могут быть приняты размещенные внутри планеты поверхность сферы или

эллипсоида известных размеров, либо поверхность, параллельная неизвестной поверхности σ планеты и находящаяся внутри последней.

Важно отметить, что потенциалографические задачи могут изучаться в дискретной постановке. Приведем пример. Пусть потенциал V заменяется потенциалом простого слоя. Если вместо непрерывной плотности μ этого слоя искать массы m_i его элементарных площадок, сконцентрированные в некоторых точках слоя, то приходим к известной задаче построения многоточечных моделей потенциала. Задавшись при этом поверхностью слоя S будем иметь линейную задачу по определению масс m_i . Если же поверхность слоя считать неизвестной, то дискретная постановка обратной потенциалографической задачи при $\kappa' = I$, $\kappa'' = 0$ охватывает общий случай построения многоточечных моделей потенциала, в которых определению подлежат массы m_i , находящиеся на поверхности S , численно определяемой искомыми точками концентрации масс ($d_i = \frac{z_i}{R}$, ν_i , λ_i ; $R = \text{const}$). Конкретная постановка одной такой задачи и решение ее даны в [8].

Заметим, наконец, что потенциалографическая задача при $\kappa' = \kappa'' = I$ в дискретной постановке при искомой поверхности S обобщает построение многоточечных моделей потенциала за счет включения в число искомых параметров этих моделей гравитационных диполей, набор которых соответствует потенциалу двойного слоя V'' .

В математическом смысле потенциалографическая задача раскрывает многообразные возможности замены объемного потенциала тела потенциалами других видов. Для геодезии эта задача позволяет потенциал притяжения планеты (полный $-V$, либо его главную часть или возмущающую $-T$) описывать различными способами, среди которых можно отыскать наиболее подходящие для тех или иных практи-

ческих целей. Заметим, что в случае представления потенциала V Земли $\kappa' \neq 0$ и $\kappa'' \neq 0$, а в случае T — $\kappa' = 0$; для гидростатически равновесных планет при описании их полного потенциала $\kappa'' = 0$. Важно также, что потенциалографическая задача допускает дискретную постановку, что, в частности, приводит, к многоточечным

и точно-дипольным моделям потенциала; кроме того, и само задание потенциала планеты может быть взято в дискретном виде. Существенно также, что поверхность S , несущая слои, может считаться искомой или может считаться заранее заданной. Все эти моменты должны быть предусмотрены детальной постановкой каждой конкретной потенциалографической задачи. Но прежде чем переходить к таковой, сделаем следующие замечания.

От поверхностей S , на которых для описания потенциала V тела суммой (3)–(5) предполагается поместить простой и двойной слои, требуется только возможность размещения на них этих слоев. Последние должны развиваться в окружающем их внешнем пространстве потенциалы притяжения, значения которых (и их производных) в точках слоев для рассматриваемой задачи несущественны. Поэтому нет необходимости брать поверхности S из класса поверхностей Ляпунова; под ними достаточно подразумевать ограниченные гладкие двухсторонние поверхности класса C^1 , именно такие, которые могут нести на себе указанные слои, при этом, как уже подчеркивалось, эти поверхности, будучи расположенными в области τ , не должны иметь общих точек с ее границей — поверхностью σ .

Поверхности S могут быть замкнутыми и могут быть незамкнутыми. Во втором случае они должны быть ограничены одной или несколькими замкнутыми кривыми. Простейшими такими незамкнутыми поверхностями S являются области некоторой плоскости, например, плоскости сечения тела τ . Очевидно, располагая слои в плоскос-

тях сечений, имеет определенный смысл выбрать сечения, проходящие через центр масс тела τ , и содержащие его диаметр, так как они - как сечения тела - наиболее полно отвечают ему в целом. Возможность использования таких плоских слоев подсказывается замечательной трактовкой [9] потенциала однородного эллипсоида с полуосями $a > b > c$ потенциалом неоднородного эллиптического слоя (диска) с полуосями $\sqrt{a^2 - c^2}$, $\sqrt{b^2 - c^2}$, расположенного в плоскости, определяемой осями эллипсоида, перпендикулярными его малой оси.

Обрисовав разнообразные возможности выбора поверхностей S для описания объемного потенциала V тела τ суммой (3)-(5), мы представим так потенциал планеты, используя именно плоские слои в ее экваториальном сечении и исходя при этом также из того, что плоскость экватора является для гидростатически равновесных планет естественной плоскостью их симметрии.

§2. Рассмотрим теперь один важный частный случай потенциалографической задачи.

Будем под S понимать площадь эллипса или круга, лежащих в экваториальной плоскости планеты и имеющих центр в центре масс планеты, возможно наибольших размеров, именно таких, что их контуры, однако, не касаются контура экваториального сечения планеты (ситуация, аналогичная таковой при введении сферы Бьерхаммара). Другими словами, за S принимаем далее площадь экваториального сечения планеты, обобщенную эллипсом или окружностью и "сжатую" незначительно к центру, именно, настолько, что ограничивающие ее эллипс или окружность становятся "почти" вписанными в это сечение. И хотя для некоторых планет (Марс, Земля) под S выгодно понимать площадь эллипса, будем все же далее - в целях описания глобального (общепланетарного) гравитационного поля планеты и ради упрощения вычислений - принимать за S круг радиуса

$$R = z_s = a_e - \xi, \quad (6)$$

где a_e - экваториальный радиус планеты, а $\xi > 0$ - малая величина.

Потенциал V планеты отнесем к вращающейся вместе с ней прямоугольной декартовой системе координат $Oxyz$, начало которой совмещено с центром масс планеты, а ось Oz совпадает с ее осью вращения. Тогда в соответствии с условиями потенциалографической задачи выразим V суммой (3) при $\kappa' = \kappa'' = 1$, слагаемые которой суть

$$V'(x, y, z) = \int_S \frac{\mu(\xi, \eta) dS}{\sqrt{(\xi-x)^2 + (\eta-y)^2 + z^2}}; \quad (7)$$

$$V''(x, y, z) = \int_S \frac{z \cdot \nu(\xi, \eta) dS}{\sqrt{(\xi-x)^2 + (\eta-y)^2 + z^2}}; \quad (8)$$

Здесь x, y, z - координаты произвольной точки P вне планеты; ξ, η - координаты текущей точки Q плоской области S ; $\mu = \mu(\xi, \eta)$ и $\nu = \nu(\xi, \eta)$ - соответственно плотность простого и момент двойного слоев, предполагаемые принадлежащими к классу функций L_2^2 .

При написании этих потенциалов использованы формулы (4) и (5), причем в последней за положительное направление нормали \bar{n} к S взято отрицательное направление оси Oz . (Заметим, что формулы (7) и (8) при $R \rightarrow \infty$ и при заданных на S в ее плоскости функциях $\mu(\xi, \eta)$ и $\nu(\xi, \eta)$ дают соответственно решение задач Дирихле и Неймана для уравнения Лапласа в случае полупространства).

Простой слой, предполагаемый находящимся на площади круга S в экваториальной плоскости планеты и развивающий вне ее и на ее поверхности потенциал (7), будем называть массовым материальным диском ММД в связи с тем, что круг (или эллипс) S - для соз-

дания им в окружающем его пространстве потенциала V' - приходится считать нагруженным поверхностными массами плотности $\mu(\xi, \eta)$, общая масса которых равна массе планеты.

Двойной слой, образованный сплошным образом расположенными на диполями, ориентированными перпендикулярно к его плоскости и развивающими в своей совокупности всюду вне его (значит, и на поверхности планеты) потенциал (8), будем именовать дипольным диском ДД на основании того, что свойства этого потенциала - как потенциала двойного слоя - обусловлены функцией распределения моментов диполей $\nu(\xi, \eta)$, создающих такой диск.

В такой предлагаемой конкретной потенциалографической задаче требуется определить плотность μ и момент ν указанных гравитирующих дисков.

Отметим сначала основные свойства потенциалов (7) и (8) этих дисков.

1-е. Площадь S гравитирующих дисков выбрана так, см. условие (6), что потенциальные функции $V'(x, y, z)$ и $V''(x, y, z)$ и их частные производные любых порядков суть функции, непрерывные всюду вне S ; значит, они и все их производные непрерывны не только во всем внешнем пространстве относительно планеты, но и на ее поверхности σ .

2-е. Из формул (7) и (8) потенциалов дисков, в сумме выражающих внешний потенциал Земли, видно, что потенциал ММД, т.е. $V'(P)$ четная функция, а потенциал ДД, т.е. $V''(P)$ - нечетная функция относительно z . Другими словами, потенциалы V' и V'' гравитирующих дисков - это суть четная и нечетная части потенциала V планеты относительно ее экваториальной плоскости. В том случае, когда для какой-либо внешней точки $P(x, y, z)$ нет ей симметричной, точнее, последняя попадает во внутрь планеты или на ее по-

верхность, то приходится понимать под потенциалом V в такой точке его аналитическое проложение извне во внутрь планеты, конечно, при условии его существования.

3-е. Вспомня разный характер убывания потенциалов слоев по мере удаления от них, отметим, что в любой внешней точке

$$|V'(P)| > |V''(P)|.$$

Дадим приближенное решение рассматриваемой потенциалографической задачи.

Будем полагать внешний потенциал V планеты заданным набором стоксовых постоянных

$$V_N = \left\{ C_{nm}, S_{nm} \right\}$$

до некоторого порядка N . На основании свойства 2-го запишем:

$$V' = V_{\text{чет}}, \quad V'' = V_{\text{неч}},$$

где $V_{\text{чет}}$ и $V_{\text{неч}}$ - соответственно четная и нечетная части потенциала V относительно z или относительно $\cos \vartheta$, где ϑ - полярное расстояние внешней точки P . Значит, исходной информацией о ММД является левая часть уравнения (7), заданная набором параметров

$$V_N' = \left\{ C_{nm}, S_{nm} \right\}_{n+m=2n}, \quad (K=0, 1, 2, \dots) \quad (9)$$

а для ДД - левая часть уравнения (8) с набором стоксовых постоянных

$$V_N'' = \left\{ C_{nm}, S_{nm} \right\}_{n+m=2K+1}. \quad (10)$$

Потенциал планеты V содержит в усеченном до N -го порядка V_N шаровых функций $(N+1)^2$ стоксовых постоянных. Легко

подсчитать, что усеченный ряд V'_N потенциала ММД имеет в своем составе $\frac{1}{2}(N+1)(N+2)$ постоянных, а в ряде V''_N потенциала ДД их общее количество равно $\frac{1}{2}N(N+1)$.

Известно, что всякая функция двух переменных $\varphi(\xi, \eta) \in \mathcal{L}_S^2$ для любого фиксированного N имеет $\frac{1}{2}(N+1)(N+2)$ степенных моментов

$$\varphi_{pq} = \int_S \varphi(\xi, \eta) \xi^p \eta^q dS, \quad (p+q \leq N). \quad (II)$$

Значит, набор (9) стоксовых постоянных, определяющий V'_N , доставляет все степенные моменты μ_{pq} плотности ММД, поэтому его плотность $\mu = \mu(\xi, \eta)$ может быть восстановлена решением усеченной (до N -го порядка) степенной проблемы моментов, конечно, при выполнении условий ее разрешимости.

Моменты μ_{pq} плотности ММД однозначно вычисляются при этом по постоянным a'_{nm} и b'_{nm} этого диска вида

$$\left. \begin{matrix} a'_{nm} \\ b'_{nm} \end{matrix} \right\} = A'_{nm} \int_S \mu z'^n \begin{cases} \cos m \lambda' \\ \sin m \lambda' \end{cases} dS \quad (I2)$$

(z', λ' - полярные координаты точки $Q(\xi, \eta)$ диска в его плоскости), которые, в свою очередь, легко получаются по соответствующим стоксовым постоянным C_{nm} и S_{nm} из их набора (9) путем сравнения коэффициентов разложения потенциала $V'(P)$ ММД в ряд шаровых функций с четными (в смысле $n+m=2k$) коэффициентами лапласова ряда потенциала $V(P)$.

Почти аналогично находится и момент $\nu(\xi, \eta)$ дипольного диска. Отличие приближенного решения уравнения (8) от описанной процедуры такового для ММД заключается в том, что таким же образом вводимые и получаемые постоянные a''_{nm} и b''_{nm} , имеющие вид (I2), но, безусловно, с функцией $\nu(\xi, \eta)$ вместо $\mu(\xi, \eta)$ и иными множителями A''_{nm} , выражаются - с точностью до коэффици-

ента, зависящего от n и m , - уже через стоксовы постоянные $C_{n+1,m}$ и $S_{n+1,m}$. Таким образом, разложение V''_N "впитывает" в себя стоксовы постоянные до $(N+1)$ -го порядка включительно.

За счет этого однозначность решения усечения степенной проблемы моментов для функции $\nu(\xi, \eta)$ до N -го порядка требует учета стоксовых постоянных планеты до $(N+1)$ -го порядка. Однако отмеченное выше 3-е свойство потенциалов гравитирующих дисков подсказывает целесообразность при их совместном приближенном построении учитывать все стоксовы постоянные Земли до заранее намеченного порядка N , находя при этом плотность $\mu(\xi, \eta)$ ММД из решения усеченной задачи до N -го порядка, а момент $\nu(\xi, \eta)$ ДД - из усеченной задачи до $(N-1)$ -го порядка.

Подчеркнем одно любопытное обстоятельство. Как известно, обратная задача теории потенциала, в которой по известному внешнему потенциалу планеты, точнее по набору ее стоксовых постоянных до некоторого порядка N , ищется плотность δ распределения ее масс, однозначного решения не имеет. При сведении этой задачи к трехмерной степенной проблеме моментов, усеченной до N -го порядка, для обеспечения единственности ее решения не хватает $\frac{1}{2}n(n-1)$ моментов на каждый n -ый порядок ($n \geq 2$). Если же искать плотность μ и момент ν гравитирующих дисков ММД и ДД этой планеты, располагая параметрами ее внешнего поля также до N -го порядка, то, как было показано, эти "плотностные" характеристики дисков могут быть определены однозначно в классе многочленов N -го и $(N-1)$ -го порядков. И хотя эти гравитирующие диски - суть абстрактные конструкции, рассмотрение их оказывается небесполезным.

§3. Из обсужденного массового материального диска ММД планеты может быть выделен меньший по размерам фокальный диск ФД, отвечаю-

ций этой планете в предположении нахождения ее в гидростатическом равновесном состоянии.

Для подтверждения этого сначала вспомним [I0], что разложение в ряд шаровых функций потенциала V^* гидростатически равновесной планеты, внешняя уровенная поверхность которой суть сфероид, содержит в себе только четные зональные гармоники. С другой стороны, в ряд точно такого же вида разлагается и потенциал неоднородного эллипсоида вращения с эллипсоидально-слоистой структурой, коэффициенты которого зависят от закона изменения плотности при переходе от слоя к слою [II]. Значит, сохраняя вне эллипсоида, объемлющего сфероид, потенциал V^* гидростатически равновесной планеты, т.е. отождествляя указанные выше два ряда по четным зональным шаровым функциям в их общей области сходимости, можно потенциал этой планеты трактовать потенциалом эллипсоида с надлежащим эллипсоидальным строением.

Практически сказанное реализуется следующим образом. Сначала, задавшись линейным масштабом построений, считая, например, заданным экваториальный или полярный радиус сфероида, найдем его поверхность по известным параметрам внешнего гравитационного поля планеты $J_{2k} = -C_{2k,0}$ ($k=0,1,2,\dots$), ее угловой скорости ω вращения и при сохранении массы планеты. Указанное можно сделать либо по методике [I2,I3], либо по формулам (27,8), (3I,7) из [I0], где, правда, последние приведены только до $k=3$. Затем на основании подходящего критерия [I4,I5,I9] аппроксимируем найденный сфероид "общепланетарным" эллипсоидом с массой, естественно равной массе планеты. Полагаем, наконец, что этот эллипсоид развивается во внешнем пространстве тот же потенциал, что и сфероид, т.е. считаем

$$J_{2k}^{\text{э.}} = J_{2k}^{\text{сф.}} = -C_{2k,0}^{\text{р.п.}}, \quad (n=2k, k=0,1,2,\dots, n \leq N)$$

где $C_{n,0}^{\text{р.п.}}$ - стоксовы постоянные реальной планеты, а надстрочные символы э. и сф. - означают эллипсоид и сфероид. Этим самым введенному квазиобщепланетарному эллипсоиду приписана эллипсоидально-слоистая структура, которая описывается формулами (5.67) из [II], выражающими коэффициенты $J_{2k}^{\text{э.}}$ через его плотность, вопроса о фактическом нахождении которой здесь не ставится.

Обсужденная процедура позволяет определить параметры такого квазиобщепланетарного эллипсоида, геометрические параметры которого практически не отличаются от таковых общепланетарного эллипсоида. Но этот эллипсоид - неуровненный, однако, во-первых, он довольно полно характеризует гидростатически равновесную планету, ибо его потенциал содержит все учтенные до N -го порядка зональные параметры планеты $J_{2k} = -C_{2k,0}$, полученные по результатам наблюдений (нечетные зональные и все тессеральные гармоники его приняты равными нулю): во-вторых, его форма и размеры наилучшим образом в определенном смысле описывает сфероид; в-третьих, распределение потенциала на его поверхности известно: оно выражается усеченным рядом V_N^* по четным полиномам Лежандра с коэффициентами J_{2k} , выводимыми из результатов наблюдений; при этом очень просто вычисляется и распределение силы тяжести на этом эллипсоиде; в-четвертых, потенциал его составляет главную часть потенциала реальной планеты.

Свойства вводимого так квазиобщепланетарного эллипсоида дают возможность принять его за нормальный эллипсоид планеты. Все же повторим еще раз: этот эллипсоид - неуровненный. Но, учитывая актуальность вопроса о выборе нормального поля, удовлетворяющего разнообразным запросам геофизики, геодезии и небесной механики, мы обращаем здесь внимание на такой возможный, альтернативный к принятому, подход к его решению. Напомним при этом, что отказ

от уровненного нормального эллипсоида в теории фигуры Земли уже был однажды предметом всестороннего обсуждения [16]. Не углубляясь в рассмотрение этого важного вопроса и не предвещая выбора в данной альтернативе, будем далее взамен нормального уровненного эллипсоида пользоваться описанным здесь квазиобщеземным эллипсоидом, понимая под последним эллипсоид, наилучшим образом аппроксимирующий сфероид и имеющий эллипсоидально-слоистую структуру.

Потенциал квазиобщеземного эллипсоида можно заменить в соответствии с классической теорией притяжения софокусных эллипсоидов, см. [9,17], потенциалом плоского слоя, расположенного в экваториальной плоскости на круге S^* с центром, совпадающим с центром эллипсоида, и с радиусом, равном половине расстояния между фокусами меридианного эллипсоида, т.е. линейному эксцентриситету семейства софокусных эллипсоидов. Этот плоский слой – фокальный диск ФД – имеет переменную поверхностную плотность $\mu^* = \mu^*(\xi, \eta)$, зависящую от закона изменения объемной плотности слоев, составляющих эллипсоид; масса этого диска равна массе планеты.

Плотность ФД $\mu^*(\xi, \eta) \in \mathcal{L}_{S^*}^2$ может быть найдена аналогично плотности $\mu(\xi, \eta)$ ММД, т.е. также из решения проблемы моментов, но при приравнении нулю всех стоксовых постоянных планеты, кроме его определяющих четных зональных J_{2k} до некоторого априори принятого их порядка N .

Выделяя из ММД основную часть ФД, надо теперь еще учесть его оставшуюся часть – ту, потенциал которой в сумме с потенциалом ФД составляет всю четную часть потенциала планеты. Этой оставшейся четной части соответствует безмассовый материальный диск – БМД с площадью S : его потенциал характеризуется всеми четными (в смысле $k+m = \text{чет.}$) стоксовыми постоянными планеты, кроме четных зональных, учтенных потенциалом ФД, – и это должно быть при-

нято во внимание при решении проблемы моментов, доставляющей плотность такого БМД.

Итак, концепция гравитирующих дисков заключается в том, что потенциал планеты (или ее "притяжение") заменяется суммой потенциалов (или "притяжений") трех круговых концентрических дисков, находящихся в плоскости экватора планеты – ФД, БМД и ДД, свойства и методика построения которых были выше очерчены. Подчеркнем лишь, что ФД характеризуют планету в предположении ее гидростатически равновесного состояния, БМД отражает негидростатические свойства планеты, обусловленные ее симметричностью относительно плоскости экватора, а ДД – антисимметричную часть ее негидростатичности.

Добавим еще, что параллельно с аналитическим решением задачи о приближенном построении гравитирующих дисков может быть дан и численный метод их конструирования, приводящий к точечно-дипольным моделям потенциала планеты.

Гравитирующие диски БМД и ДД введены, кажется, впервые, а значение ФД в теории фигуры Земли отмечено было в работе [18], где показана возможность объяснения потенциала притяжения уровненного эллипсоида распределением масс на этом диске. Здесь же он использован для объяснения притяжения гидростатически равновесной планеты и неуровненного эллипсоида с эллипсоидальной внутренней структурой. Однако наиболее естественно необходимость его введения вытекает из следующих механических соображений.

Притяжение сферически – симметричной планетой внешней точки может быть заменено, как установил Ньютон, притяжением материальной точки, расположенной в центре масс планеты – скажем массивного шарика ничтожного радиуса. А для планеты эллипсоидальной формы с эллипсоидально-слоистой структурой такой шарик, очевидно,

должен быть сплюснут в массивный "эллипсоидик". Из теоремы Маклорена о притяжении эллипсоидов следует, что указанный "эллипсоидик" - и есть как раз фокальный диск общепланетарного эллипсоида, являющийся предельным положением сплющивающегося эллипсоида, софокусного исходному [9].

Дальнейшим развитием этой прозрачной идеи является вся изложенная здесь концепция гравитирующих дисков.

Л и т е р а т у р а

1. Мещеряков Г.А. Новая интерпретация представления внешнего гравитационного потенциала планеты рядом шаровых функций, - Сб. "Геодезия, картография и аэрофотосъемка", вып.28, Львов, 1978.

2. Мещеряков Г.А. О наилучшей квадратической аппроксимации геопотенциала, - в кн. "Наблюдения ИСЗ", №20, 1980; София, БАН, 1982.

3. Лундквист С.А., Джакалия Дж.Е.О. Представление геопотенциала с помощью выборочных функций, - в сб. [6].

4. Мещеряков Г.А. О мультипольном представлении гравитационного потенциала, - в сб. "Геодезия, картография и аэрофотосъемка", вып.19, Львов, 1974.

5. Мещеряков Г.А., Марченко А.Н. О максвелловых параметрах гравитационного поля Земли, - в кн. "Наблюдения ИСЗ", №18, 1978, Варшава-Лодзь, ПАН, 1979.

6. Использование искусственных спутников для геодезии", под редакцией С.Хемриксена и др., перев. с англ., М, "Мир", 1975.

7. Пеллинен Л.П., Нейман Ю.И. Физическая геодезия; Итоги науки и техники, сер. Геодезия и аэрофотосъемка, том 18, М., ВИНТИ, 1980.

8. Марченко А.Н. О выборе стабилизатора для устойчивой аппроксимации потенциала рядом фундаментальных решений уравнения Лапласа, - в кн. Proc. Int. Symp. "Figure of the Earth's, the Moon and other Planets", Monograph Series of VUŽTK, Prague, 1983.

9. Сретенский Л.Н. Теория ньютоновского потенциала, М.-Л., ОГИЗ -Гостехиздат, 1946.

10. Жарков В.Н., Трубицин В.П. Физика планетных недр, М., "Наука", 1980.

11. Дубошин Г.Н. Небесная механика: основные задачи и методы, М., "Наука", 1968.

12. Мещеряков Г.А. Использование метода итераций при определении обобщенных фигур планет, - в кн. Proc. Int. Symp. "Figure of the Earth's, the Moon and other Planets", Monograph Series of VUŽTK, Prague, 1983.

13. Мещеряков Г.А. О сфероиде Клеро, обобщающем поверхность Марса, - в кн. "Картографирование Луны и Марса", М., "Недра", 1978.

14. Мещеряков Г.А., Волжанин С.Д. О выводе параметров общеземного эллипсоида по спутниковой информации с использованием метода L_p - оценок, - в кн.: "Международная конференция "Использование наблюдений ИСЗ для геодезии и геофизики; Тезисы докладов, СССР, Суздаль, 13-18.IX.1982.

15. Мещеряков Г.А., Волжанин С.Д., Киричук В.В. Об уравнивании геодезических измерений с учетом закона распределения ошибок, ж. "Геодезия и картография", №2, М., "Недра", 1984.

16. Мигаль Н.К. Теория совместного определения фигуры и размеров Земли, - "Научные записки ЛПИ", вып.ХУ, серия геодезия, №1, Львов, 1949.

17. Мещеряков Г.А. О представлении потенциала планеты суммой потенциалов двух простых слоев, - в сб. "Геодезия, картография и аэрофотосъемка", - вып.39, Львов, 1984.

18. Юркина М.И. О проблеме Стокса, - Изв. ВУЗов, сер. "Геодезия и аэрофотосъемка", №1, 1977.

19. Мещеряков Г.А., Волжанин С.Д. Использование метода L_p - оценок при определении параметров общеземного эллипсоида, - в сб. "Геодезия, картография и аэрофотосъемка", вып.38, Львов, 1983.

Helmut Moritz

Institute of Theoretical Geodesy
 Technical University Graz, Austria

Abstract

Hamilton's principle of least action, in the form of Lagrange's equations, was applied to the rotation of a rigid earth, e.g., by Woolard (1953) and to the rotation of an elastic earth with a liquid core by Jeffreys (1949) and Jeffreys and Vicente (1957a, b). In the form of Hamilton's canonical equations it was applied to a rigid earth by Andoyer (1923, 1926) and, most recently and accurately, by Kinoshita (1977).

Poincaré (1910) modified Lagrange's equations, using non-holonomic group variables, and applied it to the rotation of a rigid mantle with a homogeneous liquid core. Finally, Moritz (1982a) applied Poincaré's equations to the rotation of the earth model of Jeffreys - Molodensky (elastic mantle and liquid core), which results in extremely simple equations derived in (Sasao et al., 1980) in a different way.

Since the rotation of a rigid earth is well-known, the paper reviews the classical approach by Jeffreys, using holonomic variables, and, in more detail, the recent approach through Poincaré's equations using non-holonomic variables related to rotation groups.

1. Lagrange's Equations

The principles of classical dynamics are treated in any course of theoretical physics. Standard treatises are, e.g., (Goldstein, 1980) and (Lanczos, 1970); (Arnold, 1978) can be recommended as an excellent synthesis of the

classical treatment and the modern approach through the language of exterior differential forms.

Let the motion of a dynamical system (e.g., a system of point masses which are free or linked to each other, or a rigid body) be described by n (generalized) coordinates or parameters q_1, q_2, \dots, q_n , where n is called the number of degrees of freedom of the system. Their time derivatives

$$\dot{q}_r = \frac{dq_r}{dt} \quad (1-1)$$

are called (generalized) velocities.

Denote the kinetic energy of the system by T , and its potential energy by U . Then T is a quadratic form in the \dot{q}_r :

$$T = a_{rs} \dot{q}_r \dot{q}_s; \quad (1-2)$$

summation over twice repeated subscripts is implied as usual (Einstein summation convention), and the coefficients a_{rs} will in general be functions of the coordinates:

$$a_{rs} = a_{rs}(q_1, q_2, \dots, q_n). \quad (1-3)$$

The potential energy U is a function of the coordinates:

$$U = U(q_1, q_2, \dots, q_n) \quad (1-4)$$

(and possibly also of time t ; this possibility will be disregarded here).

Hamilton's principle. The equations of motion may be derived from the following principle of least action, or Hamilton's principle. We introduce the Lagrangian, or Lagrangian function, L , by

$$L = T - U \quad (1-5)$$

as the difference between kinetic and potential energy, and define the action A by the integral

$$A = \int_{t_1}^{t_2} L dt \quad (1-6)$$

of L along the trajectory from the initial point (time t_1) to the end point (time t_2) of the motion.

Then the principle of least action states that the motion is such that

$$A = \int_{t_1}^{t_2} L dt = \int_{t_1}^{t_2} (T-U) dt = \text{minimum} \quad (1-7)$$

Lagrangian equations. Using well-known methods of the calculus of variations, the condition (1-7) leads to Lagrange's equations

$$\frac{d}{dt} \left(\frac{\partial L}{\partial \dot{q}_r} \right) - \frac{\partial L}{\partial q_r} = 0 \quad (1-8)$$

a system of n ordinary differential equations of the second order for $q_r = q_r(t)$.

The geodesist knows the relation between a variational problem and a system of second-order differential equations from ellipsoidal geometry: a geodesic line, being the shortest connection between two points (on the ellipsoid or on any other smooth surface) satisfies the condition of least arc length, analogous to (1-7), and is also a solution of a second-order system of differential equations, analogous to (1-8); in this case $n = 2$.

Rotation of a rigid body. The position (or rather orientation) of a rigid body rotating around its center of mass may be defined by three Eulerian angles ϕ, θ, ψ . Then

$$q_1 = \phi, \quad q_2 = \theta, \quad q_3 = \psi \quad (1-9)$$

are the generalized coordinates describing the rotation of a rigid body such as a rigid earth; hence $n = 3$ in this case.

For a certain specification of the Eulerian angles, the expression for the kinetic energy has the form

$$T = \frac{1}{2} A(\dot{\theta}^2 + \dot{\psi}^2 \sin^2 \theta) + \frac{1}{2} C(\dot{\phi} + \dot{\psi} \cos \theta)^2 \quad (1-10)$$

which serves as an example for the general expression (1-2). The constants A and C denote the principal moments of inertia of a rigid earth, presupposing

rotational symmetry ($B = A$). The potential energy U expresses the effect of sun and moon, the lunisolar attraction.

For this case, Lagrange's equations (1-8) can be formed and, after some transformations, neglecting small terms, lead to the well-known Poisson equations

$$\begin{aligned} \dot{\theta} &= \frac{1}{C\Omega} L_2, \\ \dot{\psi} \sin \theta &= -\frac{1}{C\Omega} L_1, \end{aligned} \quad (1-11)$$

whose solution gives precession and nutation in longitude ψ and obliquity θ ; Ω is a constant average value of the earth's rotational speed, and L_1 and L_2 are appropriate components of the lunisolar torque.

These brief remarks are only intended to convey a general idea how Lagrange's equations can be applied to earth rotation in a simple but important special case. The case of a rigid earth is well known, being treated in many textbooks, cf. (Plummer, 1918; Schneider, 1981; Melchior, 1983; Moritz and Mueller, 1985). The most detailed and accurate treatment is Woolard's (1953), which has served as an official standard in astronomy until 1979.

Hamilton's canonical equations constitute a very elegant reduction of Legendre's system of n second-order differential equations to a system of $2n$ first-order differential equations. Hamilton's equations use the $2n$ canonical variables $q_1, q_2, \dots, q_n; p_1, p_2, \dots, p_n$ with

$$p_r = \frac{\partial L}{\partial \dot{q}_r};$$

they have the simple form

$$\dot{q}_r = \frac{\partial H}{\partial p_r}, \quad \dot{p}_r = -\frac{\partial H}{\partial q_r},$$

where the Hamiltonian H is defined by

$$H = T + U$$

as the sum of kinetic and potential energy.

The Hamiltonian approach has been introduced by Andoyer in 1911, cf. (Andoyer, 1923, 1926). Recently, Kinoshita (1977) has used Andoyer variables to derive the most accurate theory of precession and nutation presently available for a rigid earth; cf. also (Moritz, 1980b; Moritz and Mueller, 1985). In general books on mechanics, the Hamiltonian approach to the rotation of a rigid body is hardly found, an exception being (Arkhangelsky, 1977).

We shall not discuss the Andoyer-Kinoshita method in this paper as we shall restrict ourselves to the more realistic earth model consisting of an elastic mantle with a rigid core, which so far has not been treated by Hamiltonian methods.

2. The Method of Jeffreys and Vicente

The first to treat the rotation of an elastic earth with a liquid core by Lagrangian methods was Jeffreys (1949). This approach has been perfected by Jeffreys and Vicente (1957a, b). In what follows we shall try to outline this method in a simple way, at the risk of oversimplification because the details are enormously complicated.

A basic principal difficulty consists in the fact that the mechanics of an elastic earth is problem of continuum mechanics for which the number of degrees of freedom is infinite. In fact, a general continuous function requires for its complete description a countably infinite set of parameters, e.g., its Fourier coefficients or its spherical-harmonic coefficients, as the case may be.

The lunisolar potential, which is responsible for tidal deformation and also for precession, nutation, and forced polar motion, can be expanded in such an infinite series of spherical harmonics. Fortunately, this series converges very rapidly, so that it can be truncated after degree 2 or 3, reducing the problem to one of a finite number of degrees of freedom which can be treated by the methods of classical dynamics.

Kinetic and potential energy. Let

$$\underline{u} = (u_1, u_2, u_3) \tag{2-1}$$

be the vector describing elastic (and possibly rotational) displacement of any material point of the body; it is the vector leading from the "undeformed" to the "deformed" position of that material point and will be assumed small. The displacement \underline{u} is different for different points $\underline{x} = (x_1, x_2, x_3)$, so that it will be a function of position

$$\underline{u} = \underline{u}(x_1, x_2, x_3) ; \tag{2-2}$$

this function is assumed to be continuous.

Then the kinetic energy is expressed by

$$T = \frac{1}{2} \iiint \rho (\dot{u}_1^2 + \dot{u}_2^2 + \dot{u}_3^2) dv ; \tag{2-3}$$

ρ denotes the density, dv the element of volume, and the integral is extended over the earth. The expression may be considered a continuous analogue of (1-2), the integral corresponding to the sum implicit in (1-2) by Einstein's convention.

The potential energy is given by

$$U = \frac{1}{2} \iiint \rho \left[\frac{\partial^2 V}{\partial x_i \partial x_j} u_i u_j + \frac{\partial(V_e + V_1)}{\partial x_i} u_i + \frac{\partial V}{\partial x_j} \left(u_i \frac{\partial u_j}{\partial x_i} - u_j \frac{\partial u_i}{\partial x_j} \right) - \rho^{-1} p_{ij} \frac{\partial u_i}{\partial x_j} \right] dv . \tag{2-4}$$

Here V denotes the gravitational potential of the (undeformed) earth, V_e the lunisolar perturbing potential, V_1 the change of the gravitational potential V because of elastic deformation, and p_{ij} the stress tensor. The summation convention applies to i, j running from 1 to 3.

We shall not attempt to derive (2-4); cf. (Jeffreys and Vicente, 1957a). We point out, however, the analogy to "small oscillations" well-known from classical dynamics, for which U is a quadratic function of q :

$$U = \frac{1}{2} b_{rs} q_r q_s , \tag{2-5}$$

with constant coefficients b_{rs} . In fact, (2-4) is quadratic in the displacements

u_i , and the integral in (2-4) again corresponds to the sum implicit in (2-5).

It is important to note that so far we have regarded the earth as nonrotating, in order to simplify matters and make the situation more transparent. Rotation will be taken into account later.

Truncation. The dynamical system defined by

$$\int_{t_1}^{t_2} (\dot{T} - U) dt = \text{minimum} \quad (2-6)$$

with (2-3) and (2-4), has infinitely many degrees of freedom as we have mentioned above.

The corresponding generalized coordinates q_r would be the coefficients of some spherical-harmonic expansion of the components u_i of the displacement vector \underline{u} . Since such an expansion is linear in the coefficients, the u_i will be linear functions of the q_r .

By an appropriate truncation we can achieve that we have only a finite number n of such q_r , so that u_i will be a linear function

$$u_i = \sum_{r=1}^n c_{ir} q_r = c_{ir} q_r \quad (2-7)$$

where u_i and c_{ir} , but not q_r , will be functions of position and time:

$$u_i = u_i(x_1, x_2, x_3, t) \quad (2-8)$$

$$c_{ir} = c_{ir}(x_1, x_2, x_3, t) \quad (2-8)$$

whereas

$$q_r = q_r(t) \quad (2-9)$$

is a function of time only. The stress tensor is linearly related to u_i by the well-known elastic stress-strain relations (Hooke's law), the known external potential also has a truncated spherical-harmonic expansion, and v_1 , being the result of a small deformation, is also related linearly to u_i . Taking all this into account, we can perform the integration in (2-3) and (2-4), ob-

taining a kinetic energy of form (1-2) and a potential energy of form

$$U = \frac{1}{2} b_{rs} q_r q_s + c_r q_r \quad (2-10)$$

with constants b_{rs} and c_r , which obviously is of form (1-4). The Lagrangian equations (1-8) then give a system of linear ordinary differential equations of second order for the $q_r(t)$.

Consideration of rotation. This barest sketch of the basic idea must now be made more precise and more concrete. First of all, we must introduce a rotating frame of reference, since (2-3) and (2-4) refer to a non-rotating inertial frame. We select a frame of reference which rotates with uniform angular velocity Ω around an x_3 -axis that has a fixed direction in space; a properly "earth-fixed" reference frame will deviate little from this uniformly rotating frame. Jeffreys describes the transition from one frame to the other by a rotation matrix. It is known that every rotation matrix depends on 3 parameters (e.g., three Euler angles). Jeffreys denotes these three parameters by l' , m' , n' ; they can be supposed small since the rotation matrix relating the "earth-fixed" frame to the uniformly rotating system will deviate little from the unit matrix, but they will depend on time.

Similar to (1-9), we may put

$$q_1(t) = l', \quad q_2(t) = m', \quad q_3(t) = n' \quad (2-11)$$

for the first three Lagrangian parameters describing the rotation of the earth as a whole.

Another set of three parameters, denoted l , m , n , will describe the rotation of the liquid core with respect to the mantle, so that

$$q_4(t) = l, \quad q_5(t) = m, \quad q_6(t) = n \quad (2-12)$$

Elasticity of the mantle. We are yet to specify those parameters q_r that enter into the expansion (2-7) of the elastic displacement vector \underline{u} and that correspond to a truncated spherical-harmonic expansion.

Because of the enormous distance of sun and moon from the earth, and since

the spherical harmonics of degree 0 and 1 are to be disregarded, the term of degree 2 will be dominant; cf. (Moritz, 1980a, sec. 55). Furthermore, for earth rotation, only the order 1 is relevant (the so-called diurnal tides, cf. Melchior, 1983, p. 26). Thus, only terms proportional to

$$R_{21}(\theta, \lambda) = P_{21}(\cos\theta)\cos\lambda, \tag{2-13}$$

$$S_{21}(\theta, \lambda) = P_{21}(\cos\theta)\sin\lambda$$

will be relevant. Here θ (polar distance) and λ (longitude) are spherical coordinates, and the Legendre function P_{21} is defined by

$$P_{21}(\cos\theta) = 3\sin\theta\cos\theta. \tag{2-14}$$

Solving the partial differential equations of elasticity for the mantle, taking into account appropriate boundary conditions at the earth's surface and at the core-mantle boundary (Melchior, 1983, sec. 5.5; Moritz, 1981, secs. 7 and 8; Moritz and Mueller, 1985, secs 4.3 to 4.5), we can express everything in terms of the radial displacement u_r at the earth's surface and at the core-mantle interface, expanding into spherical harmonics and retaining only the terms (2-13):

$$u_r(R) = q_7(t)R_{21}(\theta, \lambda) + q_8(t)S_{21}(\theta, \lambda), \tag{2-15}$$

$$u_r(R_c) = q_9(t)R_{21}(\theta, \lambda) + q_{10}(t)S_{21}(\theta, \lambda).$$

Here, $R = 6371$ km and $R_c = 3485$ km denote the mean radii of the earth and the core, respectively; the coefficients $q_7(t)$ through $q_{10}(t)$ furnish the desired generalized "coordinates" describing mantle elasticity.

It is not difficult to see that exactly 4 parameters are needed to describe mantle elasticity. It is well known that the solution can be expressed in terms of three Love numbers h, k, ℓ (cf. Melchior, 1983, sec. 5.5; Moritz, 1981, p. 96). However, $h, k,$ and ℓ satisfy a linear relation which expresses the vanishing of the tangential tension. Thus we are left with two independent numbers h and ℓ , which, apart from a known factor, are nothing else than radial and tangential displacement at the earth's surface, $u_r(R)$ and $u_t(R)$. Instead of $u_t(R)$ we may also take $u_r(R_c)$, which leads to (2-15).

Lagrange's equations. Using the "rotational" parameters $q_1(t)$ to $q_6(t)$ and the "elasticity" parameters $q_7(t)$ to $q_{10}(t)$ we get a Lagrangian

$$L = L(q_1, q_2, \dots, q_{10}) \tag{2-16}$$

for a dynamic problem with 10 degrees of freedom. L will be quadratic in the q_r and can be shown to have the form

$$L = \frac{1}{2} a_{rs} \dot{q}_r \dot{q}_s - \frac{1}{2} b_{rs} q_r q_s + c_{rs} q_r \dot{q}_s - d_r q_r, \tag{2-17}$$

where the summations go from 1 to 10. The coefficients a_{rs} , etc., are constants but depend on the model assumed for the internal structure of the earth and must be computed accordingly. The presence of the "gyroscopic term" $c_{rs} q_r \dot{q}_s$ is due to the rotation of the earth (cf. Goldstein, 1980, p. 354; Lanczos, 1970, p. 122).

Finding these coefficients constitutes the main difficulty, which is enormous indeed. After that, matters are straightforward. Using (2-17), Lagrange's equations (1-8) give immediately

$$a_{rs} \ddot{q}_s + (c_{sr} - c_{rs}) \dot{q}_s + b_{rs} q_s + d_r = 0. \tag{2-18}$$

The further treatment of these linear differential equations is standard. Using complex combinations

$$\begin{aligned} q_1 + iq_2 &= Q_1, \\ q_4 + iq_5 &= Q_2, \\ q_7 + iq_8 &= Q_3, \\ q_9 + iq_{10} &= Q_4 \end{aligned} \tag{2-19}$$

(with an appropriate choice of rotation parameters it is possible to disregard n and n') we are able to reduce (2-18) to a system of four complex linear differential equations for Q_k ($k = 1, 2, 3, 4$), and "transforming to the frequency domain" by

$$Q_k(t) = Q_k^0 e^{i\sigma t} \tag{2-20}$$

we get a system of four linear algebraic equations to be solved for Q_k^0 .

The Lagrangian approach of Jeffreys and Vicente has a conceptually simple structure: once the Lagrangian (2-17) has been established, everything else follows in a logically straightforward manner. Nevertheless, the details of the computation of the coefficients a_{rs} , etc., for a given earth model are enormously complicated, and only a man of the physical insight and mathematical skill of Sir Harold Jeffreys could have devised such an approach and lead it to a successful conclusion.

In view of these difficulties, Jeffreys and Vicente (1957a, b) considered only two greatly simplified earth models: the central particle model, consisting of a homogeneous core and a central mass point representing the solid inner core, and the Roche model using a continuous density distribution in the core according to Roche's law. For the same reason, beginning at an early stage, computations were performed numerically instead of analytically, so that the physical interpretation becomes difficult. Thus this approach, though logically very elegant, is physically not completely transparent.

Therefore, Molodensky (1961), wishing to use more realistic earth models, gave up the variational approach and instead used the partial differential equations of elasticity and hydromechanics. A particularly simple and elegant solution of Molodensky's problem was provided by Sasao et al. (1980), and it turned out that these equations can be derived and physically interpreted by another variational principle which goes back to Poincaré (1901).

It is not surprising that, after 35 years of efforts, we now understand the problem better, but this would not be possible without the pioneering work of Jeffreys and Molodensky.

3. Poincaré's Equations

The rotation group. It is well known that rotation matrices \underline{A} form a **group**, so that the following properties hold:

1. The product of two rotation matrices \underline{A} and \underline{B} is again a rotation matrix $\underline{C} = \underline{A} \underline{B}$.
2. For the unit matrix \underline{I} we have $\underline{A} \underline{I} = \underline{I} \underline{A} = \underline{A}$

3. Every rotation matrix has an inverse \underline{A}^{-1} which again is a rotation matrix.

Furthermore, the inverse of a rotation matrix is simply its transpose:

$$\underline{A}^{-1} = \underline{A}^T, \quad (3-1)$$

so that

$$\underline{A} \underline{A}^T = \underline{A}^T \underline{A} = \underline{I}. \quad (3-2)$$

The matrix

$$d\underline{\Pi} = \underline{A}^{-1} d\underline{A} = \underline{A}^T d\underline{A} \quad (3-3)$$

is skew-symmetric, which immediately follows by differentiating (3-2). Thus it has the form

$$d\underline{\Pi} = \begin{bmatrix} 0 & -d\pi_3 & d\pi_2 \\ d\pi_3 & 0 & -d\pi_1 \\ -d\pi_2 & d\pi_1 & 0 \end{bmatrix} \quad (3-4)$$

On introducing the matrices

$$\underline{E}_1 = \begin{bmatrix} 0 & 0 & 0 \\ 0 & 0 & -1 \\ 0 & 1 & 0 \end{bmatrix}, \quad \underline{E}_2 = \begin{bmatrix} 0 & 0 & 1 \\ 0 & 0 & 0 \\ -1 & 0 & 0 \end{bmatrix}, \quad \underline{E}_3 = \begin{bmatrix} 0 & -1 & 0 \\ 1 & 0 & 0 \\ 0 & 0 & 0 \end{bmatrix} \quad (3-5)$$

this may be written

$$d\underline{\Pi} = \underline{E}_1 d\pi_1 + \underline{E}_2 d\pi_2 + \underline{E}_3 d\pi_3 = \underline{E}_i d\pi_i. \quad (3-6)$$

The term $\underline{E}_1 d\pi_1$ obviously represents a rotation by the infinitesimal angle $d\pi_1$ around the x_1 axis, and similar for the other terms.

It is immediately verified that the matrices \underline{E}_i satisfy the basic commutation relations

$$\begin{aligned} [E_1, E_2] &= E_3 \quad , \\ [E_2, E_3] &= E_1 \quad , \\ [E_3, E_1] &= E_2 \quad . \end{aligned} \tag{3-7}$$

The commutation symbol $[]$ stands for

$$[E_i, E_j] = E_i E_j - E_j E_i \quad , \tag{3-8}$$

$E_i E_j$ being the usual matrix product of E_i and E_j .

Eqs. (3-7) are a special case, for the rotation group, of the general commutation relations

$$[E_i, E_j] = c_{ijk} E_k \quad , \tag{3-9}$$

valid for a general continuous group, or Lie group; cf. (Smirnow, 1971) or (Choquet-Bruhat et al., 1977). The c_{ijk} are constants, called the structure constants of the group. For a general group, they run from 1 to n , n being again the number of degrees of freedom. By (3-8), the interchange of i and j means a change of sign, whence

$$c_{ijk} = -c_{jik} \quad . \tag{3-10}$$

For the rotation group we have in particular

$$\begin{aligned} c_{123} &= c_{231} = c_{312} = 1 \quad , \\ c_{213} &= c_{321} = c_{132} = -1 \quad , \end{aligned} \tag{3-11}$$

all other $c_{ijk} = 0$.

The c_{ijk} are zero for commutative (Abelian) groups.

The angular velocity component ω_i along the x_i axis may be considered a change of $d\pi_i$ with respect to time t :

$$\omega_i = \frac{d\pi_i}{dt} \tag{3-12}$$

Given ω_i , one cannot, however, integrate (3-12) to obtain coordinates π_i since the $d\pi_i$ are not, in general, perfect differentials. Nevertheless, it is useful still to regard the $d\pi_i$ as some kind of coordinates, called anholonomic coordinates, which make sense only in the infinitesimal domain; cf. (Grafarend, 1975).

The important property of the $d\pi$ is their group-invariance, whereas holonomic coordinates for the rotation group, e.g., the three Euler angles, are not group-invariant; see below.

The torque $\underline{L} = (L_1, L_2, L_3)$ is related to the rotational potential energy U by

$$-dU = L_1 d\pi_1 + L_2 d\pi_2 + L_3 d\pi_3 = L_i d\pi_i \quad , \tag{3-13}$$

so that we may write formally

$$L_i = - \frac{\partial U}{\partial \pi_i} \quad , \tag{3-14}$$

which is analogous to the relation between force \underline{F} and potential V :

$$\underline{F} = -\text{grad } V \quad \text{or} \quad F_i = - \frac{\partial V}{\partial x_i} \quad , \tag{3-15}$$

the minus sign being conventional in both cases.

Poincaré's equations. Starting again from the principle of least action (1-7), but using anholonomic coordinates $d\pi_i$ and velocities ω_i , we find Poincaré's equations of motion:

$$\frac{d}{dt} \left(\frac{\partial L}{\partial \omega_i} \right) + c_{ijk} \omega_j \frac{\partial L}{\partial \omega_k} - \frac{\partial L}{\partial \pi_i} = 0 \quad . \tag{3-16}$$

They differ from Lagrange's equations (1-8) only by the middle term, containing the structure constants c_{ijk} ; for holonomic coordinates (possible in the case of commutative or Abelian groups), they even reduce to Lagrange's equations. A derivation of (3-16) can be found in (Moritz, 1982b, c), or in (Moritz and Mueller, 1985, sec. 4.6.2).

Eqs. (3-16) were given by Poincaré (1901) explicitly with a view to application

to the problem of earth rotation, but this paper remained practically unknown to mathematicians. This is the more surprising as otherwise his work in dynamics is highly recognized by them. Recently the topic, motion on a Lie group, has become quite fashionable, cf. (Hermann, 1968; Abraham and Marsden, 1978; Arnold, 1978); none of them quotes Poincaré's paper. Nor does (Whittaker, 1961), who uses general non-holonomic coordinates (not restricted to Lie groups).

We take into account $L = T - U$ and the fact that the potential energy U does not depend on the velocities ω_i . We furthermore assume that T depends only on ω_i so that $\partial T / \partial \pi_i = 0$. Then, using (3-14), we may write Poincaré's equations (3-16) in the form

$$\frac{d}{dt} \left(\frac{\partial T}{\partial \omega_i} \right) + c_{ijk} \omega_j \frac{\partial T}{\partial \omega_k} = L_i ; \quad (3-17)$$

there is no danger to confuse the torque components L_i with the Lagrangian L

Application to Euler's equations. As an example, consider the rotation of a rigid body. Then the group under consideration is the three-dimensional rotation group, whose constants are given by (3-11). For the kinetic energy we have the simple equation

$$T = \frac{1}{2} (A\omega_1^2 + B\omega_2^2 + C\omega_3^2) , \quad (3-18)$$

where A, B, C are the principal moments of inertia, and the coordinate axes are the principal axes of inertia. Then (3-16) immediately gives

$$\begin{aligned} A\dot{\omega}_1 + (C-B)\omega_2\omega_3 &= L_1 , \\ B\dot{\omega}_2 + (A-C)\omega_3\omega_1 &= L_2 , \\ C\dot{\omega}_3 + (B-A)\omega_1\omega_2 &= L_3 , \end{aligned} \quad (3-19)$$

which are the well-known Euler equations for rigid-body rotation.

It is instructive to compare the approaches of Lagrange and Poincaré. In the Lagrangian approach, using holonomic coordinates ϕ, θ, ψ , the kinetic energy (1-10) depends on the coordinates q_r in addition to the velocities \dot{q}_r , whereas in the present approach, (3-18) depends only on the velocities ω_j . Eq. (1-10) is a quadratic form in the velocities with variable coefficients,

whereas (3-18) has constant coefficients. Furthermore, (3-18) has a very simple and symmetric form, expressing group symmetry or group invariance.

Thus the essential feature of Poincaré's approach consists in the fact that, using anholonomic variables, the group symmetry can be fully exploited.

4. Rigid Mantle and Liquid Core

Poincaré (1910) considered an earth model consisting of a rigid mantle enclosing a homogeneous liquid core. Both the earth's surface and the core-mantle interface are regarded as concentric and coaxial ellipsoids of revolution.

Poincaré uses two different approaches which both lead to the same result:

1. The core movement is treated by the equations of hydrodynamics.
2. The core movement is considered a "simple motion", reducing to a rotation of the core after an affine transformation of the ellipsoidal core-mantle interface into a sphere.

The first approach is appealing on physical grounds and is, therefore, also treated in the textbook literature; cf. (Lamb, 1932, p. 724; Melchior, 1983, p. 125). The second approach is considered by Poincaré himself simpler and more elegant; it will be briefly sketched here; for more details cf. (Moritz, 1982c; Moritz and Mueller, 1985).

The kinetic energy is given by

$$\begin{aligned} T = \frac{1}{2} (A\omega_1^2 + B\omega_2^2 + C\omega_3^2 + \\ + A_c x_1^2 + B_c x_2^2 + C_c x_3^2) + \\ + F\omega_1 x_1 + G\omega_2 x_2 + H\omega_3 x_3 , \end{aligned} \quad (4-1)$$

generalizing (3-18) because of the rotation of the core with respect to the mantle (angular velocity components x_1, x_2, x_3). Here A, B, C and A_c, B_c, C_c denote the principal moments of inertia for the whole earth and for the core, respectively. Because of symmetry we have

$$B = A , \quad B_c = A_c , \quad G = F ; \quad (4-2)$$

furthermore it may be shown that, to a sufficient approximation,

$$F = A_c, \quad H = C_c. \quad (4-3)$$

We now wish to apply Poincaré's equations (3-17). We here have six degrees of freedom: three for the rotation of the earth as a whole (ω_i) and three for the core rotation (χ_i). Thus the whole six-dimensional group relevant for the present problem consists of two independent rotation groups. The structure equations (3-7) for rotation groups give

$$\begin{aligned} [E_1, E_2] &= E_3, & [E_1^c, E_2^c] &= -E_3^c, \\ [E_2, E_3] &= E_1, & [E_2^c, E_3^c] &= -E_1^c, \\ [E_3, E_1] &= E_2, & [E_3^c, E_1^c] &= -E_2^c, \end{aligned} \quad (4-4)$$

where E_i^c denotes E_i for core rotation. Note the difference in sign due to the fact that the second rotation is with respect to the mantle whereas the first is a rotation of the mantle with respect to inertial space. Any rotation E_i commutes with any rotation E_i^c since the two rotations are independent of each other, whence

$$[E_i, E_j^c] = 0 \quad (i \text{ and } j = 1, 2, 3). \quad (4-5)$$

The six quantities $\omega_1, \omega_2, \omega_3, \chi_1, \chi_2, \chi_3$ may be identified with $\omega_1, \omega_2, \dots, \omega_6$ and $E_1, E_2, E_3, E_1^c, E_2^c, E_3^c$ with E_1, E_2, \dots, E_6 according to (3-9). The corresponding structure constants c_{ijk} are all 0, 1, or -1, according to (4-4) and (4-5).

Thus Poincaré's equations (3-17) with i, j, k running from 1 to 6, give

$$\begin{aligned} \frac{d}{dt} \left(\frac{\partial T}{\partial \omega_1} \right) - \omega_3 \frac{\partial T}{\partial \omega_2} + \omega_2 \frac{\partial T}{\partial \omega_3} &= L_1, \\ \frac{d}{dt} \left(\frac{\partial T}{\partial \omega_2} \right) - \omega_1 \frac{\partial T}{\partial \omega_3} + \omega_3 \frac{\partial T}{\partial \omega_1} &= L_2, \\ \frac{d}{dt} \left(\frac{\partial T}{\partial \omega_3} \right) - \omega_2 \frac{\partial T}{\partial \omega_1} + \omega_1 \frac{\partial T}{\partial \omega_2} &= L_3; \end{aligned} \quad (4-6)$$

$$\begin{aligned} \frac{d}{dt} \left(\frac{\partial T}{\partial \chi_1} \right) + \chi_3 \frac{\partial T}{\partial \chi_2} - \chi_2 \frac{\partial T}{\partial \chi_3} &= 0, \\ \frac{d}{dt} \left(\frac{\partial T}{\partial \chi_2} \right) + \chi_1 \frac{\partial T}{\partial \chi_3} - \chi_3 \frac{\partial T}{\partial \chi_1} &= 0, \\ \frac{d}{dt} \left(\frac{\partial T}{\partial \chi_3} \right) + \chi_2 \frac{\partial T}{\partial \chi_1} - \chi_1 \frac{\partial T}{\partial \chi_2} &= 0. \end{aligned} \quad (4-7)$$

The right-hand side of (4-7) is zero since the lunisolar torque \underline{L} acts on the whole earth; there is no external torque which would effect a relative motion of the core with respect to the mantle. This relative motion is caused purely by the rotation of the mantle which, through the ellipticity of the core-mantle interface, acts on the core through "inertial coupling" (which, e.g., also renders the rotational behavior of a raw egg different from that of a hard-boiled egg).

The further treatment is straightforward. We substitute (4-1) into (4-6) and (4-7), taking (4-2) and (4-3) into account. Then, after some algebra and neglecting small terms, the third equation of (4-6) gives, with $L = 0$ because of rotational symmetry,

$$\omega_3 = \Omega = \text{const.}, \quad (4-8)$$

and the third equation of (4-7) has the solution

$$\chi_3 = 0. \quad (4-9)$$

Introducing the complex quantities

$$\begin{aligned} u &= \omega_1 + i\omega_2, \\ v &= \chi_1 + i\chi_2, \\ L &= L_1 + iL_2, \end{aligned} \quad (4-10)$$

the first two equations of (4-6) can be combined into one complex equation, and the same can be done with the first and second equation of (4-7). The result is

$$\begin{aligned} A\dot{u} + A_c\dot{v} - i(C-A)\Omega u + iA_c\Omega v &= L, \\ A_c\dot{u} + A\dot{v} + iC\Omega v &= 0, \end{aligned} \quad (4-11)$$

which are Poincaré's equations. By a transformation to the frequency domain, putting

$$u = u_0 e^{i\sigma t}, \quad v = v_0 e^{i\sigma t}, \quad L = L_0 e^{i\sigma t}, \quad (4-12)$$

these equations can be reduced to a system of algebraic linear equations for two unknowns and thus easily solved, if the lunisolar torque L is given.

The physical meaning of the two equations (4-11) is different. The first is a consequence of the well-known angular momentum equations

$$\frac{dH}{dt} + \underline{\omega} \times H = \underline{L}, \quad (4-13)$$

which holds for an arbitrary body (rigid or not), in a system rotating with angular velocity $\underline{\omega}$; the vector H denotes angular momentum. The second equation, however, can be interpreted only in terms of the hydrodynamics of the liquid core.

Formally, however, both equations (4-11) are very similar; and the present derivation from a variational principle explains the similarities as a simple consequence of the two basic rotations, ω_i and x_i .

5. Elastic Mantle and Liquid Core

Kinetic energy. The velocity of a particle in the mantle can be split up as follows:

$$\underline{v} = \underline{v}_{\text{mantle}} = \underline{\omega} \times \underline{x} + \underline{v}_m, \quad (5-1)$$

where $\underline{\omega} \times \underline{x}$ denotes a rigid rotation and \underline{v}_m , a small deviation from rigid rotation due to elastic deformation. In a similar way, we have for a particle in the core

$$\underline{v} = \underline{v}_{\text{core}} = \underline{\omega} \times \underline{x} + \underline{x} \times \underline{x} + \underline{v}_c, \quad (5-2)$$

where, in addition to the rotation $\underline{\omega}$ of the entire earth, we have a relative

rotation \underline{x} of the core with respect to the mantle and a residual deformation \underline{v}_c .

The kinetic energy of a mass element is $\frac{1}{2} \underline{v}^2 dM$ and hence for the whole earth we have

$$T = \frac{1}{2} \iiint \underline{v}^2 dM. \quad (5-3)$$

The substitution of (5-1) for the mantle and (5-2) for the core leads rather directly to the expression

$$T = \frac{1}{2} C_{ij} \omega_i \omega_j + C_{ij}^c \omega_i x_j + \frac{1}{2} C_{ij}^c x_i x_j. \quad (5-4)$$

For a rigid body, using principal axes of inertia, the inertia tensors C_{ij} (whole earth) and C_{ij}^c (core) are diagonal, and (5-4) reduces to (4-1). For an elastic body, however, we must allow for small time-dependent deviations from diagonal form, putting

$$[C_{ij}] = \begin{bmatrix} A & 0 & 0 \\ 0 & A & 0 \\ 0 & 0 & C \end{bmatrix} + \begin{bmatrix} c_{11} & c_{12} & c_{13} \\ c_{12} & c_{22} & c_{23} \\ c_{13} & c_{23} & c_{33} \end{bmatrix}, \quad (5-5)$$

and similarly for the core. Here A, C, A_c, C_c (the last two being principal moments of inertia for the core) are constants. As regards the residual inertia tensors,

$$c_{ij} = c_{ij}(t), \quad c_{ij}^c = c_{ij}^c(t), \quad (5-6)$$

we only retain those which are related to nutation and polar motion, namely $c_{13}, c_{23}, c_{13}^c,$ and c_{23}^c . Other terms do not influence these phenomena and can be disregarded without harm. Then (5-4) takes the final form

$$T = \frac{1}{2} A(\omega_1^2 + \omega_2^2) + \frac{1}{2} C\omega_3^2 + c_{13}\omega_1\omega_3 + c_{23}\omega_2\omega_3 + \frac{1}{2} A_c(2\omega_1x_1 + x_1^2 + 2\omega_2x_2 + x_2^2) + \frac{1}{2} C_c(2\omega_3x_3 + x_3^2) + c_{13}^c(\omega_1x_3 + \omega_3x_1 + x_1x_3) + c_{23}^c(\omega_2x_3 + \omega_3x_2 + x_2x_3). \quad (5-7)$$

Potential energy. For the total potential energy U we now have to consider elasticity, so that

$$U = U_g + U_e + U_d \tag{5-8}$$

Here U_g is the gravitational potential energy related to the lunisolar torque; it is the same as U in sec. 4. Now, however, we have two additional terms related directly (U_e) and indirectly (U_d) to elastic deformation. More precisely, U_e represents the energy of the elastic forces which are a reaction of the earth (including its liquid core) to the external forces, and U_d represents the change in gravitational energy due to elastic deformation.

U_d is relatively easy to derive; we find

$$U_d = \Omega(c_{13} f_1 + c_{23} f_2) \tag{5-9}$$

where f_1 and f_2 represent the given external (lunisolar) potential; cf. eq. (5-20) below.

Then U_e can be found using a theorem given in (Love, 1927, p. 173): "The potential energy of deformation of a body, which is in equilibrium under a given load, is equal to half the work done by the external forces, acting through the displacements from the unstressed state to the state of equilibrium." The result equations we have

$$U_e = \frac{1}{2} \Omega \left[E_{11} (c_{13}^2 + c_{23}^2) + E_{22} (c_{13}^c{}^2 + c_{23}^c{}^2) + 2E_{12} (c_{13} c_{13}^c + c_{23} c_{23}^c) \right] \tag{5-10}$$

where the E_{ij} are constants only depending on the internal structure of the earth model under consideration; they can be expressed relatively easily, e.g., through the standard functions $y_1(r), y_2(r), y_3(r), y_4(r), y_5(r), y_6(r)$ of (Alterman et al., 1959).

A detailed derivation of T and U can be found in (Moritz, 1982b, secs. 6 and 7) or in (Moritz and Mueller, 1985, sec. 4.7).

We finally put

$$U_{ed} = U_e + U_d \tag{5-11}$$

for the combined energy of elastic deformation, so that the total potential energy becomes

$$U = U_g + U_{ed} \tag{5-12}$$

Application of Poincaré's equations. First we have to find the variables for the present problem. Just as in the rigid-mantle problem discussed in the preceding section, we have two rotation groups, given by the six velocities $\omega_1, \omega_2, \omega_3, \chi_1, \chi_2, \chi_3$. In addition to these rotational variables, the kinetic energy (5-7) also contains the time-variable products of inertia $c_{13}, c_{23}, c_{13}^c, c_{23}^c$; and also the potential energy depends on these variables; cf. (5-9) and (5-10). Thus we have four additional degrees of freedom, which describe the elastic deformation. They are ordinary (holonomic) variables q_7, q_8, q_9, q_{10} , so that the usual Lagrange equations (1-8) hold for them. (This also fits into the group-theoretic scheme, with π_i instead of q_i for $i = 7, 8, 9, 10$, the corresponding subgroup being Abelian with zero c_{ijk} .)

The Poincaré equations (4-6) and (4-7) finally remain the same since we have two independent rotation groups as in sec. 4. In addition to these six equations we have

$$\frac{\partial(T-U)}{\partial q_i} = 0, \quad i = 7, 8, 9, 10,$$

which follows from (1-8) since $T-U$ does not contain the corresponding \dot{q}_i . Since only U_{ed} , but not U_g , depends on these q_i , this reduces to

$$\begin{aligned} \frac{\partial T}{\partial c_{13}} &= \frac{\partial U_{ed}}{\partial c_{13}}, & \frac{\partial T}{\partial c_{23}} &= \frac{\partial U_{ed}}{\partial c_{23}}, \\ \frac{\partial T}{\partial c_{13}^c} &= \frac{\partial U_{ed}}{\partial c_{13}^c}, & \frac{\partial T}{\partial c_{23}^c} &= \frac{\partial U_{ed}}{\partial c_{23}^c}. \end{aligned} \tag{5-13}$$

The 10 equations (4-6), (4-7), and (5-13) relate and determine the 10 quantities $\omega_1, \omega_2, \omega_3, \chi_1, \chi_2, \chi_3, c_{13}, c_{23}, c_{13}^c$, and c_{23}^c .

We note that the torque components L_i are the same as in sec. 4, namely purely gravitational: since U_{ed} does not depend on the rotational variables,

we have

$$L_i = - \frac{\partial U}{\partial \pi_i} = - \frac{\partial U}{\partial \pi_i} g_i, \quad (5-14)$$

representing the usual components of the lunisolar torque.

The rest is straightforward. We substitute (5-7) into (4-6) and (4-7). The third equations of the two systems again give

$$\begin{aligned} \omega_3 &= \Omega = \text{const.}, \\ x_3 &= 0. \end{aligned} \quad (5-15)$$

The complex combination of the first two equations of each system yields

$$\begin{aligned} A\dot{u} - i(C-A)\Omega u + A_c(\dot{v} + i\Omega v) + \Omega(\dot{c} + i\Omega c) &= L, \\ A_c\dot{u} + A_c\dot{v} + iC_c\Omega v + \Omega\dot{c}_c &= 0, \end{aligned} \quad (5-16)$$

with (4-10) and

$$c = c_{13} + ic_{23}, \quad c_c = c_{13}^c + ic_{23}^c. \quad (5-17)$$

The complex combination of the results of (5-13) gives with $f = f_1 + if_2$:

$$\begin{aligned} u &= E_{11}c + E_{12}c_c + f, \\ v &= E_{12}c + E_{22}c_c, \end{aligned} \quad (5-18)$$

which may be inverted to yield

$$\begin{aligned} c &= D_{11}(u-f) + D_{12}v, \\ c_c &= D_{12}(u-f) + D_{22}v. \end{aligned} \quad (5-19)$$

The four equations (5-16) and (5-19) determine the four complex unknowns u , v , c , c_c in the usual manner. We finally note that f is related to the given lunisolar torque L by

$$f = iL/(C-A)\Omega. \quad (5-20)$$

Discussion. Eqs. (5-16) and (5-19) probably constitute the simplest formulation of the Jeffreys-Molodensky liquid core problem. They are due to Sasao et al. (1980), who derived them using the equations of elasticity and of hydrodynamics, corresponding to "Poincaré's first method" as mentioned at the beginning of sec. 4. For a rigid earth, with $c_{ij} = 0$, they reduce to Poincaré's equations (4-11) as they should. The remarkable achievement of Sasao et al. (1980) was to show that the generalization of (4-11) to an elastic mantle can be made in such a simple way. That means, the resulting equations were simple, but their derivation was rather complicated and difficult.

The present approach, corresponding to "Poincaré's second method", tries to conform to the useful guideline that simple results should be derived in a simple way. The logical simplicity is expressed by the fact that the equations of hydrodynamics are not needed and both equations (5-16) are derived in a unified way.

The internal structure of the earth only enters through the coefficients D_{ij} or E_{ij} which, besides permitting a simple physical interpretation as coefficients in the elastic energy (5-10), can easily be expressed by means of standard functions and computed for arbitrary (basically radially symmetric) earth models featuring a heterogeneous liquid core and even a solid inner core.

With respect to the Lagrangian approach of Jeffreys and Vicente outlined in sec. 2, the simplification is achieved by using non-holonomic rotational variables and, as elastic variables, the products of inertia c_{13} , c_{23} , c_{13}^c and c_{23}^c instead of the radial displacements according to (2-15).

REFERENCES

- Abraham, R.A., and Marsden, J.E. (1978): Foundations of Mechanics, 2nd ed., Benjamin-Cummings, Reading, Mass.
- Alterman, Z., Jarosch, H., and Pekeris, C.L. (1959): Oscillations of the earth, Proc. R.Soc., A, 252, 80-95, London.

- Andoyer, M.H. (1923, 1926): *Cours de Mécanique Céleste*, Gauthier-Villars, Paris.
- Arkhangel'sky, Yu.A. (1977): *Analytical Dynamics of a Rigid Body* (in Russ.), Nauka Press, Moscow.
- Arnold, V.I. (1978): *Mathematical Methods of Classical Mechanics*, Springer, New York.
- Choquet-Bruhat, Y., de Witt-Morette, C., and Dillard-Bleick, M. (1977): *Analysis, Manifolds and Physics*, North-Holland Publ.Co., Amsterdam.
- Goldstein, H. (1980): *Classical Mechanics*, 2nd ed., Addison-Wesley, Reading, Mass.
- Grafarend, E.W. (1975): Three-dimensional geodesy I: the holonomy problem, *Z. Vermessungswesen*, 100, 269-281.
- Hermann, R. (1968): *Differential Geometry and the Calculus of Variations*, Academic Press, New York.
- Jeffreys, H. (1949): Dynamic effects of a liquid core, *Mon.Not.R.Astr.Soc.*, 109, 670-687.
- Jeffreys, H., and Vicente, R.O. (1957a): The theory of nutation and the variation of latitude, *Mon.Not.R.Astr.Soc.*, 117, 142-161.
- Jeffreys, H., and Vicente, R.O. (1957b): The theory of nutation and the variation of latitude: the Roche model core, *Mon.Not.R.Astr.Soc.*, 117, 162-173.
- Kinoshita, H. (1977): Theory of the rotation of the rigid earth, *Celestial Mech.*, 15, 277-326.
- Lamb, H. (1932): *Hydrodynamics*, Cambridge Univ.Press (reprinted by Dover Publ.).
- Lanczos, C. (1970): *The Variational Principles of Mechanics*, 4th ed., Univ. of Toronto Press.
- Love, A.E.H. (1927): *A Treatise on the Mathematical Theory of Elasticity*, Cambridge Univ.Press (reprinted by Dover Publ.).
- Melchior, P. (1983): *The Tides of the Planet Earth*, 2nd ed., Pergamon Press, Oxford.
- Molodensky, M.S. (1961): The theory of nutation and diurnal earth tides, *Comm.Obs. R.Belgique*, 188, 25-56.
- Moritz, H. (1980a): *Advanced Physical Geodesy*, H. Wichmann, Karlsruhe, and Abacus Press, Tunbridge Wells, Kent.
- Moritz, H. (1980b): Theories of nutation and polar motion I, Report 309, Dept. Geod.Sci., Ohio State University.
- Moritz, H. (1981): Theories of nutation and polar motion II, Report 318, Dept. Geod.Sci., Ohio State University.
- Moritz, H. (1982a): A variational principle for Molodensky's liquid-core problem, *Bull.Géod.*, 56(4), 364-380.
- Moritz, H. (1982b): Theories of nutation and polar motion III, Report 342, Dept. Geod.Sci., Ohio State University.
- Moritz, H. (1982c): Variational methods in earth rotation, in: H. Moritz and H. Sünkel (eds.), *Geodesy and Global Geodynamics*, Comm.No. 41, Geod.Inst., Technical Univ., Graz, Austria.
- Moritz, H. and Mueller, I.I. (1985): *Earth Rotation: Theory and Observation*, F. Ungar, New York.
- Plummer, H.C. (1918): *An Introductory Treatise on Dynamical Astronomy*, Cambridge Univ.Press (reprinted by Dover Publ.).
- Poincaré, H. (1901): Sur une forme nouvelle des équations de la mécanique, *C.R. Acad.Sci. Paris*, 132, 369-371.
- Poincaré, H. (1910): Sur la précession des corps déformables, *Bull.Astron.*, 27, 321-356.
- Sasao, T., Okubo, Sh., and Saito, M. (1980): A simple theory on the dynamical effects of a stratified fluid core upon nutational motion of the earth, in: E.P. Fedorov, M.L. Smith, and P.L. Bender (eds.), *Nutation and the Earth's Rotation*, 165-183, D. Reidel, Dordrecht, Holland.
- Schneider, M. (1981): *Himmelsmechanik*, 2nd ed., Bibliographisches Institut, Zürich.

Smirnow, W.I. (1971): Lehrgang der höheren Mathematik, vol. III/1, 6th ed.,
VEB Deutscher Verlag der Wissenschaften, Berlin.

Whittaker, E.T. (1961): A Treatise on the Analytical Dynamics of Particles and
Rigid Bodies, 4th ed., Cambridge Univ.Press.

Woolard, E.W. (1953): Theory of the rotation of the earth around its center
of mass, Astron.Papers for the American Ephemeris and Nautical Almanac,
XV, 1, Washington, D.C.

SECULAR AND LONG TERM VARIATIONS IN POLAR MOTION
FROM CLASSICAL AND DOPPLER OBSERVATIONS

A. Poma* and E. Proverbio**

Abstract. The existence of secular and low frequency variations
in the spectrum of polar motion has been reported in a large
number of works and discussed by several authors.

However, the reality and the geophysical and/or meteorologi-
cal causes of these phenomena are still a matter of discussion
chiefly because the only long series of pole coordinates are
essentially the ones based on the results of the five ILS sta-
tions.

The comparison of classical series (ILS and BIH) of polar
coordinates with those derived from Doppler observations lead
to the emphasizing of some characteristic features in the se-
cular polar motion in accordance with the crustal motion model.

1. Introduction

The observed Earth's polar motion emphasized the existence
of free variations (The Chandlerian wobble) primarily caused
by the complex internal structure of the Earth and its elasti-
city, and forced variation (annual and short term fluctuations)
due to the mechanical interaction of the solid Earth with its

* Stazione Astronomica Inter. di Latitudine, Cagliari, Italy

** Istituto di Astronomia e Fisica Superiore, Cagliari, Italy

atmosphere and hydrosphere.

The evidence of secular and long term variation in polar motion has been from time to time denied or explained by means of kinematic and dynamics models. Therefore the existence of similar secular motion shown in the ILS since 1900 and BIH since the 1956 polar coordinates (Poma & Proverbio, 1976) seems to testify to the reality of such a motion.

A plausible geophysical mechanism of polar motion drift is based on the possibility of changes in the products of inertia of the Earth due to large scale mass displacement like the deglaciation of polar cap effects and concomitant sea level changes (Dickman, 1979; Nakiboglu & Lambeck, 1980); but the difficulty of deriving in such a way the amplitude of secular drift calls for further research in this direction.

The comparison of the mean BIH pole of inertia with the mean pole derived from C_{21} and S_{21} by GEM 6 and GEM 8 shows the existence of secular variation in very poor agreement (Poma & Proverbio, 1979); it confirms the difficulty of the analysis based on the measurement of the Earth's pole of inertia and urges the furthering of studies in this problem.

On the other hand the motion of the Earth's crust according to the plate tectonics theory causes secular variation in latitude and longitude of the astronomical stations, as has been put in evidence by Proverbio & Quesada (1974). In fact the existence of single movements in the continental plates does not disagree with the existence of a global movement in the Earth's crust.

Though the changes in the products of inertia of the Earth due to tectonic global movement do not influence secular polar

motion by more than 10% of the observed value (Han-Shou Liu et al., 1974), variations in the zenith of the stations caused by global crustal motion could simulate the secular and long term variations observed in the coordinates of the pole of the Earth. An attempt to explain the observed motion of the pole by taking into account the Eötvös weak force, tending to move the continent toward the equator, was made some time ago by Mikhallov (1971) and the results confirmed the possibility of applying such a model to try to explain the observed drift of the Earth's pole.

2. Analysis of the observed secular motion

One of the critical questions in the discussion of whether the observed secular and long-period terms in the polar motion are a real phenomena or whether these variations are only a consequence of the local effects in the mean latitude of the observing stations essentially concerns the data set: most of the results were based on the observations of the five ILS stations, a number which often has been considered to be too small to allow reliable conclusions.

About ten years ago, an attempt was made (Poma & Proverbio, 1976) to derive secular polar motion starting from the data of the polar co-ordinates supplied by the BIH, practically independent of those from the ILS.

By comparing ILS and BIH values over the period 1956-1974 an evident similarity of the drifts of the ILS and BIH pole was shown. Considering the large number of instruments operating in the BIH collaborating stations, this result was, in our opinion, reliable evidence of the reality of secular polar motion. However, the non-homogeneity in the BIH system before

and after 1962.0 caused doubt about this conclusion.

For these reasons and since we have now at our disposal homogeneous data of 22 years from BIH a new analysis is here undertaken.

The source of data are:

for the period 1955.9 - 1961.9 BIH values are from Bulletins Horaires (series 4-5) of BIH taking into account the corrections which refer these results to the 1968 BIH system given in Annual Reports of the BIH; later values for 1962.0 to 1984.0 are from the BIH Annual Reports (values for every 1/20th year).

ILS values are from the Annual Reports and the Monthly Notes of the IPMS.

In order to remove the Chandler and annual components the ILS and BIH co-ordinates (x, y) have been filtered with F60 (six - year running means) which eliminates or strongly reduces periods ≤ 6 years. The mean annual values of the filtered co-ordinates x F60 and y F60 (barycentres of the polar wobble) are given in Table 1 and plotted in Fig. 1, where an averaged value of 0°037 is removed from (x F60)_{ILS}; the BIH values before 1962.0 are joined by hatched lines. The annual mean differences between BIH and ILS pole positions are also listed in Fig. 1 and shown at the top of Fig. 2.

A visual examination of these diagrams clearly suggests some considerations:

a) there is a significant similarity in the variation of the BIH and ILS y-coordinates;

b) the trend in y appears fairly to be a linear drift with superimposed oscillation of little amplitude

Table 1.

Annual means of the polar co-ordinates (x, y) after smoothing with a F60 filter (unit: 0°001)

Year	BIH		ILS		BIH-ILS	
	x	y	x	y	x	y
1959	+ 59	+ 185	+ 67	+ 196	- 8	- 11
60	48	194	65	200	17	6
61	33	202	60	203	27	1
62	20	215	50	209	30	+ 6
63	8	224	41	217	33	7
64	- 1	233	37	222	38	11
65	- 4	238	30	226	34	12
66	- 4	240	23	233	27	7
67	0	243	19	241	19	2
68	+ 1	241	17	243	16	- 2
69	2	244	22	247	20	3
70	6	246	32	251	26	5
71	10	251	43	252	33	1
72	15	251	56	250	41	+ 1
73	17	250	64	247	47	3
74	21	253	66	250	45	3
75	23	255	67	250	44	5
76	24	256	66	251	42	5
77	24	261	75	257	51	4
78	24	268	92	264	68	4
79	27	275				
80	27	279				

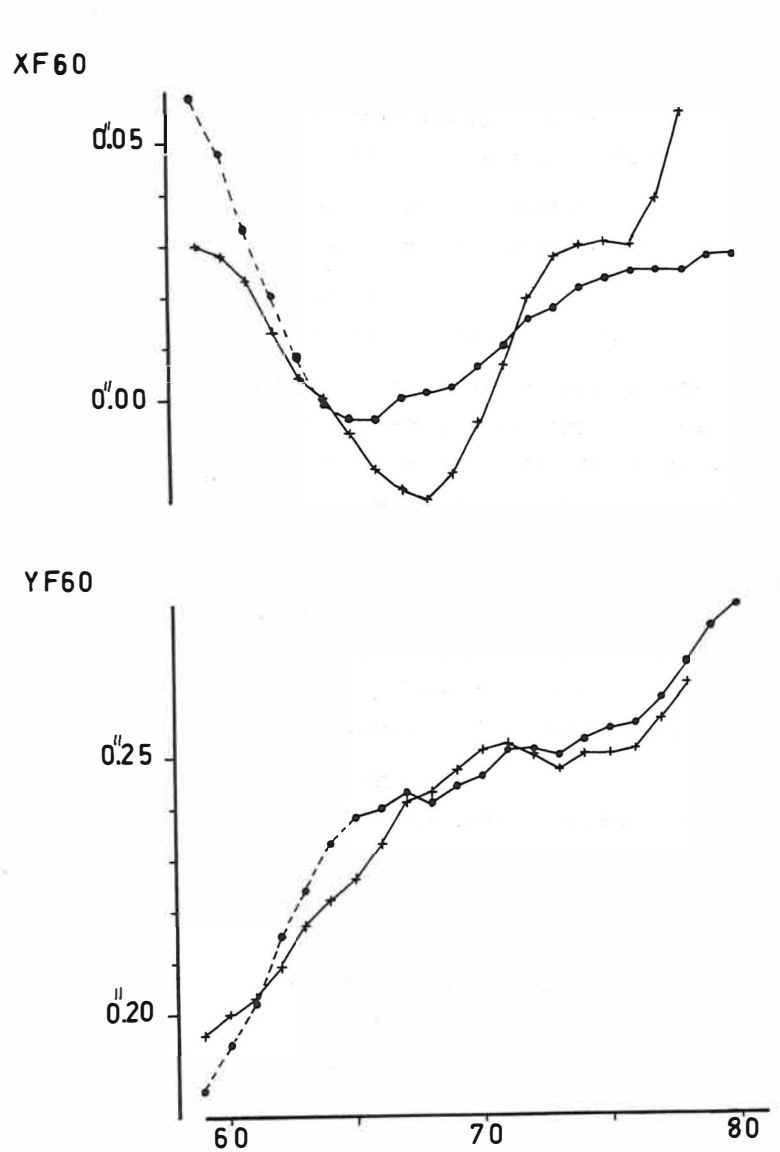


Fig. 1. Annual means of the polar co-ordinates filtered with F60 : BIH (•) and ILS (+).

• BIH
+ ILS - 0.037

• BIH
+ ILS

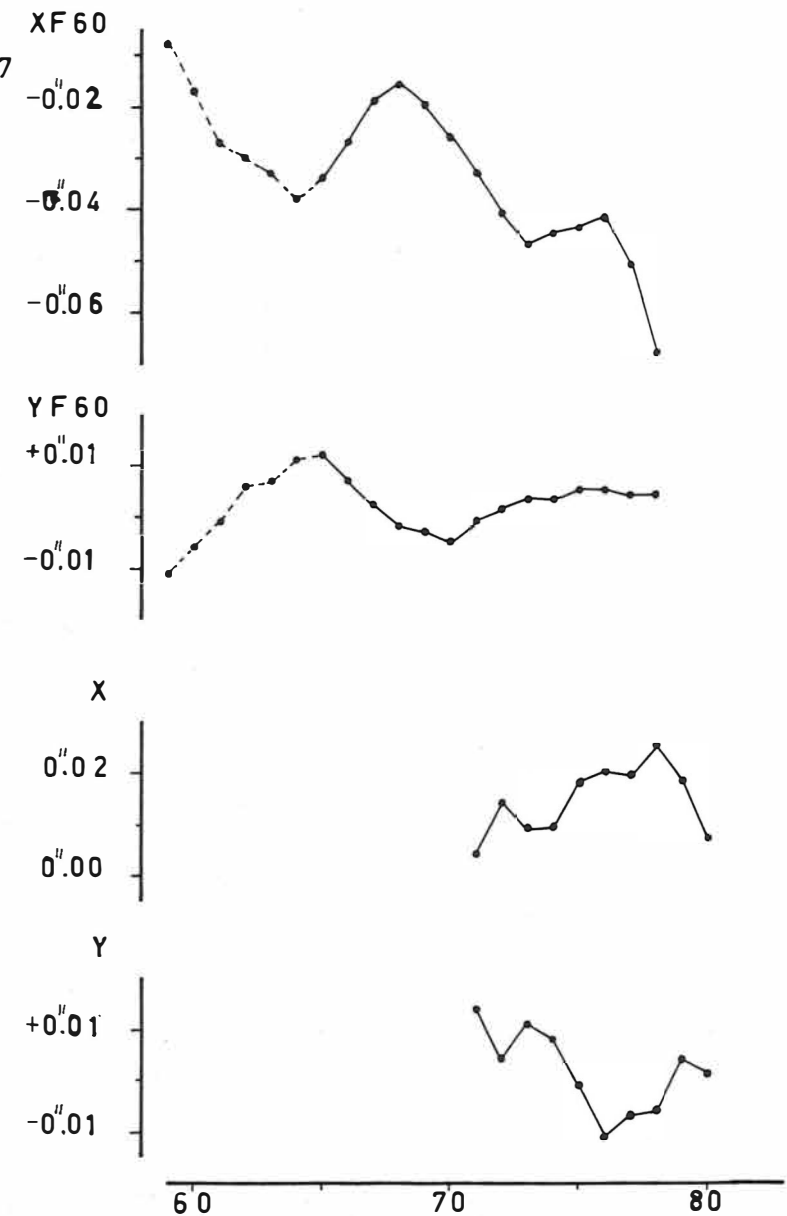


Fig. 2. Yearly mean differences of the polar co-ordinates: BIH - ILS after filtering with F60 (top) and BIH - DMA (bottom).

- c) there is no evidence of discontinuity in the BIH y-coordinates before 1962.0
- d) the x-coordinate shows the existence of long term fluctuation whereas there is evidence of the existence of little secular trend.

Points (b) and (d) are in agreement with a former analysis of the ILS data over the period 1902-1960 (Proverbio et al. 1971).

These conclusions are also supported by numerical results. Solutions for a linear rate of drift by least squares give for dy/dt

		dy/dt (0".001/yr)		dy/dt (0".001/yr)
1965 - 1978	BIH	2.0	ILS	2.0
1959 - 1978	BIH	3.5	ILS	3.3
1959 - 1980	BIH	3.5		
1965 - 1980	BIH	2.4		
1965 - 1978	BIH-ILS	0.0		
1959 - 1978	BIH-ILS	0.2		

The formal uncertainty is about 0".0002

It must be noted that these estimates concerning the y-coordinate could be slightly affected by the presence of systematic variations superimposed upon the linear drift. It is interesting to note that, when the linear term given before is removed from the BIH data, residuals suggest the existence of additional periodic terms.

However, there can be little doubt that this linear variation represents a real secular drift. If this secular motion does not

exist it might be expected that the ILS pole should move with respect to BIH pole. No evidence for such a motion over a long period is shown in our results.

Systematic differences between the y-coordinate of the BIH and ILS systems exist, but they are small.

A comparison with other systems of polar coordinates further confirms our conclusions. Markowitz (1982) has estimated the rate dy/dt from the IPMS from the 1962 to 1981 and finds

$$dy/dt = 0".0026/yr \\ \pm .0004$$

We have also computed the drift between the y-coordinates of the BIH and DMA systems. The latter are the coordinates of the pole obtained by the Defense Mapping Agency from Doppler observations of Transit satellites. By using the annual mean BIH-DMA differences published by BIH (Annual Report for 1980) and plotted in the bottom of Fig. 2 we have:

$$(dy/dt)_{BIH-DMA} = - 0".0016/yr$$

over the period 1971-1980.

Taking into account the value found by Markowitz (1982) from DMA data from 1970 to 1981

$$(dy/dt)_{DMA} = 0".0055/yr \\ \pm .0008$$

we may conclude

$$\text{Drift } y(\text{ILS}) \approx \text{Drift } y(\text{BIH}) \ll \text{Drift } y(\text{DMA})$$

However, a much longer series is necessary to have a significant estimate of the DMA drift.

On the contrary, the x-coordinate shows large and apparently systematic variations. We shall discuss this point later.

Bearing in mind the trend in x shown in Fig. 1 and Fig. 2, it is difficult to obtain a reliable value for a drift because the estimate of the apparent rate of drift depends upon the period in which the data are computed. Moreover it may be seen that the BIH-ILS differences are larger in x than they are in y. However, even if no conspicuous evidence appears, there is a discrete similarity between the pattern of the BIH and ILS x-coordinate.

3. Conclusions.

According to available literature the mean rotation pole as determined for many years by ILS, has an apparent drift (see e.g. Markowitz, 1982).

$$dx/dt = 0''.0009/yr,$$

$$dy/dt = 0''.0034/yr,$$

However, the reality of this secular motion has been and still is questioned and often attributed to the local non polar effects of the ILS stations, mainly Ukiah (Jatskiv, 1981). In particular, several attempts have been made recently to calculate the possible apparent displacement of the mean pole due to the drifting of the stations as a consequence of plate tectonics (Dickman, 1977, Soler and Mueller, 1978) but without great success, all the models generating an apparent drift of the rotation pole a magnitude smaller than the observed value.

Table 2 shows, for example, the results obtained by Soler and Mueller.

The apparent displacement (Δx , Δy) of the mean pole over 70 years has been derived from the changes in latitude and longitude of each station of the ILS and IPMS network, computed by using eight absolute plate velocity models of Solomon et al. (1975).

Several conclusions follow from the tabulated results:

- a) The computed drift of the mean pole is generally greater in the direction of the x-axis than along the y-axis.
- b) All eight models provide, for the ILS and IPMS pole, practically the same Δy displacement.
- c) If the number of the observing stations increases as is the case of the IPMS network, the displacement of the mean pole along the x-axis is reduced.

After comparing these results with those obtained by us in the above section we believe that the preponderance of evidence fairly suggests that secular motion is a real phenomenon quite free from the influence of local effects.

Such effects, of course, exist and are almost certainly less important in the BIH and IPMS network because a large number of stations tends to average them better.

Local effects may play a role in the observed fluctuations of the x-coordinate. It should be investigated better. But they cannot have significant effect on the secular motion since the observed drift chiefly occurs along the y-axis and agreement between ILS, BIH, IPMS and DMA observations as regards the y component is good.

Table 2

Apparent displacement (in meters) of the mean pole over 70 years from ILS and IPMS observatoires for different absolute plate velocity models.

Model	Δx		Δy	
	ILS	IPMS	ILS	IPMS
A3 Uniform drag coefficient beneath all plates	1.59	1.00	0.25	0.28
B3 Drag beneath continents only	0.75	0.23	0.50	0.50
B4 Continents have 3 times more drag than oceans	1.23	0.65	0.35	0.37
C3 Drag opposing horizontal translations of slabs, oceanic subduction zone only	1.75	1.17	0.12	0.13
C4 Same but including Arabian and Himalayan trenches	1.60	1.00	0.10	0.16
D1 Maximum pull by slabs plus plate drag	0.65	0.12	0.12	0.13
E2 Drag beneath 8 mid-plate hot spots	0.53	0.96	-0.34	-0.30
E3 Drag beneath 19 hot spots	0.97	0.48	0.11	0.11

The models of plates are described in (Solomon et al., 1975)

The values of the apparent displacements Δx and Δy of the mean pole are taken from (Soler and Mueller, 1978)

It may be of interest to recall the results reported by Yumi and Wako (1970); by the adoption of local drifts at Mizusawa and Ukiah they computed the resulting motion of the ILS pole and found a reduction of about 1/2 in the x-component and only 20% in the y-component.

It is also noticeable the agreement found by McCarthy (1972) between the observed secular trend of the latitude of Washington and the change in the same latitude derived from ILS secular motion.

Again, this reasonably agrees with our conclusions because the Washington latitude is very sensitive to the variation of the pole along the y-axis.

Therefore, unless new techniques (such as Laser, VLBI, etc.) give results very different in the near future, the reality of secular motion of the pole cannot, in our opinion, be dismissed.

As discussed in Section 1, however, the discovery of the origin and the physical mechanism causing this motion remains a more difficult task. Further details are given in an article being prepared.

We thank Mr. Vincenzo Gusai for drawing the figures and Mrs. Rosanna Lepori for typewriting the manuscript.

References

- Dickman, S.R., 1977, *Geophys. J.R. Astr. Soc.*, 51, 229-244.
- Dickman, S.R., 1979, *Geophys. J.R. Astr. Soc.*, 57, 41-50.
- Han-Shou Liu, Carpenter, L., Agreen, R.W., 1974, *J.G.R.*, 79, 4379-82.
- Markowitz, Wm, 1982, Report to IAU Commissions 19 and 31, Patras, Greece.
- McCarthy, D.D., 1972, in Rotation of the Earth, Melchior P. and Yumi S. (eds), Reidel, Dordrecht, Holland.
- Mikhailov, A.A., 1971, *Sov. Astr.*, 14, 1035-37.
- Nakiboglu, S.M., Lambeck, K., 1980, *Geophys. J. R. Astr. Soc.*, 62, 49-58.
- Poma, A., Proverbio, E., 1976, *Astron. & Astrophys.* 47, 105-111.
- Poma, A., Proverbio, E., 1979, in Time and Earth's Rotation, McCarthy D.D. and Pilkington J.D.H. (eds), Reidel, Dordrecht, Holland.
- Proverbio, E., Carta, F., Mazzoleni, F., 1971, *Rendic. Semin. Fac. Scienze Univ. Cagliari*, XLI, 3-42.
- Proverbio, E., Quesada, V., 1974, *J.G.R.*, 79, 4941-43.
- Soler, T., Mueller, I.I., 1978, *Bull. Geod.*, 52, 39-57.
- Solomon, S.C., Sleep, N.H., Richardson, R.M., 1975, *Geophys. J.R. Astr. Soc.*, 42, 769-801.
- Yatskiv, Ya.S., 1981, In Reference Coordinate System for Earth Dynamics, Gaposchkin E.M. and Kolaczek B. (eds), Reidel, Dordrecht, Holland.
- Yumi, S., Wako, Y., 1970, In Earthquake Displacement Fields and the Rotation of the Earth, L. Mansinha et al. (eds), Springer-Verlag, N.York.

ON THE CONVERGENCE PROBLEM OF THE SATELLITE DERIVED SPHERICAL HARMONIC EXPANSION OF THE GEOPOTENTIAL AT THE EARTH'S SURFACE

Lars E. Sjöberg
The Royal Institute of Technology
Department of Geodesy
S-100 44 STOCKHOLM, Sweden

ABSTRACT

The problem of downward continuing a satellite derived series of spherical harmonics of the Earth's gravity field to the surface is considered. An error formula is derived, which agrees with that given by M.S. Petrovskaya and N.I. Lobkova. Despite of Ch. Jekeli's extensive numerical study it is concluded that the error of a high degree harmonic expansion ($N \geq 300$) is not yet satisfactorily known.

1. Introduction

During the last 15 years several geodesists have discussed and attempted to solve the problem of convergence of the spherical harmonic expansion of the Earth's external gravity field. Outside the minimum sphere bounding all mass of the Earth (the atmosphere is neglected) the convergence of the series is doubtless. The problem occurs when applying the exterior type of series within the bounding sphere and, in particular, at the surface of the Earth.

A "proof of divergence" of the series was given by Morrison (1970). However the proof was based on the erroneous statement that the series of spherical harmonics diverges if its subseries of zonal harmonics diverges.

A "proof of convergence" of the series was given by Arnold (1978) for a very general topography of the surface of the Earth. See also Arnold (1980). However, it is easy to find a counter-example to Arnold's very general result. For example, the radius of convergence of the exterior harmonic series of the potential of a homogeneous, oblate ellipsoid equals the focal distance (see for instance MacMillan, 1958). If the focal distance (ae) exceeds the length of the semi-minor axis (b) there will be regions on the surface of the ellipsoid around the poles where the radius vector r satisfies $b \leq r < ae$. In these

regions the external type of spherical harmonic expansion diverges in contrast to Arnold's proofs of convergence.

Another example of a divergent series was demonstrated by Sjöberg (1980). For a homogeneous ellipsoid with a disturbing spherical mass (M) in its interior it was shown that the exterior type of harmonic series does not always converge at the surface. At points located within the geocentric sphere through the centre of M (the sphere of convergence) the series diverges.

Moritz (1978) paid attention to the approximation theorems of Krarup-Runge and Keldych-Lavrentiev. See also Colombo (1982). These theorems prove the existence of a potential regular down to an internal sphere and approximating the potential of the Earth in its exterior arbitrarily well. "As a practical consequence we recognize that it is always possible to consider the earth's external potential as a 'convergent potential'." (Moritz, *ibid.*)

Although we agree with Moritz' statement, this does not prove anything about the convergence of the actual harmonic series of the exterior geopotential. Thus we prefer to formulate the relevant problem as follows (Sjöberg, 1980):

"Given a spherical harmonic series V_N (truncated at degree N) of the earth's external gravitational potential (V), it is required to reveal whether there is an optimum degree of expansion of V_N , for which degree $|V_N - V|$ is a minimum. Only if $|V_N - V|$ is negligible and the minimum of this error occurs at a very high degree, beyond practical limits, we may regard the series V_N as 'practically convergent'."

In Freeden and Karsten (1982) and Jong (1982) methods are given of how to determine approximating potentials regular down to an internal sphere in accordance with the approximation theorems. All methods are based on surface data. However these methods do not solve the above stated problem.

In Sjöberg (1980) the divergence was shown for a very simple Earth model. The minimum $|V_N - V|/\gamma < 1$ mm occurred at $200 < N \leq 400$ ($\gamma = 978$ Gal). Jekeli (1981, 1982) has studied the problem in a much more refined Earth model based on elevation elements of resolution 0.6 (= 67 km). Based on a method given by Petrovskaya (1979) [cf. formula (2.12) below] he computed the downward continuation error of the height anomalies and gravity anomalies (the difference

between the exterior and inner harmonic series) to degree 300. These errors attained RMS values from $0.3 \mu\text{m}$ to 0.4 mm (and $0.02 \mu\text{Gal}$ to $4 \mu\text{Gal}$, respectively) in areas ranging from near the equator to the vicinity of the pole. From this result Jekeli drew the conclusion that "the estimation of point or mean gravity anomalies and geoid undulations (height anomalies) using the outer series expansion to degree 300 anywhere on the earth's surface is practically unaffected by the divergence of the total series". This conclusion appears to solve the downward continuation problem of the harmonic series.

Below we will approach the downward continuation problem following the line of Sjöberg (1977). In the final discussion we will return to Jekeli's result, and we will also give a numerical example.

2. Formulas for solution of the problem

The Newtonian potential of the Earth in an arbitrary point P is

$$V = \iiint_V \frac{\rho}{\ell} dv \quad (2.1)$$

where

v = volume of the Earth

$\mu = G\rho$; G = Newton's constant of gravitation

ρ = density of mass

$\ell = (r_i^2 + r^2 - 2r r_i \cos \psi)^{1/2}$

r_i = geocentric radius of the current point (P_i)

r = geocentric radius of P

ψ = geocentric angle between P and P_i

At an arbitrary point outside the bounding sphere of radius R (i.e. for $r > R$) the reciprocal distance ℓ^{-1} may be expanded $\{P_n(\) = \text{Legendre's polynomial}\}$

$$\ell^{-1} = \frac{1}{r} \sum_{n=0}^{\infty} \left(\frac{r_i}{r}\right)^n P_n(\cos \psi) \quad (2.2)$$

Inserting this series expansion into (2.1) and changing the order of summation and integration we obtain

$$V = \frac{1}{r} \sum_{n=0}^{\infty} \iiint_{\sigma} \mu \left(\frac{r_i}{r}\right)^n P_n(\cos \psi) dv \quad (2.3)$$

For points inside the bounding sphere ($r < R$) the series (2.2) does not converge and the validity of (2.3) is doubtful. A general series expansion for $r < R$ is

$$V = \frac{1}{r} \sum_{n=0}^{\infty} \iiint_{\sigma} \left[\int_0^r \mu \left(\frac{r_i}{r}\right)^n + \int_r^{r_s} \mu \left(\frac{r_i}{r}\right)^{n+1} \right] P_n(\cos \psi) dv \quad (2.4)$$

where r_s is the radius of a current point at the surface of the Earth ($r \leq r_i \leq r_s$) and σ is the unit sphere. Thus the possible error of extending formula (2.3) inside the bounding sphere is given as the difference between (2.3) and (2.4) (Cook, 1967; Levallois, 1969; Sjöberg, 1977):

$$\delta V(N) = \frac{1}{r} \sum_{n=0}^N \iiint_{\sigma} \int_r^{r_s} \mu \left[\left(\frac{r_i}{r}\right)^n - \left(\frac{r_i}{r}\right)^{n+1} \right] P_n(\cos \psi) dv \quad (2.5)$$

where N approaches infinity. In practice, however, we know the spherical harmonic coefficients corresponding to (2.3) only to a finite degree (N). Subsequently the "downward continuation error" of a series expansion (2.3) to degree N may be represented by (2.5). If for an arbitrary $\epsilon > 0$ there exists a number N_0 such that

$$|\delta V(N)| < \epsilon \quad \text{for } N > N_0 \quad (2.6)$$

then formula (2.3) is convergent. Even if this is not the case in the strict sense, we define (2.3) as "practically convergent" if the minimum of $|\delta V(N)|$ is negligible and N_0 is beyond practical limits.

Let us assume that the density (μ) is constant for each latitude and longitude (i.e. independent of r_i). Then formula (2.5) may be rewritten (cf. Sjöberg, 1977 and 1980)

$$\delta V(N) = \sum_{n=0}^N \iiint_{\sigma} \mu I(r, r_s) P_n(\cos \psi) d\sigma \quad (2.7a)$$

where

$$I(r, r_s) = r^2 \begin{cases} 0 & \text{if } r \geq r_s \\ \frac{(r_s/r)^{n+3} - 1}{n+3} - \frac{(r_s/r)^{-(n-2)} - 1}{n-2} & \text{if } r < r_s, n \neq 2 \\ \frac{(r_s/r)^5 - 1}{5} - \ln(r_s/r) & \text{if } r < r_s, n = 2 \end{cases} \quad (2.7b)$$

Formula (2.7) was recommended by Sjöberg (1980) for investigation of the convergence of $\delta V(N)$ with N for a known topography. As the density of the topography is not known in detail, μ was assumed to be constant for the entire topography (above the sphere of radius r).

It was shown in Sjöberg (1977) and Jekeli (1981) that the "downward continuation error" representation according to (2.7) is unlikely large for small N and decreases for increasing N . As this formula is the difference between two series of very different nature, the exterior and the inner series, it is possible that it includes also some contribution that vanishes when N approaches infinity. If $\delta V(N) \rightarrow 0$ as $N \rightarrow \infty$ the series (2.3) is strictly convergent.

We will now exclude the always converging parts of (2.5), extracting a possibly divergent formula. From the notations

$$r_i = r + H$$

we obtain the series expansions

$$\left(\frac{r_i}{r}\right)^{n+2} = 1 + (n+2) \left(\frac{H}{r}\right) + \frac{(n+2)(n+1)}{2} \left(\frac{H}{r}\right)^2 + \frac{(n+2)(n+1)n}{2 \cdot 3} \left(\frac{H}{r}\right)^3 + \dots \quad (2.8a)$$

and

$$\left(\frac{r}{r_i}\right)^{n-1} = 1 - (n-1)\left(\frac{H}{r}\right) + \frac{(n-1)n}{2}\left(\frac{H}{r}\right)^2 - \frac{(n-1)n(n+1)}{2 \times 3}\left(\frac{H}{r}\right)^3 + \dots \quad (2.8b) \quad \frac{1}{4\pi} \iint_{\sigma} f(Q) \delta_N(\psi_{PQ}) d\sigma_Q \rightarrow f(P) \quad N \rightarrow \infty \quad (2.10)$$

Inserting these expansions into (2.5) with

$$dv = r_i^2 dH d\sigma$$

we arrive at

$$\delta V(N) = \delta V^{(0)}(N) + \delta V^{(1)}(N) + \delta V^{(2)}(N) + \dots \quad (2.9a)$$

where

$$\delta V^{(0)}(N) = \iint_{\sigma} \int_0^H \mu H \delta_N(\psi) dH d\sigma \quad (2.9b)$$

$$\delta V^{(1)}(N) = \frac{1}{r} \iint_{\sigma} \int_0^H \mu H^2 \delta_N(\psi) dH d\sigma \quad (2.9c)$$

and

$$\delta V^{(2)}(N) = \frac{1}{3r^2} \iint_{\sigma} \int_0^H \mu H^3 Q_N(\psi) dH d\sigma \quad (2.9d)$$

where

$$\delta_N(\psi) = \sum_{n=0}^N (2n+1) P_n(\cos \psi)$$

and

$$Q_N(\psi) = \frac{1}{2} \sum_{n=0}^N (2n+1)(n+1) n P_n(\cos \psi)$$

Let the spherical harmonic expansion of a function f be convergent. Then it is easily shown that

If the point of computation (P) is located on or outside the surface of the Earth, then

$$f(P) = \int_0^H \mu H dH = 0$$

and

$$f(P) = \int_0^H \mu H^2 dH = 0$$

and it follows that (2.9b) and (2.9c) vanish as N approaches infinity:

$$\delta V^{(0)}(N) \rightarrow 0 \quad \text{and} \quad \delta V^{(1)}(N) \rightarrow 0 \quad \text{as} \quad N \rightarrow \infty$$

Thus we are left with (2.9d) and higher-order terms (see 2.9a) as the possible divergent downward continuation error. Assuming that the density of the topography is constant (2.9d) may be written

$$\delta V^{(2)}(N) = \frac{\mu}{12r^2} \iint_{\sigma} H^4 Q_N(\psi) d\sigma \quad (2.11)$$

Except for the sign the formulas (2.9d) and (2.11) agree with formulas (15) and (24) of Petrovskaya and Lobkova (1982) derived from Brovar's integral formula. Furthermore they presented the following formula (with opposite sign)

$$\delta V^{(2)}(N) = \frac{r}{6\pi} \iint_{\sigma} \Delta g \left(\frac{H}{r}\right)^3 Q_N(\psi) d\sigma \quad (2.12)$$

where Δg is the gravity anomaly at the surface of the Earth. Jekeli (1981, 1982) gave a similar formula where Δg is replaced by a surface density (in practice derived from surface gravity anomalies).

3. Some numerical results and discussion

Petrovskaya and Lobkova (1982) derived a closed formula for the function $Q_N(\psi)$:

$$2 Q_N(\psi) = \frac{2(N+1)}{(1-t)^2} \{P_{N+1}(t) - P_N(t)\} + \frac{(N+1)^2}{1-t} \{(N+2) P_N(t) - N P_{N+1}(t)\} \quad (2.13)$$

where

$$t = \cos \psi$$

(Note that we have slightly corrected their formula.)

Finally Petrovskaya and Lobkova (ibid.) gave the formula

$$Q_N(0) = N(N+1)^2(N+2)/4$$

This formula is given in Table 1 for some N.

Table 1. $Q_N(0) = N(N+1)^2(N+2)/4$

N	100	200	300	400	500
$Q_N(0)$	2.60×10^7	4.08×10^8	2.05×10^9	6.46×10^9	1.58×10^{10}

In Figure 1 we illustrate $Q_N(\psi) \sin \psi$ for $N = 100$ and 300 and for comparison we give also $F(\psi) = 1/2 S(\psi) \sin \psi$, where $S(\psi)$ is Stokes' function. From the figure we conclude that $F(\psi)$ is much smoother than $Q_N(\psi)$, which fluctuates

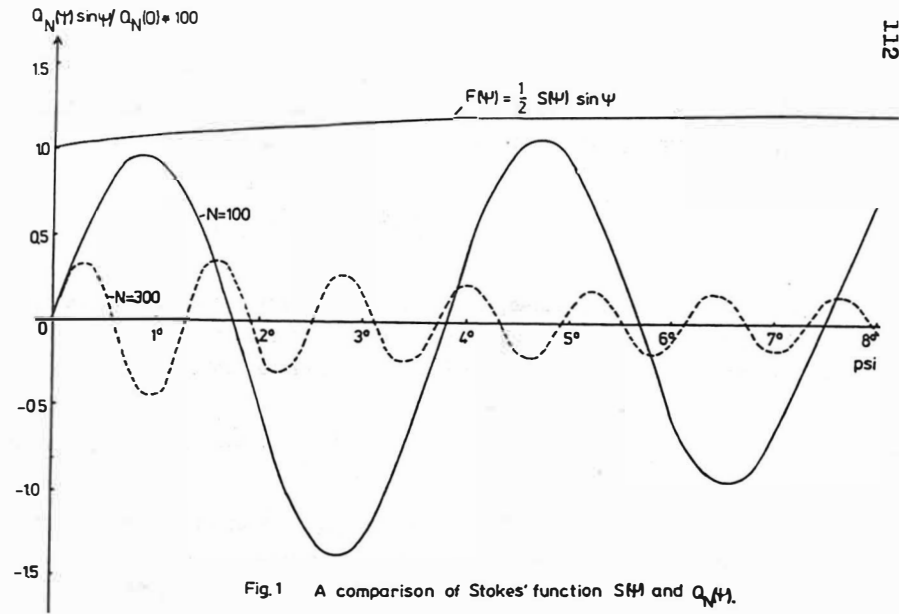


Fig.1 A comparison of Stokes' function $S\psi$ and $Q_N\psi$.

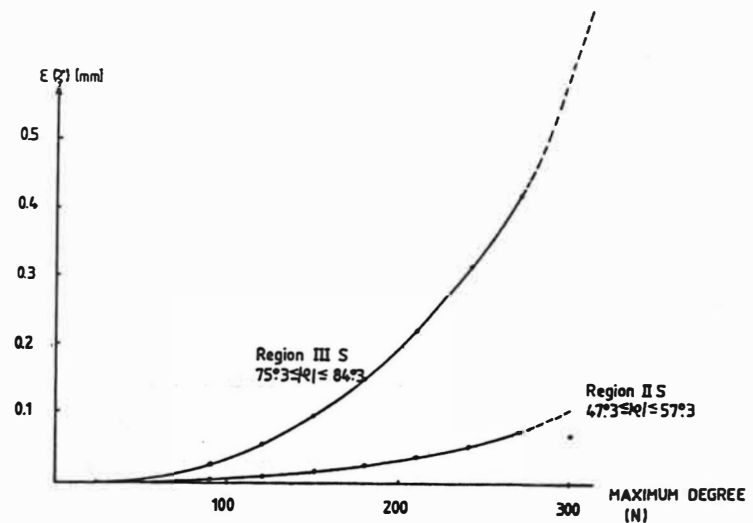


Fig.2 The downward continuation error of the geopotential as a function of the degree of this expansion. Data from Jekeli (1981), Table 5.

more and more around the ψ -axis as N increases (the period is approximately $2\pi/N$). This effect and the roughness of argument H^4 of (2.9d) and (2.11) or $\Delta g H^3$ of (2.12) implies that the result of a numerical application is very sensitive to the size of the used blocks or compartments for the numerical integration. Jekeli (1981) used the block size 0.6° . Some of his results are given in Figure 2. He suggested that the reduced downward continuation error at the degree 300 is a consequence of the different nature of the exterior and interior series of expansion. On the contrary we believe that this result is a smoothing effect due to too large blocks (0.6°) for this high degree expansion. In addition one has to consider that the topographic data was actually limited to 1° block size and that within this limit down to 0.6° the data was artificially generated.

Jekeli's excellent work is certainly the most extensive contribution so far to solve the downward continuation problem. However from the above concerns we conclude that the size of the error of high degree spherical harmonic expansions ($N \geq 300$) is still an open question.

4. An Example

A disturbing point mass M is located outside the mean earth sphere of radius R_0 (see Figure 3).

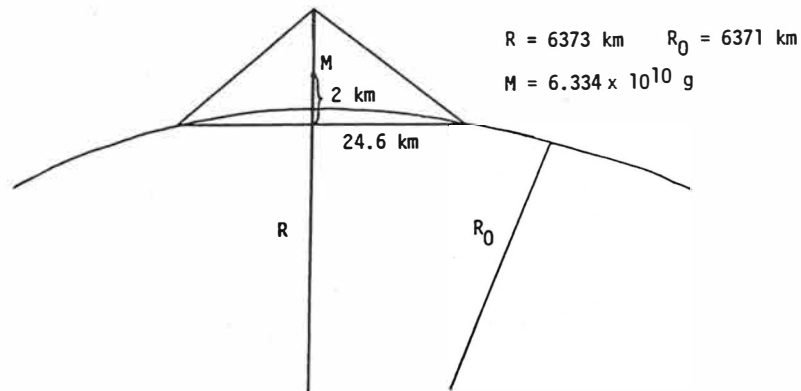


Figure 3. Molodenskii's mountain.

In an arbitrary point $P(r, \psi)$ outside M (ψ = spherical distance from the center of M to P , r = geocentric distance to P) the disturbing potential originated in M is given by:

$$T = \mu / (R^2 + r^2 - 2Rrt)^{1/2} ; \quad \mu = GM \quad (4.1)$$

where

G = constant of gravitation

R = geocentric radius of the center of M

$t = \cos \psi$

Let T be represented by the following truncated series of Legendre's polynomials:

$$T_N = \frac{\mu}{R} \sum_{n=0}^N \left(\frac{R}{r}\right)^{n+1} P_n(t) \quad (4.2)$$

and the downward continuation error becomes $T_N - T$. The computations for $r < R$ show errors oscillating around the zero-axis with a typical minimum of its envelope at some high degree. These minima are given in Table 2 for various spherical distances (ψ) to the disturbing mass. The table shows that the external spherical harmonic representation of this model within the bounding sphere has serious limitations.

Table 2. Numerical results with formulas (4.1) and (4.2).

N_{opt} = optimum degree of truncation of envelope.
 $\gamma = 978$ Gal.

ψ	T/γ [mm]	N_{opt}	$ T_N - T /T$ [%]
10'	23.0	1896	44.4
13'	17.8	1458	51.3
15'	15.5	1265	49.2
17'	13.7	1749	46.1
20'	11.6	1487	42.3
25'	9.3	1620	38.0
30'	7.8	1710	34.8
1°	3.9	1575	24.6
3°	1.3	1605	14.2
5°	0.8	1647	11.0
10°	0.4	1632	7.7
20°	0.2	1626	5.5

References

- Arnold, K., 1978, The spherical-harmonic expansion of the gravitational potential of the Earth in the external space and its convergence. Gerlands Beitr. Geophysik, Vol. 87, No. 2, 81-90.
- Arnold, K., 1980, Picone's theorem and the convergence of the expansion in spherical harmonics of the gravitational potential of the Earth in the external space. Boll. di Geofisica Teorica ed Applicata, Vol. 22, No. 86, 95-103.
- Colombo, O.L., 1982, Convergence of the external expansion of the gravity field inside the bounding sphere. Manuscripta Geodaetica, Vol. 7, 209-246.
- Cook, A.H., 1967, The determination of the external gravity field of the Earth from observations of artificial satellites. Geophysical Journal of the Royal Astronomical Society, Vol. 13, 297-312.
- Freedon, W. and H. Kersten; 1982, An extended version of Runge's theorem. Manuscripta Geodaetica, Vol. 7, 267-278.

Jekeli, Ch., 1981, The downward continuation to the Earth's surface of truncated spherical and ellipsoidal harmonic series of the gravity and height anomalies. Department of Geodetic Science and Surveying, Report No. 323, The Ohio State University.

Jekeli, Ch., 1982, A numerical study of the divergence of spherical harmonic series of the gravity and height anomalies at the Earth's surface. Bull. Géod., Vol. 57, 10-28.

Jong, G., 1982, Convergence in the mean of the spherical harmonics expansion of the Earth's gravity field. Manuscripta Geodaetica, Vol. 7, 247-266.

Levallois, J.J., 1969, Note sur la convergence du développement du potentiel en harmoniques spheriques. Proc. of the IVth Symposium on Mathematical Geodesy, Trieste, Italy.

MacMillan, W.D., 1958, The Theory of the Potential. Dover Publ Inc., New York.

Moritz, H., 1978, On the convergence of the spherical harmonic expansion for the geopotential at the Earth's surface. Boll. di Geodesia e Scienze Affini, No. 2-3, 363-381.

Morrison, F., 1969, Validity of the expansion of the potential near the surface of the Earth. Proc. of the IVth Symposium on Mathematical Geodesy, Trieste, Italy, 95-106.

Petrovskaya, M.S., 1979, Upward and downward continuations in the geopotential determination. Bull. Géod., Vol. 53, 259-271.

Petrovskaya, M.S. and N.I. Lobkova, 1982, On refinement of relations between Stokes' constants and surface gravitational data. Manuscripta Geodaetica, Vol. 7, 21-36.

Sjöberg, L., 1977, On the errors of spherical harmonic developments of gravity at the surface of the Earth. Department of Geodetic Science, Report No. 257, The Ohio State University.

Sjöberg, L., 1980, On the convergence problem for the spherical harmonic expansion of the geopotential at the surface of the Earth. Boll. di Geodesia e Scienze Affini, Vol. 39, No. 3, 261-271.

On the comparison of the results of two different E-W-strainmeters
operating at Tiefenort in the period 1978 - 1984

Simon, D.^{x)}; Karmaleeva, R. M.; Latynina, L. A.^{xx)}

Summary

The paper contributes to the possible application of tidal strainmeters for measurements of recent crustal movements.

The records of two E-W-strainmeter of different type were analyzed. The instruments are measuring since 1978 simultaneously at the Tiefenort station, 5 meters distant from each other.

The first result of the comparison between the corresponding tidal, thermoelastic and secular components of the records of both the strainmeters was that there are no essential instrumental falsifications. It seems that the use of laser interferometric calibration methods and the good protection of the instruments against meteorological influences allows the neglect of the instrumental disturbance components in the first approximation.

As the second main result of the simultaneous strainmeter records at the Tiefenort station must be regarded the detection of significant local components induced by the cavity effect and the pressure of the overburden.

By measurements with two strainmeters operating in the vertical direction it was shown that the amplitudes of the above mentioned local components can be diminished distinctly by an optimal choice of the measuring places.

In this connection are to consider several regulas resulting from the model calculations of HARRISON /1976/ concerning the cavity effect in tunnel-like galleries and from the calculated loading pressure situation around such tunnels.

It was shown in the case of the vertical strainmeter measurements carried out at the Tiefenort station that the consideration of such regulas leads to a decrease of the local components (cavity effect and loading influence) of about one order of magnitude.

x) Akademie d. Wiss. d. DDR, Zentralinstitut für Physik der Erde
Potsdam, Telegrafenberg

xx) Akademie d. Wiss. d. UdSSR, Institut für Physik der Erde, Moskau

Zusammenfassung

Die Aufzeichnungen zweier Strainmeter unterschiedlichen Typs, die seit 1978 an der Station Tiefenort 5 m voneinander entfernt in E-W-Richtung aufgestellt sind, werden analysiert. Es zeigten sich keine wesentlichen instrumentell bedingten Störungen, da die Geräte gut gegenüber äußeren Einflüssen geschützt sind und mit einem interferometrischen Verfahren mit Hilfe eines Lasers geeicht werden.

Mit zwei Vertikalstrainmetern konnte gezeigt werden, daß der Einfluß lokaler Strainstörungen durch eine geeignete Wahl des Aufstellungsortes um etwa eine Größenordnung reduziert werden kann. In diesem Zusammenhang sind die Ergebnisse der Modellrechnungen von HARRISON /1976/ bezüglich der Hohlraumeffekte und die Einflüsse der Luftdruckbelastungen zu beachten.

Certain errors of the measurements of recent crustal movements are difficult to detect since the data were received from measuring campaigns which differ very much in time. There are no informations concerning the processes which run down in the time between the measuring campaigns. As a consequence several authors propose continuous tilt and strain records in special test areas.

It seems that long-basis watertube tiltmeters are suitable instruments for such a purpose, since the results of tilt measurements at the Königstein station are in a good agreement with the correspondend datas of the precision nivellements (LORENZ /1984/).

Concerning the possible application of tidal strainmeters for measurements of recent crustal movements there are no experiences. In the most papers the strainmeter records are to short for a determination of the secular components (VARGA /1984/). For the estimation of the secular strain rates and

- the instrumental errors
- the meteorological strain components
- and the influences of the local cavity distribution, geology and topography, respectively

better founded informations are to receive from simultaneous records of strainmeters of different type.

In the present paper are used for this purpose the records of two horizontal E-W-strainmeters of different type operating at the Tiefenort station in 1978-1984. The instruments, a wire strainmeter with a length of 24.99 m and a quartz tube one of 26.30 m are installed 5 meters distant from each other. The first part of the records of the quartz tube strainmeter was excluded from the analysis, since as a consequence of certain irregularities of the records R. M. KARMALEEVA found a crack in the quartz tube and changed a part of it in May, 1980. Since the repair the instrument works normal.

Both the instruments are calibrated by magnetostrictive lengthenings of the measuring normals. The amplitudes of the magnetostrictive impulses were determined by laser interferometric measurements with an accuracy of about $\pm 2\%$. The accuracy of the relative calibration reach $\pm 0.5\%$. A digital output of the strainmeters in short time steps allows the elimination of heating influences of the calibration coil and the small tidal

variation in the time of calibration.

First informations concerning the amplitudes of the instrumental and local strain components induced by the cavity effect were deduced from the observed parameters of the tidal strain waves. For this purpose are used the harmonic constants of the lunar diurnal and semidiurnal waves O_1 and M_2 , which contain only small meteorological constituents.

Table 1 shows that the difference between the observed amplitudes of the large O_1 waves is smaller than the error of the absolute calibration.

The little amplitudes of the M_2 waves are a consequence of a zero amplitude of the corresponding body strain wave appearing in the geocentric latitude of 51.3° N, calculated for the Earth model of WAHR /1982/. The latitude of the Tiefenort station is about 50.8° N, therefore in the observed M_2 wave the ocean loading component dominates.

On the other hand the ocean loading component of the observed O_1 wave is very small since in the Atlantic the ocean tides with the period of the O_1 wave reach only 1 % - 10 % of that of the corresponding M_2 waves. Consequently it is possible to estimate the amplitude of the local component of the O_1 wave by a comparison of the observed and the theoretical "in phase" components of O_1 . The observed amplitude is about 7 % larger than the calculated one.

This amplitude difference was interpreted mainly as an influence of the cavity effect. Since the instruments are installed between the walls of the gallery and near the end of it (fig. 2), where according to the model calculations of HARRISON /1976/ the cavity effect usually has a relative maximum.

On the other hand the influences of the local geology and topography are considered as to be small since the salt deposit near the station is homogeneous and the relief of the Earth surface near the station is rather small.

Fig. 1 shows the long periodic components of the strainmeter records. Here as before in the case of the tidal waves the outputs of both the instruments agree very good. The main components of strain variations in the period range of half a day to several years was measured by the two strainmeters of different type with comparable amplitudes and phases. Therefore, if we analyse these components, it seems to be possible to neglect the instrumental errors of the records in the first approximation.

In fig. 1 at the first sight are to distinguish two different components of the long periodic strain variations: the first one has a period of about one year, the second one seems to be a linear component.

In order to explain the yearly period measurements of rock temperature begun in June 1982 at 7 different boreholes located inside and outside of the station. The drill holes are 40 cm deep and equipped with reading thermometers having a graduation of 0.01° C or 0.1° C, respectively. The locations of the measuring places are shown in fig. 2.

Two different streams of fresh air flow along the boundaries of the station, which is protected against the air streams by thick walls and double doors. During the period 1982 - 1984 inside the station no variation of rock temperatures were measured within $\pm 0.01^\circ$ C. But outside of the station at the measuring places No. 1 and 7 located at distances of about 300 m or 400 m respectively, from the entrance of the station, the double amplitudes of the yearly temperature variations reach about 6° C or 9° C, respectively (fig. 3).

These differences between the temperature waves are caused by the different distances of the measuring places to the corresponding shafts. Inside of the amplitude differences the temperature waves are very similar. For instance in the very hot and long summer 1983 the rock temperature was higher over a period of about 4 month than the maximal temperature in the last rainy summer. And in the winter 1983/84 the rock temperature was lower during 3 month than the corresponding minimal temperature of the winter 1982/83. These phenomena are measured analogously at both the measuring places 1 and 7. Such seasonal differences from one year to the next one are important for the interpretation of long periodic strain variations.

In fig. 4 the horizontal strain variations are compared with the rock temperature curves measured in both the boreholes number 1 and 7. For the explanation of the observed strain variations the rough drawing on the right hand of the figure is used.

In the cold season - here between November 1983 and March 1984 - the rock are cooling and contracting consequently the salt rock in the stations area not withstanding the constant rock temperature here must expand. The strain velocity is proportional to the heat transfer or to the temperature differences between salt rocks and the air masses.

Additional measurements of two vertical strainmeters confirm this explanation. The first instrument is installed between roof and floor, the second one in a bore hole drilled in the ground of a gallery. A rough drawing in the lower part of fig. 4 explains the situation.

According to our idea a horizontal expansion of the stations area in the wintertime must produce a diminishing of the distance between roof and floor of the cavity and a vertical dilatation in the ground of it, since the floor moves upwards.

Such movements are visible in fig. 5. For the comparison of the records of the vertical strainmeters it was necessary to exclude from the record of the floor - roof strainmeter a linear component induced by influences of the pressure of overburden. This loading component has a velocity of about $2 \cdot 10^{-6}$ /year. After that the records of both the vertical strainmeters and of the horizontal one are in a good agreement with our model.

For instance in the last winter - between November 1983 and March 1984 - the horizontal EW strainmeter and the borehole instrument have measured expansion movements, but the floor-roof vertical strainmeter a compression. The thermoelastic components of the records of both the vertical strainmeters are quite symmetrically with reference to the time axis.

The records of the vertical strainmeters and the rock temperature data are useful for an exact elimination of the thermoelastic components of the horizontal strain records. This work is not yet finished. Therefore fig. 6 shows only a rough approximation of the non-thermoelastic component of the horizontal strain variations. It seems to be a linear component with a yearly strain rate of about $2 \cdot 10^{-7}$ (dilatation).

The observed velocity of the secular strain component agrees good with the mean strain rates, which were calculated for adjoining regions, for example for the Saxonian one. Here THURM /1974/ calculated a mean strain rate of about $3 \cdot 10^{-7}$ /year for the EW direction, using the results of two trigonometric measuring campaigns which differ in time by about 60 years.

As a consequence of this and due to the good agreement between the records of two parallel instruments of different type operating at the Tiefenort station during a period of about 4 years tidal strainmeters may be suitable instruments for measurements of recent crustal movements too. For the determination of the yearly strain rates of recent crustal movements from strainmeter records shorter measuring periods are necessary than in the case of trigonometric measurements (for instance 6 years instead of 60 years). Therefore a continuous control of the strain velocity in special test areas by means of such instruments seems to be possible.

Furthermore the measuring results of both the vertical strainmeters have shown that essential improvements of the regional representativeness of the measured strain rates and the tidal parameters may be reached by changes of the measuring places.

Both the instruments differ only in the location and in the manner of installation; their measuring systems are quite the same.

The records of the floor-roof vertical strainmeter are disturbed by large local loading and meteorological components. These effects are diminished in the case of the bore hole instrument as follows

1. the mining loading strain is diminished by a factor of $K_1 \approx 10$ (see fig. 4)
2. the barometric pressure effects (loading and instrumental ones) are diminished by a factor of 8 (absolutely) or 3, relatively,
3. the cavity effect seems to be smaller than 1 %, since the first harmonic analysis of a record of 110 days results a M_2 -Amplitude of

$$e_{rr}^{obs}(M_2) = 35.66 \cdot 10^{-10} ;$$

the corresponding theoretical amplitude was calculated according to the Earth model of WAHR

$$e_{rr}^o(M_2) = 35.93 \cdot 10^{-10} .$$

Analogous improvements of the regional representativeness of the measuring results are to reach in the case of horizontal strainmeters too. For this purpose we must consider several regulas resulting from the model calculations of HARRISON /1976/

Table 1. Station Tiefenort/GDR
Tidal results of the EW strainmeter 1978 - 1984

year	record. month	$e_{\lambda\lambda}(O_1)$ wire $A \times 10^{-10}$ \approx	$e_{\lambda\lambda}(O_1)$ tube $A \times 10^{-10}$ \approx	record. month
1978	12	72.184 0.97 ⁰		
1979	12	71.643 1.16 ⁰		
1980	12	71.872 2.95 ⁰	72.213 1.16 ⁰	6
1981	12	72.338 3.83 ⁰	70.645 1.74 ⁰	12
1982	12	74.220 3.75 ⁰	74.624 2.24 ⁰	12
1983	12	72.300 1.51 ⁰	71.798 1.97 ⁰	12
1984	6	72.571 2.51 ⁰	71.637 0.85 ⁰	6
mean		72.590 2.38 ⁰ 0.762 1.19 ⁰	72.183 1.59 ⁰ 1.481 0.57 ⁰	
WAHR model		67.368 0 ⁰	body strain wave	
year	record. month	$e_{\lambda\lambda}(M_2)$ wire $A \times 10^{-10}$ \approx	$e_{\lambda\lambda}(M_2)$ tube $A \times 10^{-10}$ \approx	record. month
1978	12	5.042 -64.82 ⁰		
1979	12	4.708 -68.62 ⁰		
1980	12	4.921 -56.48 ⁰	4.912 -64.48 ⁰	6
1981	12	4.665 -66.99 ⁰	4.827 -58.53 ⁰	12
1982	12	4.897 -64.23 ⁰	4.372 -56.44 ⁰	12
1983	12	4.500 -58.23 ⁰	4.394 -59.52 ⁰	12
1984	6	4.980 -59.47 ⁰	4.558 -62.46 ⁰	6
mean		4.816 -62.69 ⁰ 0.195 4.65 ⁰	4.613 -60.29 ⁰ 0.247 3.19 ⁰	
WAHR model		1.557 0 ⁰	body strain wave	

concerning the cavity effect in galleries or tunnels of elliptic cross-sections and the loading pressure situation around such tunnels.

The amplitudes of the local strain components induced by loading influences and the cavity effect have a relative minimum at measuring places in the floor and near the symmetry axis of the gallery and distant from its ends.

Fig. 7 shows the old and the new manner of installation of the horizontal strainmeters at the Tiefenort station.

The first instrument is installed about 1 m above the floor between the walls of the gallery and near the end of it. The second strainmeter operates in an artificial cleft with a depth of about 80 cm drilled into the floor near the middle axis of the gallery and distant from its end.

Two NS instruments installed in the old and the new manner record simultaneously since the autumn of 1984. For the determination of the amplitudes of the different local components a recording period of about 1 year seems to be necessary.

References

- HARRISON, J.C.: Cavity and Topographic Effects in Tilt and Strain Measurements
Geoph. Res., Vol. 81 (1976), S. 319-328
- LORENZ, G.: Stationäres hydrostatisches Präzisions-Neigungssystem
5th Int. Symp. "Geodesy and Physics of the Earth", Magdeburg, 23.-29. Sept. 1984
- THURM, H.: Horizontale Dislokationen und Deformationen der Erdkruste in der Elbtalzone
Geod. Geoph. Veröff. R. III H 35 (1974), S. 6-20
- VARGA, P.: Long-time variations recorded by extensometers
J. of Geophysics Vol. 55 (1984), S. 68-70
- WAHR, J.M.: Computing tides, nutations, and tidally-induced variations in the earth's rotation rate for a rotating elliptical earth
In "Geodesy and Geodynamics", Mttlg. d. Geod. Inst. TU Graz (1982), 41. Folge.

List of figure captions

- Fig. 1. The longperiodic components of the EW strainmeter records
W wire instrument; Q quartz tube instrument
- Fig. 2. Map of the station and its surroundings
← fresh air streams
T1, ... T7 measuring places of the rock temperature
EW I, EW II (tube) measuring places of the horizontal
VI, VII (borehole) and vertical strainmeters
- Fig. 3. Results of the rock temperature measurements 1982 - 1984 in the boreholes T1 - T7
- Fig. 4. Lefthand: comparison between the records of the EW strainmeter EW I and the results of rock temperature measurements in the borehole T1;
Righthand, upper part: model of the horizontal strain variations inside and outside of the station during the wintertime;
Righthand, lower part: model of the vertical strain variations inside the station during the wintertime
- Fig. 5. Comparison between the longperiodic components of the records of the horizontal strainmeter EW I, the vertical strainmeter VI and VII, respectively
- Fig. 6. The linear component of the long periodic strain variation in the EW direction 1978 - 1984 (instrument EW I)

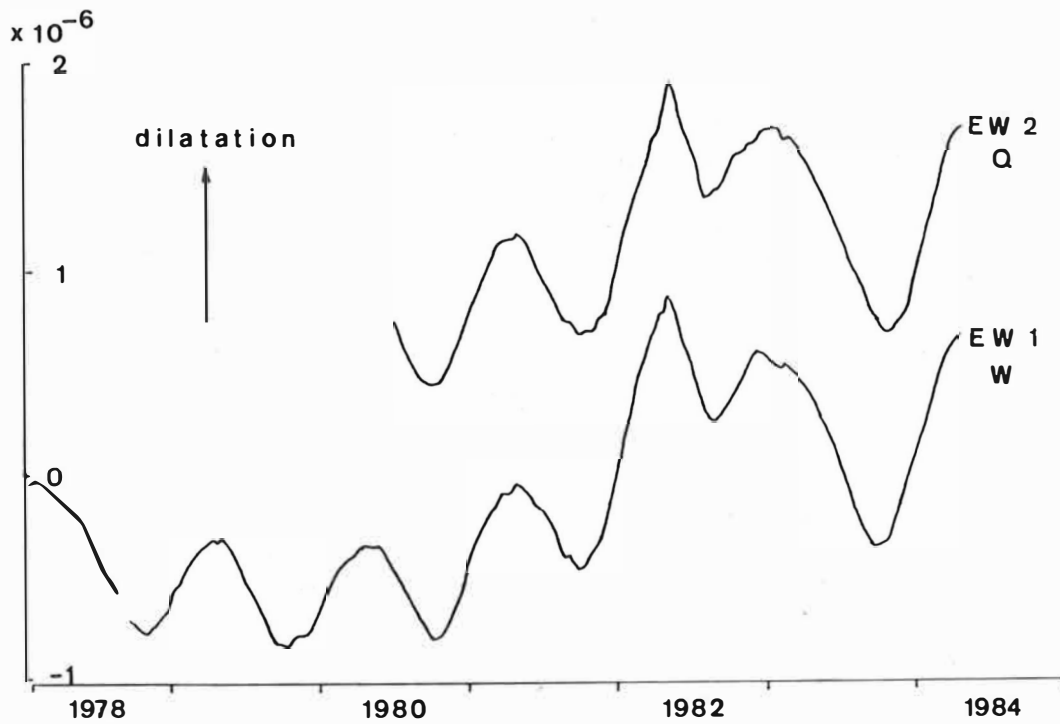


Fig. 1

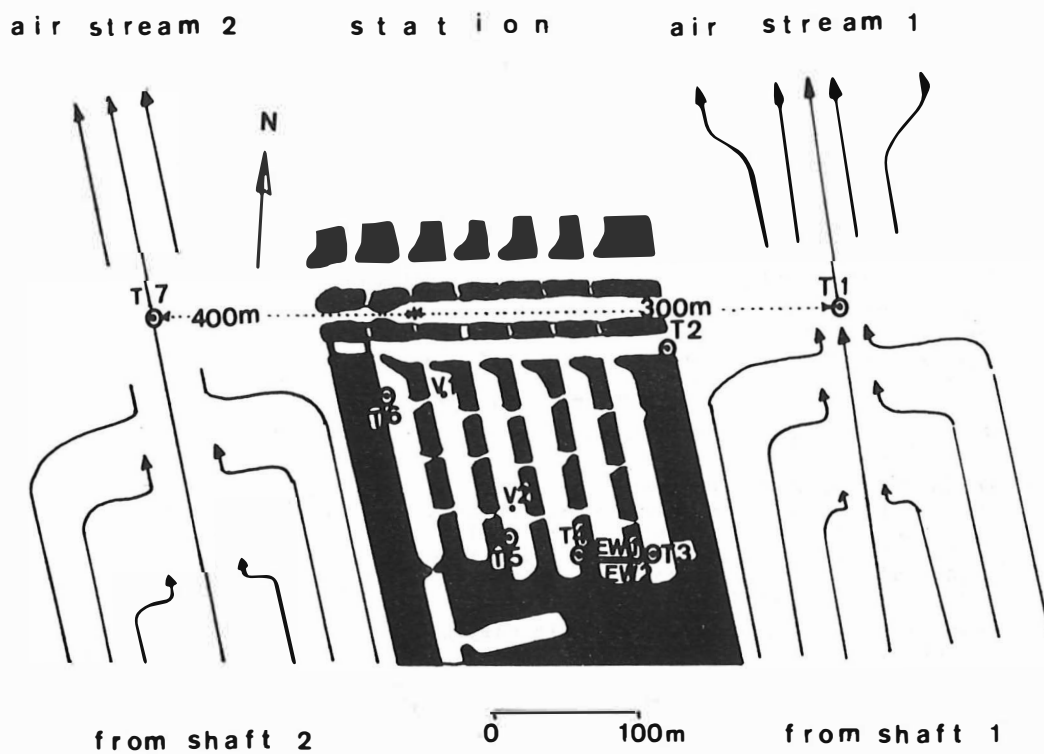


Fig. 2

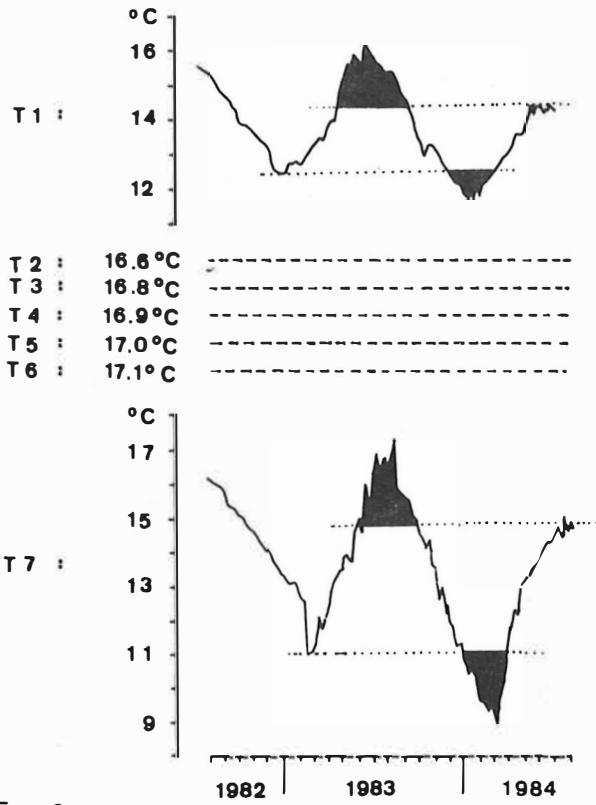


Fig. 3

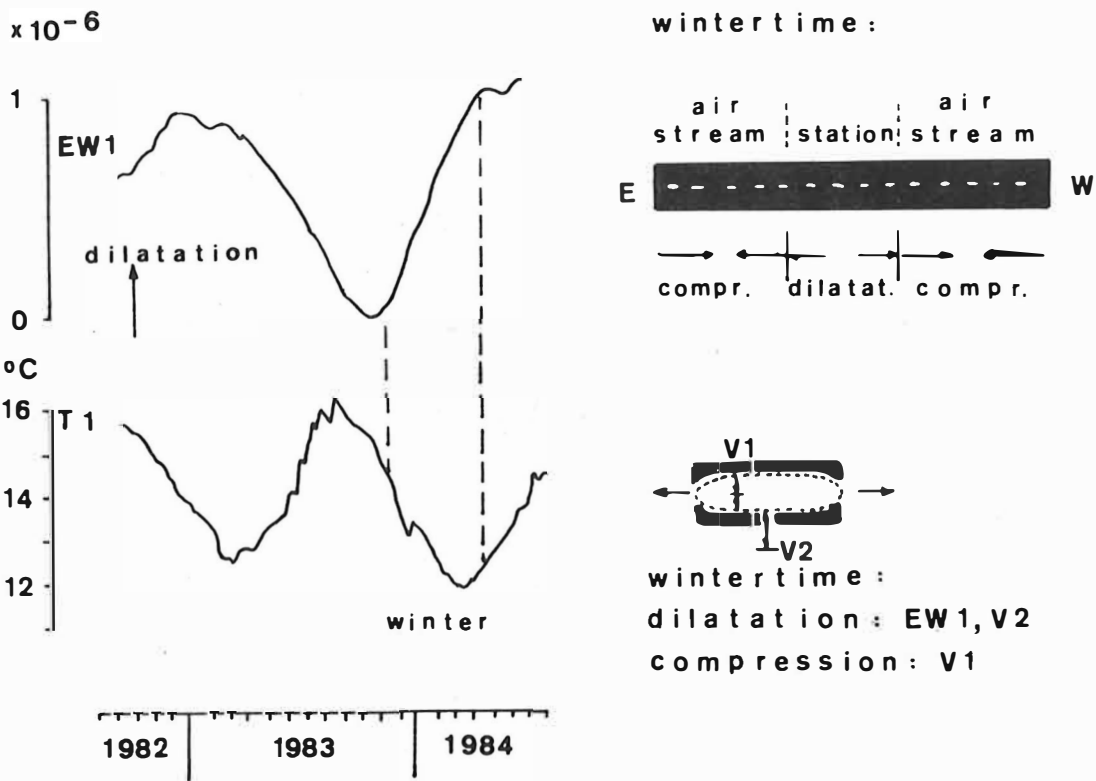


Fig. 4

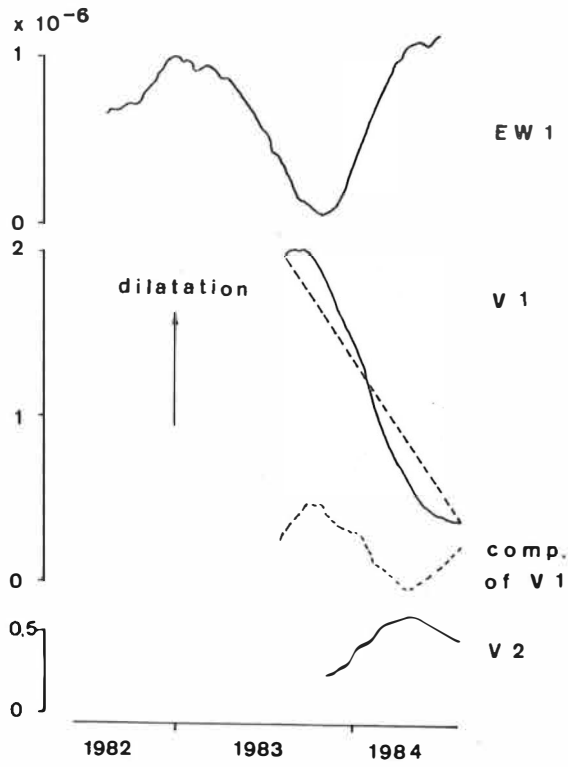


Fig. 5

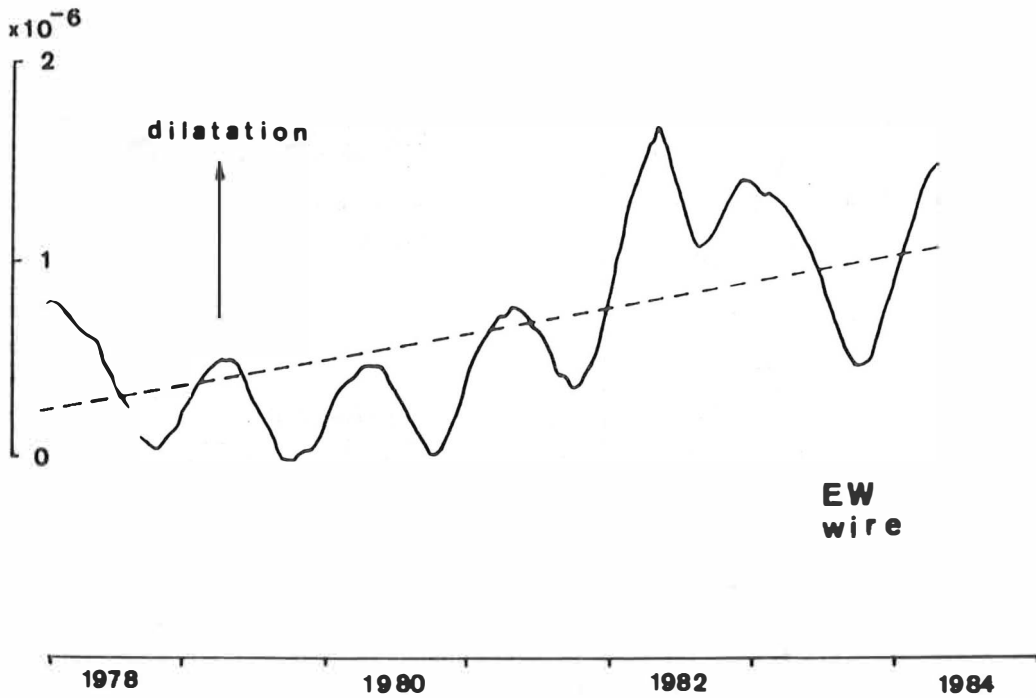


Fig. 6

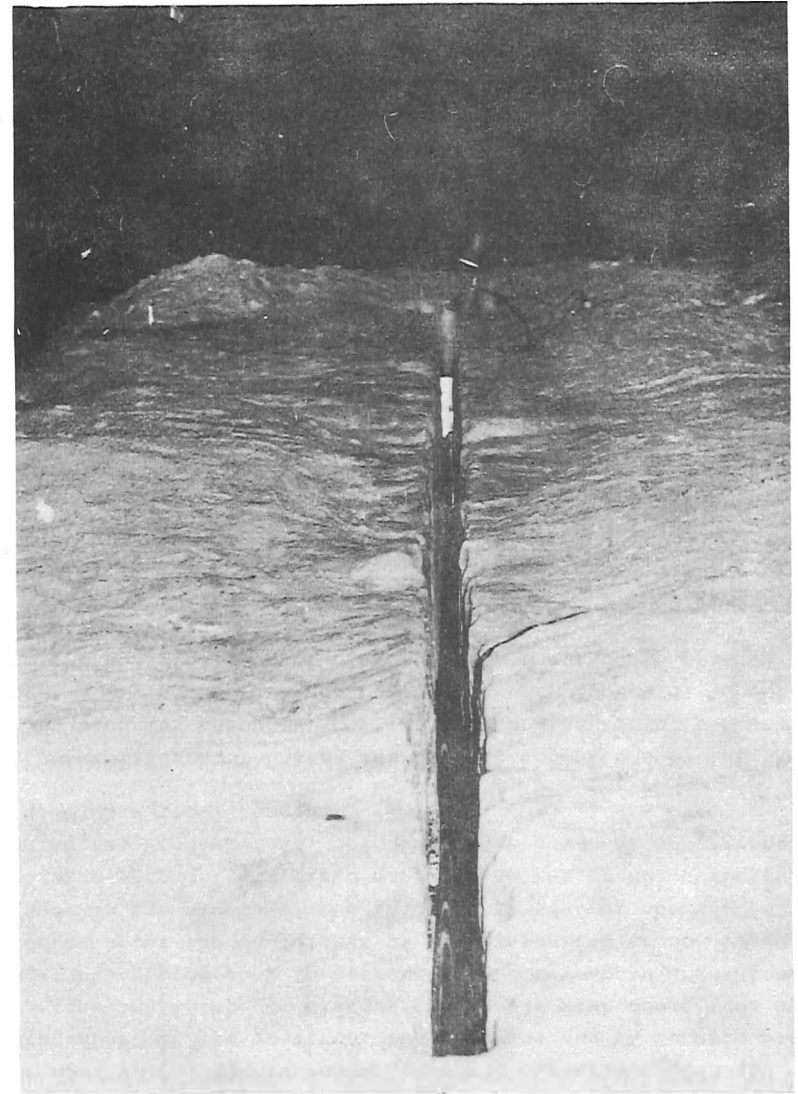
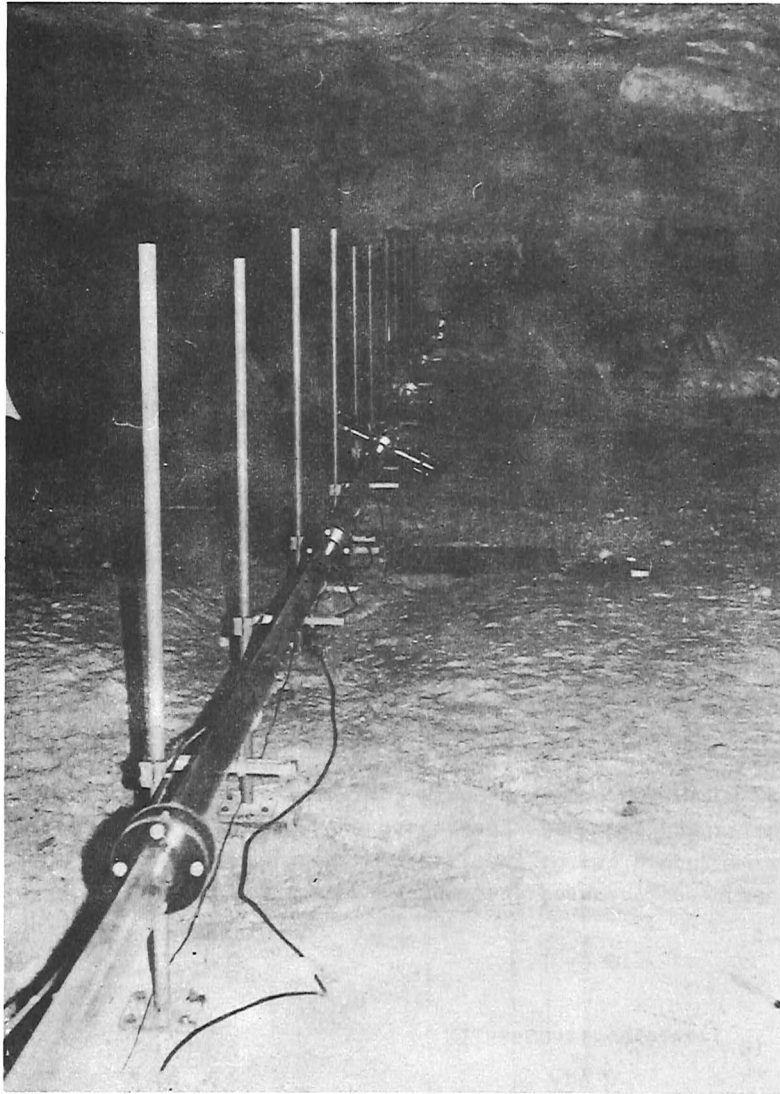


Fig. 7

The old and the new manner of installation of horizontal strainmeters at the Tiefenort station

Planets around Barnard's star? ¹⁾

by

Klaus-Günter Steinert ²⁾

Summary

From Analyses of long-focus observations unseen objects may be found from perturbations in the proper motions of a star. The question is discussed under what conditions it should be possible to detect planets around the nearby Barnard's star.

Zusammenfassung

Aus Untersuchungen von photographischen Beobachtungen an langbrennweitigen Instrumenten können aus den Störungen der Eigenbewegungen eines Sterns unsichtbare Objekte gefunden werden. Es wird die Frage diskutiert, unter welchen Bedingungen es möglich sein sollte, Planeten um den benachbarten Barnardschen Stern zu entdecken.

1. Introduction

In 1844 F.W. Bessel pointed out that irregularities in the proper motions of stars indicate the existence of unseen companions. Indeed some decades later companions of Sirius and Procyon announced by Bessel were found by Clark in 1862 and by Schaeberle in 1896 resp. with visual refractors. The history of discovering the planets Neptune and Pluto is very similar.

¹⁾ Mitteilung des Lohrmann-Observatoriums der TU Dresden Nr. 52

²⁾ Technische Universität Dresden, Sektion Geodäsie und Kartographie. DOR-8027 Dresden, Mommsenstraße 13

By means of long-focus photographic astrometry 50 years ago the first unseen companion of a star, that means the component of a visual binary (Ross 614) was discovered from series of observations and analyses of the perturbation in proper motion over nine years. Twenty years later the object was seen and photographed in its apastron. The next one was VW Cephei. Since this time the method of discovering double star companions by long-focus photography in astrometry was developed and there is no doubt about the usefulness of it. Systematic search began already in the middle of the thirties at several observatories. Intensive work in this field was done at the Sproul Observatory Swarthmore, Pennsylvania, using the well known 61 cm refractor with 10.93 m focal length.

As the amplitudes of unseen astrometric companions of the explored binaries are about 0.1", the determination of period, excentricity and periastron passage is very accurate. To determine the perturbations of a star's proper motion in principle Schlesinger's method of dependences is used. To avoid effects of magnitude equation it is necessary to select reference stars having magnitudes of the same order as the objects (field stars) to be investigated. The period of observation depends of course on the period of orbital motion of a star and its companion around their common barycenter.

In the case of faint nearby visual binaries as a rule this astrometric technique is quite valuable and may be regarded as fully developed (v.d. Kamp, 1981).

2. Barnard's star

Besides this it should be possible to apply this method of finding companions of stars from perturbations in their proper motion for the discovery of planets around nearby stars. It is evident that in this case the necessary accuracy is the larger the more distant the star and the closer the planet is to it. Of course the demanded accuracy also depends on the mass ratio of star and planet.

The smallest stars have about 0.07 times the solar mass. Smaller objects are according to our present knowledge black dwarfs, and if smaller than 0.005 solar masses planets, that means objects which are not able to develop nuclear energy. Compared to this Jupiter's mass is 0.001 solar mass.

After W.D. Heintz (1980) it is necessary to secure an accuracy in determining the perturbations of proper motions, and to derive the existence of a perturbing body better than 0.01" over a long period of observations. Because the orbital period of a presumed planet is previous unknown, the series of observations must be extended over some decades. In the case of Barnard's star Peter van de Kamp (1981, 1983) has used observations with the Sproul refractor started in 1938. That means for his latest results v.d. Kamp (1983) could use the material of 1200 nights from 44 years (1938 - 1982), each night with about four plates, each of them with up to 5 expositions. Since 1975 v.d. Kamp made some analyses for finding planets around Barnard's star from the perturbations of its proper motion. The results obtained by him depend on the boundary conditions considered by van de Kamp. With the following dates for Barnard's star: Red dwarf; apparent magnitude 9.5^m; spectral type M 5; mass 0.14 solar masses; parallax 0.547"; distance 6.0 light years; proper motion 10.31 "/year v.d. Kamp (1983) got from the analysis of perturbations in proper motion the following results: there are existing two planets around Barnard's star, having radii of circular orbits 2.7 and 3.9 astronomical units resp., masses of 0.6 and 0.4 times the mass of Jupiter resp. and orbital periods of 12 and 20 years resp.. Representations of the perturbation curves of Barnard's star caused by these presumed planets are to be found in v.d. Kamp's publications (1981, 1983). The curves having a semi-amplitude of 0.01" or 0.5 μm in the focal plane of the Sproul refractor are calculated from so called normal points, i.e. mean values of alpha and delta over one year.

This interesting result of P.v.d. Kamp is not without con-

tradiction by other authors. Especially W.D. Heintz (1980) from Sproul observatory negates absolutely the reality of the planets found by v.d. Kamp. His main contra-arguments are:

- v.d. Kamp's curves mentioned above reflect instrumental errors which can also be found from observations of other stars made at the Sproul refractor
- a systematical accuracy of 0.01" can not be reached from photographic plates over a field of 20', as it was used by v.d. Kamp with the Sproul refractor; that means 10⁻⁵ relatively
- proper motion and parallax of Barnard's star are very large compared with the presumed perturbations.

These contra-arguments are to be compared with P.v.d. Kamp's results and discussed to consider some facts for clearing up the problem, because it is of cosmogonic importance and indirectly it is connected with SETI.

3. Conclusions

In the opinion of the author there are some facts pro and contra the results as well of v.d. Kamp as of Heintz.

An accuracy of 10⁻⁵ can be reached in photographic astrometry. That was proved with plates of the 2-m-Schmidt in the Lohrmann-program. Main condition for this is of course a long-time constancy of the instrument's adjustment.

Such a constancy may be doubted for the Sproul refractor, because there were some changes in the construction and adjustment of the instrument. The dates of these events were 1941.82, 1949.21, 1957, and 1966. It is very likely that they have influenced anyhow the results of v.d. Kamp's analysis of the proper motion of Barnard's star in spite of reductions because of variations of the instrumental equation connected with these events. The simultaneous variation in both coordinates alpha and delta also point in this direction.

Using different time intervalls of Sproul observations lead to different results for the presumed planets as is shown in v.d.

Kamp's book "Stellar Paths" (1981).

Barnard's star moves very fast. Its distance from the sun becomes smaller. Therefore proper motion and parallax are changing. To avoid systematic influences accuracies of 0.2 % and 4 % resp. are necessary, what is possible to be reached as mentioned above.

The fact of using only four reference stars for the determination of the perturbations of Barnard's star is an other weak point for deriving the existence of planets around it, particularly because of the altering of a reference star's influence to the position of the field star. Barnard's star changes his position at the plate relatively to the tangential point of the Sproul objective for 5 mm per 10 years.

The author agrees with P.v.d. Kamp (1983) and with W.D. Heintz (1980): it is possible to find planets around nearby stars with the photographic method. However there must be fulfilled all conditions to avoid systematical influences from the instrument, from the reference stars, and from the measurement of the plates.

And indeed it seems there are not yet series of observations with the quality needed and having the necessary length.

References

- Heintz, W.D. (1980): Die Sterne 56 (1980), Heft 1, pp. 55 - 58
 v.d. Kamp, P.(1981): Stellar Paths, Reidel Publishing Company Dordrecht, Boston, London
 v.d. Kamp, P.(1983): Astronomische Nachrichten 304 (1983), No. 3, pp. 97 - 100

Jiří Trešl

Geophysical Institute, Czechosl.Acad.Sci.,
 Boční II, Spořilov, CS - 141 31 Praha 4

Summary

Some geodynamic effects arising due to deformation of the Earth are investigated. In undeformed state the Earth is replaced by a sphere with radially depending density. Its deformed state is described by displacement vector field. Corresponding density disturbances are expressed in terms of the density and displacements. Further, displacement vector field is decomposed into irrotational and solenoidal parts. Gravitational changes on the Earth's surface are composed from:

- i/ the changes due to density disturbances inside the Earth
- ii/ the changes due to deformations of the density interfaces
- iii/ the changes due to radial displacement of the observational point

Mathematical expressions are derived for the deflections of the vertical, the displacements of the principal axes of inertia, the changes of Earth's rate of rotation and its centre of gravity in terms of the density disturbances.

1. Introduction

The mass distribution in the Earth's interior and the shape of its surface depend on working of external and internal force fields. Generally, it is changing with time. However, such changes evoke a number of geodynamic effects: the variation of the gravitational field and rate of rotation, the displacement of the principal axes of inertia and the centre of gravity.

From external disturbing factors, the tidal effects due to planetary attraction are most important. The study of this phenomena has long history and forms an independent part of geodynamics [1].

In this paper, we will study the geodynamic consequences of Earth's deformation. Solving this problem, we choose a kinematic approach (the deformations are considered given a priori). As a result, we will derive expressions, describing above mentioned geodynamic effects in terms of the density disturbances arising from deformation.

2. Displacement field in spherical geometry

According to fundamental theorem of vectoranalysis, any displacement vector field \vec{u} may be resolved into irrotational and solenoidal parts

$$(1) \quad \vec{u} = \vec{u}_1 + \vec{u}_2, \quad \text{rot } \vec{u}_1 = 0, \quad \text{div } \vec{u}_2 = 0.$$

Eqs.(1) will be satisfied by putting

$$(2) \quad \vec{u}_1 = \text{grad } \varphi, \quad \vec{u}_2 = \text{rot } \vec{A}.$$

The quantities φ, \vec{A} are called scalar and vector potentials. Introducing spherical co-ordinates r, ϑ, λ we can expand φ in the following manner

$$(3) \quad \varphi(r, \vartheta, \lambda) = \sum_{n=0}^{\infty} \sum_{m=0}^n \varphi_n(r) P_n^m(z) [a_n^m \cos m\lambda + b_n^m \sin m\lambda],$$

where $P_n^m(z)$ are associated Legendre polynomials and $z = \cos \vartheta$.

The solenoidal part of the displacement field can be written as

$$(4) \quad \vec{u}_2 = \text{rot}(\vec{A}_r + \vec{A}_t) = \text{rot } \vec{A}_r + \text{rot } \vec{A}_t = \vec{u}_2^T + \vec{u}_2^S,$$

where \vec{A}_r , resp. \vec{A}_t is vector potential in direction of the position vector \vec{r} , resp. in direction perpendicular to \vec{r} . Therefore, we may put

$$(5) \quad \vec{A}_r = T \vec{r}, \quad \vec{A}_t = \text{rot}(S \vec{r}) = \text{grad } S \times \vec{r}.$$

Here so-called toroidal and spheroidal defining scalars [2] T, S can be again divided into their spherical harmonics components

$$(6) \quad \begin{bmatrix} S(r, \vartheta, \lambda) \\ T(r, \vartheta, \lambda) \end{bmatrix} = \sum_{n=0}^{\infty} \sum_{m=0}^n \begin{bmatrix} S_n(r) \\ T_n(r) \end{bmatrix} P_n^m(z) \left\{ \begin{bmatrix} c_n^m \\ e_n^m \end{bmatrix} \cos m\lambda + \begin{bmatrix} d_n^m \\ f_n^m \end{bmatrix} \sin m\lambda \right\}$$

3. Density disturbances

Let us consider a volume element $d\tau$ and corresponding mass element dm . In reference state before deformation is

$$(7) \quad dm = F_0(\vec{r}) d\tau,$$

where $F_0(\vec{r})$ is density in a point with position vector \vec{r} . In disturbed state after deformation it holds

$$(8) \quad dm = F(\vec{r} + \vec{u}) d\tau',$$

where \vec{u} is displacement vector and $d\tau'$ deformed volume element. In view of \vec{u} is small quantity, we can write

$$(9) \quad F(\vec{r} + \vec{u}) = F_0(\vec{r}) + f(\vec{r}) + \vec{u} \cdot \text{grad } F_0(\vec{r}).$$

Here f is density disturbance, which is supposed to be small. The change of a volume element is given by expression [3]

$$(10) \quad d\tau' = (1 + \text{div } \vec{u}) d\tau.$$

From the condition of equality of right-hand sides of Eqs.(7),(8) with a view to (9),(10) we arrive at

$$(11) \quad f = -(\vec{u} \cdot \text{grad } F_0 + F_0 \text{div } \vec{u}) = -\text{div}(F_0 \vec{u}).$$

This formula gives density disturbance as a function of reference density and displacement.

We will suppose radially dependent density in the reference state: $F_0(\vec{r}) = F_0(r)$. Then, with a view to (1),(2) Eq.(11) reduces to

$$(12) \quad f = -(u_r F_0' + F_0 \Delta \varphi),$$

where the prime indicates a derivative with respect to radial coordinate r . Further, in spherical coordinates holds [4]

$$(13) \quad \Delta \varphi = \frac{1}{r^2 \sin \vartheta} \left[(r^2 \varphi')' \sin \vartheta + \frac{\partial}{\partial \vartheta} \left(\sin \vartheta \frac{\partial \varphi}{\partial \vartheta} \right) + \frac{1}{\sin \vartheta} \frac{\partial^2 \varphi}{\partial \lambda^2} \right].$$

Finally, after expression of the radial displacements from Eqs.(2),(4), (5) we arrive at

$$(14) f = \sum_{n=0}^{\infty} \sum_{m=0}^n \left[\alpha_n(r) (\alpha_n^m \cos m\lambda + \beta_n^m \sin m\lambda) + \beta_n(r) (c_n^m \cos m\lambda + d_n^m \sin m\lambda) \right] P_n^m(z) = \sum_{n=0}^{\infty} \left[\alpha_n(r) Y_n^\alpha(\vartheta, \lambda) + \beta_n(r) Y_n^\beta(\vartheta, \lambda) \right],$$

where radial functions $\alpha_n(r)$, $\beta_n(r)$ are defined as follows

$$(15) \alpha_n(r) = \frac{F_0}{r^2} \left[n(n+1)\varphi_n - (r^2\varphi_n')' \right] - F_0'\varphi_n',$$

$$(16) \beta_n(r) = -\frac{n(n+1)}{r} F_0' S_n.$$

4. Gravitational effects due to density disturbances inside the Earth

Let us suppose Earth's model according to Fig.1. Here outer surface $r=R$ corresponds to Earth's surface and $r=R_1$ corresponds to core-mantle boundary.

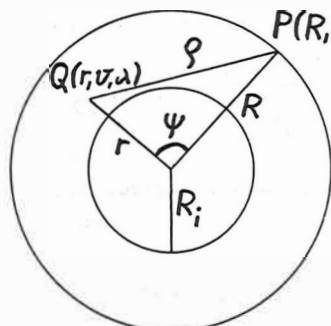


Fig.1

$$(17) T_1(P) = \varpi \int_{R_1}^R \int_0^{2\pi} \int_0^\pi f(Q) \varrho^{-1} r^2 \sin\vartheta \, dr \, d\vartheta \, d\lambda,$$

where P denotes a fixed point at the Earth's surface and Q current point of integration. From the theory of spherical harmonics are known following formulae [5]

$$(18) \frac{1}{\varrho} = \sum_{n=0}^{\infty} \frac{r^n}{R^{n+1}} P_n(\cos\psi), \quad r \leq R,$$

$$(19) 4\pi Y_n(\theta, \lambda) = (2n+1) \int_0^\pi \int_0^{2\pi} Y_n(\vartheta, \lambda) P_n(\cos\psi) \sin\vartheta \, d\vartheta \, d\lambda.$$

Then, after integration of Eq.(17) we obtain

$$(20) T_1(P) = 4\pi\varpi \sum_{n=0}^{\infty} \frac{Y_n(\theta, \lambda)}{(2n+1)R^{n+1}},$$

where

$$(21) Y_n = Y_n^\alpha \int_{R_1}^R \alpha_n(r) r^{n+2} \, dr + Y_n^\beta \int_{R_1}^R \beta_n(r) r^{n+2} \, dr.$$

The change of gravitational acceleration is

$$(22) \delta g_1(P) = -\frac{\partial T_1}{\partial R} = 4\pi\varpi \sum_{n=0}^{\infty} \frac{(n+1)Y_n(\theta, \lambda)}{(2n+1)R^{n+2}}.$$

Finally, changes in the direction of the vertical are

$$(23) e_{1,\vartheta}(P) = \frac{\partial T_1}{gR\partial\theta} = \frac{4\pi\varpi}{g} \sum_{n=0}^{\infty} \frac{\partial Y_n(\theta, \lambda)}{(2n+1)R^{n+2} \partial\theta},$$

$$(24) e_{1,\lambda}(P) = \frac{\partial T_1}{gR\sin\theta\partial\lambda} = \frac{4\pi\varpi}{g\sin\theta} \sum_{n=0}^{\infty} \frac{\partial Y_n(\theta, \lambda)}{(2n+1)R^{n+2} \partial\lambda}.$$

5. Gravitational effects due to deformation of the density interfaces

Our density model $F_0(r)$ contains two clean-cut density interfaces: core-mantle boundary $r=R_1$ and Earth's surface $r=R$. Clearly, there are jumps in the reference density $\Delta F_0(R_1) = \delta_1$ and $\Delta F_0(R) = \delta$. We will investigate corresponding gravitational effects by means of simple layers with surface densities

$$(25) \mu \left[\left(\begin{matrix} R_1 \\ R \end{matrix} \right), \vartheta, \lambda \right] = \left(\begin{matrix} \delta_1 \\ \delta \end{matrix} \right) u_r \left[\left(\begin{matrix} R_1 \\ R \end{matrix} \right), \vartheta, \lambda \right],$$

where u_r denotes radial component of the displacement. Further, at the interfaces we can use developments in surface spherical harmonics

$$(26) u_r \left[\left(\begin{matrix} R_1 \\ R \end{matrix} \right), \vartheta, \lambda \right] = \sum_{n=0}^{\infty} \sum_{m=0}^n \left[\left(\begin{matrix} u_{ni}^m \\ u_n^m \end{matrix} \right) \cos m\lambda + \left(\begin{matrix} v_{ni}^m \\ v_n^m \end{matrix} \right) \sin m\lambda \right] P_n^m(z) = \sum_{n=0}^{\infty} \left[\left(\begin{matrix} U_{ni} \\ U_n \end{matrix} \right) (\vartheta, \lambda) \right].$$

The potential arising from the deformation of Earth's surface is given by

$$(27) \quad T_2(P) = \alpha \epsilon R^2 \int_0^{2\pi} \int_0^\pi u_r(R, \vartheta, \lambda) \vartheta^{-1} \sin \vartheta \, d\vartheta \, d\lambda.$$

Now, we must separate two cases. First, if the observational point P is rising, then its radial distance $r_p > R$ because $u_r(P) > 0$.

In this case

$$(28) \quad \frac{1}{\vartheta} = \sum_{n=0}^{\infty} \frac{R^n}{r_p^{n+1}} P_n(\cos \Psi),$$

$$(29) \quad T_2(P) = 4\pi\alpha\epsilon\delta \sum_{n=0}^{\infty} \frac{U_n(\theta, \lambda) R^{n+2}}{(2n+1)r_p^{n+1}}.$$

On the other hand, for sinking point P is $r_p < R$, $u_r(P) < 0$ and

$$(30) \quad \frac{1}{\vartheta} = \sum_{n=0}^{\infty} \frac{r_p^n}{R^{n+1}} P_n(\cos \Psi),$$

$$(31) \quad T_2(P) = 4\pi\alpha\epsilon\delta \sum_{n=0}^{\infty} \frac{U_n(\theta, \lambda) r_p^n}{(2n+1)R^{n+1}}.$$

Finally, for unchanged point P $u_r(P) = 0$ / Eqs.(29),(31) reduce to

$$(32) \quad T_2(P) = 4\pi\alpha\epsilon\delta R \sum_{n=0}^{\infty} \frac{U_n(\theta, \lambda)}{2n+1}.$$

The derivative of Eqs.(29),(31) with respect to $(-r_p)$ and putting $r_p = R$ gives

$$(33) \quad \delta g_2(P) = 4\pi\alpha\epsilon\delta \sum_{n=0}^{\infty} \frac{n+1}{2n+1} U_n(\theta, \lambda), \quad u_r(P) > 0,$$

$$(34) \quad \delta g_2(P) = -4\pi\alpha\epsilon\delta \sum_{n=0}^{\infty} \frac{n}{2n+1} U_n(\theta, \lambda), \quad u_r(P) < 0.$$

The changes in the direction of the vertical are found from (32)

$$(35) \quad e_{2\vartheta}(P) = \frac{4\pi\alpha\epsilon\delta}{g} \sum_{n=0}^{\infty} \frac{\partial U_n(\theta, \lambda)}{(2n+1)\partial\theta},$$

$$(36) \quad e_{2\lambda}(P) = \frac{4\pi\alpha\epsilon\delta}{g \sin\theta} \sum_{n=0}^{\infty} \frac{\partial U_n(\theta, \lambda)}{(2n+1)\partial\lambda}.$$

In the similar way, the potential arising from deformation of Earth's core-mantle boundary is given by

$$(37) \quad T_2^i(P) = 4\pi\alpha\epsilon\delta_i R_i \sum_{n=0}^{\infty} \frac{U_{ni}(\theta, \lambda)}{2n+1}, \quad \varrho = \frac{R_i}{R}.$$

From this expression we immediately obtain

$$(38) \quad \delta g_2^i(P) = 4\pi\alpha\epsilon\delta_i \sum_{n=0}^{\infty} \varrho^{n+2} \frac{n+1}{2n+1} U_{ni}(\theta, \lambda),$$

$$(39) \quad e_{2\vartheta}^i(P) = \frac{4\pi\alpha\epsilon\delta_i}{g} \sum_{n=0}^{\infty} \varrho^{n+2} \frac{\partial U_{ni}(\theta, \lambda)}{(2n+1)\partial\theta},$$

$$(40) \quad e_{2\lambda}^i(P) = \frac{4\pi\alpha\epsilon\delta_i}{g \sin\theta} \sum_{n=0}^{\infty} \varrho^{n+2} \frac{\partial U_{ni}(\theta, \lambda)}{(2n+1)\partial\lambda}.$$

6. Gravitational effects due to surface deformation at the observational point

Owing to radial displacement, the observational point $P(R, \theta, \lambda)$ is shifted in $P'(R+u_r, \theta, \lambda)$. Corresponding disturbing potential will be

$$(41) \quad T_3(P) = \frac{d}{dR} \left(\frac{\alpha M}{R} \right) u_r = - \left(\frac{\alpha M}{R^2} \right) u_r = -g u_r,$$

where M is the mass of the Earth. Disturbing gravitational effect is

$$(42) \quad \delta g_3(P) = - \frac{\partial T_3}{\partial R} = - \frac{2\alpha M}{R^3} u_r = - \frac{2}{R} g u_r.$$

The changes in the direction of the vertical, resulting from a surface deformation at the observational point are

$$(43) \quad e_{3\vartheta}(P) = - \frac{\partial u_r}{R \partial \theta} = - \frac{1}{R} \sum_{n=0}^{\infty} \frac{\partial U_n(\theta, \lambda)}{\partial \theta},$$

$$(44) \quad e_{3\lambda}(P) = - \frac{\partial u_r}{R \sin\theta \partial \lambda} = - \frac{1}{R \sin\theta} \sum_{n=0}^{\infty} \frac{\partial U_n(\theta, \lambda)}{\partial \lambda}.$$

7. The disturbance in the Earth's rate of rotation

Assume the Earth in the shape of a rotational ellipsoid, in the centre of which, O, we shall place the origin of rectangular co-ordinate system xyz. The z-axis is identical with minor axis of the ellipsoid (positive direction to the north). The x-axis is defined by the intersection of the equatorial plane and the prime meridian and the y-axis makes up the clockwise system.

In the reference state before deformation the Earth rotates about z-axis with angular rate of rotation ω_0 . The principal moment of inertia with regard to z-axis is C_0 . If the displacement field is axisymmetric it holds

$$(45) \quad C = C_0 + \delta C, \quad \omega = \omega_0 + \delta\omega, \quad \delta C \ll C_0, \quad \delta\omega \ll \omega_0.$$

According to third Euler's equation [6]

$$(46) \quad \frac{d}{dt} (C\omega) = 0, \quad C\omega = \text{const.}$$

Then, with a view to (45) we arrive at

$$(47) \quad \frac{\delta\omega}{\omega_0} = - \frac{\delta C}{C_0}.$$

It is sufficient to calculate small quantity δC in a spherical approximation according to formula

$$(48) \quad \delta C = \int_0^R \int_0^\pi \int_0^{2\pi} f(r, \nu) r^2 \sin^2 \nu d\varphi + \int_0^R \int_0^\pi \delta u_r(R, \nu) R^2 \sin^2 \nu dS + \\ + \int_0^R \int_0^\pi \delta_i u_r(R_i, \nu) R_i^2 \sin^2 \nu dS_i = \delta C_1 + \delta C_2 + \delta C_3,$$

where

$$(49) \quad \begin{bmatrix} d\varphi \\ dS \\ dS_i \end{bmatrix} = \begin{bmatrix} r^2 dr \\ R^2 \\ R_i^2 \end{bmatrix} \sin \nu d\nu d\alpha.$$

Clearly, δC_1 expresses the influence of density disturbances in Earth's mantle, whereas δC_2 and δC_3 are resulting from deformations of density interfaces. According to Eq.(14), the zonal part of density disturbance is given by

$$(50) \quad f(r, \nu) = \sum_{n=0}^{\infty} [a_n \alpha_n(r) + c_n \beta_n(r)] P_n(z).$$

Taking into account developments (26) we obtain after integration

$$(51) \quad \delta C_1 = \frac{8\pi}{3} \int_{R_i}^R [a_0 \alpha_0(r) + c_0 \beta_0(r)] r^4 dr - \\ - \frac{8\pi}{15} \int_{R_i}^R [a_2 \alpha_2(r) + c_2 \beta_2(r)] r^4 dr.$$

$$(52) \quad \delta C_2 = \frac{8\pi}{15} \delta R^4 (5u_0 - u_2),$$

$$(53) \quad \delta C_3 = \frac{8\pi}{15} \delta_i R_i^4 (5u_{0i} - u_{2i}).$$

8. The displacements of principal axes of inertia

In the reference state before deformation are co-ordinate axes x,y,z identical with principal axes of inertia. The tensor of inertia

$$(54) \quad T_{ij} = \begin{bmatrix} T_{11} = A & 0 & 0 \\ 0 & T_{22} = A & 0 \\ 0 & 0 & T_{33} = C \end{bmatrix}$$

contains only diagonal terms. If the mass distribution becomes axially asymmetric, then will be

$$(55) \quad T_{ij} = \begin{bmatrix} T_{11} = A' & T_{12} = -F & T_{13} = -E \\ T_{21} = -F & T_{22} = A' & T_{23} = -D \\ T_{31} = -E & T_{32} = -D & T_{33} = C' \end{bmatrix}$$

To the first order accuracy, for directional cosines ξ, η, ζ of the new principal axis of inertia z' then holds [7]

$$(56) \quad \xi = - \frac{E}{C-A}, \quad \eta = - \frac{D}{C-A}, \quad \zeta = 1.$$

The products of inertia may be calculated from

$$(57) \quad \begin{bmatrix} E \\ D \end{bmatrix} = \int_0^R \int_0^\pi \int_0^{2\pi} f(r, \nu, \alpha) r^2 \sin \nu \cos \nu \begin{bmatrix} \cos \alpha \\ \sin \alpha \end{bmatrix} d\varphi + \\ + \int_0^R \int_0^\pi u_r(R, \nu, \alpha) \delta R^2 \sin \nu \cos \nu \begin{bmatrix} \cos \alpha \\ \sin \alpha \end{bmatrix} d\varphi + \\ + \int_0^R \int_0^\pi u_r(R_i, \nu, \alpha) \delta_i R_i^2 \sin \nu \cos \nu \begin{bmatrix} \cos \alpha \\ \sin \alpha \end{bmatrix} dS_i = \\ = \begin{bmatrix} E_1 \\ D_1 \end{bmatrix} + \begin{bmatrix} E_2 \\ D_2 \end{bmatrix} + \begin{bmatrix} E_3 \\ D_3 \end{bmatrix}.$$

With a view to well-known formula [8]

$$(58) \int_{-1}^{+1} P_1^k(z) P_n^m(z) dz = \frac{2(n+m)!}{(2n+1)(n-m)!} \delta_{km} \delta_{1n},$$

where δ_{km} is Kronecker's symbol, we obtain from (57)

$$(59) \begin{bmatrix} E_1 \\ D_1 \end{bmatrix} = \frac{4\pi}{5} \left[\begin{pmatrix} a_2^1 \\ b_2^1 \end{pmatrix} \int_{R_i}^R \alpha_2(r) r^4 dr + \begin{pmatrix} c_2^1 \\ d_2^1 \end{pmatrix} \int_{R_i}^R \beta_2(r) r^4 dr \right].$$

By substituting (26) into (57) we get after integration

$$(60) \begin{bmatrix} E_2 \\ D_2 \end{bmatrix} = \frac{4\pi}{5} \delta R^4 \begin{bmatrix} u_2^1 \\ v_2^1 \end{bmatrix}, \quad \begin{bmatrix} E_3 \\ D_3 \end{bmatrix} = \frac{4\pi}{5} \delta_i R_i^4 \begin{bmatrix} u_{2i}^1 \\ v_{2i}^1 \end{bmatrix}.$$

9. The change of the centre of gravity

In the reference state before deformation, the centre of gravity is located in the origin of co-ordinate system xyz . After deformation it is shifted and its new position vector is $\vec{r}_0(x_0, y_0, z_0)$. It holds

$$(61) \vec{r}_0 = \frac{1}{M} \int_{R_i}^R \int_{\pi}^{2\pi} \int_{\theta}^{\theta} f(r, \vartheta, \lambda) \vec{r} d\tau + \frac{1}{M} \int_{\pi}^{2\pi} \int_{\theta}^{\theta} u_r(R_i, \vartheta, \lambda) \delta \vec{r} dS + \\ + \frac{1}{M} \int_{\pi}^{2\pi} \int_{\theta}^{\theta} u_r(R_i, \vartheta, \lambda) \delta_i \vec{r} dS_i = \vec{r}_{01} + \vec{r}_{02} + \vec{r}_{03},$$

where M is the mass of the Earth and $\vec{r}(x, y, z)$ the position vector of density disturbance. After integration we arrive at

$$(62) \vec{r}_{01} = \frac{1}{\bar{F} R^3} \left[\begin{pmatrix} a_1^1 \\ b_1^1 \\ a_1^0 \end{pmatrix} \int_{R_i}^R \alpha_1(r) r^3 dr + \begin{pmatrix} c_1^1 \\ d_1^1 \\ c_1^0 \end{pmatrix} \int_{R_i}^R \beta_1(r) r^3 dr \right],$$

$$(63) \vec{r}_{02} = \frac{\delta}{\bar{F}} (u_1^1, v_1^1, u_1^0), \quad \vec{r}_{03} = \frac{\delta_i}{\bar{F}} (u_{1i}^1, v_{1i}^1, u_{1i}^0),$$

where \bar{F} is mean density of the Earth.

10. Conclusion

The model analysis we have carried out indicates that gravitational changes can arise mainly due to local deformation at the point of observation and at its near surroundings.

On the other hand, the displacement of the principal axes of inertia, the changes of Earth's rate of rotation and its centre of gravity may occur only due to planetary deformations of global character. Some estimates for the case of deformation of Earth's core-mantle boundary are given in [9], [10].

REFERENCES

- [1] P. Melchior: The tides of the planet Earth. Oxford 1978.
- [2] E.C. Bullard, H. Gellman: Homogeneous dynamos and terrestrial magnetism. Phil. Trans. Roy. Soc. London, A247 (1954), 213.
- [3] L.D. Landau, E.M. Lifschitz: Lehrbuch der theoretischen Physik. Bd. VII: Elastizitätstheorie. Berlin 1975.
- [4] Ch. B. Officer: Introduction to theoretical geophysics. Berlin 1974.
- [5] W.A. Heiskanen, H. Moritz: Physical geodesy. San Francisco 1967.
- [6] W.H. Munk, G.T.F. Macdonald: The rotation of the Earth. Cambridge 1960.
- [7] P. Melchior: Physique et dynamique planétaires (vol.1). Bruxelles 1971.
- [8] G. Korn, T. Korn: Mathematical handbook for scientists and engineers. New York 1968.
- [9] J. Trešl: The effect of the irregularities of the shape of the Earth's core-mantle boundary on the observed acceleration of gravity. Studia geoph. et geod., 25 (1981), 5.
- [10] J. Trešl: The effect of the irregularities of the shape of the Earth's core-mantle boundary on pole wandering. Studia geoph. et geod., 25 (1981), 124.

On the Long-wavelength Correlation between Gravity and Topography

by

C.C. Tscherning
Geodætisk Institut
Gamlehavn Alle 22
DK-2920 Charlottenlund
Danmark

Abstract:

Spherical-harmonic expansions of the topography, the topographic-isostatic reduction potential and the gravity potential of the Earth (OSU78, OSU81, GEM10C) now exist complete to degree (N) and order 180.

A correlation analysis of the various fields by degree has been made. While the general correlation between gravity and topography for the sets OSU78 and 81 is around 50% for $N > 15$, the correlation with GEM10C is considerably lower for $N > 36$. This indicates that this set is unreliable above this degree.

The topographic-isostatic reduction potential may be computed either rigorously by integrating the topography and its compensation or by condensating the topography and its compensating masses. In the last case the spherical harmonic coefficients of the isostatic reduction potential are related in a simple linear manner to the spherical harmonic coefficients of the expansion of the topographic heights.

An optimal depth of compensation for each degree has been determined by requiring the reduced field to be as smooth as possible. Depths between 35 and 15 km were found for $N > 20$, which are much lower than the values found earlier by Rapp using another optimal depth principle.

It was found that the correlation between the primitive condensated topographic-isostatic potential coefficients showed a higher correlation with the OSU78 and 81 sets than did the rigorously computed coefficients derived at Technische Universität Graz. Since this is opposite to what should be expected, the quality of these coefficients must be in doubt.

1. Introduction

Spherical-harmonic expansions of the topography, the rock-equivalent topography, the topographic-isostatic reduction potential and the gravity potential of the Earth now exist complete to degree (N) and order 180.

The coefficients are of varying quality. But it is difficult to know how good or how bad the sets are. "Good" or "bad" also depends on for which purpose one wants to use the coefficients.

An important application is in the area of gravity field modelling, where the contribution from either the potential of the (isostatically compensated) topography or from the expansion of the gravity potential in subtracted from the observations. In both cases a considerable smoothing is expected, which if achieved should facilitate the use of various approximation or prediction techniques.

A necessary, but not sufficient, condition for a large smoothing to be achieved is the occurrence of a strong correlation between the various spherical harmonic coefficients. If the correlation is below 50% no smoothing is achieved. A small correlation also indicates inconsistencies between coefficient sets, which in principle should represent the same information. This is used as an indicated for the quality of the various sets.

Since a strong correlation may exist even in cases where two sets differ by a large scalefactor, so-called smoothing coefficients are introduced. These quantities are used to describe quantitatively the smoothing per degree achieved. Furthermore, the quantities are used to determine optimal depths of compensation, defined as the depths where the largest smoothing is achieved.

2. Correlation and smoothing

Let us regard the spherical harmonic expansions of two functions with fully normalized coefficients $(\bar{C}_{nm}, \bar{S}_{nm})$ and $(\bar{A}_{nm}, \bar{B}_{nm})$, respectively.

The correlation by degree is then

$$\rho_n = \frac{\sum_{m=0}^n (\bar{C}_{nm} \bar{A}_{nm} + \bar{S}_{nm} \bar{B}_{nm})}{(\sigma_n^2(A, B) \sigma_n^2(C, S))^{\frac{1}{2}}} \quad (1)$$

with the degree-variances

$$\sigma_n^2(C, S) = \sum_{m=0}^n (\bar{C}_{nm}^2 + \bar{S}_{nm}^2) \quad (2)$$

$$\sigma_n^2(A, B) = \sum_{m=0}^n (\bar{A}_{nm}^2 + \bar{B}_{nm}^2) \quad (3)$$

It is obvious, that the correlation may be high, even if the two sets differ by a scale factor, so the correlation is not necessarily a good measure for an agreement or disagreement between two sets. In fact, it is of more importance in physical geodesy to know which degree of smoothing we obtain, if we subtract one set from the other.

A measure for the smoothing per degree is

$$S_n = \frac{\sum_{m=0}^n ((A_{nm} - C_{nm})^2 + (B_{nm} - S_{nm})^2)}{\sigma_n^2(A, B)} \quad (4)$$

The correlation between various potential coefficient sets are shown in Table 1. Here OSU78 is described in Rapp (1978), OSU81 in Rapp (1981), GEM10C in Lerch et.al.(1981), "rock eq" in Rapp (1982) and "topiso" in Grassegger and Wotruba (1983).

We should naturally expect a very strong correlation between the coefficient sets for the spherical harmonic representation of the gravity potential, W , since the expansions have been computed using very much the same data. But this is not the case. OSU78 and 81 seems to be in agreement, but GEM10C shows little correlation with the two OSU sets for $n > 40$.

We would also expect that a good gravity potential coefficient set should show a strong correlation with the expansion of the potential of the topography. This is clearly the case for the two OSU sets, but the topography and GEM10C shows very little correlation by degree. From this one may conclude, that the intermediate wavelength ($40 < n < 120$) information in the two OSU sets is the most reliable. For the very long wavelength coefficients, we know that GEM10C is identical to GEM10B, which has given excellent results for all types of orbit computations (S. Klosko, private communication).

Furthermore, it is interesting to see that the in principle rigorously computed coefficients of the isostatic reduction potential show less correlation with the OSU78 and 81 sets, than the coefficients computed based on the attraction of a condensed topography. It may therefore be suspected that the former set of coefficients contain numerical errors. That this is possible has been admitted by our Austrian colleagues (Sünkel, 1984, private communication).

Similar phenomena, exposing less reliable coefficients, can be seen when regarding the smoothing coefficients, Fig. 1 - 9. However, the level of smoothing obtained when subtracting the potential of the isostatically compensated topography depends on the adopted depth of isostatic compensation, D .

The degree-variances obtained from the potential of a topographic expansion with coefficients \bar{A}_{nm} and \bar{B}_{nm} and its isostatic compensation are (Lambeck, 1978, p. 592)

$$\sigma_n^2(D) = \left(\frac{3\rho_c}{\bar{\rho}}\right)^2 \frac{1}{(2n+1)^2} \left[1 - \left(\frac{R-D}{R}\right)^n\right]^2 \sigma_n^2(A, B) \quad (5)$$

where ρ_c is the average crustal density, $\bar{\rho}$ the average Earth density and R the mean Earth radius. The square-root of this equation gives basically the relation between the individual coefficients.

This has been used by Rapp (1982) in order to find compensation depths, so that

$$\sigma_n^2(D) \approx \sigma_n^2(C, S),$$

(where the C_{nm}, S_{nm} set was the OSU81 set).

The result was rather large depths of 50 km. However, if we instead suppose that the optimal depth is attained where the smoothing is largest, then the results in Fig. 10 and 11 are obtained. Here more realistic depths of between 15 and 30 km are obtained for $N > 15$. In general the estimated values will be too small, due to the large noise in both coefficient sets. (The depths were found by linearising eq. (5) and solving for D in a least-squares adjustment with one unknown).

In general it is surprising to see that the smoothing coefficients are close to or larger than 1, indicating no smoothing. This is reflected in the results given in Table 2, which show the variation of the geoid undulations and gravity anomalies before and after the subtraction of the potential of the isostatically compensated, but condensed, topography.

3. Conclusion

The analysis of the correlation between various sets of potential coefficients or expansions of the potential of the topography shows unexpected low values and also large variations in the values as a function of the degree. This points at some sets as being of lesser quality than others.

The variation of the smoothness coefficients as a function of adopted depth of compensation shows that it may be useful to use varying depths of compensation for varying degree. However, the smoothing achieved by subtracting the effect of the topography (to degree and order 180) is very small for the geoid and also rather small for gravity anomalies. This is in contrast to results obtained in local areas, where a 25% smoothing generally is obtained by subtracting local topographic effects.

References

Grasegger, J. and M.Wotruba: Geoidbestimmung, Berechnung an der TU Graz, 1. Teil. In: Das Geoid in Oesterreich, pp. 117-124, Geod. Arb. Oesterreichs Int. Erdmessung, Neue Folge, Band III, 1983.

Lambeck, K.: Methods and geophysical applications of satellite geodesy. Reports on Progress in Physics, Vol. 42, pp. 547-628, 1979.

Lerch, F.J., B.Putney, S.Klosko and C.Wagner: Goddard Earth Models for Oceanographic Applications (GEM 10B and 10C). Marine Geodesy, Vol. 5, pp. 145-187, 1981.

Rapp, R.H.: A Global 1 deg. x 1 deg. Anomaly Field Combining Satellite, Geos-3 Altimeter and Terrestrial Data. Dep. of Geodetic Science Report No. 278, The Ohio State University, Columbus, Ohio, 1978.

Rapp, R.H.: The Earth's gravity field to degree and order 180 using SEASAT altimeter data, terrestrial gravity data, and other data. Reports of the Department of Geodetic Science and Surveying No. 322, The Ohio State University, Columbus, Ohio 1981.

Rapp, R.H.: Degree variances of the Earth's potential, topography and its isostatic compensation. Bulletin Geodesique, Vol. 56, No. 2, pp. 84-94, 1982.

Table 2 - page 143

Table 1. Correlations between sets of potential coefficients for varying degree, n, in %

Coeff. set n	OSU 78 OSU 81	OSU 78 GEM10C	OSU 78 topiso	OSU 81 topiso	GEM10C topiso	OSU 78 rockeq	OSU 81 rockeq	topiso rockeq
2	100	100	-44	-43	-43	-44	-43	99
4	100	100	45	46	30	47	47	99
6	100	100	34	33	32	46	45	97
8	99	98	43	42	37	36	34	96
10	97	94	65	68	68	66	68	97
12	97	92	-2	4	8	2	8	94
14	91	79	55	56	52	54	60	94
16	91	84	47	52	45	50	60	96
18	92	78	65	66	59	55	59	93
20	90	75	53	56	48	57	62	91
22	90	78	51	46	42	49	49	91
24	91	81	62	53	39	61	52	93
26	89	67	64	68	59	61	67	95
28	89	75	61	60	50	70	67	92
30	86	55	59	59	28	59	62	95
35	91	65	60	61	38	57	56	91
40	92	72	59	62	47	58	64	91
45	93	77	60	63	47	61	63	90
50	95	85	58	64	52	54	59	88
55	95	78	58	57	49	58	57	88
60	95	75	63	64	42	66	67	89
65	94	70	57	59	46	61	63	86
70	95	70	60	62	44	58	61	85
75	93	62	44	49	29	56	56	79
80	94	65	56	56	44	57	57	78
85	91	65	44	46	34	50	50	78
90	91	53	35	37	28	47	50	75
95	91	52	51	59	38	52	58	74
100	90	49	50	48	31	50	54	66
105	92	49	56	57	39	60	62	73
110	91	50	53	53	31	60	60	73
115	91	55	43	43	24	50	50	60
120	91	45	46	50	24	50	57	72
125	90	39	56	54	20	58	57	66
130	88	36	41	42	20	49	54	58
135	86	30	33	42	2	47	49	57
140	87	27	47	49	9	55	56	62
145	86	19	35	36	6	49	47	57
150	82	30	36	42	7	40	52	49
155	83	19	34	33	6	41	41	55
160	80	10	31	32	6	46	50	51
165	86	6	37	38	3	56	52	57
170	83	12	26	24	0	40	44	48
175	84	6	31	33	-3	47	52	43
176	80	5	28	30	10	39	42	52
178	80	9	43	43	1	45	48	56
179	81	5	43	45	0	48	54	56
180	82	7	32	41	8	40	48	55

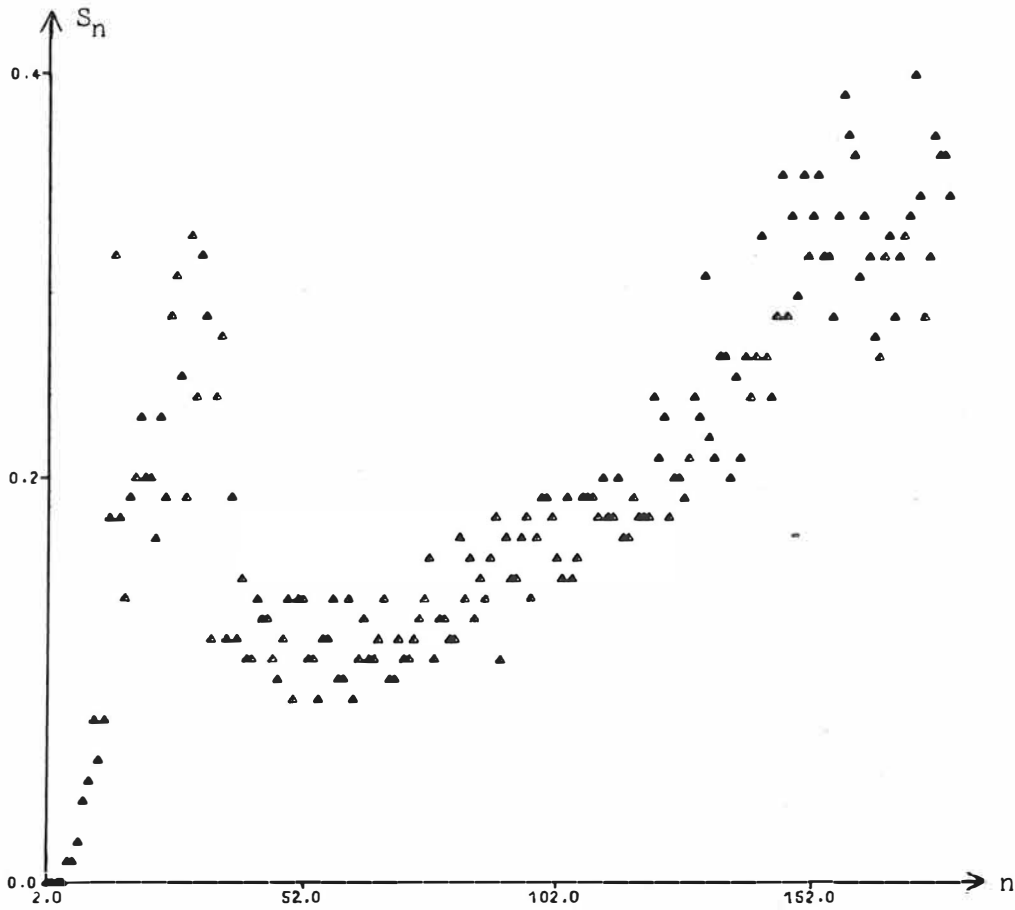


Fig 1. Smoothness coefficients S_n based on coefficients $\{A_{nm}, B_{nm}\} = \{\text{OSU 81}\}$ and $\{C_{nm}, S_{nm}\} = \{\text{OSU 78}\}$. Note the jump at degree 30

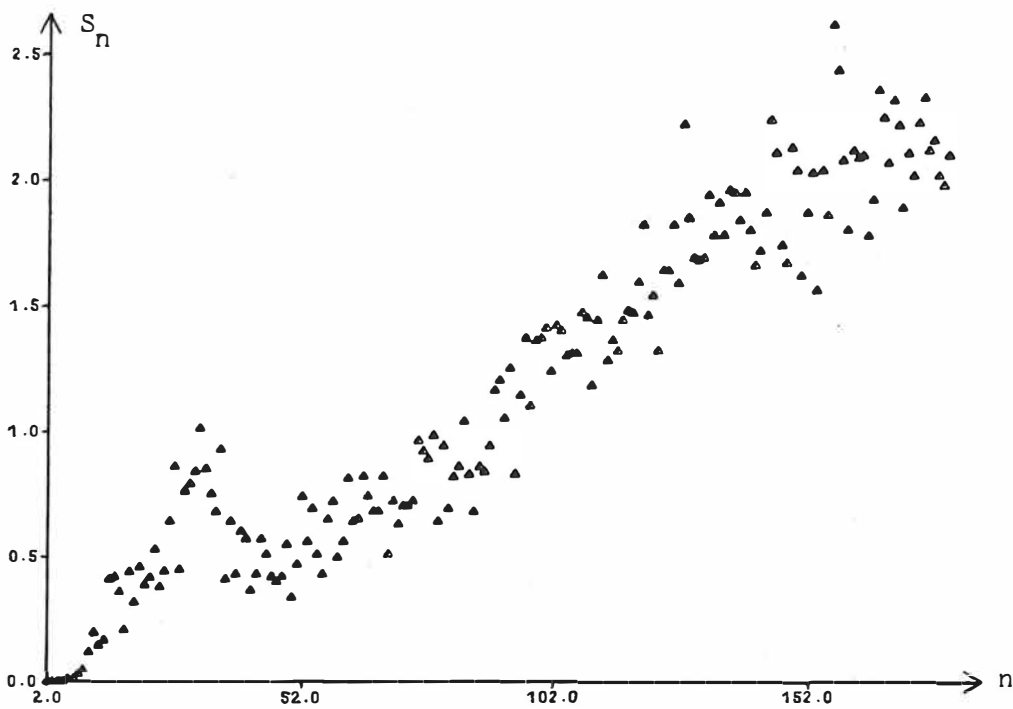


Fig. 2. Smoothness coefficients S_n based on coefficients $\{A_{nm}, B_{nm}\} = \{\text{OSU 78}\}$ set and $\{C_{nm}, S_{nm}\} = \{\text{GEM 10 C}\}$ set.

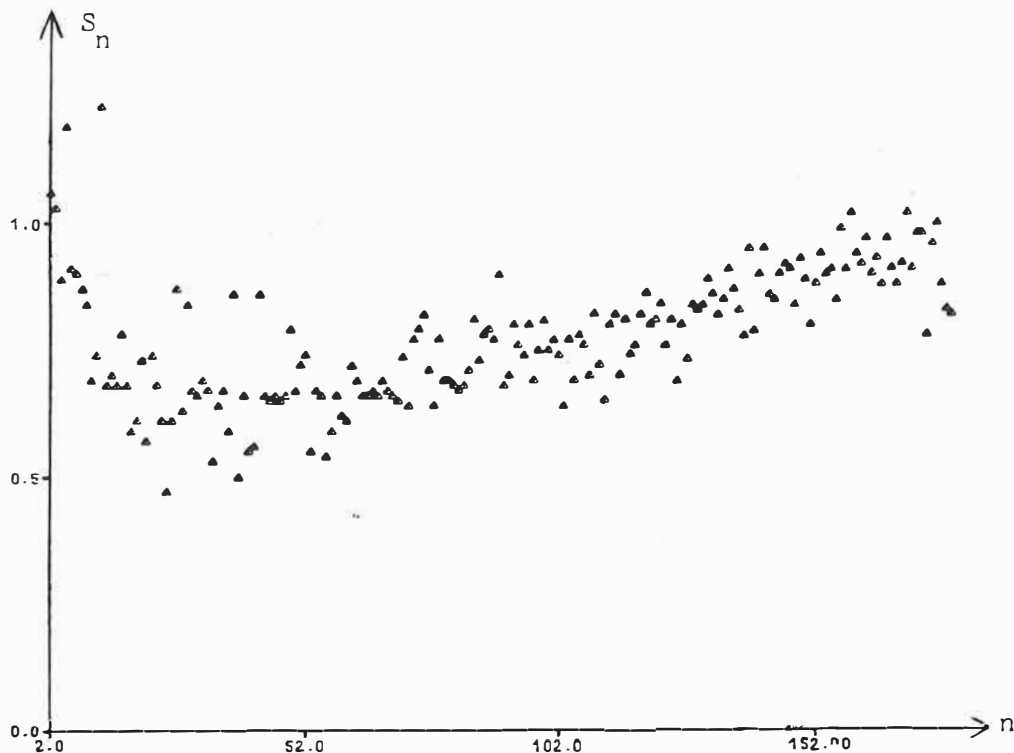


Fig 3. Smoothness coefficients S_n based on coefficients $\{A_{nm}, B_{nm}\} = \{\text{OSU 78}\}$ set and $\{C_{nm}, S_{nm}\} =$ coefficients of the topographic-isostatic reduction potential. Note the linear trend for $n > 30$.

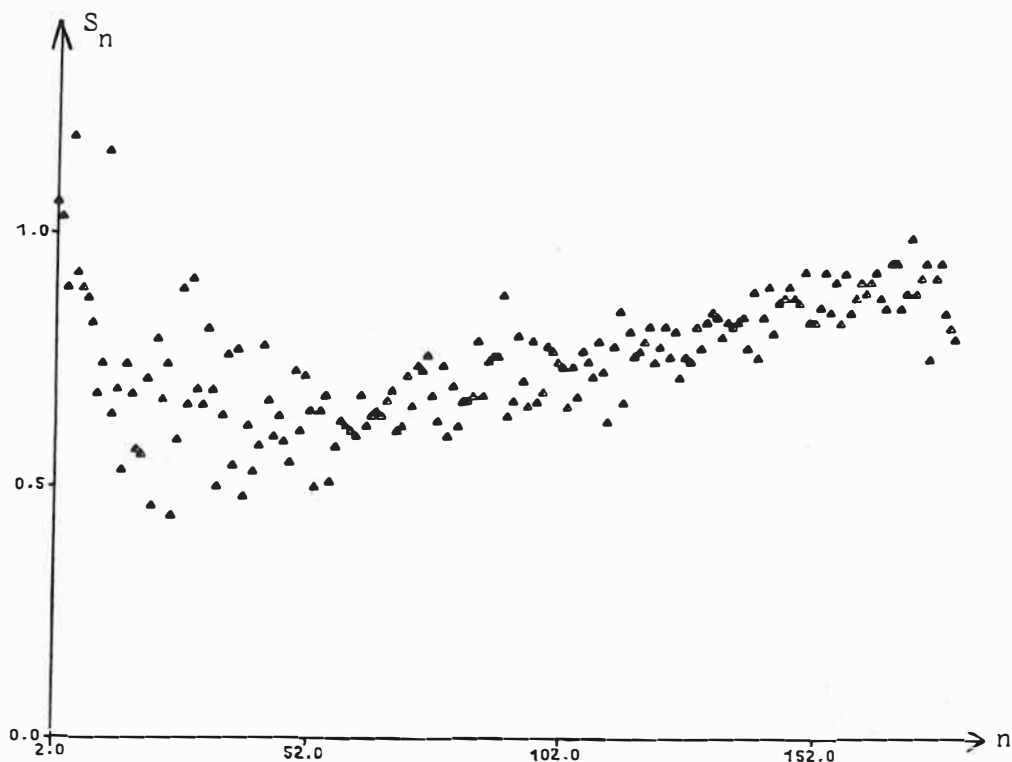


Fig. 4. Smoothness coefficients S_n based on coefficients $\{A_{nm}, B_{nm}\} = \{\text{OSU 81}\}$ set and $\{C_{nm}, S_{nm}\} =$ coefficients of the topographic-isostatic reduction potential. Note the linear trend for degree > 30 .

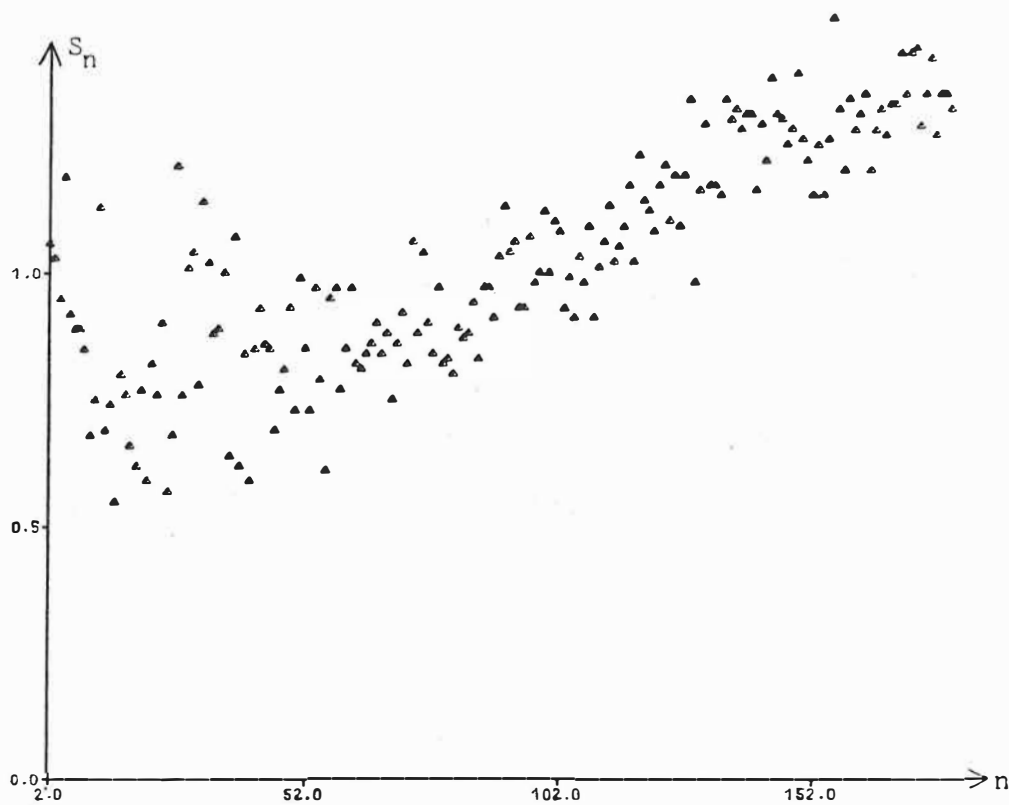


Fig. 5. Smoothness coefficients S_n based on $\{A_{nm}, B_{nm}\} = \{\text{GEM10 C}\}$ and $\{C_{nm}, S_{nm}\} =$ coefficients of the topographic-isostatic reduction potential. Note, that $S_n > 1$ for the majority of the values of n .

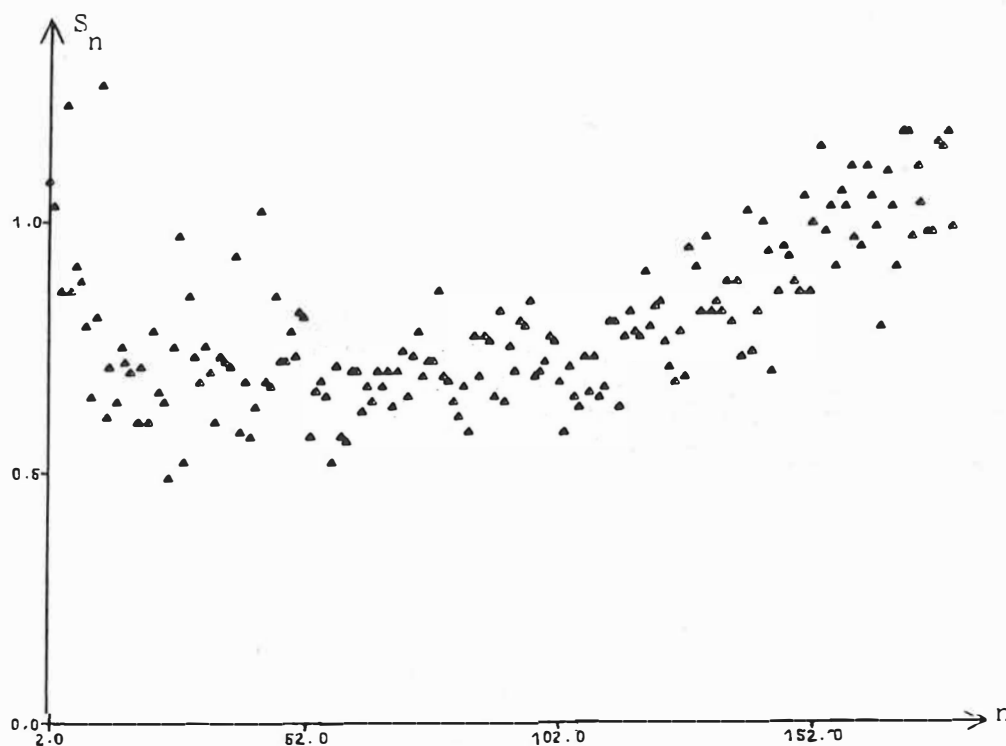


Fig. 6. Smoothness coefficients S_n based on coefficients $\{A_{nm}, B_{nm}\} = \{\text{OSU78}\}$ set and the coefficients $\{C_{nm}, S_{nm}\}$ of the potential of the condensed rock-equivalent topography, compensated at $D = 30$ km.

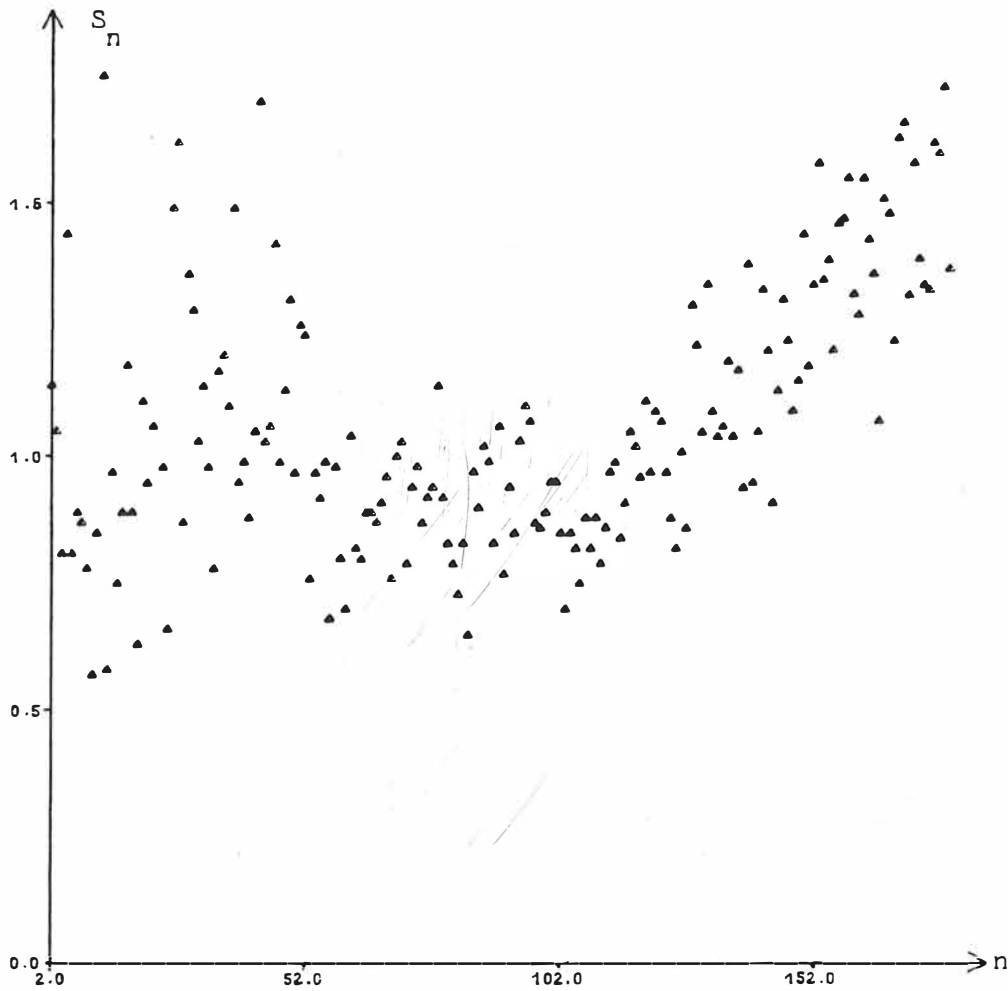


Fig. 7. Smoothness coefficients S_n based on coefficients $\{A_{nm}, B_{nm}\} = \{\text{OSU 78}\}$ set and $\{C_{nm}, S_{nm}\}$ of the potential of the condensed rock-equivalent topography, compensated at $D = 50$ km.

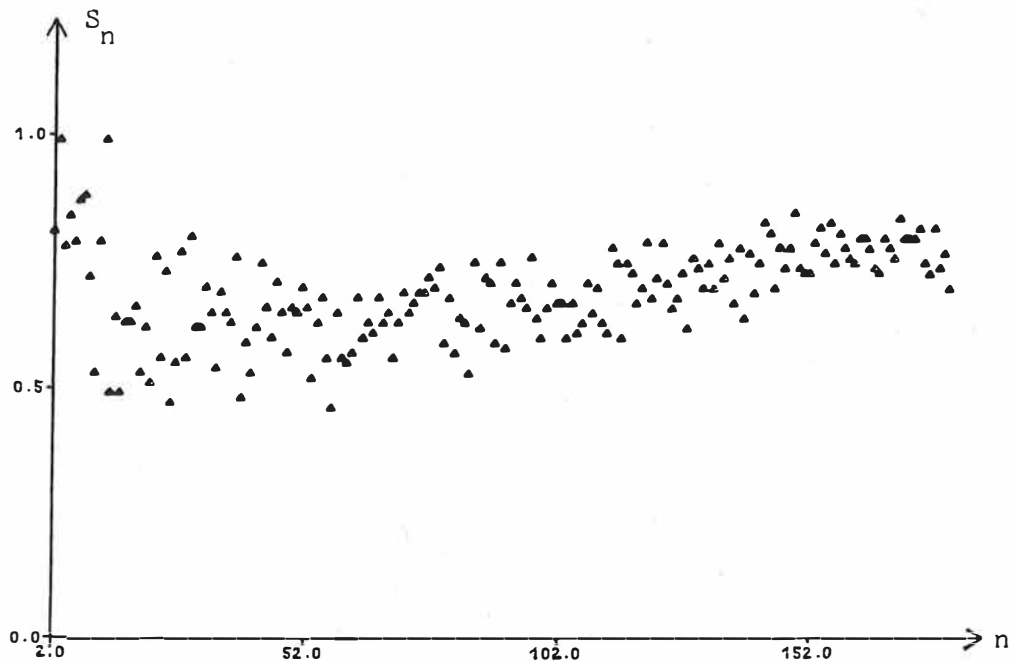


Fig. 8. Smoothness coefficients S_n based on coefficients $\{A_{nm}, B_{nm}\} = \{\text{OSU 78}\}$ and $\{C_{nm}, S_{nm}\}$ derived from rock-equivalent topography using optimized depths, cf. Fig. 10.

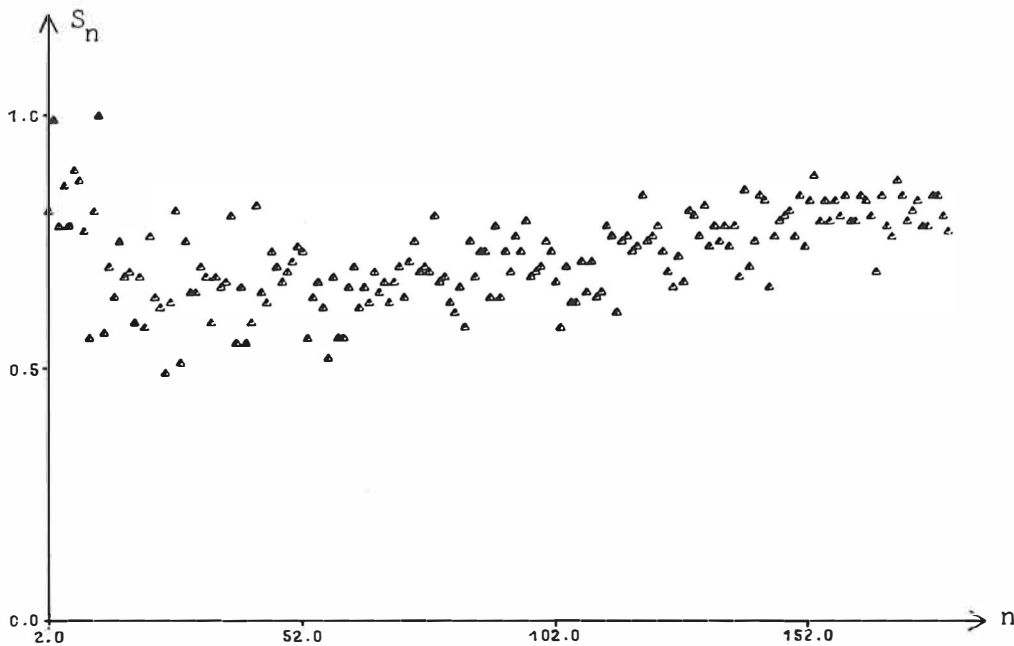


Fig. 9. Smoothness coefficients S_n based on coefficients $\{A_{nm}, B_{nm}\} = \{\text{OSU 81}\}$ set and $\{C_{nm}, S_{nm}\}$ derived from coefficients of rock-equivalent topography using optimized depths, cf. Fig. 11.

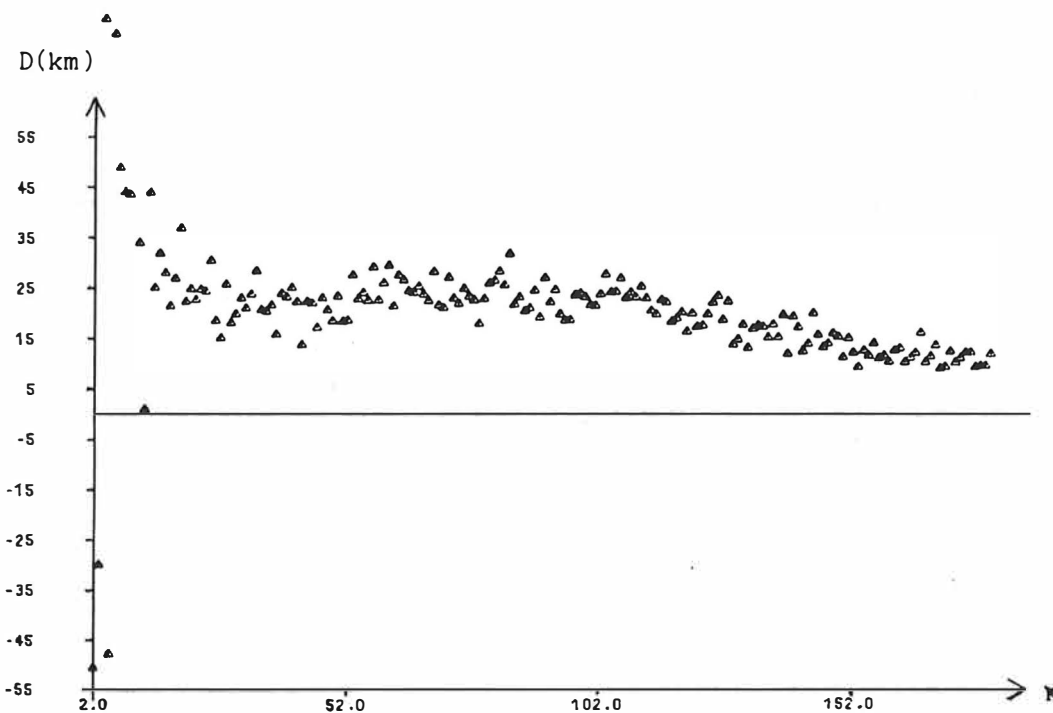


Fig. 10. Optimal depths of compensation, D , as a function of degree, computed using $\{\text{OSU 78}\}$ set and the coefficient of the rock-equivalent topography. Note, that some values are negative. However, they are very uncertain.

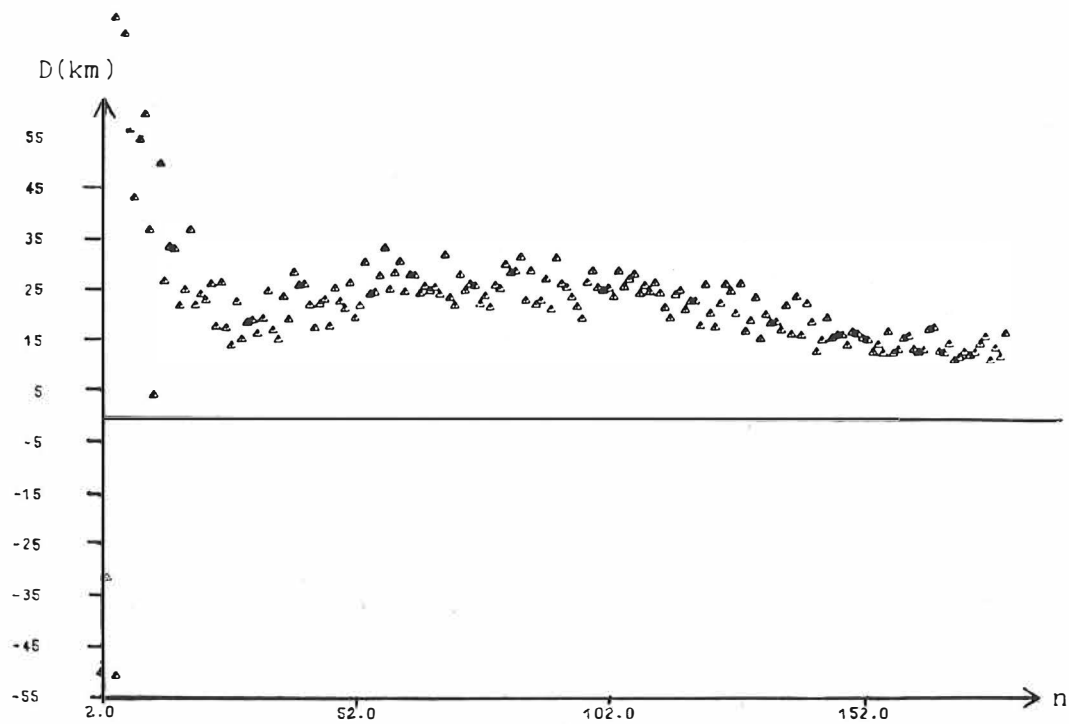


Fig. 11. Optimal depth's of compensation, D , as a function of degree, computed using {OSU 81} set and the coefficients of the rock-equivalent topography.

Table 2. Mean sq. variation of geoid heights and gravity anomalies from various sets of potential coefficients complete to degree and order 180, or computed from differences between such sets.

Coefficient set (1)	(2)	Mean square variation derived from set (2)			
		Geoid m**2	Gravity mgal**2	Geoid m**2	Gravity mgal**2
OSU1978	none			915.9	551.6
	top.-iso., D=30	15.4	125.4	933.9	441.1
	rock eq., D=20	10.5	115.4	925.2	431.8
	rock eq., D=25	16.3	167.6	930.8	434.8
	rock eq., D=30	23.2	226.8	937.7	446.7
	rock eq., D optimal	110.9	143.6	805.0	408.0
OSU1981	none			921.3	585.8
	OSU1978	915.9	551.6	3.5	82.0
	top.-iso., D=30	15.4	125.4	938.7	460.7
	rock eq., D=20	10.5	114.4	930.0	446.2
	rock eq., D optimal	113.1	166.1	808.3	419.7
GEM10C	none			920.9	467.6
	OSU1978	915.9	551.6	7.7	307.2
	top.-iso., D=30	15.4	125.4	940.0	445.7
top.iso.	rock eq., D=30			1.9	92.3

The set rock eq.. is the coefficients of the potential of the rock-equivalent topography, condensed, and with its isostatic compensation at the depth D. D optimal means that the different compensation depths have been used for different degrees, so that the best agreement with the coefficient set (1) was obtained.

Polar Motion Between 1900.0 and 1984.0 as Determined
by Different Techniques¹⁾

by

J. Vondrák²⁾

SUMMARY

Polar motion between 1900.0 and 1984.0 as determined by classical astrometry (till 1973.0) and the BIH combination of classical astrometry and modern techniques (after 1973.0) is studied with stress on periods equal to one year and longer. Carter's hypothesis on the frequency modulation of Chandler wobble is supported; non-linear relationship between frequency and amplitude can explain the observed phase shifts with rms error $\pm 16^\circ$. Westward secular drift of the mean pole ($0.00329''/y$ in the direction $78^\circ 2' W$) is confirmed, being present also in modern data. The most probable period of Markowitz wobble is found to be 27.5y but its real existence is highly improbable; it is not present after 1962.0, when more reliable data are available.

- 1) This paper is in print with the European geophysical journal *Annales Geophysicae*
- 2) Astronomical Institute of the Czechoslovak Academy of Sciences, Budečská 6, 120 23 Praha 2, Czechoslovakia

Xia Jiongyu

(Institute of Geodesy and Geophysics, Academia Sinica)

Abstract

This paper has given three formulas of the earth tidal correction in astronomical time and latitude observations. And it has also compared and calculated two of them, i.e. the formulas (2) and (3). The main conclusions are as follows:

1. The Wahr formula is more complete than the other^s in theory and is suitable for calculating the correction of each single wave.
2. The equilibrium tidal formula is fit for calculating the correction of all tidal waves. The maximum errors in the equation (2) in this article are $\pm 0^s.00002$ for time and $\pm 0".0003$ for latitude respectively, which satisfy the present requirement of $0".001$.
3. The calculation of 11 main tidal waves shows that the earth tidal correction in astronomical time and latitude observation is not the same as the ocean tidal one, in which the several main waves are only needed. It is necessary for the earth tidal correction to calculate as much as possible waves. Therefore the equilibrium tidal formula may more suitable in practice.

Reference

1. BIH Annual Report for 1971
2. Xu Houze and Mao Huiqin, Symposium of Astro-Geodynamics, 145-152, Published by Shanghai Observatory(1979)
3. Xia Jiongyu, Symposium of Astro-Geodynamics, 153-157, Published by Shanghai Observatory(1979)
4. Wahr, J. M., Geophys. J. R. Astro. Soc., 64(1981), 677-703
5. Yokoyama, K., The guide line in the reduction of observations for optical astrometry during the main campaign in project MERIT(1983)
6. Guinot, B., Astronomy and Astrophysics, Vol.8, No.1(1970), 26-28
7. Cartwright, D. E. and Anne C. Edden, Geophys. J.R. Astro. Soc., 33(1973), 253-264
8. Cartwright, D. E. and Tayler, R. J., Geophys. J.R. Astro. Soc., 23(1971), 45-74
9. Xia Jiongyu, ACTA Geodaetica et Geophysica, No. 6(1984), (in press)

On the Comparison and Choice between the Formulas of the Earth Tidal Correction in Astronomical Time and Latitude Observation

1) Introduction

With the improvement of astronomical observation and the development of theory of the earth rotation, the earth tidal effects on astronomical observation should be considered. BIH has corrected the lunar tidal effects on the classical results since 1971.^[1] In 1978, we proposed a formula for correcting astronomical time and latitude observations due to the change in the local vertical by the earth tides.^{[2][3]} Our formula has been used for reducing astronomical observations in China during MERIT main campaign. In 1981, J. Wahr also gave a formula for correcting colatitude and longitude when he investigated the earth tide for a elastic, oceanless, elliptical and rotating earth.^[4] The Wahr formula may be adopted in reducing classical astronomical observations during MERIT main campaign by IPMS.^[5] This paper has compared these formulas theoretically and choiced the one which may be the most suitable in practice.

1) The Formulas

Due to the change in vertical by earth tides there are three formulas yet used for calculating the effects of the vertical change on the observed time latitude results.

1. BIH formula

In the annual report of BIH for 1971, adopting directly the results obtained by B. Guinot, who had analysed BIH data, a group of formulas for correction to time observations due to the change in the vertical by the moon were given. Actually the following formula has been adopted since 1972 by BIH.

$$\begin{aligned} \Delta\varphi = & -0.00866\Lambda(1.0045 + 0.165\cos g_0)[(1-3\sin^2\delta_0)\sin 2\varphi - 2\cos 2\varphi \sin 2\delta_0 \cos t \\ & + \sin 2\varphi \cos^2\delta_0 \cos 2t] \\ \Delta u = & -0.00115467\Lambda(1.0045 + 0.165\cos g_0)[t\varphi \sin 2\delta_0 \sin t + \cos^2\delta_0 \sin 2t] \end{aligned} \quad (1)$$

where g , δ_0 and t are the mean anomaly, declination and hour angle of the moon respectively. $\Lambda = 1+k-1$, in which k and 1 are Love numbers, here the adopted value of $1+k-1$ is 1.20.

2. Our Formula

In 1978, we had proposed a formula based on the equilibrium tidal theory for standard spherical rigid earth.

$$\begin{aligned} d\varphi = & \Lambda_2 \left(\frac{a}{R_e}\right) \sum_{j=1,2} a_j \left(\frac{c}{r}\right)_j^3 \cos \delta_j \sin \delta_j \cos A_j + \Lambda_3 \left(\frac{a}{R_e}\right)^2 b_1 \left(\frac{c}{r}\right)_1^4 (5\cos^2 \delta_1 - 1) \sin \delta_1 \cos A_1 \\ \cos \varphi du = & \Lambda_2 \left(\frac{a}{R_e}\right) \sum_{j=1,2} c_j \left(\frac{c}{r}\right)_j^3 \cos \delta_j \sin \delta_j \sin A_j + \Lambda_3 \left(\frac{a}{R_e}\right)^2 d_1 \left(\frac{c}{r}\right)_1^4 (5\cos^2 \delta_1 - 1) \sin \delta_1 \sin A_1 \end{aligned} \quad (2)$$

where $j=1,2$ denotes the moon and the sun respectively. $a/R_e = 0.998332 + 0.001668 \cos 2\varphi$ is the ratio of the geocentric distance and the equatorial radius at geographical latitude φ . $(c/r)_j$ is the ratio of the mean distance and the instantaneous one from the tidal generating celestial body j to the earth. δ_j and A_j are the zenith distance and azimuth of the celestial body j respectively. Λ_2 and Λ_3 are the co-Love numbers

for the second degree and the third degree respectively. a_j , b_j , c_j and d_j are the constants relating to the mass of the celestial body j and earth as well as R_e and C . Here $a_1 = 0''.034768$, $a_2 = 0''.015967$, $b_1 = 0''.000288$, $c_1 = 0''^S.002318$, $c_2 = 0''^S.001064$, $d_1 = 0''^S.000019$.

3. Wahr Formula

In 1981 J. Wahr gave a formula for correcting astronomical co-latitude and longitude due to the change in vertical by earth tides.

$$\delta\theta = \frac{1}{R(\theta)} H_2^m \times 10^2 [LAT0 \partial_\theta Y_2^m + LAT1 \partial_\theta Y_{2+2}^m + LAT2 \frac{1}{\sin\theta} Y_{2+1}^m + LAT3 \frac{1}{\sin\theta} Y_{2-1}^m]$$

$$\sin\theta \delta\lambda = \frac{1}{R(\theta)} H_2^m \times 10^2 [LONG0 \frac{m}{\sin\theta} Y_2^m + LONG1 \partial_\theta Y_{2+1}^m + LONG2 \partial_\theta Y_{2-1}^m] \quad (3)$$

where θ and λ are co-latitude and eastward longitude. $Y_p^m(\theta, \lambda)$ are spherical harmonics. $R(\theta)$ is the geocentric distance of a observed point, $R(\theta) = r_0 \frac{1}{\sqrt{1 - e^2 \cos^2 \theta}}$, $r_0 = 6371 \text{ km}$ is the mean radius of the earth. $e = 0.00334$ is the earth's ellipticity. H_2^m represent the frequency-dependent tidal potential amplitudes in meters observed at the equator directly adopted from reference [7] and [8]. The scalars $LAT0$, $LAT1$, $LAT2$, $LAT3$, $LONG0$, $LONG1$, and $LONG2$ are dimensionless factors and in general are frequency dependent.

111) Comparisons

1. In Principles

Based on the equilibrium theory the formulas (1) and (2) are derived from the changes in vertical due to the earth tides. In the formula (1) the moon upto 2 degree is only considered, and the ratio of the mean distance from the moon to the earth and the instantaneous one contains only $\cos \theta$. But the formula (2) includes all the terms for the moon upto 3 degree and for the sun upto 2 degree. Although the formula (3) is also derived from the change in vertical due to the earth tides, it is based on the Wahr's model, i.e. a elastic, elliptical, oceanless and rotating earth. In his theory the tidal generating force is expressed the sum of the spherical harmonics, therefore the formula (3) can directly calculate the amplitude of the variations of co-latitude and longitude for each single tidal wave. And the dimensionless factors are in general frequency dependent.

2. In Calculating Methods

Since the formulas (1) and (2) both are based on the equilibrium tidal theory, the calculating procedure of them are also the same. Thus the comparisons between the formulas (2) and (3) have only been done below. The formula (3) originally gives the amplitude of the changes in co-latitude and longitude caused by the corresponding tidal waves. For the convenience of the comparison the time factor $e^{i\omega t}$ should be added. Moreover the formulas (2) and (3) are developed into the zonal term, diurnal term and semi-diurnal one.

i. $l=2$, $m=0$ (zonal term)

In this case the values of each dimensionless factor is not frequency-dependent, so the formula (3) for zonal term becomes

$$\delta\theta_{2,0} = \frac{10^2}{R(\theta)} (1.14441 \sin 2\theta - 0.00185 \sin 4\theta - 0.00020 \cos 2\theta) \xi H(\omega_i) \cos \omega_i t$$

$$\delta\lambda_{2,0} = 0 \quad (4)$$

Also for zonal term the formula (2) is

$$d\varphi_{2,0} = A_2 \left(\frac{a}{R_e}\right) \sum_{j=1,2} \left[a_j \left(\frac{c}{r}\right)_j^3 (3 \sin^2 \delta_j - 1) \sin 2\varphi \right]$$

$$dU_{2,0} = 0 \quad (5)$$

ii. 1=2, m=1 (diurnal term)

In the case each dimensionless factor is frequency-dependent, the formula (3) becomes

$$\delta\theta_{2,1} = \frac{10^2}{R(\theta)} \sum_i \left[H(\omega_i) (-0.77255 \text{LATO} \cos 2\theta - 0.23654 \text{LAT1} (7 \cos 4\theta + \cos 2\theta) \right. \\ \left. - \text{LAT2} (0.807955 \cos 2\theta + 0.484773) - 0.34549 \text{LAT3}) \sin \omega_i \right] \quad (6)$$

$$\delta\lambda_{2,1} = \frac{10^2}{R(\theta)} \sum_i \left[H(\omega_i) (-0.77255 \text{LONG0} - 0.34549 \text{LONG2}) \cos \omega_i \right]$$

The corresponding formula derived from (2) diurnal term is

$$d\varphi_{2,1} = A_2 \left(\frac{a}{R_e}\right) \sum_{j=1,2} \left[a_j \left(\frac{c}{r}\right)_j^3 \sin 2\delta_j \cos t_j \right] 2 \cos 2\varphi$$

$$dU_{2,1} = -A_2 \left(\frac{a}{R_e}\right) \sum_{j=1,2} \left[c_j \left(\frac{c}{r}\right)_j^3 \sin 2\delta_j \sin t_j \right] 2 \sin 2\varphi \quad (7)$$

iii. 1=2, m=2 (semi-diurnal term)

Like the zonal term each dimensionless is not frequency-dependent, the formula derived from (3) for this term is

$$\delta\theta_{2,2} = \frac{10^2}{R(\theta)} (-0.46838 \sin 2\theta + 0.00117 \sin 4\theta) \sum_i H(\omega_i) \cos \omega_i$$

$$\delta\lambda_{2,2} = \frac{10^2}{R(\theta)} 0.93942 \sum_i H(\omega_i) \sin \omega_i \quad (8)$$

The corresponding formula derived (2) is

$$d\varphi_{2,2} = -A_2 \left(\frac{a}{R_e}\right) \sum_{j=1,2} \left[a_j \left(\frac{c}{r}\right)_j^3 \cos^2 \delta_j \cos 2t_j \right] \sin 2\varphi$$

$$dU_{2,2} = -A_2 \left(\frac{a}{R_e}\right) \sum_{j=1,2} \left[c_j \left(\frac{c}{r}\right)_j^3 \cos^2 \delta_j \sin 2t_j \right] \quad (9)$$

From the formula (4) to (9) it seems that the formula originally derived from the formula (3) contain more terms than those derived from the formula (2). The additional term can be regarded as the modified term caused from Wahr model. According to Wahr's theory, LAT0 and LONG0 are corresponding to $-(1+k-1)$ for 2 degree. The others scalars are small quantities, the values of which are between -0.008 to 0.005 . Thus their effects can be neglected. The Table 1 gives the modified amplitudes of the variations of latitude and time for main tidal waves at observatories in China. The maximum modified amplitudes are $0''.00048$ for latitude and $0^s.000001$ for time respectively.

As we mentioned above, the formula (3) is suitable for calculating the corrections of single wave. And the adopted dimensionless factors are sometime varied with the frequency of the wave. In contrast with the formula (3), the formula (2) contains all term for the moon upto 3 degree and the sun upto 2 degree and adopts in general the same values of $1+k-1$ for the all tidal waves in the same degree.

3. Comparisons with Results

In reference^[4] the maximum errors of the formula (2) were estimated, which are $\pm 0''.0003$ for latitude and $\pm 0^s.00002$ for time respectively.

In order to know the differences between the calculated corrections obtained by the formulas (2) and (3), several calculations have been finished in the year of 1983 at Wuchang Time Observatory. In calculations $\lambda_2=1.2148$ and LAT0, LAT1, LAT2, LAT3, LONG0, LONG1 and LONG2 are directly taken from reference [4]. The results are compared as follows:

i. By using the formula (6), $\delta\theta_{2,1}$ and $\delta\lambda_{2,1}$, included 22 main diurnal waves, have been calculated. And $d\varphi_{2,1}$ and $du_{2,1}$ according to the formula (7) have been calculated for all tidal waves upto 2 degree. Then the maximum differences between these at the same epoch may reach $0''.0011$ for latitude and $0^s.0006$ for time respectively. It is obvious that the differences are caused by the different numbers of the waves and the different values of the dimensionless factor.

ii. The latitude and time corrections for M+S, Mf, K1, O1, P1, Q1, Mm, M2, N2, S2 and K2 have been calculated by using two kind of formulas derived from the formulas (2) and (3). The maximum differences between the calculated results for each corresponding wave are listed in Table 2. The adopted amplitudes of each wave and the differences between λ_2 and LAT0, LONG0 used for calculations are listed in Table 2 too. Table 2 shows that the maximum differences caused by K1 wave can reach $0''.00031$ for $d\varphi$ and $0^s.0000007$ for du and are almost one order larger than the theoretical modified values listed in Table 1. The main reason is the different values of the corresponding dimensionless factors adopted in the calculations. The maximum differences between the above 11 main waves by the formula (3) and the all waves by the formula (2) may reach $0''.0028$ for latitude and $0^s.00021$ for time respectively. Both the differences excess the present requirement of $0''.001$.

IV. Conclusions

1. The BIH formula, which the lunar effects are only considered, is fit for BIH because the solar effects are absorbed in local seasonal correction in BIH reducing method. Although this formula is useful in practice for BIH, it is not reasonable in conception.
2. The Wahr formula is more complete in theory and fit for calculating for single wave. It can also consider the frequency-dependent of the scalars. But it is not convenience even impossible for the large number of waves.
3. Our formula (2), the accuracy of which satisfys the present requirement of $0''.001$, is convenience for all the waves involved. Adopting Doodson's coefficients for the waves, it can also be used to calculate the tidal effects on astronomical observations for individual wave, namely the frequency-dependent of the Love numbers can be considered.
4. As mentioned above, it is important how to elect appropriately the values of Love numbers.
5. According to our point of view, the earth tidal correction for astronomical observations, is not the same as the ocean tides, should need the tidal waves as much as possible. Thus our formula may be more suitable in practice.

Table 1 Modified Amplitudes

units: 0".00001 ($\Delta d\varphi$)
0^S.000001 (Δdu)

Tidal Waves	Yunnan		Wuchang		Shanghai		Purple Mountain		Shaanxi		Tianjin		Beijing	
	$\Delta d\varphi$	Δdu												
M2	0.3	0.0	1.0	0.0	1.1	0.0	1.3	0.0	1.7	0.0	2.5	0.0	2.6	0.0
S2	0.2	0.0	0.5	0.0	0.5	0.0	0.6	0.0	0.8	0.0	1.2	0.0	1.2	0.0
N2	0.1	0.0	0.2	0.0	0.2	0.0	0.2	0.0	0.3	0.0	0.5	0.0	0.5	0.0
K2	0.0	0.0	0.1	0.0	0.1	0.0	0.2	0.0	0.2	0.0	0.3	0.0	0.3	0.0
K1	4.0	0.6	3.9	0.8	3.9	0.8	3.9	0.9	3.7	1.0	3.3	1.1	3.1	1.2
O1	2.9	0.5	2.8	0.6	2.8	0.6	2.7	0.6	2.6	0.7	2.3	0.8	2.2	0.8
P1	1.3	0.2	1.3	0.3	1.3	0.3	1.3	0.3	1.2	0.3	1.1	0.4	1.0	0.4
Q1	0.6	0.1	0.5	0.1	0.5	0.1	0.5	0.1	0.5	0.1	0.4	0.2	0.4	0.2
Mo+So	2.3	-	3.2	-	3.3	-	3.4	-	3.9	-	4.6	-	4.8	-
Mm	0.3	-	0.4	-	0.4	-	0.4	-	0.4	-	0.5	-	0.5	-
Mf	0.5	-	0.7	-	0.7	-	0.7	-	0.8	-	1.0	-	1.0	-

Table 2

Tidal Waves	H _i (m)	D _i	$\Delta d\varphi_{max}$ (0".00001)	Δdu_{max} (0 ^S .000001)	$\lambda_2 - \lambda_{ATo} $	$\lambda_2 - \lambda_{ONGo} $
M2	0.63189	0.90812	4	3	0.0022	0.0012
S2	0.29400	0.42286	1	1	0.0022	0.0012
N2	0.12099	0.17387	1	1	0.0022	0.0012
K2	0.07996	0.11506	0	1	0.0022	0.0012
K1	0.36878	-0.53050	31	7	0.0478	0.0488
O1	-0.26221	0.37689	8	3	0.0038	0.0048
P1	-0.12203	0.17554	4	2	0.0148	0.0158
Q1	-0.05020	0.07216	2	1	0.0028	0.0038
Mo+So	-0.31455	0.73869	1	-	0.0002	-
Mm	-0.03158	0.08254	0	-	0.0002	-
Mf	-0.06663	0.15642	0	-	0.0002	-

ОБ УЧЕТЕ ВЛИЯНИЯ ГОРИЗОНТАЛЬНЫХ ПЕРЕМЕЩЕНИЙ
ЛИТОСФЕРНЫХ ПЛИТ ПРИ ОБРАБОТКЕ НАБЛЮДЕНИЙ В
ГЛОБАЛЬНОЙ СЕТИ ГЕОДИНАМИЧЕСКИХ СТАНЦИЙ (НА
ПРИМЕРЕ ГЕОСС-РЕА)

Я.С.Яцкив, Н.Т.Миронов

Главная астрономическая обсерватория АН УССР

Резюме

На основе модели тектоники плит *RM2*, предложенной Минстером и Джорданом, определены кинематические параметры движений литосферных плит относительно евразийской плиты (модифицированная модель *RM2-REA*).

Выполнено сравнение теоретически предвычисленных по этой модели изменений угловых расстояний между точками земной поверхности с данными астрономических и доплеровских наблюдений. Показано, что модель *RM2-REA* не противоречит данным наблюдений и может использоваться в качестве начального приближения при уточнении модели мгновенной кинематики литосферных плит и учета горизонтальных смещений станций в сети ГЕОСС-РЕА.

Summary

Ya.S.Yatskiv, N.T.Mironov

On reducing the effect of horizontal displacements of the lithospheric plates from the observations carried out by global geodynamic network (on example the GEOSS-REA network).

On the base of plate tectonic model *RM2* by Minster and Jordan [1] the displacements of the lithospheric plates relative to the EURA-plate are calculated. This modified relative model is called *RM2-REA*. Relative changes of angular distances between the stations predicted by means of the *RM2-REA* model are compared with the observational data (BIH data and Doppler satellite data for the periods 1968-1982 and 1973-1983 respectively).

It is shown that the *RM2-REA* model does not contradict to the observations and could be used for the reduction purpose.

Построение мгновенной кинематической модели движения литосферных плит занимает центральное место в современной тектонике плит. Это обусловлено, с одной стороны, тем, что до сих пор не установлен механизм тектоники плит. С другой стороны, перемещения литосферных плит выступают в роли «помех» при обработке наблюдений в сети опорных геодинимических станций, предназначенной для установления земной системы координат, определения параметров вращения Земли и т.п.

В последние годы общее признание получили модели абсолютных и относительных перемещений плит, построенные Минстером и Джорданом / 1 /. Были предприняты многочисленные попытки проверки этих моделей по данным наблюдений, а также независимого определения кинематических параметров движения литосферных плит / 2-4 /.

Исследования кинематики плит наталкиваются на значительные трудности, обусловленные следующими обстоятельствами:

- (1) при построении существующих моделей кинематики плит преимущественно использовались геофизические сведения о движениях вблизи границ литосферных плит, где могут происходить значительные локальные деформации. В то же время станции, ведущие высокоточные астрономические и геодезические наблюдения, расположены, как правило, вдали от таких границ;
- (2) для получения более менее надежных оценок скоростей перемещений плит применяется осреднение движений за многие миллионы лет. Возникает вопрос о соответствии такого «осредненного» движения и современных мгновенных перемещений плит;
- (3) эффективные глобальные модели тектоники плит могут включать ограниченное число больших литосферных плит, относительные движения которых с некоторой точностью описывают движение

всей земной поверхности. На самом деле литосфера разбита на значительно большее число мелких плит, перемещения которых могут существенно отличаться от глобальных;

- (4) в большинстве работ для проверки моделей кинематики плит использовались данные об изменениях координат точек земной поверхности, которые зависят от стабильности принятой системы отсчета, учета векового движения полюса и других систематических эффектов. Измерения угловых расстояний между станциями наблюдений, длин хорд и базисов практически не использовались для этой цели. Чтобы преодолеть эти трудности были предложены проекты построения глобальных сетей станций с целью надежного обнаружения современных горизонтальных перемещений плит / 5,6 /.

Мы предприняли новую попытку сравнения существующей модели кинематики плит *RM2* с данными наблюдений с целью выяснения ее пригодности для учета влияния движения плит при обработке наблюдений в сети опорных геодинимических станций ГЕОСС-РЕА. Эта сеть, охватывающая Восточную Европу и Азию, включает в себя также несколько станций, расположенных на Северо-Американской и других плитах. Наблюдения этих и дополнительных станций, будучи приведенными в единую систему с евразийскими станциями, должны обеспечивать лучшую обусловленность систем уравнений и разделение неизвестных (параметры вращения Земли, элементы орбиты и др.).

2. МОДИФИКАЦИЯ КИНЕМАТИЧЕСКОЙ МОДЕЛИ *RM2*

Модель относительного движения литосферных плит *RM2*, построенная Минстером и Джорданом на основе тщательно отобранного наблюдательного материала, позволяет элементарным путем рассчитывать линейную скорость относительного движения для произвольной

точки рассматриваемых плит. Так как нас интересуют перемещения плит относительно Евразии, то на основе RM2 нами была построена модифицированная кинематическая модель RM2-REA (см. табл. I). При этом Евразийская плита считалась неподвижной, а относительное перемещение остальных плит по сферической Земле описывалось тремя параметрами - координаты полюса вращения плит ($\Phi_k \wedge_k$) и ее угловая скорость Ω_k .

В таблице I и последующих таблицах приняты сокращенные английские обозначения основных литосферных плит: Евразийская (EURA), Тихоокеанская (PFC), Северо-Американская (NOAM), Южно-Американская (SOAM), Африканская (AFRC), Индийская (INDI), Антарктическая (ANTA), Кокос (COCO), Наска (NAZC), Карибская (CARB) и Аравийская (ARAB).

Таблица I

Модифицированная модель RM2 (RM2-REA)

Единицы: Φ, \wedge, β_Φ и β_\wedge в градусах
 Ω и β_Ω в $1 \cdot 10^6$ град/год

	Φ_k	β_Φ	\wedge_k	β_\wedge	Ω_k	β_Ω
I	2	3	4	5	6	7
AFRC	25.17	5.69	338.80	1.71	0.104	0.013
ANTA	16.27	10.71	109.03	3.41	0.070	0.003
ARAB	29.82	5.00	358.33	9.48	0.357	0.037
CARB	-40.98	28.24	88.33	19.25	0.136	0.044
COCO	21.83	1.56	242.66	2.05	1.424	0.050
INDI	19.71	0.56	38.45	1.58	0.698	0.015
NAZC	48.75	6.60	260.84	3.53	0.577	0.037
NOAM	-65.84	13.55	312.48	1.31	0.231	0.016

I	2	3	4	5	6	7
	-60.64	3.57	101.07	1.30	0.977	0.022
	-78.47	16.51	115.78	18.69	0.288	0.012

Примечание: Принято, что плиты вращаются относительно EURA против часовой стрелки.

3. ЗАВИСИМОСТЬ МЕЖДУ НАБЛЮДАЕМЫМИ ВЕЛИЧИНАМИ И КИНЕМАТИЧЕСКИМИ ПАРАМЕТРАМИ ПЛИТ

действительными или фиктивными наблюдаемыми величинами, характеризующими изменения положений точек земной поверхности, являются изменения географических или прямоугольных геоцентрических координат станций наблюдений, угловых расстояний между станциями, длин хорд и базисов, соединяющих рассматриваемые станции наблюдений. Пусть Φ_{ki}, \wedge_{ki} - географические координаты i -ой станции, расположенной на k -ой плите; $\Phi_k, \wedge_k, \Omega_k$ - кинематические параметры плиты. В / 2,5/ приведены формулы, связывающие изменения координат i -ой точки за единицу времени Δt (для удобства примем $\Delta t = 1$); с кинематическими параметрами k -ой плиты:

$$\Delta \Phi_{ki} = - \Omega_k \cos \Phi_k \sin (\wedge_k - \wedge_{ki})$$

$$\Delta \wedge_{ki} = \Omega_k \sin \Phi_k - \Omega_k \cos \Phi_k \cos (\wedge_k - \wedge_{ki}) \operatorname{tg} \Phi_{ki}$$

Аналогичные формулы могут быть записаны и для изменений прямоугольных координат $\Delta X_{ki}, \Delta Y_{ki}$ и ΔZ_{ki} . Принимая во внимание, что вектор вращения k -ой плиты относительно e -ой плиты равен $\vec{\Omega}_{k,e} = \vec{\Omega}_k - \vec{\Omega}_e$, легко находим соотношения для изменений угловых расстояний ΔS_{ij} между станциями наблюдений.

$$\Delta S_{ij} = \frac{R_{k,e}}{\sin S_{ij}} \left[\sin \Phi_{k,e} \cos \varphi_i \cos \varphi_j \sin (\lambda_i - \lambda_j) - \right. \quad (2)$$

$$\left. - \cos \Phi_{k,e} \sin \varphi_i \cos \varphi_j \sin (\lambda_{k,e} - \lambda_j) + \right.$$

$$\left. + \cos \Phi_{k,e} \cos \varphi_i \sin \varphi_j \sin (\lambda_{k,e} - \lambda_i) \right]$$

где $\sin S_{ij} = \sin \{ \arccos [\sin \varphi_i \sin \varphi_j + \cos \varphi_i \cos \varphi_j \cos (\lambda_i - \lambda_j)] \}$
 $0 < S_{ij} < 180^\circ$.

Изменения ΔS_{ij} можно также выразить через изменения географических или прямоугольных геоцентрических координат рассматриваемых точек Земли. Зависимость изменения длин хорд, соединяющих i -ую и j -ую станции, от кинематических параметров относительного движения двух плит имеет вид:

$$\Delta d_{ij} = (x_i z_j - z_i x_j) R_{k,e} \cos \Phi_{k,e} \sin \lambda_{k,e} + \quad (3)$$

$$+ (x_j y_i - x_i y_j) R_{k,e} \sin \Phi_{k,e} +$$

$$+ (z_i y_j - y_i z_j) R_{k,e} \cos \Phi_{k,e} \cos \lambda_{k,e}$$

По данным табл.1 и формулам (1-3) легко получить теоретически предвычисленные изменения координат станций, угловых расстояний между станциями и хорд.

Сравнивая наблюдение значения $\Delta \varphi^\circ$, $\Delta \lambda^\circ$, ΔS° и Δd° с теоретически предвычисленными на основании кинематической модели тектоники плит, можно судить о пригодности модели для описания современных движений плит и, в принципе, уточнить кинематические параметры плит.

4. ХАРАКТЕРИСТИКА НАБЛЮДАТЕЛЬНЫХ ДАННЫХ ОБ ИЗМЕНЕНИИ ПОЛОЖЕНИЙ ТОЧЕК ЗЕМЛИ

В качестве исходного наблюдательного материала нами взяты изменения астрономических координат станций, участвовавших в работе МБВ в 1968-1982 гг., а также вычисленные по доплеровским наб-

людениям ИСЗ движения станций за 1973-1983 гг. / / . Что касается астрономических данных, то мы использовали т.н. коэффициенты a , принятые МБВ для характеристики отклонений координат станций от системы МБВ 1968 года. Применяя регрессионный анализ этих коэффициентов, нами были найдены изменения координат станций МБВ за один год. Так как на Евразийской плите находится большое количество станций наблюдений, были найдены осредненные по блокам (размером $30^\circ \times 30^\circ$) изменения координат $\Delta \lambda^\circ$ и $\Delta \varphi^\circ$. Все станции были распределены по плитам в соответствии с общепринятыми границами плит^{*}). В табл.2 и 3 приведены сведения о массивах астрономических и доплеровских данных, где $\langle \delta \rangle$ - среднее значение среднеквадратической ошибки определения скорости перемещения станции по каждой координате, выраженное в единицах $1 \cdot 10^6$ градусов/год.

Таблица 2. Распределение массива астрономических данных по плитам

Название плиты	Количество станций (или блоков)	$\langle \delta \rangle_{\Delta \varphi}$	$\langle \delta \rangle_{\Delta \lambda}$
ЕУРА	5	± 0.13	± 0.60
НОАМ	4	0.50	0.60
СОАМ	4	0.34	2.00

Как видно из табл.2 и 3, точность определения скоростей движений станций по доплеровским наблюдениям примерно в три раза выше по сравнению с астрономическими определениями этих движений.

* В первом варианте японские станции были отнесены к Евразийской плите, а во втором - исключены из рассмотрения.

Таблица 3. Распределение массива доплеровских данных по плитам

Название плиты	Количество станций (или блоков)	$\langle \delta \rangle_{\Delta\varphi}$	$\langle \delta \rangle_{\Delta L}$
EUR A	4	0.15	0.19
NOAM	8	0.23	0.32
INDI	3	0.12	0.15
PCFC	3	0.10	0.16

Примечание: В отличие от работы / 4 / в Индийскую плиту были включены станции, расположенные на Филиппинах и в Австралии.

5. СРАВНЕНИЕ НАБЛЮДЕННЫХ И ТЕОРЕТИЧЕСКИ ПРЕДВЫЧИСЛЕННЫХ ПО МОДЕЛИ ТЕКТониКИ ПЛИТ ИЗМЕНЕНИЙ УГЛОВЫХ РАССТОЯНИЙ МЕЖДУ СТАНЦИЯМИ

В настоящей работе мы рассматриваем скорости изменений угловых расстояний между станциями, которые в отличие от изменений координат не зависят от выбора системы координат и ее стабильности.

В табл.4 и 5 приведены средние значения квадратов изменений угловых расстояний между станциями до и после учета кинематики плит (ΔS_{ij}^o - наблюдаемые величины, ΔS_{ij}^c - теоретически предвычисленные), найденные по астрономическим и доплеровским наблюдениям соответственно.

Таблица 4. Средние значения квадратов величин ΔS_{ij}^o , и $(\Delta S_{ij}^o - \Delta S_{ij}^c)$

Название плиты	$\langle (\Delta S_{ij}^o)^2 \rangle$	$\langle (\Delta S_{ij}^o - \Delta S_{ij}^c)^2 \rangle$
NOAM	0.632	0.606
SOAM	3.086	2.982

Таблица 5. Средние значения квадратов величин ΔS_{ij}^o и $(\Delta S_{ij}^o - \Delta S_{ij}^c)$

Название плиты	$\langle (\Delta S_{ij}^o)^2 \rangle$	$\langle (\Delta S_{ij}^o - \Delta S_{ij}^c)^2 \rangle$
NOAM	0.149 (0.082)	0.155 (0.076)
INDI	1.206 (0.863)	0.607 (0.502)
PCFC	0.300 (0.097)	0.266 (0.332)

Примечание: В скобках указаны значения, полученные по второму варианту (станция в Мидзусава исключена).

Как видно из табл.4 и 5, учет влияния перемещенной плит (модель RM2) в большинстве случаев уменьшает значение среднего квадрата угловых расстояний между станциями, т.е. модель кинематики плит в среднем не противоречит результатам современных наблюдений за движениями станций.

Нами предпринята попытка уточнения по указанным выше наблюдательным данным кинематические параметры движения плит относительно Евразии (см. табл.6).

Таблица 6. Поправки к принятым значениям кинематических параметров (модель *RM2*) и их ошибки.

Название плиты	Наблюдения	$d\varphi$	$\delta(d\varphi)$	$d\lambda$	$\delta(d\lambda)$	$d\Omega$	$\delta(d\Omega)$
NOAM	ASTR	-50	±145	+131	±208	-0.232	±0.434
NOAM	DOP	0	38	59	76	-0.435	0.129
SOAM	ASTR	86	100	-74	153	0.415	1.167
INDI	DOP	-22	36	-104	64	0.586	0.491
PCFC	DOP	-20	10	54	43	0.337	0.296

Единицы: поправки координат полюса вращения в градусах,
поправка угловой скорости вращения в $1 \cdot 10^6$ град/год.

Из полученных нами результатов можно сделать следующие выводы:

1. Модель кинематики плит *RM2* в принципе может служить в качестве исходного стандарта при обработке наблюдений в сети ГЕОСС-РЕА и уточнении кинематических параметров.
2. Астрономические определения скоростей движений станций уступают по точности современным доплеровским определениям. Их привлечение для уточнения параметров тектоники плит вряд ли целесообразно.
3. Для уверенного определения кинематических параметров движения плит необходимо существенно повысить точность определения скоростей движения станций наблюдений, их угловых расстояний и хорд (примерно на порядок по сравнению с имеющимися данными).

ЛИТЕРАТУРА

1. Minster J.B., Jordan T.H., Present-day Plate Motions, JGR, vol.83, N B11, 1978.
2. Arur M.G. and Mueller I.I. Latitude Observations and the Detection of Continental Drift. Journ.of Geophys.Res., vol.76,N 8, p.2071-2176, 1971.
3. Drewes H. A Geodetic Approach for the Recovery of Global Kinematic Plate Parameters, Bull.Geod., 56, 1982, p.70-79.
4. Anderle R.J. and Malyevac C.A. Plate Motions Computed from Doppler Satellite Observations presented at Symposium 2 of the XVIII General Assembly of IUGG, Hamburg, 1983.
5. Drewes H. Design of a Global Geodetic Network for Geodynamics, Proc.of the International Symposium on Geodetic Networks and Computations, Munich, 1981. Veröffentlichungen der Deutschen Geodätischen Kommission.Reihe B, Heft N 258/11, 1982
6. Geodetic Monitoring of Tectonic Deformation toward a Strategy. Panel on Crustal Movement Measurements. Washington,D.C.1981.

ГЛАВНОЕ УПРАВЛЕНИЕ ГЕОДЕЗИИ И КАРТОГРАФИИ ПРИ
СОВЕТЕ МИНИСТРОВ СССР
ЦЕНТРАЛЬНЫЙ ОРДЕНА "ЗНАК ПОЧЕТА" НАУЧНО-ИССЛЕДОВАТЕЛЬСКИЙ
ИНСТИТУТ ГЕОДЕЗИИ, АЭРОСЪЕМКИ И КАРТОГРАФИИ
им. Ф.Н. КРАСОВСКОГО

О ПРИЛИВНЫХ ПОПРАВКАХ В ГЕОДЕЗИИ

М.И. Юркина

ПРЕДСТАВЛЕНО 5-му МЕЖДУНАРОДНОМУ СИМПОЗИУМУ
"ГЕОДЕЗИЯ И ФИЗИКА ЗЕМЛИ"

Литература

Groten E. 1981. Reply to M. Ekman's "On the definition of gravity, remarks on "A remark on M. Heikkinen's paper "On the Honkasalo term in tidal corrections to gravimetric observations". Bulletin géodésique, 55, N 2, 169.

Honkasalo T. 1964. On the tidal gravity correction. Bollettino di geofisica teorica ed applicata, 6, N 21, 34-36, Marzo.

Zeman Antonin. 1981. Problem Honkasalovy opravy v teorii vysek. Sbornik referátu z celostátního semináře, konaného ve dnech 20-24.10.1980 ve Zvíkovském Podhradí, díl I Geofyzikální ústav CSAV. Praha. Geofyzika n.p. Brno. Brno, 81-83.

Резюме: Во всех точных геодезических измерениях при заметных приливных влияниях необходимо приведение к одному моменту времени или постоянному влиянию прилива. Обсуждение вопроса об исключении этого постоянного во времени приливного влияния необходимо начинать с анализа основных зависимостей теории Молоденского. Если приливный эффект будет исключен из аномалий силы тяжести и восстановлен в связи высоты квазигеоида и возмущающего потенциала, этот эффект не следует исключать из результатов геометрического нивелирования. Вопрос о начале счета высот не связан с вопросом о фигуре среднего уровня моря.

Во влияниях Луны и Солнца на Землю и ее гравитационное поле можно выделить члены, которые зависят от широты места и не зависят от времени. Их называют постоянными. Можно считать, что фигура твердой Земли, а не только уровень моря сформировались под влиянием этих членов.

Международная геодезическая ассоциация на заседаниях в Канберре в 1979 г. приняла решение о полном исключении приливных влияний из всех геодезических измерений.

Это решение соответствует требованиям теории фигуры Земли, согласно которой аномалии силы тяжести должны отражать только аномальные массы внутри Земли. Тогда задачу об определении аномальной части земного гравитационного поля по аномалиям силы тяжести можно ставить как краевую.

Возмущающий потенциал T можно определить так

$$T = W - P - U, \quad (I)$$

где W - потенциал силы тяжести g Земли, включающий постоянные члены P влияний Луны и Солнца, U - потенциал силы тяжести нормального (отсчетного) эллипсоида. Потенциал T будет отражать только влияние аномальных масс внутри земной поверхности, вне этой поверхности потенциал T будет гармонической функцией: удовлетворяет уравнению, называемому именем Лапласа, и на бесконечности регулярен (стремится к нулю). Найдем теперь связь возмущающего потенциала T и высоты квазигеоида при учете приливных влияний.

Можно представить

$$W = W_0 - \int g dh, \quad (2)$$

где W_0 - потенциал силы тяжести в исходном пункте счета высот,

dh - элементарное нивелирное превышение; криволинейный интеграл должен быть вычислен от упомянутого исходного пункта до исследуемой точки. Величины W_0 , g и dh содержат в себе постоянные влияния Луны и Солнца. Согласно теории Молоденского полагаем

$$-\int g dh = U(B, H_Q) - U_0, \quad (3)$$

$$U = U(B, H_Q) + \frac{\partial U}{\partial H} \zeta, \quad (4)$$

где B - геодезическая широта. Поскольку высота H над нормальным эллипсоидом не известна, потенциал U разложен в ряд Тейлора, первый член справа в последней зависимости определен решением предыдущего уравнения, определяющего нормальную высоту H_Q исследуемой точки. Способы решения этого уравнения хорошо отработаны. Присутствие в величинах g и dh приливных влияний не препятствует решению, ζ обозначает дополнение нормальной высоты H_Q до полной высоты исследуемой точки над нормальным эллипсоидом. Если величину ζ отложить по нормалью к этому эллипсоиду от его поверхности, концы отрезков ζ образуют поверхность, называемую Молоденским квазигеоидом.

Заметив

$$\frac{\partial U}{\partial H} = -\gamma \quad (5)$$

и подставив зависимости (3) - (5) в исходное выражение потенциала T , можно найти

$$\zeta = \frac{T}{\gamma} - \frac{W_0 - U_0}{\gamma} + \frac{P}{\gamma}. \quad (6)$$

Краевое условие можно получить, продифференцировав

исходное выражение (1) по высоте

$$\frac{\partial T}{\partial H} = \frac{\partial W}{\partial H} - \frac{\partial P}{\partial H} - \frac{\partial U}{\partial H}. \quad (7)$$

Здесь

$$\frac{\partial W}{\partial H} = -g, \quad (8)$$

величина $\frac{\partial U}{\partial H}$ с необходимой здесь точностью не известна и опять может быть выражена с помощью ряда Тейлора

$$\frac{\partial U}{\partial H} = \left(\frac{\partial U}{\partial H} \right)_{H_Q} + \frac{\partial^2 U}{\partial H^2} \zeta = -\gamma_{H_Q} - \frac{\partial \gamma}{\partial H} \zeta. \quad (9)$$

Исключив высоту ζ квазигеоида с помощью полученного выше выражения, получаем краевое условие

$$\frac{\partial T}{\partial H} - \frac{T}{\gamma} \frac{\partial \gamma}{\partial H} = -g + \gamma_{H_Q} - \frac{W_0 - U_0}{\gamma} \frac{\partial \gamma}{\partial H} + \frac{P}{\gamma} \frac{\partial \gamma}{\partial H} - \frac{\partial P}{\partial H}, \quad (10)$$

где

$$\frac{\partial P}{\partial H} = -\Delta\gamma = +0,031(1 - 3 \sin^2 B) \text{ мгал.}$$

Коэффициент этой формулы приведен без учета упругих деформаций твердой Земли, т.е. результат Honkasaalo 1964 поделен на использованный им множитель 1,2 за упругость твердой Земли. По поводу этого множителя см. Grotef 1981, где указана литература по обсуждаемой теме, и ниже. Таким образом, при выделении из потенциала силы тяжести Земли приливного влияния, возникает косвенный эффект - предпоследний член справа в (10).

Член, содержащий разность $W_0 - U_0$, можно определить по астрономо-геодезическим и спутниковым данным, все остальные члены справа можно получить из измерений и вычислений. Представив потенциал T распределением простого слоя на земной поверхности, что возможно, поскольку этот потенциал создан распределением аномальных масс внутри Земли, можно получить интегральное уравнение теории Молоденского. Решение этого уравнения определяет T . Вычислив по формуле (6) высоту ζ квази-

геоида, можно найти полную высоту H над нормальным эллипсоидом.

В измеряемые элементы поля необходимо вводить поправки за разность действительного полного влияния Луны и Солнца и соответственных постоянных членов. Именно такую приливную поправку рекомендовал вводить в измеряемые величины силы тяжести $H_{\text{поправка}}$ и в нивелирование, следуя $H_{\text{поправка}}$, $Zelman$ 1981. Такие приливные поправки позволяют привести все измерения к одинаковому расположению внешних возмущающих масс и как бы к одному моменту времени. В этом случае в реальном потенциале силы тяжести Земли сохраняется постоянный член влияния Луны и Солнца, результаты нивелирования можно будет непосредственно сравнивать со средними уровнями морей, но в аномалиях силы тяжести этот постоянный член будет исключен и такие аномалии можно использовать в известных формулах теории фигуры Земли. Добавив к вычисленной по этим формулам аномальной составляющей некоторого элемента поля соответственное влияние нормального эллипсоида, постоянный член влияния Луны и Солнца, а при желании их полное влияние в определенный момент времени, можно получить нужный элемент реального гравитационного поля Земли. Следует заметить, что зависящая от времени часть влияний Луны и Солнца на геометрическое нивелирование весьма мала сравнительно с современной точностью, носит случайный характер и потому, как правило, пренебрегаема. Такой подход к учету влияний Луны и Солнца на гравитационное поле Земли вполне аналогичен принятому способу исключения влияния центробежной силы из аномалий силы тяжести. Влияние центробежной силы, как известно, сохраняется в реальном потенциале силы тяжести Земли, и, соответственно, в нормальных высотах.

Задачу теории фигуры Земли можно решить при ином подходе к учету приливных влияний. А именно, в соответствии с решением Международной геодезической ассоциации можно исключить приливный эффект из всех геодезических измерений, решить краевую задачу, выразить нужный элемент гравитационного поля и в нем восстановить приливное влияние. Полная высота некоторой

точки земной поверхности над отсчетным эллипсоидом является элементом чисто геометрическим и от гравитационного поля не зависит. При обоих подходах к учету приливных влияний эта величина должна получиться одинаковой. Так и будет, если последний член формулы (6) и соответственное влияние в величине W_0 будут исключены из связи высоты квазигеоида и возмущающего потенциала и отнесены к зависимости (3). Но в этом случае реальный уровень моря окажется заведомо неуровенной поверхностью и нельзя будет результаты геометрического нивелирования непосредственно использовать для изучения уровней морей. Ниже будет показано, что влияние постоянного приливного эффекта на результаты нивелирования заметно и не считаться с ним нельзя. Состояние теории уровня моря не позволяет вычислять с достаточной точностью соответственные поправки в этот уровень.

Для оценки постоянного влияния Луны и Солнца на результаты нивелирования можно воспользоваться расчетом $Zelman$ 1981. Однако представляется неправильным использовать при таком расчете содержащий числа Лява множитель за упругие деформации твердой Земли, поскольку введение этого множителя предполагает кратковременность действия возмущающей силы. Эти упругие деформации $Zelman$ 1981 оценил в + 5,7 см на экваторе и - 11,4 см на полюсах. Сравнительно с точностью гравиметрических измерений, необходимой для решения задач теории фигуры Земли, соответственные погрешности малы. Однако они могут составить несколько сотых миллигала, т.е. быть заметными при современной точности гравиметрических измерений. Более правильным представляется считать Землю твердой при расчете рассматриваемого постоянного влияния и вводить поправку только за соответственное смещение уровней поверхностей. Без учета коэффициента за упругие деформации Земли, из формул $Zelman$ следует

$$\Delta H = 0,27 (\gamma_i n^2 B - \gamma_i n^2 B_0) \text{ м.}$$

Величина $\gamma \Delta H$ определяет разность потенциалов P в иссле-

дуемой точке и исходном пункте нивелировок. Если отсчетную точку поместить на полюсе, то на экваторе $\Delta H = 0,3$ м, что в общем согласуется с оценкой *Нонкаса́ло*. Расхождение со средним уровнем моря получается значительным. Как указал *Земан 1981*, таким образом, например, может быть искусственно создана разность уровней Балтийского и Адриатического моря величиной около 7,2 см, что превышает ошибки нивелирования на таком расстоянии.

При установлении знака поправки следует иметь в виду, что удаление постоянных влияний Луны и Солнца снимает дополнительное экваториальное вздутие уровенных поверхностей на Земле и увеличивает разность высот в точках, одна из которых расположена под экватором, а другая – в средней полосе.

Вопрос об изучении относительных уровней морей с помощью нивелирования не следует смешивать с вопросом о среднем уровне моря как отсчетной поверхности. Такой отсчетной поверхностью геодезисты не пользуются, несмотря на утверждения учебников геодезии и в частности *Нонкаса́ло*, выбирая за отсчетную согласно определению Брунса ту уровенную поверхность, которая проходит через исходный нуль счета высот.

Нонкаса́ло получил свой результат осреднением за 18,6 года – оборот узла лунной орбиты. Для сравнения результатов гравиметрических измерений – приведения их к одному моменту времени вполне достаточно поправка *Нонкаса́ло*, тем более, что при вычислении смешанной аномалии силы тяжести необходимо дополнительное вычисление косвенного эффекта.

При изучении движения искусственных спутников Земли, влияние Луны и Солнца должно быть принято во внимание непосредственно. Коэффициенты разложения геопотенциала по сферическим функциям или другие данные о гравитационном поле Земли должны соответствовать только реальной Земле, т.е. в этом случае нужен потенциал $U + T = W - P$. При согласовании спутниковых и наземных данных нужно принять во внимание потенциал P .

ANELASTICITY IN THE EARTH'S MANTLE:
 IMPLICATIONS FOR THE FREQUENCY
 DEPENDENCE OF LOVE NUMBERS

J. Zschau
 Institute of Geophysics, Christian Albrechts
 University, Kiel, West Germany

Analytical formulas are developed which describe the anelastic and viscous behaviour of solids by means of an absorption band as deduced from a Gaussian distribution of relaxation times. These formulas are applied to the Earth's mantle in order to explain post glacial rebound data as well as various observations of anelasticity over a frequency range of more than seven decades including the seismological band as well as free oscillations and the Chandler Wobble. In fitting the parameters of the absorption band to the observations, the effect of composition, structure, phase transitions, pressure and temperature on the anelastic behaviour is accounted for by making use of the empirical relationship

$$G^* = c \frac{Q\eta}{S_0}$$

where G^* is Gibb's free energy of a relaxation process, $Q\eta$ the seismic parameter, S_0 ambient density and c a constant which is only dependent on the relaxation mechanism itself. This relationship is shown to be well fulfilled for solid state self-diffusion in various solids like metals, halides and oxides including minerals important in the mantle.

Connected with the Gaussian absorption band it yields a theoretical model of inelasticity in the mantle which is in excellent agreement with current knowledge on transient and steady state viscosities as well as with attenuation and dispersion observations between 1 sec and 435 days in period. Based on this model the Earth global Love numbers are calculated for different frequencies. It turns out that the Love numbers entering into Earth tidal and rotational problems are significantly different from those valid in the frequency band of seismology. The difference is an increase in the Love numbers of 2 to 3% if the Earth's short period tidal deformation is considered. It is higher for longer periods of loading and results in an 8 days lengthening of the Chandler Wobble period at 435 days.